

Reviews and syntheses: Review of proxies for low-oxygen paleoceanographic reconstructions

Babette A. A. Hoogakker¹, Catherine Davis², Yi Wang³, Stephanie Kusch⁴, Katrina Nilsson-Kerr⁵, Dalton S. Hardisty⁶, Allison Jacobel⁷, Dharma Reyes Macaya^{1,8,9}, Nicolaas Glock¹⁰, Sha Ni¹⁰, Julio Sepúlveda¹¹, Abby Ren¹², Alexandra Auderset¹³, Anya Hess¹⁴, Katrin J. Meissner¹⁵, Jorge Cardich¹⁶, Robert Anderson¹⁷, Christine Barras¹⁸, Chandranath Basak¹⁹, Harold J. Bradbury²⁰, Inda Brinkmann²¹, Alexis Castillo⁹, Madelyn Cook^{22,23}, Kassandra Costa²⁴, Constance Choquel²¹, Paula Diz²⁵, Jonas Donnenfeld²⁶, Felix J. Elling²⁷, Zeynep Erdem²⁸, Helena L. Filipsson²¹, Sebastian Garrido¹, Julia Gottschalk²⁹, Anjaly Govindankutty Menon¹⁰, Jeroen Groeneveld³⁰, Christian Hallmann^{31,32}, Ingrid Hendy²², Rick Hennekam³³, Wanyi Lu³⁴, Jean Lynch-Stieglitz³⁵, Lelia Matos^{36,37}, Alfredo Martínez-García³⁸, Giulia Molina^{36,37}, Práxedes Muñoz³⁹, Simone Moretti³⁸, Jennifer Morford⁴⁰, Sophie Nuber¹², Svetlana Radionovskaya⁴¹, Morgan Reed Raven⁴², Christopher J. Somes⁴³, Anja S. Studer⁴⁴, Kazuyo Tachikawa⁴⁵, Raúl Tapia³⁰, Martin Tetard⁴⁶, Tyler Vollmer³⁵, Xingchen Wang⁴⁷, Shuzhuang Wu⁴⁸, Yan Zhang⁴⁹, Xinyuan Zheng⁵⁰, Yuxin Zhou⁴²

15

¹The Lyell Centre, Heriot-Watt University, Edinburgh, EH14 4AP, UK

²Department of Marine, Earth, and Atmospheric Sciences, North Carolina State University, Raleigh, NC 27695, USA

³Tulane University, New Orleans, LA70118, USA

⁴Institute of Marine Sciences, University of Quebec Rimouski, Rimouski, QC G5L 3A1, Canada

20 ⁵Department of Earth Sciences, University of Bergen and Bjerknes Centre for Climate Research, Bergen, 5007, Norway

⁶Department of Earth and Environmental Sciences, Michigan State University, East Lansing, MI 48824, USA

⁷Department of Earth and Climate Sciences, Middlebury College, Middlebury, VT 05753, USA

⁸Center for Marine Environmental Sciences, University of Bremen, Bremen, 28359, Germany

25 ⁹Centro de Investigación y Estudios Avanzados del Maule, Universidad Católica del Maule, Campus San Miguel, Talca, 3460000, Chile

¹⁰Institute for Geology, Hamburg University, Hamburg, D-20146, Germany

¹¹Department of Geological Sciences and Institute of Arctic and Alpine Research, University of Colorado Boulder, CO 80309, USA

¹²Department of Geosciences, National Taiwan University, Taipei 106, Taiwan

30 ¹³School of Ocean and Earth Science, University of Southampton, Southampton, SO14 3ZH, UK

¹⁴Department of Earth and Planetary Sciences, Rutgers, the State University of New Jersey, NJ 08854, USA

¹⁵Climate Change Research Centre and ARC Centre of Excellence for Climate Extremes, University of New South Wales, Sydney, NSW 2052, Australia

¹⁶CIDIS-Facultad de Ciencias e Ingeniería, Universidad Peruana Cayetano Heredia, Lima, Lima 15102, Peru

35 ¹⁷Lamont-Doherty Earth Observatory of Columbia University, NY 10964, USA

¹⁸Laboratoire de Planétologie et Géosciences, Université d'Angers, 49000 Angers, France

¹⁹Department of Earth Sciences, University of Delaware, Newark, DE 19716, USA

²⁰Department of Earth, Ocean and Atmospheric Sciences, University of British Columbia, Vancouver, V6T 1Z4, Canada

²¹Department of Geology, Lund University, Lund, 223 63, Sweden

40 ²²Department of Earth and Environmental Sciences, University of Michigan, Ann Arbor, MI 48109, USA

²³Department of Geosciences, University of Arizona, Tucson, AZ 85721, USA

²⁴Department of Geology and Geophysics, Woods Hole Oceanographic Institution, MA 02543 USA

²⁵Centro de Investigación Mariña, XM1, Universidade de Vigo, Vigo, 36310 Spain

- 26College of Earth, Ocean, and Atmospheric Sciences, Oregon State University, Corvallis, OR 97331, USA
- 45 27Leibniz-Laboratory for Radiometric Dating and Isotope Research, Christian-Albrecht University of Kiel, Kiel, 24118, Germany
- 28Department of Marine Microbiology & Biogeochemistry, NIOZ Royal Netherlands Institute for Sea Research, 't Horntje (Texel), 1797 SZ, The Netherlands
- 29Institute of Geosciences, Kiel University, Kiel, 24118, Germany
- 50 30Institute of Oceanography, National Taiwan University, Taipei 106, Taiwan
- 31GFZ German Research Centre for Geosciences, Potsdam, 14473, Germany
- 32Institute of Geosciences, University of Potsdam, Potsdam, 14476, Germany
- 33NIOZ Royal Netherlands Institute for Sea Research, Department of Ocean Systems, Den Burg (Texel), 1790 AB, The Netherlands.
- 55 34State Key Laboratory of Marine Geology, Tongji University, Shanghai 200092, China
- 35School of Earth and Atmospheric Sciences, Georgia Institute of Technology, Atlanta, GA 30332, USA
- 36Centre of Marine Sciences (CCMAR), University of Algarve, Faro, 8005-139, Portugal
- 37Marine Geology and Georesources Division, Portuguese Institute for the Sea and Atmosphere (IPMA), Lisbon, 1495-165, Portugal
- 60 38Max Planck Institute for Chemistry, Mainz, 55128, Germany
- 39Departamento de Biología Marina, Universidad Católica del Norte, Coquimbo, Chile
- 40Chemistry Department, Franklin & Marshall College, Lancaster, PA 17604, USA
- 41Department of Earth Sciences, University of Cambridge, Cambridge, CB23EQ, UK
- 42Earth Science Department, University of California, Santa Barbara, CA 93106, USA
- 65 43GEOMAR Helmholtz Centre for Ocean Research Kiel, Kiel, 24148, Germany
- 44Department of Environmental Sciences, University of Basel, Basel, 4056, Switzerland
- 45Aix Marseille Univ, CNRS, IRD, INRAE, Coll France, CEREGE, Aix-en-Provence, 13331, France
- 46GNS Science, Lower Hutt, 5040, New Zealand
- 47Morrissey College of Arts and Sciences, Boston College, MA 02467, USA
- 70 48Institute of Earth Sciences, University of Lausanne, Lausanne, CH-1015, Switzerland
- 49Ocean Sciences Department, University of California, Santa Cruz, CA 95064, USA
- 50Department of Earth and Environmental Sciences, University of Minnesota Minneapolis, MN 55455, USA

Correspondence to: Babette A.A. Hoogakker (b.hoogakker@hw.ac.uk) and Catherine Davis (cdavis24@ncsu.edu)

75 **Abstract.** A growing body of observations reveals rapid changes in both the total inventory and distribution of marine oxygen over the latter half of the 21st century, leading to increased interest in extending oxygenation records into the past. Use of paleo-oxygen proxies have the potential to extend the spatial and temporal range of current records, bound pre-anthropogenic baselines, provide datasets necessary to test climate models under different boundary conditions, and ultimately understand how ocean oxygenation responds beyond decadal scale changes. This review seeks to summarize the current state-of-

80 knowledge about proxies for reconstructing Cenozoic marine oxygen: sedimentary features, sedimentary redox-sensitive trace elements and isotopes, biomarkers, nitrogen isotopes, foraminiferal trace elements, foraminiferal assemblages, foraminiferal morphometrics, and benthic foraminifera carbon isotope gradients. Taking stock of each proxy reveals some common limitations as the majority of proxies function best at low-oxygen concentrations and many reflect multiple environmental drivers. We also highlight recent breakthroughs in geochemistry and proxy approaches for constraining pelagic (in addition to

85 benthic) oxygenation that are rapidly advancing the field. In light of both the emergence of new proxies and the persistent multiple driver problem, the need for multi-proxy approaches and FAIR data storage and sharing is emphasized. Continued

refinement of proxy approaches and both proxy-proxy and proxy-model comparisons are likely to support the growing needs of both oceanographer and paleoceanographers interested in paleo-oxygenation records.

1 Introduction

90 Dissolved oxygen in the oceans is necessary to sustain aerobic life, control biogeochemical processes, and is closely linked to carbon remineralization, export, and storage. Oxygen in the ocean has declined since at least the mid-20th century. This decrease has been observed in estuaries and coastal regions (Diaz & Rosenberg, 2008; Rabalais 2009, Rablais et al., 2010; Conley et al., 2011), continental shelves, and the open ocean (Schmitko et al., 2017; Chan et al., 2008; Bograd et al., 2008; Breitburg et al., 2018; Keeling et al., 2009; Levin, 2018; Stramma et al., 2008; Stramma et al., 2010). Direct measurements of
95 oxygen have only been routine for decades at most, and even then, are spatially limited. Inaccessible subsurface regions and open ocean features, such as oxygen minimum zones (OMZs), are especially difficult to monitor. Thus, proxies are required to extend modern records and investigate long-term drivers of deoxygenation.

Drivers of ocean deoxygenation include 1) ocean warming, causing decreasing oxygen solubility in seawater and increasing remineralization, 2) increased productivity leading to higher subsurface oxygen utilization during respiration, and 3) decreased
100 ventilation, due to changes in circulation or stratification (Keeling et al., 2009; Breitburg et al., 2018). These drivers can influence ocean deoxygenation on different timescales and to different degrees. Warming is a key driver of modern deoxygenation in the open ocean as well as in coastal systems (Schmitko et al., 2017; Levin, 2018; Rabalais et al., 2010). In coastal systems, anthropogenic nutrient increases (eutrophication) from activities such as sewage efflux and fertilizer input, is frequently the primary cause of deoxygenation on short time scales (Rabalais et al., 2010; Breitburg et al., 2018). Productivity
105 changes can also be important in driving decadal (Deutsch et al., 2011, 2014) to centennial and longer scale changes in open ocean settings (e.g., Dickens and Owen, 1994; Hendy et al., 2004). Ventilation changes may act across different scales of space and time. For example, deoxygenation induced by stratification can be variable on timescales of days to years and beyond, especially in coastal regions and restricted basins (reviewed in Rabalais et al., 2010). However, seawater oxygen content is also responsive to ventilation changes on centennial, millennial and longer time scales, associated with changes in deep water
110 source, upwelling, overturning circulation, ocean gateway dynamics, and the geometry of whole ocean basins (Hoogakker et al., 2015; Fyke et al., 2015; Cardich et al., 2019; Auderset et al., 2022; Hess et al., 2023; Khon et al., 2023).

Climate models indicate that a decrease in dissolved oxygen concentrations will continue for hundreds to thousands of years into the future (Bahl et al., 2019; Kwiatkowski et al., 2020; Oschlies 2021; Gulev et al., 2021). The combined effect of future warming and seawater oxygen depletion could have adverse impacts on the marine environment, potentially culminating in a
115 mass extinction rivalling those in Earth's past (Penn and Deutsch, 2022). The latest state-of-the-art coupled climate models capture the global observational trend in the upper ocean within the conservative end of uncertainty levels (Takano et al., 2023), which are high due to spatiotemporal data sparsity (Ito, 2021). However, models still underestimate deoxygenation in the deep ocean and do not reproduce the observed patterns in the tropical thermocline (Oschlies, 2018; Kwiatkoswki et al.,

2020), where the persistent oxygen deficient zones exist. This mismatch is likely due to unresolved circulation, mixing, and transport processes, misrepresentation of respiratory oxygen demand, missing biogeochemical feedback mechanisms, and insufficient simulation length to reach equilibrium in the deep ocean (Oschlies, 2018). To better constrain biological and physical processes in the ocean and improve their representation in models (see supplementary information for details), we need dedicated observational programs. We also need proxy-based oxygen reconstructions from the geologic past when the climate system was different to present day to test numerical models and to improve process understanding.

Interest in seawater oxygen proxies is increasing, partly due to current trends of ocean deoxygenation and uncertainties about the future at different timescales. A methodological overview of proxies was included in Moffitt et al. (2015). Since this review was published, methodological developments, updates, and insights have emerged that were not captured previously, or were applied to older sediments. This review is limited to proxies that can be applied through the Cenozoic (i.e. the last 66 million years), although we briefly touch upon some well-studied earlier examples, such as Cretaceous oceanic anoxic events (OAEs). The focus on the Cenozoic, when our oceans were overall well oxygenated, allows an investigation of scenarios and timescales most immediately relevant to inform the future.

Extending modern records into the past provides baselines for pre-industrial marine oxygen content and necessary data to test climate models under different boundary conditions from today and improve process understanding. While the past is only a partial analogue to the future, it can provide a portfolio of oxygen scenarios to bound future projections. This is especially the case for past climate episodes that were characterized by greenhouse gas concentrations similar to projected future levels. In step with the growing interest in modern and future ocean oxygen, there has been rapid proxy development over the past decades. Implementation of new technologies as well as a burgeoning interest in paleo-oxygenation has led to an influx of new proxies and refocusing and advancement of established proxies.

This review aims to provide an overview of the current state of proxy development at a pivotal moment for the field. We summarize the major classes of proxies for the benefit of both new and experienced paleoceanographers, and those working in adjacent fields. It is our hope that an introduction to and update of the suite of available proxies will increase their utility for those interested in marine oxygen research. Moreover, we hope that a clear discussion of current limitations and future directions can pave the way for improving the tools at our disposal for generating new paleo-oxygenation records.

2 Proxies

Proxies provide indirect representations of environmental variables in circumstances where they cannot be measured directly, such as the geological past. Examples include seawater temperature, pH, and dissolved oxygen. A proxy is a measurable physical or chemical variable that is conserved in a natural climate archive and allows us to infer information about the variable of interest in a qualitative or quantitative manner. To build a useful proxy, it is important to understand how the proxy relates to the variable of interest and what other environmental parameters might influence the proxy pre- and post-deposition in

sediments. This involves understanding the biology (especially if the proxy is captured in fossil and organic material), chemistry, and physics of both proxy and sedimentary systems.

155 Paleo-oxygen proxies are generally developed and calibrated through a combination of theoretical, empirical, and experimental approaches. Examples of theoretical approaches to proxy development can be subfields of geochemistry such as inorganic and organic geochemistry of sediments and biogenic calcites. For example, a theoretical understanding of redox potential can lead to robust predictions about concentrations of elements and ions across oxygen gradients, and thus whether one would expect redox-sensitive elements to be found in higher or lower abundance in sediments or biogenic minerals. Theoretical approaches generally require empirical validation as many complexities remain difficult to model. For example, redox-associated chemistry and incorporation of products into biogenic minerals is biologically mediated, and influenced by other environmental (e.g., temperature) variables, and taxa-specific dynamics related to their life cycle, metabolism and ontogeny. As a result, theoretical approaches are usually limited to the identification of proxies of interest and qualitative predictions.

160 The use of recently deposited sediments on the seafloor (frequently referred to as 'core-tops') recovered across natural oxygen gradients is the most frequent empirical approach. Core-top calibrations can be critical for proxies that require timescales or depositional environments difficult to replicate in a laboratory setting, such as foraminiferal assemblages, sedimentary features, and sedimentary trace metals. This approach has the benefit of testing how a proxy manifests in the complex natural environment. One key limitation is the need to deconvolve highly correlated environmental controls, such as productivity, organic carbon content, and oxygen, which are classically difficult to disentangle as drivers of foraminiferal assemblages (Gooday, 2003). This may also impact most other proxies, including the isotopic composition of nitrogen ($\delta^{15}\text{N}$) and organic matter. The second key limitation of core-top calibrations is the no-analogue problem; extrapolation beyond modern examples may be required to describe paleo-oxygen environments which are unlike current conditions, particularly during the more extreme events of ocean deoxygenation found in the geologic record. Furthermore, core-tops are not always modern in age, due to extremely low sedimentation rates, dissolution and hiata caused by winnowing currents or active tectonic activity (Mekik and Anderson, 2018; Erdem et al., 2016). Sediment trap studies and plankton tows are other examples of important, yet less-frequently used empirical approaches.

175 Experimental approaches are often considered the 'gold-standard' for quantitative calibration of single-driver proxies. As of now, most paleo-oxygen proxies are qualitative or semi-quantitative. Experimental approaches have the benefit of allowing for single controlling variables to be isolated and have been used to greatest effect so far in biogenic calcites. However, there are a few drawbacks to this approach. The first is that proxies are removed from the complexities of the natural environment, thus results must be validated with field observations where possible. In other cases, the timescales (e.g., sedimentary features, sedimentary trace metals) or complex initial conditions (e.g., biomarkers assemblages) necessary to replicate natural observations are difficult or impossible to generate in a laboratory setting.

2.1 Proxy material

185 Sediments provide the backbone for any marine paleo-environmental reconstruction along with its preserved or fossilized biogenic materials. This can include morphologically identifiable skeletal material such as foraminiferal tests or diatom frustules, or ‘molecular fossils’.

Our review of the various proxy methods is split into a traditional overview of sediments as proxy carriers (section 4), followed by a discussion of sedimentary redox trace elements and isotopes (section 5), organic proxies (section 6), and nitrogen isotopes (section 7). Following this, part of the nitrogen isotope section (8), and sections 9 to 11 (foraminiferal trace elements
190 foraminiferal assemblages, foraminiferal morphometrics, and benthic foraminifera carbon isotope gradients respectively) use foraminifera as proxy carriers, which are introduced below.

Foraminifera (Kingdom Chromista; Infrakingdom: Rhizaria; Order: Foraminiferida) are amoeboid protists characterized by a cytoplasmic body and a shell or ‘test’ comprising one or more interconnected chambers. The test wall can be made of agglutinated particles, organic material, or biomineralized crystals of calcite, aragonite, or rarely silica (Loeblich and Tappan,
195 1988). Calcareous tests, in particular, are frequently preserved in marine sediments after death or reproduction (Debenay, 2012). As a result, a rich fossil record of calcareous foraminifera extends from the Cambrian into the present (Loeblich and Tappan, 1988; Sen Gupta, 2003; Debenay, 2012). Foraminifera have colonized a diversity of environments. The majority are benthic, where they occupy virtually every water depth and substrate, on and into the sediment (e.g., Vickerman, 1992; Gooday, 2003, Sen Gupta, 1999). Others are planktic, with habitats ranging from the ocean’s surface into the mesopelagic (Schiebel &
200 Hemleben, 2017). As a result, foraminifera can offer a near continuous record of ecological succession, with individual shells capturing environmental conditions over their week to years-long lifespans.

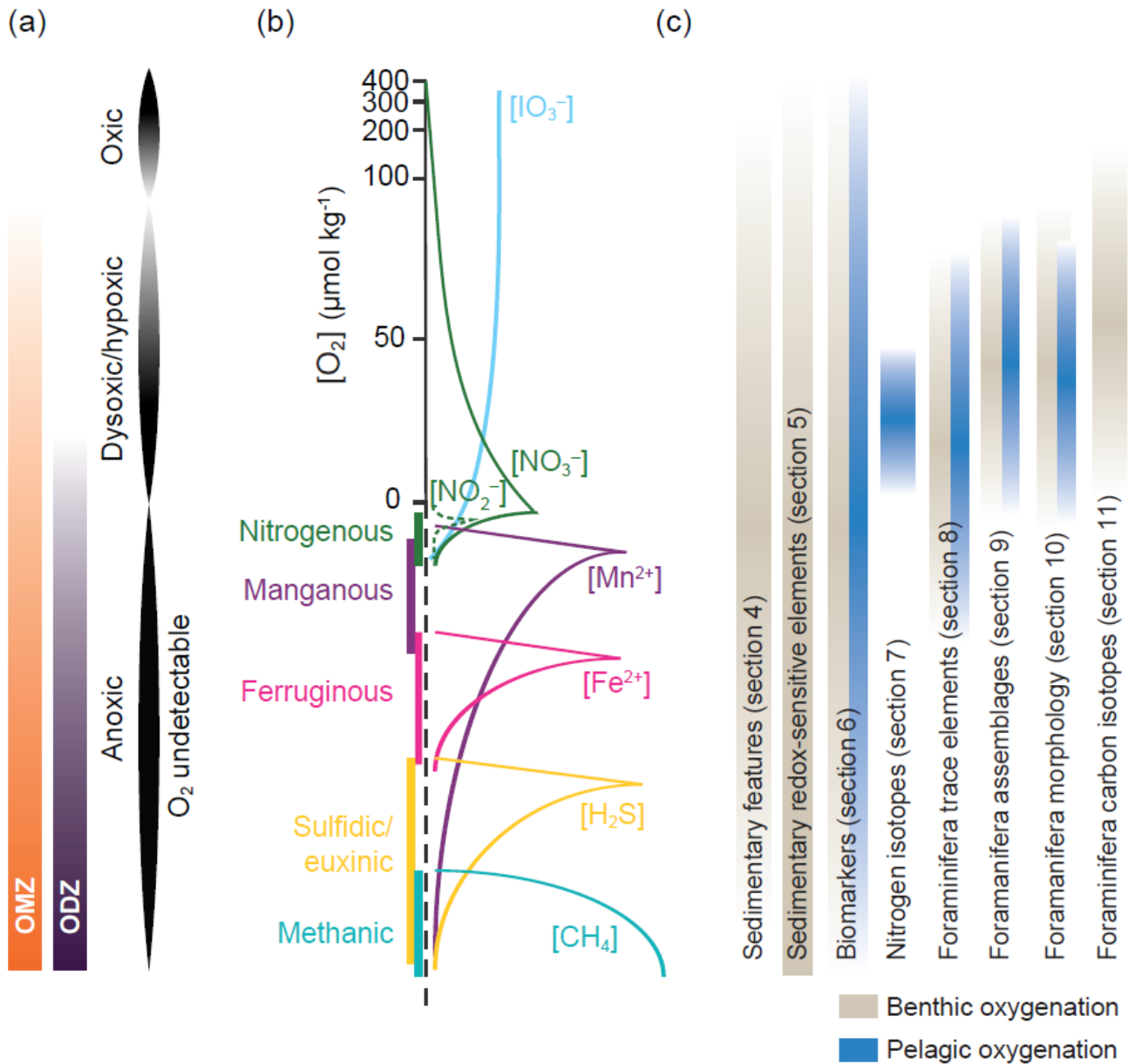
The most diverse and abundant living group of foraminifera are the Rotaliida. Calcification and morphology of this group is different from other groups (e.g., Miliolida, Nodosariida, and Robertinida)(de Nooijer et al., 2023). Calcareous hyaline foraminifera, Rotaliida, diversified during the Cretaceous, and are the basis of several proxy methods using foraminifera
205 (sections 8-11), limiting these to the late Cretaceous until recent (Tappan and Loeblich, 1988; Kaiho, 1994). Other groups, such as Nodosariidae, are sometimes used in paleoenvironmental reconstructions, but have differing calcification mechanisms resulting in marked differences in geochemistry from the more common Rotaliida (de Nooijer et al., 2023; Pacho et al., 2023). Fully planktic Rotaliida foraminifera evolved from benthic orders starting in the middle Jurassic (Boudagher-Fadel, 2015), meaning that proxy applications are more limited in time than those of benthic foraminifera.

210 Living benthic foraminifera are found both on the sediment surface (epifaunal), and throughout at least the top 10 cm of the sediment (infaunal), although the proportion of the total population decreases rapidly with increasing depth (Corliss, 1985; 1991). Moreover, some benthic foraminifera can migrate vertically within sediments, with their habitat depths and position in the sediment column influenced by the organic matter flux and availability of resources such as oxygen (Bernhard, 1992; Barmawidjaja et al., 1995; Loubere et al., 1993; Linke and Lutze, 1993; Jorissen et al., 1995; Geslin et al., 2004). Planktic
215 foraminiferal inhabit the water column above the seafloor, with most species having a near-surface habitat (Schiebel and

Hemleben, 2017). Benthic foraminifera therefore can record variations in bottom water oxygen concentrations in locations where the seafloor is within a low oxygen environment. Planktic foraminifera proxies can provide information about both open ocean oxygen conditions and the extent of low oxygen zones, such as OMZ's.

220 **3 Terminology and units**

As will be evident from the discussion of the different proxies, the nomenclature to define different oxygenation 'zonations' has historically been inconsistent and confusing (Canfield and Thamdrup, 2009). This can be ascribed in part to the interdisciplinarity of modern oxygen research. Classically, geochemists define an oxic zone as one supporting aerobic metabolism, followed by an oxygen-depleted zone, sometimes referred to as suboxic, where metabolism is supported by
225 nitrate-, manganese (Mn)- and iron (Fe)- reduction, and an anoxic zone where metabolism is supported by sulphate reduction and methanogenesis (Froelich, 1979; Berner, 1981). However, this scheme has been regarded as confusing and contradictory by Canfield and Thamdrup (2009) who proposed instead to use terminal electron acceptors and respiration processes to define chemical/metabolic zones (Fig. 1). Ecologists and biologists have frequently focused on oxygen levels associated with negative outcomes for aerobic organism (fish, crustaceans, etc.), and have defined a sublethal threshold and lethal oxygen
230 concentrations, which greatly vary among taxa and may be influenced by other factors such as temperature (Vaquer-Suyter and Duarte, 2008). This sublethal threshold is referred to as hypoxia. It leads to mortality events, loss in biodiversity, habitat reduction, predation potential and disruption of life cycling (Service, 2004; Rabalais et al., 2002). Some literature additionally uses the term 'suboxia' as an intermediate between either 'oxic' and 'hypoxic' or 'hypoxic' and 'anoxic'. The dearth of observational oxygen data at the full range of spatial and temporal scales applicable to either geochemical or ecological systems
235 further complicates definition in terminology. We further note the use of Oxygen Deficient Zone (ODZ), a term which is primarily used to describe a region where oxygen is low enough to allow for denitrification or other anaerobic metabolisms. The term OMZ is used more broadly to refer to regions of notably low oxygen at a variety of thresholds, frequently defined by dissolved oxygen content. With this usage, all ODZs are also OMZs, however the reverse is not always the case and both terms are used here in different contexts. To avoid confusion between the different terms used, an illustrative Fig.1 is provided
240 to give a sense of the zonation, chemical speciation and metabolic processes, alongside the 'oxygen working' range of the different proxies. While 'anoxic' is consistently used to describe no (or undetectable) oxygen, other terms are used to describe different oxygen ranges by different authors. This is represented by varying opacity in Fig. 1 to represent the oxygen ranges often associated with these terms. Similarly, units for dissolved oxygen vary markedly, most frequently reported as ml/L, mg/L, % saturation, or $\mu\text{mol/kg}$. Unfortunately, conversions are not always straight forward as density needs to be considered.
245 Here we favour $\mu\text{mol/kg}$ for consistency, but occasionally reference oxygen in other units when referencing previously published work.



250 Figure 1: Overview of oxygen "stage" nomenclature used in this review. A) shows the ranges most often associated with the
 255 descriptive terms OMZ, Oxygen Deficient Zone (ODZ), anoxia, dysoxia/hypoxia, and anoxia in seawater. In B) oxygen
 concentrations are shown on a log linear scale along with a simplified schematic of several proxy-relevant components of other
 redox-sensitive reactions. Chemical concentrations other than oxygen are non-dimensional, but all relate to scales in both A) and
 C). The redox ladder is modified from Canfield and Thamdrup (2009). C) shows the ranges of oxygen and/or redox chemistries over
 which different proxy types can be used to reconstruct paleo-environments, based on proxies applied to sediment samples. Proxy
 types are ordered as they are discussed in the manuscript, with section numbers associated with each. Proxy types shown in grey

can be used to reconstruct oxygen from benthic settings, those in blue can be used for pelagic settings. Variations in thickness and opacity denote uncertainty and differing usage of terminology.

260 4 Sediment properties as proxies

Reconstructions of past marine environments rely on sediment samples from deep sea cores, or outcrops of uplifted marine sediments. Sedimentary observations form the backbone of metadata essential to support the growing arsenal of proxies employed to define Earth's biogeochemical evolution. In particular, quantitative mineralogy and lithologic descriptions should accompany sample archives to support existing and future geochemical proxy measurements and interpretations. This is critical as a given proxy may only be applicable to specific rock types or biogenic material or may be interpreted in different ways depending on mineralogy or lithology. Programs like IODP (International Ocean Discovery Program) have prioritized presenting lithologic metadata alongside formalized and accessible sample archives. However, samples collected by individual labs may not be associated with these data and/or be archived in an accessible way. Recently developed databases, such as the Sedimentary Geochemistry and Paleoenvironment Project (SGP), are working to circumvent some of these issues by requiring lithologic context and detailed sediment descriptions to accompany geochemical data submissions. Importantly, sedimentary features are crucial to guide sample selection for quantitative analyses, especially intervals that are of interest because of specific redox characteristics. For example, descriptors such as changes in organic carbon content, laminae, and the deposition of pyrites can be useful first indicators of sedimentary redox/oxygen changes.

4.1 Historical based sedimentary redox / bottom water oxygen reconstructions

275 The presence/absence of laminae (Fig. 2) has historically played an important role in reconstructing low-oxygen systems, and they remain a popular tool today. The presence of laminae is a key indicator of conditions that are inconsistent with the survival of benthic fauna beyond seasonal timescales, although microbioturbation of laminated sediments, not visible to the naked eye, have been described (Pike et al., 2001). Importantly, laminae can result from factors unrelated to redox changes, and thus need to be interpreted with caution. For instance, laminated sediments are commonly found associated with diatom mats or giant diatoms, where diatom mats (e.g., *Thalassiothrix* spp.) suppress benthic activity (e.g., King et al., 1995; Kemp et al. 1996, 2000, 2006; Grigorov et al., 2002). Laminae can also form due to grain size changes and particle sorting in sediment gravity flows, sediment-bed interaction, and seasonal to interannual changes in the grain size of settling particles (Kemp 1996, O'Brien 1996).

In addition to laminations, biofacies oxygen indices considering bioturbation, fauna, diversity, body size, and trophic levels, 285 have been used to characterize paleoredox conditions, including specific oxygen levels (Rhoads and Morse, 1971; Behl and Kennett, 1996; Sperling et al., 2022). For instance, ichnological analysis has been widely applied to investigate ocean oxygenation (e.g., OAEs, glacial cycles, and hyperthermals) because different biofacies correspond to specific ranges of oxygen, such as anoxic, suboxia (low oxygen), and dysoxia (e.g., Casanova-Arenillas et al., 2022, Nicolo et al., 2010;

Rodríguez-Tovar et al., 2011; Rodríguez-Tovar et al., 2021). However, trace fossil occurrences could be impacted by both
290 bottom water and pore water conditions. In some cases, trace fossils were produced during later favourable conditions (i.e.
during diagenesis), and such traces are independent of the anoxic pore water conditions but attributed to connections with
favourable more oxygenated bottom waters (e.g., Rodríguez-Tovar et al., 2021). Other environmental conditions, including
food availability (e.g., organic carbon supply) and sedimentation rates, all need to be considered when interpreting ocean
oxygenation (Rodríguez-Tovar et al., 2022). Recent work further demonstrates that carnivory and vision are linked to
295 environmental oxygen levels (Sperling et al., 2013; McCormick et al., 2019). These indices have been used to reconstruct
oxygen trends during the evolution of early animal life (Sperling et al., 2015; Canfield and Farquhar, 2009; Boyle et al., 2014;
Tarhan et al., 2015; van de Velde et al., 2018), oxygen impacts on mass extinctions (Reddin et al., 2020; Sampaio et al., 2021),
as well as local oxygen levels independent of broader evolutionary context.

The presence and relative abundance of pyrite, and observations of its crystal structure can be indicators of water column
euxinia (Fig. 2). Specifically, the size distribution of framboidal pyrite may reflect formation in euxinic versus more oxidizing
300 water columns. Smaller framboids found in the Black Sea, for example, are interpreted to reflect a fast growth rate within the
euxinic water column, as opposed to formation under longer timescales within sulphidic sediments (Wilkin et al., 1996; 1997a;
1997b; Wignall and Newton, 1998). The size fraction of pyrite framboids has been applied within OAEs, but also other
intervals, with widespread geochemical evidence of marine anoxia (Wilkin et al., 1996; Wignall et al., 2005; Kuroda et al.,
305 2005; Jenkyns et al., 2010). Because syngenetic pyrite can incorporate or absorb trace elements (Huerta-Diaz and Morse,
1992), the trace element content of pyrite is also an important paleoredox archive (Large et al., 2014).

4.2 Non-destructive methods for sediment analyses

Observations of sedimentary facies are used as a first-order evaluation of the depositional environment. Traditional methods
(e.g., non-destructive core description and physical property measurements) are a fast, low-cost qualitative way to interpret
310 redox/oxygen conditions. Over the past few decades, there have been important technological advances to describe
sedimentary features in quantitative and non-destructive ways. Analytical instruments and imaging technology (e.g.,
microtomography, X-ray fluorescence (XRF) scanner, multi-sensor core logger, scanning electron microscopy) can further
improve the spatial and temporal resolution of the sedimentological and physical property measurements (see below), allowing
non-destructive and 3D detection of various sedimentary features on the sub-millimetre to micron scale.

315 **X-ray computed tomography (CT)** is a high-resolution (~0.1-1 mm) imaging technique that allows visualization of 3D
structure of objects, determined by X-ray attenuation associated with variations of density and element compositions in
sedimentary records (Fig. 2, see reviews by Mees, 2003 and St-Onge, 2007). Standard-resolution CT imaging can be used on
both whole round and section halves of sediment cores with minimal pretreatment. As a non-destructive method, it has been
used to determine physical properties of sediments (e.g., density, porosity, and grain size (Fortin, 2013; Tanaka, 2011; Orsi,
320 1994; Amos, 1996; Mena, 2015) and to identify benthic communities (e.g., bioturbation analysis and trace fossil
detection/ichnological analysis in the sediments (Dorador, 2020; Rodriguez-Tovar, 2022)). Microstructure information

obtained using standard-resolution CT has greatly improved the accuracy of sedimentological description, whereas physical property data are critical for understanding oxygen penetration in the sediment profile and subsequent diagenetic processes controlled by pore water redox concentrations.

325 **Multi-Sensor Core Logger (MSCL)** or **Multi-Sensor Track (MST)** is widely used for continuous measurements of physical properties on centimetre scales in either whole round or section halves of sediment cores. These core loggers are usually equipped with detectors for measuring magnetic susceptibility, gamma ray density, natural gamma radiation, p-wave velocity, and resistivity, which provides density, porosity, and Fe-bearing mineral information for first order evaluation of ambient redox state in pore waters.

330 **XRF scanners** measure the relative abundance of elements (from Al to U, following the periodic table) on section half sediment cores at sub-millimetre to centimetre (i.e. high-resolution) scales in a non-destructive manner (Fig. 2., Croudace 2006, Croudace 2015, 2019). XRF data are considered semi-quantitative as elemental variability in the sediment cores is measured as counts and not concentrations. XRF data quality is affected by X-ray tube ageing, water content, smoothness of the sample surface, and grain size (Böning et al., 2007; Tjallingii et al., 2007; Weltje and Tjallingii, 2008). Thus, appropriate
335 sample preparation (e.g., core scraping and use of a thin polyester XRF film to smooth the surface) is required for high-quality data acquisition (Löwemark et al., 2019). Additionally, sediment composition (e.g., organic carbon and calcium carbonate content) may affect XRF counts because lighter elements (e.g., carbon, nitrogen, and oxygen) are outside of the XRF detection range. For instance, higher sedimentary organic carbon can dilute the number of counts for all elements (Löwemark et al., 2010). Normalization of the absolute counts with respect to an element that is less affected by biological and diagenetic
340 processes (e.g., normalizing to Al or Ti) is used to assess the relative variability of elemental compositions (Löwemark et al., 2010). Despite the limitations, scanning XRF is able to provide high-resolution data with fast and non-destructive measurements, allowing a first-order assessment of redox-sensitive element abundance (e.g., molybdenum, uranium, and manganese) prior to more labour-intensive analyses (e.g., solution-based bulk elemental concentration analyses, as discussed in Section 5).

345

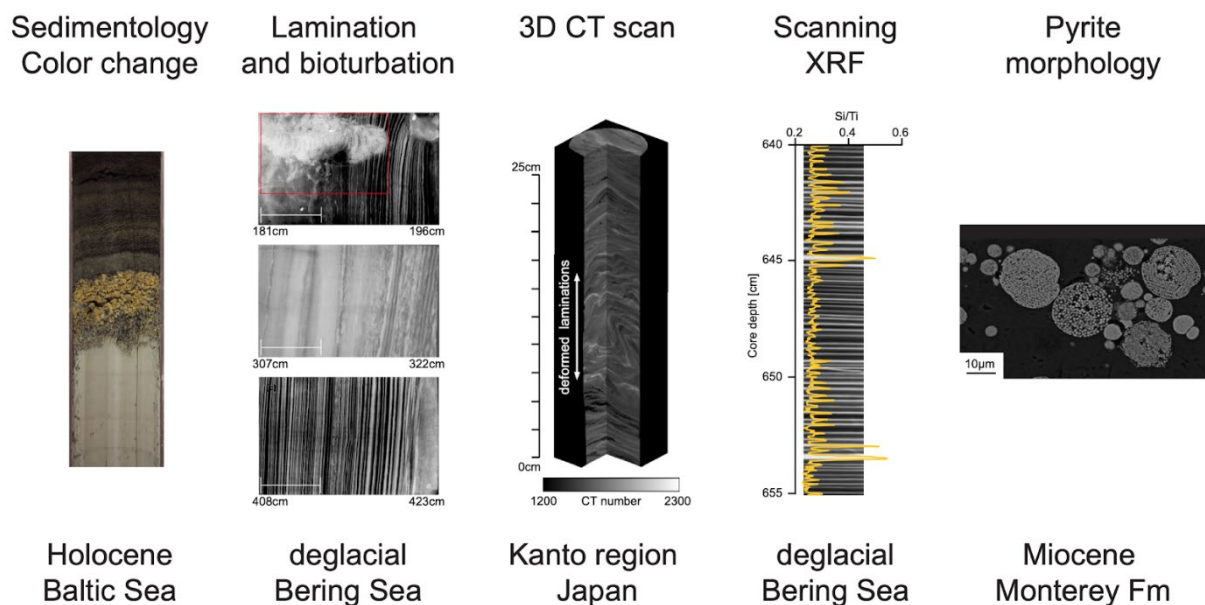


Figure 2: Examples of sedimentary features discussed in the main text. Left to right: clay to laminated gyttja sediments at the transition from Baltic Ice Lake to Littorina Sea in the early Baltic Sea Holocene; laminae from the Bering Sea ODZ during the last deglacial; 3D CT scan from sediments deformed during the 2011 Tohoku Earthquake from offshore Japan; SEM image of framboidal pyrite from the Miocene Monterey Formation of California, USA (adapted after Berndmeyer et al., 2012; Kühn et al., 2014; Nakashima and Komatsubara, 2018).

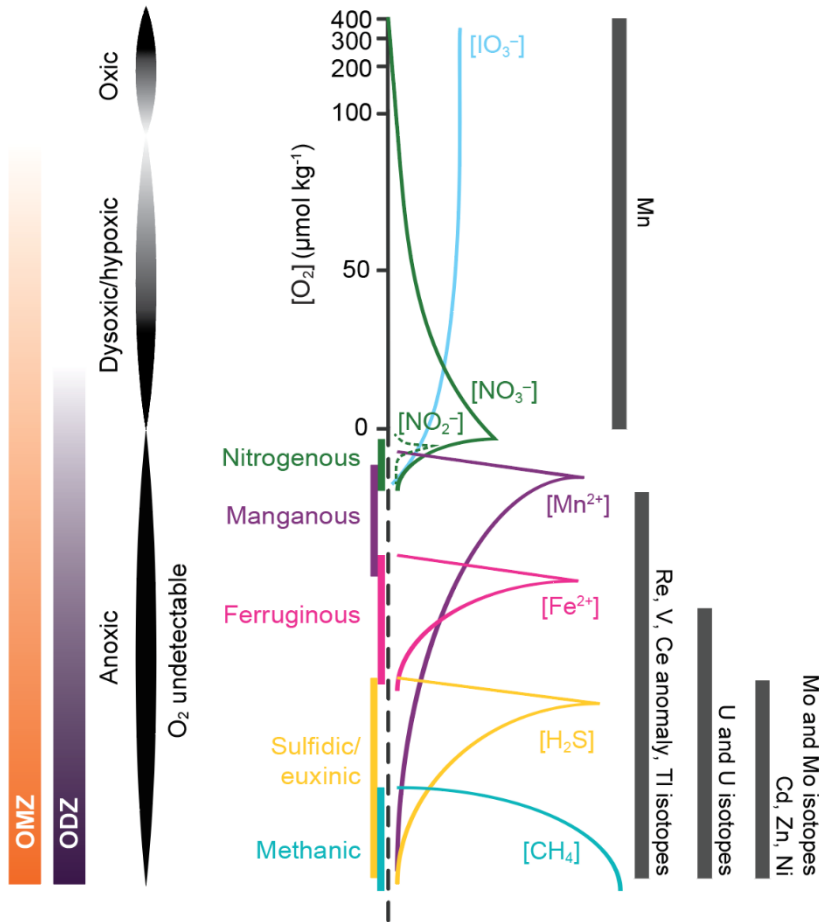
5 Sedimentary redox trace elements and isotopes

5.1 Introduction

The potential for the concentrations of trace metals in sediments to act as proxies for past Earth surface conditions has been recognized since early observation of metal enrichments in organic-rich sediments (Goldschmidt, 1954). Trace metals provide some of the most commonly used proxies for the reconstruction of paleo-redox conditions in sediments (Algeo, 2004; Algeo & Maynard, 2004; Algeo & Rowe, 2012; Bennett & Canfield, 2020; Algeo & Li, 2020; Brumsack, 2006; Calvert & Pedersen, 1996; Little et al., 2015; Morford & Emerson, 1999; Nameroff et al., 2004; Scott & Lyons, 2012; Sweere et al., 2016; Tribovillard et al., 2006; Calvert & Pedersen, 2007; Zhou & McManus, 2023).

Sedimentary trace metal enrichments are associated with precipitation and/or adsorption of metals from the ambient bottom and/or pore waters along a redox gradient (redox potential Eh) primarily controlled by decomposition of organic carbon using various oxidants (Calvert and Pederson, 2007, Froelich et al., 1979). These redox reactions proceed in a well-defined sequence (Fig. 3), during which trace metals may be scavenged from ambient waters and subsequently enriched in sediments (i.e. authigenic enrichment as distinct from detrital input) as a result of changes in valence state (e.g., Mn, U, Re, and Mo) and/or speciation (e.g., Cd, Ni, and Zn with solid phase precipitation but no valence change) (Algeo & Li, 2020). Because sedimentary Eh varies in response to both bottom water oxygen availability and the rain rate of organic carbon, reconstructions using redox-

sensitive elements to reconstruct bottom water oxygen must explicitly account for changes in the rain rate of organic carbon (see Section 5.4.1).



370 **Figure 3: Redox ladder (modified from Fig. 1 in the introduction) and redox-sensitive trace metals and metal isotopes discussed in this section. Dissolved oxygen ranges for OMZs, ODZs, anoxia, dysoxia/hypoxia (low-oxygen), are labelled in the figure. The redox ladder is modified from Canfield and Thamdrup (2009). The oxygen/redox potential range for use of each redox-sensitive metal and metal isotope redox proxy is shown as coloured bars on the right.**

Trace element analysis has the advantage of facilitating "multi-proxy" data acquisition. Sedimentary trace metal concentration measurements are free from vital effects compared to trace metal incorporation into biogenic carbonate (e.g., foraminifera shells, see Section 8), and are particularly valuable when carbonate preservation is poor and sediments have remained relatively undisturbed post-deposition. Recently, a better understanding of redox-sensitive metal preservation in surface sediments and applications of statistical techniques have made it possible to quantify dissolved oxygen concentrations in some coastal systems of the Eastern Pacific (Valdés et al., 2021; Sánchez et al., 2022; Costa et al., 2023), opening the door for additional regional redox-sensitive trace metal calibrations and creating new possibilities for quantitative oxygen reconstructions.

375
380

In addition to redox-sensitive metal concentrations isotopic fractionation these metals (e.g., Mo, U, Cr, and Fe) may occur during the exchange between seawater and other ocean sinks/sources (e.g., scavenging from reducing water columns) in various redox environments, making those isotope systems potential redox proxies. Technical advances in mass spectrometry have allowed measurements of “non-traditional” stable metal isotope systems and enabled their use in reconstructions of past ocean oxygenation changes (e.g., Andersen et al., 2017; Kendall et al., 2017; Severmann et al., 2008; Frei et al., 2011). Compared to authigenic enrichments, redox-sensitive metal isotope proxies may allow for more (semi-) quantitative redox reconstructions via isotope mass balance, and potentially provide a more globally integrated perspective on ocean oxygen variability.

Trace element enrichments and their isotopes have provided key insights into ocean processes on various timescales (from Precambrian to present; Table 1) and research is ongoing to refine the interpretations of these proxies to shed new light on our understanding of global ocean oxygen responses to variations in Earth’s climate and other environmental variables.

Table 1: Summary of redox trace elements and isotopes that can provide insights into ocean oxygenation from Precambrian to present.

Proxy	Typical marine concentration of aqueous species	Marine isotope composition (\pmSD)	Ocean residence time (years)	Example Reference
Mn	~1.8 nmol/kg	N/A	10-40	Bender et. al., 1977
Ce/Ce*	5 pmol/kg	N/A	50-130	Alibo and Nozaki, 1999
$\delta^{53}\text{Cr}$	4 nmol/kg	0.44 – 1.53‰ (?)	~3,000	Qin and Wang, 2017
U and $\delta^{238}\text{U}$	13.4 nmol/kg	-0.39‰	400,000	Lau et al., 2019
Re and $\delta^{187}\text{Re}$	~40 pmol/kg	-0.17 \pm 0.12‰	130,000	Dickson et al., 2020
V and $\delta^{51}\text{V}$	~35 nmol/kg	0.2 \pm 0.07‰	~91,000	Nielsen, 2021

Mo $\delta^{98}\text{Mo}$	104 nmol/kg	$2.34 \pm 0.1\%$	440,000	Kendall et al., 2017
$\epsilon^{205}\text{Tl}$	65 nmol/kg	$-6 \pm 0.3 \epsilon$ unit	~20,000	Owens 2019

395

5.2 Materials needed and analytical methods

Quantitative elemental concentrations are measured on dried sediments, which are either fully or partially dissolved (i.e. leached) to target authigenic phases. Samples are generally treated using bulk digestion methods such as acid digestion and alkaline fusion, depending on the sediment composition and elements of interest. To avoid contamination, all sample preparation should be performed in metal-clean laboratories with acid-cleaned vessels and trace-metal grade chemicals. Acid digestion and alkaline fusion are commonly used to dissolve sediment to analyse major, minor, and trace elements.

Major and minor element compositions can be measured using quantitative X-ray fluorescence (XRF), inductively coupled plasma optical emission/atomic emission spectroscopy (ICP-OES or ICP-AES), atomic absorption spectrophotometry (AAS), and microwave plasma atomic emission spectroscopy (MP-AES); whereas minor and trace elements may be measured using inductively coupled plasma mass spectrometry (ICP-MS) that has a lower detection limit.

Quantification of redox-sensitive metal enrichment (Metal_{EF}) may be determined following Tribovillard et al. (2006) (Eq. 5.1) and Böning et al. (2009) (Eq. 5.2):

410 Equation 5.1 $\text{Metal}_{\text{EF}} = (\text{Metal}/\text{NE})_{\text{sample}} / (\text{Metal}/\text{NE})_{\text{background}}$

where NE corresponds to the element for normalization.

415 Equation 5.2 $\text{Metal excess (normalized by Al)} = \text{Metal}_{\text{sample}} - (\text{Metal}/\text{Al})_{\text{background}} * \text{Al}_{\text{sample}}$

The upper continental crust has been widely used as a lithogenic background reference (Rudnick and Gao, 2003). Because lithogenic background ratios may vary by region, by source materials (e.g., aeolian, river sediment input, and coastline or glacial erosion), and by timescales, care should be taken to determine and cite an appropriate value (see Section 5.4.2).

Metal isotope measurements often target authigenic phases to avoid contamination from detrital components. As such, diluted acids (e.g., diluted HCl and HNO₃) or weaker acids (e.g., acetic acid) are used in the partial digestion or leaching process. Leaching methods vary between and within labs even for the same isotope measurements (e.g., U isotopes (Tissot et al., 2018)). Initial sample reconnaissance experiments should be used to determine the optimal leaching procedure. For high-precision

stable metal isotope analysis, it is generally necessary to purify the element of interest from sample matrices to avoid possible spectral or non-spectral interferences on the instrument (e.g., through column chemistry).

425 Metal stable isotopes are now analysed routinely using thermal ionization mass spectrometry (TIMS) or multi-collector ICP-
 MS (MC-ICP-MS) instruments (Table 2). Precise and accurate stable isotope ratio measurements on either type of instrument
 depends on robust correction of instrumental mass bias produced during analysis (e.g., double spike and sample-standard
 bracketing method) (e.g., Sibert et al., 2001; Ripperger et al., 2007; Tian et al., 2019; Nielsen et al., 2016; Nielsen et al., 2004;
 Wu et al., 2016). Additionally, metal stable isotopes can be measured by *in situ* techniques, including secondary ion MS
 430 (SIMS) and laser ablation MC-ICP-MS, which has shown unique potential in unravelling micron-scale information from
 samples with complex textures or zonation that are otherwise inaccessible by bulk analysis. Currently, *in situ* stable isotope
 analysis is more frequently used in studies of high-temperature and cosmogenic processes, as well as environmental conditions
 of early Earth. This leaves ample opportunities to adapt existing *in situ* methodologies and develop new ones for more recent
 paleoceanographic research.

435

Table 2: Quantitative analytical methods for trace metals and metal isotopes.

Analysis	Digestion method	Instrument	Quality control
Bulk major elements	Full digestion (alkaline fusion or acid digestion)	ICP-OES (rapid and cost efficient), solution-based or laser ablation (for LiBO ₂ fused beads) ICP-MS (low detection limit), XRF, AAS	Instrumental drift correction (e.g., internal standards) and standard reference materials
Bulk minor-trace elements	Full digestion (alkaline fusion or acid digestion)	Usually ICP-MS, solution-based or laser ablation of LiBO ₂ fused beads	Instrumental drift correction (e.g., internal standards) and standard reference materials
Stable metal isotopes	Leaching authigenic phases	TIMS, (laser ablation) MC-ICP-MS, and <i>in situ</i> SIMS	Double spike and sample-standard bracketing

5.3 Redox-sensitive metal and metal isotope proxies

5.3.1 Redox-sensitive metal proxies with valence state changes by redox potential

440 **5.3.1.1 Manganese**

Manganese (Mn) has three oxidation states (II, III, and IV). The reduced forms of Mn are soluble in low-oxygen waters (< 10 μmol O₂) (Madison et al., 2013; Oldham et al., 2017), which include Mn(II) and soluble Mn(III) complexed by inorganic or organic ligands (Mn(III)-L) (Oldham et al., 2015). The oxidized form of Mn(IV) forms solid Mn(IV) oxides. Consequently, the residence time of dissolved Mn in the oxygenated deep ocean is on the order of 10-40 years (Bender et. al., 1977;

445 Klinkhammer & Bender, 1980; Hayes et al., 2018). As reduced Mn(II) can be oxidized to Mn(III)/Mn(IV) oxyhydroxides with even micromolar levels of oxygen concentrations (Tebo et al., 2004; Morgan, 2005; Clement et al., 2009), sedimentary Mn enrichment can be used as an oxic indicator in pore waters (Burdige & Gieskes, 1983; Froelich et al., 1979; Calvert & Pedersen, 1996). However, free Mn(II) can also precipitate as MnCO₃ and/or co-precipitate with authigenic calcite in reducing pore waters with high alkalinity for example when methanogenesis occurs (Calvert and Pedersen, 1996; Mucci, 2004), which may
450 lead to a false positive for oxic conditions. Thus, Mn should be evaluated simultaneously with other redox-sensitive metals.

5.3.1.2 Iron

The iron paleoredox proxy can be used to distinguish oxic, ferruginous, and euxinic water column settings (reviewed in Raiswell et al., 2018). In oxic environments, Fe exists as Fe (oxyhydr)oxides, including ferrihydrite, lepidocrocite (γ -FeOOH), goethite (α -FeOOH), hematite (α -Fe₂O₃), maghemite (γ -Fe₂O₃), and magnetite (Fe₃O₄). As the ambient water becomes depleted
455 in oxygen, Fe (oxyhydr)oxides can be reduced to Fe(II). With sulphide production during sulphate reduction, reduced Fe(II) can be converted to Fe sulphides that include mackinawite (FeS), greigite (Fe₃S₄), and pyrite (FeS₂). In strongly reducing waters (e.g., methanic conditions), siderite (FeCO₃) can also form. Combined with Fe sulphides, carbonate-bearing Fe and Fe (oxyhydr)oxides make up the highly reactive Fe pool, because these forms of Fe readily react with free sulphide (e.g., HS⁻) in early diagenetic stages. By leaching out different Fe phases, Fe speciation uses highly reactive Fe (Fe_{HR}) / total Fe (Fe_T), and
460 pyrite Fe (Fe_{py}) / Fe_{HR} to distinguish oxic, ferruginous, and sulphidic conditions. Modern sediment calibrations indicate a threshold of Fe_{HR}/Fe_T >0.38 for anoxic water columns. Under anoxic regimes (Fe_{HR}/Fe_T>0.38), Fe_{py}/Fe_{HR} has been used to differentiate sulphidic (Fe_{py}/Fe_{HR}>0.7~0.8) from ferruginous (Fe_{py}/Fe_{HR}<0.7) waters. When Fe_{HR}/Fe_T<0.38, and/or high Fe_{py}/Fe_{HR} values (>0.8) have also been used to indicate oxic water columns with pore water sulphide accumulation in organic rich sediments.

465 5.3.1.3 Uranium, rhenium, and vanadium

Uranium (U), rhenium (Re), and vanadium (V) behave conservatively in seawater – the residence time in the ocean is ~750,000 years for Re (Akintomide et al., 2021), ~300,000-600,000 years for U (Dunk et al., 2002; Ku et al., 1977; McManus et al., 2005; Morford and Emerson, 1999, Lau, et al., 2019), and ~50,000-100,000 years for V (Shiller and Boyle, 1987; Tribovillard et al., 2006, Nielsen 2021). As a result, sedimentary concentration changes of U, Re, and V on time scales shorter than tens of
470 thousands of years are likely not a response to the changes in the dissolved concentration in the overlying water column. Instead, the downward flux of metal reduction, in accordance with the redox potential of the pore water, is likely the driver of the sedimentary variations (Böning et al., 2004; Colodner et al., 1995; Sundby et al., 2004), making these elements potentially useful oxygen indicators.

Rhenium exists as ReO₄⁻ in oxic waters, but can be reduced to Re(IV) oxides (e.g., ReO₂) in reducing environments. Redox
475 potential of the Re(VII)/Re(IV) couple is higher than that of U(VI)/U(IV), situated between MnO₂/Mn(II) (manganous) and Fe³⁺/Fe²⁺ (ferruginous) and is similar to the redox potential of NO₃⁻/NO₂⁻ (Bratsch 1989, Algeo & Li, 2020). Re preservation

in sediment could also be associated with thiolation of ReO_4^- to particle-reactive $\text{ReO}_n\text{S}_{4-n}^-$ which enhances its particle reactivity towards iron sulphides (Akintomide et al., 2021) and/or co-precipitation with the Fe-Mo-S phase in sulphidic waters (waters in which oxygen is undetected and sulphide is present) (Helz and Dolor, 2012; Helz, 2022). Free sulphide levels in the most sulphidic water columns are still insufficient to support thiolated ReO_4^- as major species due to higher required sulphide levels relative to molybdate thiolation (Helz and Dolor, 2012; Vorlicek et al., 2015). However, this potential exists in euxinic pore waters (Akintomide et al., 2021). Less is known about Re isotopes and their usefulness for constraining past changes in ocean oxygenation although early studies are working to constrain the Re isotope mass balance (Dellinger et al., 2021; Dickson et al., 2020).

Vanadium mainly occurs as V(V) in oxic waters in the form of vanadate (e.g., HVO_4^{2-} and H_2VO_4^-). However, unlike U and Re, vanadate can be scavenged by adsorption onto Fe-Mn (oxyhydr)oxides and clay minerals (e.g., Wehrli and Stumm 1989; Morford and Emerson, 1999). The redox potential of the V(V)/V(IV) is similar to that of the Re(VII)/Re(IV) couple (Algeo and Li, 2020). Thus, as oxygen draws down, vanadate can be reduced to the V(IV) species (vanadyl, VO^{2+} and $\text{VO}(\text{OH})^{3+}$) by organic compounds, which can co-precipitate/complex with mineral particles and organic matter (Emerson & Huested, 1991; Algeo and Maynard, 2004). Under more reducing conditions (e.g., sulphidic), vanadyl might be further reduced to the V(III) species by free sulphide in the ambient waters, which precipitate as solid oxides (V_2O_3) or hydroxides (VOOH) (Wanty and Goldhaber, 1992). Despite the different authigenic enrichment mechanisms, V reduction and sequestration into sediments still begin under low-oxygen conditions, making it a tracer of such conditions.

In oxic water columns, U exists as the soluble U(VI) and binds to carbonate ions forming $\text{Ca}_2\text{UO}_2(\text{CO}_3)_3$ (Endrizzi & Rao, 2014, Langmuir, 1978). Redox potential of the U(VI)/U(IV) couple is below that of the $\text{Fe}^{3+}/\text{Fe}^{2+}$ couple but above $\text{SO}_4^{2-}/\text{H}_2\text{S}$ (Fig. 1, Morford and Emerson, 1999; Zheng et al., 2002). In reducing environments, U(VI) turns into U(IV) in the form of the solid uraninite (UO_2) or adsorbs onto sediment solids, which may involve biologically mediated processes (Crusius et al., 1996; Klinkhammer and Palmer, 1991; McManus et al., 2005; Zheng et al., 2002; Lovley et al., 1991; McManus et al., 2006; Stirling et al., 2015; Rolison et al., 2017).

As discussed above, soluble U(VI) can be reduced to insoluble U(IV). The sedimentary U sequestration process also introduces significant isotopic fractionation (e.g., Zhang et al., 2020), as the nuclear volume effect causes a preferential removal of the heavy ^{238}U relative to the lighter ^{235}U isotope. Because of the long residence times of U ($\sim 3\text{-}6 \times 10^5$ years; Dunk et al., 2002), the isotopic composition of U in seawater is globally homogenous (-0.39‰ in the modern ocean; Andersen et al., 2017). Uranium uptake in reducing sediments is the primary U sink in the global ocean, and, hence, seawater $\delta^{238}\text{U}$ changes can be associated with the extent of sea floor anoxia (e.g., Lau et al., 2019; 2020).

Oxic sediment deposits that record the seawater U isotope value (e.g., shallow marine carbonates and Mn oxide crusts) have been used to infer the areal extent of anoxic sinks in the global ocean using isotope mass-balance models (e.g., Zhang et al., 2018; 2020). However, post-depositional diagenesis of carbonate could result in much larger offsets from the seawater U isotope value (e.g., Chen et al., 2022). In contrast, sediments deposited within anoxic conditions, such as organic-rich black shales, will typically record enriched $\delta^{238}\text{U}$ values during more intense anoxia, although the expression of isotope enrichment

is complicated by processes that vary across depositional environments (e.g., diffusion of U between the sediment-water interface and the zone of U reduction within the sediment; see Andersen et al., 2014). Long-lasting anoxia/euxinia within restricted basins (e.g., limited water renewal) are shown to have a larger fractionation factor from seawater ($\sim+0.5$ to $+0.7\%$ based on modern observation) due to diffusion limitations of U (VI) in shallow sediments, where most U reduction occurs (e.g., Lau et al., 2020). Within anoxic facies, carbonate-associated-uranium isotopes have also been used to infer local deoxygenation in sediments, with the large advantage that this proxy is not significantly impacted by post-depositional oxidation (Clarkson et al., 2021b).

5.3.1.4 Molybdenum

In oxic waters, Mo primarily exists as soluble molybdate (Mo(VI)O_4^{2-}) and behaves conservatively ($\sim 440,000$ years residence time) (Miller et al., 2011). However, $\sim 30\text{--}50\%$ of molybdate may be sequestered through adsorption onto Mn and Fe (oxyhydr)oxides in oxic waters (Kendall et al., 2017). Unlike the low-oxygen indicators (e.g., U, Re, and V), reductive Mo removal requires sulphidic conditions that lead to progressive thiolation of molybdate (thiomolybdate series $\text{Mo(VI) O}_x\text{S}_{4-x}^{2-}$, $x=0\text{--}4$) (Hlohowskyj et al., 2021). Thiomolybdates are particle reactive and readily scavenged into sediments and onto iron sulphides (Freund et al., 2016). Mo removal from sulphidic pore waters had been associated with a $[\text{H}_2\text{S}]$ threshold of $> 11 \mu\text{mol}$ (when MoS_4^{2-} starts to dominate in the waters, Helz et al., 1996). Yet, recent studies have suggested that under weakly sulphidic conditions ($[\text{H}_2\text{S}] < 11 \mu\text{M}$), intermediate thiomolybdate species could be the dominant Mo species in the water column that contribute to Mo sequestration (e.g., Tessin et al., 2019). Multiple pathways have been proposed for Mo removal from sulphidic waters, including: (1) the organic matter (OM) pathway that leads to Mo (IV or VI)-OM complexes (Dahl et al., 2017); (2) the Fe-sulphide pathway that has thiolated Mo adsorption to iron sulphide phases with subsequent Mo(VI) reduction to Mo(IV) (Miller et al., 2020) and/or that incorporates Mo(IV) into Mo-Fe-S structures such as $\text{FeMoS}_2(\text{S}_2)$ (Helz and Vorlicek, 2019); and (3) the biological pathway that implies biological uptake (e.g., by sulphate reducing bacteria) and Mo reduction by enzymes (e.g., Dahl et al., 2017). Authigenic Mo enrichment has thus been interpreted as an indicator of sulphidic environments provided that coeval enrichments of other redox-sensitive trace metals (e.g., U or Re that are not scavenged by Mn oxides in oxic environments) are observed.

As discussed above, in sulphidic environments Mo from oxic waters (mostly as MoO_4^{2-}) is converted into particle-reactive thiomolybdate species in the presence of free sulphide. During this transformation the Mo isotopes are fractionated, with the more sulphidised thiomolybdate species becoming isotopically lighter relative to seawater (He et al., 2022; Kerl et al., 2017; Tossell, 2005). The Mo isotopic composition of mildly euxinic sediments is, thus, expected to be lighter than the seawater value ($\sim -2.34\%$ in the modern ocean; Nakagawa et al., 2012; Nägler et al., 2013). Low $\delta^{98}\text{Mo}$ values of sediments deposited in such environments can be modelled assuming higher scavenging rates for the more sulphidised Mo species, allowing semi-quantitative reconstructions of H_2S concentrations (Dahl et al., 2010; Matthews et al., 2017; Sweere et al., 2021). However, in strongly sulphidic conditions (e.g., the Black Sea), the conversion of MoO_4^{2-} to MoS_4^{2-} (the most sulphidised species) is near-

complete (Erickson and Helz, 2000), such that little-to-no fractionation is expressed (Tossell, 2005). The sedimentary $\delta^{98}\text{Mo}$ values therefore approach seawater compositions (Neubert et al., 2008; Brüske et al., 2020).

In conclusion, sedimentary Mo isotopes can be used to trace the local euxinic water-column conditions when the global seawater Mo isotopic composition is known or close to modern values (e.g., Holocene/Pleistocene to Paleocene sediments, Andersen et al., 2018; Azrieli-Tal et al., 2014, Hardisty et al., 2021; Matthews et al., 2017, Sweere et al., 2021, Riedinger et al., 2021). Environments with quantitative drawdown of dissolved Mo may also be studied to infer global seawater $\delta^{98}\text{Mo}$ values to estimate global-scale extends of oxic-anoxic-euxinic Mo sinks on geological timescales (e.g., Dahl et al., 2021; Dickson and Cohen, 2012; Dickson et al., 2016). Sedimentary (co-)variations in $\delta^{98}\text{Mo}$ and $\delta^{238}\text{U}$ have also been applied to trace past changes in ocean oxygenation, especially on orbital to million year timescales (e.g., Andersen et al., 2020; Chen et al., 2015; Chiu et al., 2022; Clarkson et al., 2021; Dahl et al., 2010; Dickson, 2017; Gordon et al., 2009; Hardisty et al., 2021; Kendall et al., 2015; Sweere et al., 2021; Wang et al., 2016; Zhang et al., 2018).

555 **5.3.2 Trace metal proxies with speciation changes in sulphidic waters (cadmium, zinc, and nickel)**

Unlike the previously discussed metals, Cd, Zn, and Ni behave like micronutrients, with a depletion in the surface ocean due to phytoplankton uptake and increasing concentrations at depth due to decomposition of organic material (Bruland, 1983; Flegal, Sanudo-Wilhelmy, & Sceflo, 1995; Nozaki, 1997; Bruland & Lohan, 2003). Authigenic metal enrichments in the sediments primarily occur in sulphidic waters because they can either form insoluble sulphides (e.g., Cd and Zn; Rosenthal et al., 1995; Tribovillard et al., 2006; Little et al., 2015) and/or can be incorporated into the pyrite structure (e.g., Ni, Huerta-Diaz and Morse, 1992; Large et al., 2014), making them a possible tracer of sulphidic conditions. However, we note that Ni has also been linked to sinking fluxes of organic material in upwelling regions because of its close link with productivity and less diagenetic alteration associated with sedimentary sulphur and manganese cycling (Böning et al., 2015).

5.4 Factors controlling trace metal preservation/metal isotope fractionation

565 In addition to redox potential and organic carbon rain rate, sedimentary enrichments of trace metals can be altered by several processes, which may affect delivery to the sediments and result in remobilization/recycling in the sediment pore waters. These caveats may lead to decoupled sedimentary responses from the water column oxygen variability.

Due to anthropogenic activities, coastal marine ecosystems are susceptible to pollution by potential contaminant metals and metalloids from industrial, domestic and harbour waste. Some pollutant metals that have adverse impacts on aquatic life and human health are also redox sensitive, such as Mo, Zn, B, Mn, Ba, Co, Ni, Sr, Cr, Cd, Zr, V, Cu, Ce. In some regions, the concentrations of these elements have recently increased and the values do not align with increases in lithogenic background inputs (Muñoz et al., 2022; Valdés et al., 2023). As river sediments may concentrate and deliver anthropogenically-sourced metals during transport to the ocean (Pizarro et al., 2010; Yevenes et al., 2018), using standard lithogenic background corrections may overestimate enrichment factors as the authigenic fraction will be augmented with the anthropogenic input.

575 In regions with high anthropogenic input, it is thus recommended to use the local lithogenic background in the region of study
(e.g., crust, river, dust, wetland sediment) (Muñoz et al., 2022, 2023; Valdés & Tapia, 2019; Valdés et al., 2023).

5.4.1 Organic carbon and trace element burial

Because redox potentials vary as a function of both reductant and oxidant availability, enrichments of trace elements in
sediments could result from bottom water oxygen availability and/or the rain rate of organic material. For example, glacial
580 authigenic U enrichments in the Southern Ocean have been found to occur primarily as a function of changes in export
production (e.g., Chase et al., 2001; Kumar et al., 1995). As some redox-sensitive metals (e.g., Mo, V, Ni, and Cd) can be
concentrated in phytoplankton due to biological uptake, they are also efficiently transported to the sediments via bio-detritus
and particulate organic matter (e.g., in upwelling areas) (Böning et al., 2004; Muñoz et al., 2012; Valdés et al., 2014; Castillo
et al., 2019; Nameroff et al., 2004; Muñoz et al., 2023). Thus, to isolate bottom water oxygen concentrations, reconstructions
585 using redox-sensitive trace elements must be accompanied by independent constraints on the supply of particulate organic
carbon (e.g., Anderson et al., 2019; Bradtmiller et al., 2010; Jaccard et al., 2009; Jacobel et al., 2020; Pavia et al., 2021). It is
particularly important that proxies for organic carbon flux are independent from oxygen, rendering classic proxies like total
organic carbon (TOC) ineffective since its sedimentary abundance is itself a function of oxic respiration (e.g., Burdige, 2007;
Tyson, 2020). For a description of marine organic compounds that are susceptible to oxygen see Section 6 on organic
590 biomarkers as proxies for seawater oxygen.

Trace element enrichment proceeds according to sequential redox thresholds, and attempts have been made to define bottom
water oxygen ‘thresholds’ below which redox-sensitive trace elements would be expected to become enriched in the sediments
(e.g., Algeo & Li, 2020; Bennett & Canfield, 2020). Unfortunately, this approach is inappropriate for reconstructing bottom
water oxygen concentrations because variations in organic carbon can be the primary determinant of trace element enrichment.

595 5.4.2 Detrital influences on authigenic enrichments of trace metals

Shifts in sedimentary elemental compositions may be associated with changing proportions of sediment sources (e.g.,
lithogenous, biogenous, and hydrogenous) with inherently different elemental matrices. For example, nearshore sediments are
highly influenced by terrestrial inputs (e.g., fluvial and aeolian sediments) and organic fluxes from primary productivity,
whereas deep-sea sediments generally receive only the finest fraction of lithogenic particles (e.g., clays from dust). Estimates
600 of authigenic concentrations are based on an assessment of the lithogenic contribution (detrital) using Al as the most common
approximation. This is based on the conservative behaviour of Al during weathering and soil formation, and the assumption
that Al concentrations are very similar in most common sedimentary rocks (Calvert and Pedersen, 2007), which may not hold
true on a global scale. Titanium has also been used for normalization for lithogenic contribution, but the concentration of this
element is more variable than Al in different rock types (Calvert and Pedersen, 2007). Additionally, the estimate of detrital
605 contributions assumes that the detrital element (e.g., Al) analysed is only in the aluminosilicate fraction. Therefore, estimations

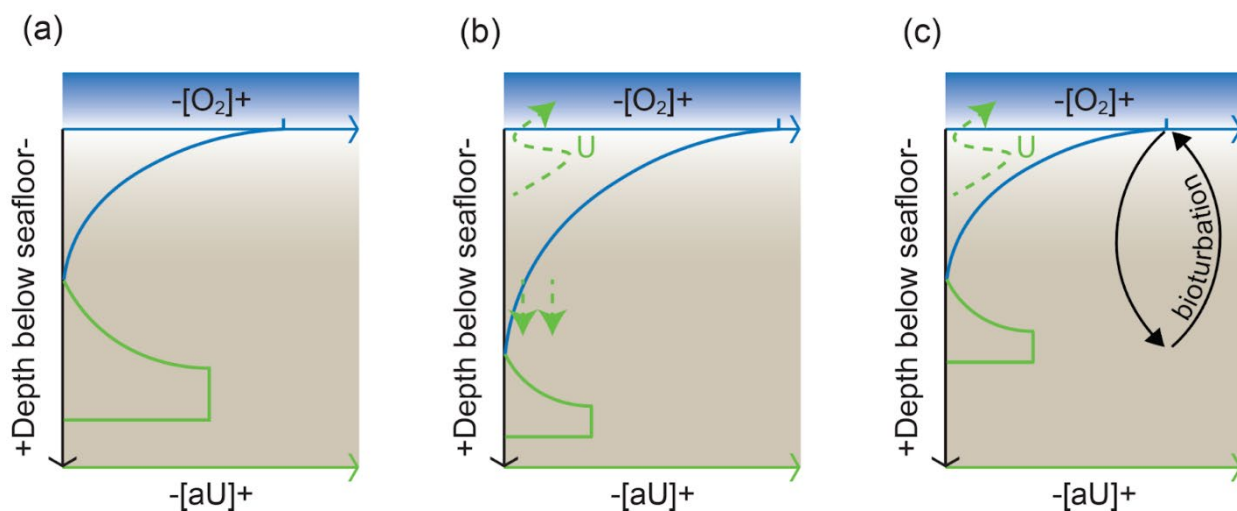
attributed to other phases (e.g., hydrogenous) could be underestimated (Van der Weijden, 2002). Caution should be employed when correlating normalized data because it could modify the original correlations between elements (Cole et al., 2017).

5.4.3 Post-depositional diagenetic effects on sedimentary trace metals

610 As with many other proxies, the utility of redox-sensitive metals as a paleo-oxygen indicator relies on the post-depositional persistence, or preservation, of the initial redox signal. Modifications to trace element distributions during diagenesis include: wholesale overprinting of sedimentary redox signals (e.g., Jacobel et al., 2020; Zheng et al., 2002), partial removal (e.g., Bonatti et al., 1971; Chase et al., 2001; Jacobel et al., 2017; Jung et al., 1997; Morford et al., 2009), and oxidation and down-core precipitation along concentration gradients (Colley et al., 1989; Colley and Thomson, 1985; Jacobel et al., 2017; Olson et al., 2017, McKay et al., 2014, Anschutz et al., 2002, Deflandre et al., 2002).

615 One of the most significant pore water alterations that can modify the original sedimentary metal enrichment signal is post-depositional organic matter remineralization, which progressively consumes pore water oxygen and changes local redox potential (Morford and Emerson, 1999; Nameroff et al., 2002) (Fig. 1). As oxygen is depleted, Fe/Mn (oxyhydr)oxides are reduced to release Mn(II) and Fe(II) that diffuse into the pore waters. Aqueous Mn(II) may diffuse upwards until it reaches oxygenated pore waters and can re-precipitate as Mn oxides (Lynn and Bonatti, 1965; Burdige & Gieskes 1983). As a result,
620 a post-depositional Mn spike may occur right above the depth where the pore water oxygen concentration goes to zero (Burdige & Gieskes, 1983; Froelich et al., 1979). Preservation of this peak is affected by subsequent variability in the oxygen penetration depth (e.g., Finney et al., 1988; Mangini et al., 2001, Anschutz et al., 2002, Deflandre et al., 2002). Shoaling of the oxygen penetration depth would push the Mn peak into reducing pore waters, in which it will dissolve and diffuse upwards, leaving no trace of the former peak (Froelich et al., 1979). In contrast, if the oxygen penetration depth increases in the sediment, the
625 Mn peak will be preserved because it will remain within the oxygen-rich zone (e.g., Froelich et al., 1979; Mangini et al., 1990, Deflandre et al., 2002). Therefore, it has been proposed that peaks in authigenic Mn concentrations in sediments are best interpreted as pore water oxygen concentrations increasing over time rather than indicators for (static) high oxygen concentrations (e.g., Volz et al., 2020; Pavia et al., 2021).

Reductive dissolution of Fe/Mn (oxyhydr)oxides may lead to additional metal release as they are carrier phases for many trace
630 metals (Algeo & Tribovillard, 2009; Scholz et al., 2011, 2017). For instance, remobilized V due to Mn oxide reductive dissolution (Seralathan and Hartmann, 1986; Legeleux et al., 1994; Hastings et al., 1996) may either diffuse upward into bottom waters (Heggie et al., 1986; Shaw et al., 1990) or diffuse downwards and re-precipitate at a deeper sediment depth (Colley et al., 1984; Jarvis and Higgs, 1987). Post-depositional build-up of reducing conditions (e.g., sulphate reduction) would also facilitate additional trace metal sequestration (e.g., Mo) by sedimentary organic material and/or sulphides (e.g., pyrite or
635 other metal sulphides) (Al-Farawati & van den Berg, 1999; Erickson & Helz, 2000; Helz et al., 1996; Helz & Vorlicek, 2019). Remobilization of authigenic U has also been studied extensively in regions characterized by large oscillations in pore water redox potential (e.g., Morford et al., 2009). When pore water oxygen increases, U remobilization may occur and allow U diffusion to the overlying bottom water and/or re-precipitation at a deeper depth (Fig. 4).



640

Figure 4: Schematic of authigenic U (aU) post-depositional diagenesis, after Jacobel et al. (2020). A) In a baseline scenario, the relatively low-oxygen concentration at a certain depth below seafloor (blue line) leads to aU precipitation (green line). B) As the bottom water oxygen concentration and the depth of oxygen penetration both increase, a portion of the previously precipitated aU becomes remobilized and diffuses upwards (green arrow). The rest of the remobilized U re-precipitates downcore. C) Bioturbation (black arrows) may also mix aU-containing sediment upward and exposings it to a better-oxygenated environment, where aU may be remobilized and released back into the bottom water (Morford et al., 2009).

645

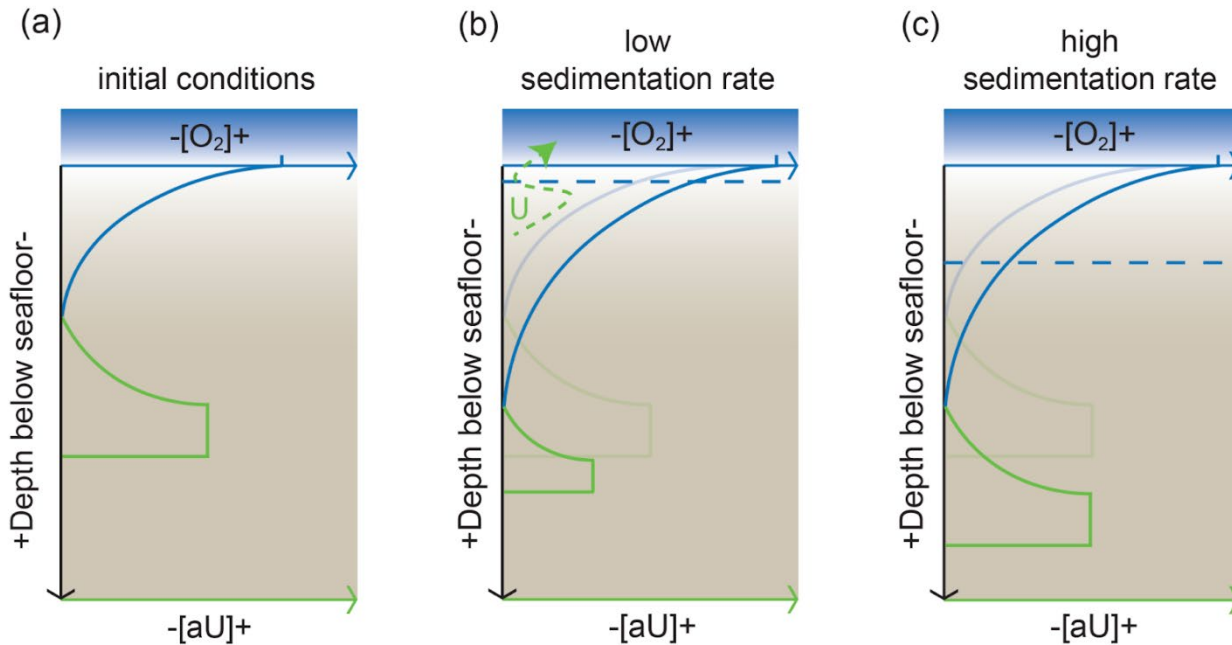
These observations have several important implications. An absence of redox-sensitive metal enrichment cannot be taken as evidence that such conditions were absent, as short-lived events may not be recorded. This is especially true in environments with accumulation rate less than 2 (Jung et al., 1997; Mangini et al., 2001) or 3 cm kyr⁻¹ (Jacobel et al., 2020), where pore waters may retain active redox fronts long after the time of initial deposition, especially if sedimentary organic carbon is low. Caution is also needed in interpreting the shape of sedimentary enrichment features as primary signals and both the sharpness of peaks and their temporal structure (Crusius and Thomson, 2000; Jacobel et al., 2020, 2017; Thomson et al., 2000) may be modified post-depositionally.

655 5.4.4 Sedimentation rate changes

The impact of sedimentation rate on authigenic enrichment should also be considered when evaluating metal accumulation. Changes in sedimentation rate would be expected to impact accumulation since sedimentation rate directly influences the rate of organic carbon respiration and depth of bioturbation. Sedimentation rate has been used as a proxy for the flux of organic carbon to the sediment-water interface, with higher rates associated with more reducing conditions and a shoaling of the oxygen penetration depth (Boudreau, 1994; Tromp et al., 1995). A shallower oxygen penetration depth would reduce pore water exposure to oxygen and allow a better preservation of trace metals (Fig. 5). A special case is the occurrence of instantaneous depositional events (e.g., turbidite layers), which could introduce pulses of sediment delivery that significantly reduce oxygen

660

665 exposure of the underlying sediments. Rapid sediment accumulation would then facilitate build-up of reducing pore waters that lead to diagenesis (e.g., Fe/Mn reduction) (Anschutz et al., 2003, McKay et al., 2014, Wang et al., 2019). However, an increase in the rate of non-reactive sediment accumulation can also dilute the relative concentrations of organic matter and trace metals while reducing the downward diffusion of dissolved gasses (oxygen) or aqueous species (trace metals, sulphate). Modelled authigenic Mo and U as a function of sedimentation rate show dramatic decreases in their authigenic concentration with increasing sedimentation rate (Liu and Algeo, 2020; Hardisty et al., 2018; Morford et al., 2007).



670 **Figure 5: Schematic of aU preservation in sediments with varying sedimentation rates, after Costa et al (2018). A) In a baseline scenario, the relatively low-oxygen concentration at a certain depth below seafloor (blue line) leads to aU precipitation (green line). B) When sedimentation rates are low (dashed blue line is the original seafloor position), as the bottom water oxygen concentration increases, aU remobilization takes place and preservation is poor. C) When sedimentation rates are high, aU is insulated from the oxygen penetration down the sediments and the aU signal is better preserved.**

675 5.4.5 Particulate shuttle and basin effect on trace metal delivery to the sediments

In many cases, trace metal enrichments may be controlled by a ‘particulate shuttle’ (e.g., particulate Fe/Mn (oxyhydr)oxides and phytoplankton remains, Zheng et al., 2002; Algeo and Tribovillard, 2009; Tribovillard et al., 2012; Sweere et al., 2016; Scholz et al., 2017; Ho et al., 2018; Severmann et al., 2008; Muñoz et al., 2023) and the resupply of certain trace metals (‘basin reservoir effect’; e.g., Algeo and Lyons et al., 2006). Due to affinity of Mo on Fe/Mn (oxyhydr)oxides, molybdate adsorbs onto particulate Fe/Mn oxyhydroxides in the oxic waters while being transferred through the water column. These particles are then reduced when oxygen is depleted in the ambient waters releasing molybdate that either diffuses back into the water column or is scavenged in the sulphidic sediments (Morford and Emerson, 1999; Morford et al., 2005). The latter process accelerates the transfer of authigenic Mo to the sediment relative to other redox-sensitive trace metals (e.g., U) that are not

680

685 affected by the particulate shuttle, leading to elevated authigenic Mo/U ratios in the sediments (e.g., Cariaco Basin, Algeo and Tribovillard, 2009). Operation of particulate Fe-Mn (oxyhydr)oxide shuttles occurring close to a (variable) redoxcline in the water column could thus be interpreted from Mo-U covariation in the sediments.

On the other hand, dissolved trace element supply is limited in hydrographically restricted basins compared to the open ocean. Subsequent scavenging of certain trace metals may deplete the dissolved metal reservoir in the water column. Consequently, trace metal enrichment can vary considerably in restricted ocean areas compared to an open ocean setting (Algeo and Lyons, 690 2006; Algeo and Rowe, 2012; Sweere et al., 2016; Algeo and Li, 2020; Bennett and Canfield, 2020). For instance, dissolved Mo/U in the Black Sea is lower than that in the open ocean due to continuous scavenging of Mo in the water column, leading to lower authigenic (Mo/U) ratio (Algeo and Tribovillard, 2009). Redox-sensitive enrichments may thus vary significantly in different depositional systems depending on metal delivery from the water column. The relationship between Mo and U enrichment factors (M_{EF} and U_{EF}) to establish the shuttle effect and to infer the oxygenation conditions of the depositional 695 environment can be found from the model proposed by Algeo & Tribovillard (2009) and Tribovillard et al. (2012).

It is necessary to take site-specific impacts and changes in environmental variables through time, such as organic carbon rain rate, into account when linking trace metal enrichments to redox conditions for each individual depositional system (Algeo and Li, 2020).

5.4.6 Interpretive approaches for reducing uncertainty

700 Several studies have applied the use of a suite of elements, including ratios and corrections for detrital phases, to compensate for some of the issues mentioned above, exploiting the variable response of different elements to the array of controlling parameters (Algeo and Lyons, 2006; Crusius et al., 1996; Jones and Manning, 1994). A recent review finds some redox dependency for all studied trace element ratios, but also stresses several complications, including the need for these proxies to be carefully calibrated for each individual setting (Algeo & Liu, 2020).

705 With an understanding of individual preservation mechanisms, the use of multiple redox proxies leads to a more nuanced interpretation of past conditions. Chromium, Re and Mo have been used to discern the global extent of anoxic and sulphidic conditions, respectively (Reinhard et al., 2013). Molybdenum and U have similarly been used to distinguish between sulphidic or non-euxinic conditions and changes over time while also providing evidence for water mass restriction (Zhang et al., 2022; Algeo and Tribovillard, 2009). Although it is possible that Re and Mo co-precipitate, varying Re/Mo ratios might provide 710 evidence for dissolution of other carriers thereby increasing the delivery of Re or Mo to pore waters (Helz, 2022). For instance, in the Humboldt upwelling ecosystem (Northern Chile and central Peru) Mo/U and Re/Mo ratios have been used to differentiate suboxic (low-oxygen and non-euxinic) from anoxic conditions in the depositional environment (Salvatteci et al., 2014, 2016; Valdés et al., 2014, 2021; Castillo et al., 2017). Higher Re/Mo and lower Mo/U than the seawater value (Crusius et al., 1996) would reflect suboxic (low-oxygen) conditions in the absence of H₂S (Tribovillard et al., 2006, Algeo and Tribovillard, 2009).

715 On the contrary, in the presence of reducing and occasionally sulphidic bottom waters, Mo accumulation increases relative to U, implying that the Mo/U ratio in sediments could be equal to or higher than that of the water column (molar ratio of $7.53 \pm$

0.25, Millero, 1996). However, the fidelity of these interpretations hinges on a clear understanding of differing authigenic preservation mechanisms, redox or non-redox related (e.g., organic carbon flux, particulate shuttle and basin reservoir effect), and the potential for diagenetic loss that would compromise the record.

720 Other empirical geochemistry proxies have also been proposed to evaluate depositional settings (Algeo & Liu, 2020 and references therein) (e.g., restricted basins vs. continental margins with intensive upwelling). For instance, a decrease in sedimentary Mo/TOC ratios has been associated with water mass restriction in anoxic marine environments (e.g., in a silled basin) based on the observation that water column Mo can be depleted in stagnant basins (Algeo and Lyons, 2006). Based on the close association of Cd and productivity (Section 5.3.2, Horner et al., 2021), elevated Cd/Mo ratios may be used to indicate
725 upwelling zones on the continental margin. Low sedimentary Cd/Mo (close to seawater value) caused by metal depletion in sulphidic water columns, along with high Co/Mn values attributed to a dominated river supply over a deep metal source (e.g., from upwelling) have been used to indicate restricted basin environments (Sweere et al., 2016). We caution that these empirical relationships require a better mechanistic understanding for trace metal cycling and can only be used in the marine environments where they have been calibrated.

730 **5.5 Future perspectives**

5.5.1 Towards quantitative oxygen proxies on a local scale

A few recent studies have investigated the potential for using redox-sensitive trace metals in quantitative oxygen reconstructions, especially on a local scale where other contributing factors to metal enrichments are less variable (e.g., sedimentation rates and lithogenic background). For instance, Costa et al. (2023) develop U/Ba as a local- to regional-specific
735 bottom water oxygen proxy, which explicitly takes organic carbon rain rate into account via normalization with respect to Ba. Local U/Ba calibrations for the Arabian Sea, Eastern Equatorial Pacific (EEP) and Western Equatorial Pacific suggest that U/Ba may be used to capture bottom water oxygen concentrations in regions with $>50 \mu\text{mol kg}^{-1}$ oxygen and high oxygen variability (several tens of $\mu\text{mol kg}^{-1}$). This shows the potential for redox-sensitive trace element concentrations to be quantitatively related to bottom water oxygen when the flux of organic carbon is accounted for. Wang et al. (2023) used
740 existing shale trace metal concentration data and machine learning technique to quantitatively reconstruct oxygen in different Phanerozoic depositional environments (e.g., euxinic basins vs. open ocean OMZs).

5.5.2 A better understanding of trace metal delivery to the sediments in the GEOTRACES era

Extensive water column analyses on redox-sensitive trace metals and metal isotopes are essential for revealing their global
745 distribution, source and sink fluxes, and preservation mechanisms in the sediments. The GEOTRACES program has provided a unique service for mapping dissolved and particulate trace metal (e.g., Mn) and metal isotope distribution in the modern ocean (Schlitzer et al., 2018), allowing a direct comparison with core-top trace metal and metal isotope measurements. The

750 GEOTRACES data may also advance our understanding of the mass balance and potential isotopic fractionation of multiple trace metals resulting from incorporation or adsorption. These are critical for improving metal isotope mass balance modelling that has been used in quantitative global oxygen reconstructions (e.g., Lau et al., 2019). Future coordinated efforts to expand routine analysis to more redox-sensitive trace metals and metal isotopes (e.g., with robust method development and participation of more research groups), as well as *in situ* surface sediment collection, would significantly advance proxy development and improve the knowledge of proxy controls and potential caveats.

5.5.3 Expanding metal isotope applications in the Cenozoic through proxy development

755 Apart from the U and Mo isotope systems discussed above, many other “non-traditional” isotope systems are being actively explored as important redox tracers. Due to the very long residence time of some trace metals compared to seawater (Section 6.2.3), other metal isotope proxies have been investigated to study ocean oxygen variability on shorter (e.g., orbital) timescales. For instance, chromium (Cr, residence time of ~10 kyr, Reinhard et al. 2014) isotopes in sediments deposited under sulphidic water columns (e.g., Cariaco Basin off the Venezuela coast) may record seawater values due to quantitative Cr removal from water columns (Gueguen et al., 2016; Reinhard et al., 2014). Another promising global oxygen content tracer is provided by thallium (Tl) isotopes, which have been shown to be primarily controlled by the global Mn oxide burial on timescales of 10^6 years (Nielsen et al. 2011, 2019, Owens et al. 2017). Quantitative Tl removal has been observed in reducing pore waters (with Mn reduction, Ahrens et al., 2021) and a recent core-top calibration suggests that authigenic Tl isotopic compositions can faithfully record the seawater value if pore water is reducing at/near the sediment-water interface leading to complete Tl sequestration from ambient pore waters (Wang et al., 2022). As criteria for determining the fidelity of sedimentary Tl isotope records are developed, paleo-reconstructions of seawater Cr, Tl and other isotopic compositions in the future will ultimately help reveal variations in Tl global ocean content on millennial to orbital timescales, with important implications for marine carbon storage that may have driven the glacial-interglacial transitions (e.g., Wang et al., 2024).

770 In addition to assessment of global ocean oxygen levels, there is demand for local oxygen reconstructions. This task can be suitably undertaken by proxies with residence times similar to, or shorter than, the average ocean mixing time of ~1,000 yrs. A promising proxy is cerium (Ce, residence time on the order of ~50–100 years, (Alibo and Nozaki, 1999)) and Ce isotope ratios. Experiments have shown that oxidative adsorption of dissolved Ce onto Mn oxides can produce ~0.5‰ fractionation in $^{142}\text{Ce}/^{140}\text{Ce}$ with adsorbed Ce being isotopically light, whereas Ce adsorption onto Fe oxides or Ce oxidation by oxygen produces a smaller Ce isotope fractionation of ~0.2‰ or less (Nakada et al., 2013). This contrasting behaviour in stable Ce isotope fractionation implies a close link between Ce isotope variations and Mn cycling. However, a modern calibration of the Ce isotope system in marine environments is lacking.

6 Biomarkers

6.1 Organic Matter and Lipid Biomarkers

780 Organic matter encompasses a wide spectrum of carbon-based compounds of primarily biological origin, which are principally based on carbon-carbon and/or carbon-hydrogen bonds (Killops and Killops, 2005). From a quantitative perspective, most organic matter reaching marine sediments derives from phytoplankton sources from the surface ocean, with additional contributions from bacteria and archaea involved in autotrophic chemosynthesis and heterotrophic processes, particularly in ODZs (Wakeham, 2020). Terrestrially derived organic matter can also be important along continental margins (e.g., Bianchi et al., 2018). Killops and Killops (2005), Eglinton and Repeta (2014), and Peters et al. (2005) provide detailed reviews on the production, composition, degradation, and preservation of organic matter in marine and terrestrial environments.

785 From a compositional perspective, organic matter largely consists of a few compound classes, including proteins (amino acids), carbohydrates, nucleotides, nucleic acids, and lipids (Killops and Killops, 2005, Peters et al., 2005). Although the former often predominate quantitatively in fresh organic matter (Wakeham et al., 1997), lipids offer by far the largest range of applications in paleoceanography due to their preservation potential in sedimentary systems (Briggs and Summons, 2014; Luo et al., 2019). Lipids include a wide-range of compounds that are all characterized by their relatively small molecular size and their mostly hydrophobic nature. This makes them insoluble in water and soluble in organic solvents, such as alkanolic acids, mono/di/triglycerides, waxes, phospho- and glycolipids, lipopolysaccharides, isoprenoids, hopanoids, steroids, terpenes, and also pigments, as well as their intact or fragmented fossil remains (Peters et al., 2005). In living cells, lipids play a central role as structural components of membranes, for energy storage, and as signalling molecules (Hazel & Williams, 1990; van Meer et al., 2008; Harayama et al., 2018). Their intact structure includes a recalcitrant hydrocarbon skeleton that can contain functional moieties such as unsaturations (double bonds) and functional groups (e.g., ester and ether bonds, ketyl, hydroxyl, and carboxyl or amine groups).

790 The versatility of lipids as the basis of paleoceanographic proxies can be explained by (a) their overall preservation potential in sedimentary systems over geological time scales, (b) their chemotaxonomic and metabolic association with biological sources, (c) their role in controlling cellular physiological processes that lead to lipid remodelling (e.g., degree of unsaturation or cyclization) in response to environmental stressors (e.g., temperature, oxygen, salinity), and (d) the preservation of stable isotope signatures (primarily carbon and hydrogen, but also nitrogen and sulphur) in their backbone skeletons (e.g., Eglinton & Eglinton, 2008; Eglinton and Repeta, 2014; Peters et al., 2005). Below we provide a brief overview of these processes and how they relate to the reconstruction of redox processes in paleoceanographic studies. Importantly, lipid biomarker applications in paleoceanography follow two approaches: 1) inferring specific source organisms or metabolisms (chemotaxonomy) prevalent in OMZ settings using intentionally biosynthesized compounds and their degradation products, and 2) inferring redox conditions using lipid degradation products that only form under oxygen-deficient conditions and may either have ubiquitous sources or no known biological sources (orphan biomarkers). In case of chemotaxonomic approaches,

810 it should be kept in mind that, while other sources of biomarkers may exist or may be discovered in the future (outlined below), independent sedimentological evidence can provide source constraints in a given setting (see section 4).

6.2 Lipid Preservation and Redox Potential

The accumulation and preservation of organic material and lipids in marine sediments hinges on a series of physical and biogeochemical factors. These factors include (a) the amount of primary productivity in surface waters, (b) the processes
815 controlling sinking fluxes and attenuation rates of particulate organic matter in its journey through the water column to the seafloor (e.g., availability and composition of ballast material, lateral transport/advection, degree of heterotrophic remineralization), (c) the nature and composition of the organics reaching the sediment/water interface, (d) the redox potential of the depositional environment, (e) the rates of sediment accumulation and burial, (f) the presence of protective minerals (specifically clays), and (g) the availability of reduced sulphur species (e.g., Hedges and Keil, 1995; Blair and Aller, 2012).
820 From their biosynthesis in cells to their preservation in sediments, lipids are subjected to a continuum of post-depositional transformations that modify their physico-chemical properties. Initially, these transformations are driven by diagenesis, predominantly microbial enzymatic degradation influenced by the redox potential, that lead to the hydrolysis of polar head groups, and/or the loss of functional groups, and/or the aromatization of ring structures, and the saturation of double bonds (Killops and Killops, 2005; Peters et al., 2005). As sedimentary systems become impacted by tectonic processes and enhanced
825 temperature and pressure gradients, catagenesis and metagenesis lead to changes in the three-dimensional configuration of the molecules (stereochemistry) and finally to their thermal cracking (Peters et al., 2005). Whereas the absolute abundance of organic material and lipids decreases along this continuum, the relative abundance of lipids within the total organic material pool increases as a consequence of their higher degradation resistance and preservation potential compared to other compound classes such as carbohydrates and nucleic acids (Briggs and Summons, 2014; Luo et al., 2019). Despite the loss of structural
830 information that lipids endure during degradation, their backbone skeletons preserve diagnostic paleoceanographic information that can be preserved for up to ~1.64 billion years, depending on factors such as oxygen exposure time and thermal maturity (Luo et al., 2019). Thus, since some lipids are more labile (i.e. more prone to degradation) than others (i.e. more recalcitrant), their utility as paleoceanographic proxies is determined by their preservation potential in sedimentary systems over geological time scales (Fig. 6).

835 The sensitivity of organic matter preservation to bottom water oxygen has been long debated (Pedersen et al., 1992; Paropkari et al., 1992, 1993). Processes such as oxygen exposure time, the adsorption to mineral phases, and the rate of sediment accumulation have been shown to have the greatest impact (Hedges and Keil, 1995; Hartnett et al., 1998; Burdige, 2007; Zonneveld et al., 2010; Arndt et al., 2013; Hemingway et al., 2019). Organic matter and lipid preservation are enhanced by reducing conditions at the water-sediment interface and within the sediment through (a) reduced exposure time to oxygen-
840 utilizing enzymes, (b) decreased bioturbation, and (c) interactions with reduced sulphur species that lead to lipid sulphurization (e.g., Kohnen et al., 1991). Thus, variable organic matter and lipid preservation, as well as the extent of lipid sulphurization, provide a means of estimating past changes in bottom water oxygen. Empirical studies of organic matter preservation across a

range of bottom water oxygen levels in the Arabian Sea find enhanced preservation of as much as an order of magnitude when bottom water oxygen levels fall below a threshold ranging between 20 and 50 $\mu\text{mol kg}^{-1}$ (Cowie et al., 2014; Keil & Cowie, 1999; Koho et al., 2013; Rodrigo-Gámiz et al., 2016). Similarly, enhanced accumulation rates and/or preservation of TOC and specific biomarkers under low-oxygen conditions has been found in sediments of the Arabian Sea (Sinninghe Damsté et al., 2002c; Woulds et al., 2009) and off the east coast of the U.S. (Prah et al., 2001). These studies have shown that the preservation response of biomarkers is nonlinear and that there is a range of sensitivities among different lipid classes to bottom water oxygen.

Anderson et al. (2019) reported that, compared to bulk productivity proxies like opal and Ba_{xs} , the accumulation rates of algal lipid biomarkers in sediments deposited during the last glacial period in the Central Equatorial Pacific Ocean were five times greater than during the early Holocene due to low bottom water oxygen. This interpretation is consistent with independent bottom water oxygen constraints at these sites during the last glacial period (20-50 $\mu\text{mol kg}^{-1}$) compared to modern bottom water oxygen concentrations ($\sim 170 \mu\text{mol kg}^{-1}$) (Hoogakker et al., 2018; Umling & Thunell, 2018; Jacobel et al., 2020). Jacobel et al. (2020) demonstrated that when biomarkers are measured in parallel with inorganic proxies for productivity such as opal and Ba_{xs} , it is possible to discriminate between production and preservation as factors causing changes in concentration or accumulation rate of TOC or of individual compounds, such as oxygen diffusion into the sediments following an increase in bottom water oxygen. The impacts of post depositional organic matter or biomarker oxidation, a process sometimes referred to as “burndown” (e.g., Colley et al., 1989; Colley and Thomson, 1985; De Lange, 2008, 1986; Prah et al., 1989), can be reduced by working at locations with high sediment accumulation rates.

The accumulation and preservation of organic matter and biomarkers can also be enhanced through sulphurization, in which organic matter and organic compounds react with sulphide (H_2S , HS^-) and/or polysulphides (S_x^{2-}), removing functional groups and generating cross-linked polymers that can be relatively resistant to breakdown by microbial exoenzymes (Sinninghe Damsté et al., 1988; Boussafir and Lallier-Vergès 1996; Van Kaam-Peters et al., 1998). Through these reactions, lipid biomarkers can be bound to high-molecular-weight organic matter (kerogen) via monosulphide (C-S-C) or disulphide (C-S-S-C) bonds (Vairavamurthy et al. 1992; Amrani and Aizenschtat 2004; Kutuzov 2019). These bonds can be broken during catagenesis (Keleman et al., 2012) or by chemical desulphurization in the lab (Orr and White 1990; Prah et al., 1996; Adam et al., 2000). S-bound and especially disulphide-bound lipids appear to form during very early sedimentation and diagenesis, sometimes prior to the appearance of detectable dissolved sulphide in pore water (Francois, 1987). Early sulphurization can trap biomarker signals before diagenetic reworking and can make these S-bound lipids a relatively high-fidelity archive of biomarker information. In both modern and ancient sediments, S-bound lipid distributions are often distinct from free (extractable) lipids, reflecting important aspects of environmental oxygenation such as pigments, steroid distributions, and C- or S-isotope compositions (Kohnen et al., 1991b; Wakeham et al., 1995; Kok et al., 2000; Rosenberg et al., 2018; Ma et al., 2021). Sulphide in the environment may also contribute to the stabilization of free lipids by reducing double bonds (Hebting

et al., 2006). Reconstructions of lipid distributions from sulphidic environments should consider the potential for sulphurization to transform, bias, and/or preserve biomarker information.

Understanding the location and timing of sulphurization also provides insights into the distribution and intensity of anoxia. For example, intervals of enhanced sulphurization and preservation of carbohydrate-derived organic matter in a TOC-rich
880 Jurassic black shale were attributed to photic zone euxinia during deposition (Boussafir et al., 1995; van Kaam-Peters et al., 2003; van Dongen et al., 2006). Changes in sulphurization intensity have also been linked to shifts in the distribution of anoxia across OAE2 (Raven et al., 2018). Sulphurization intensity can be approximated by S:C molar ratios, where values greater than about 0.02 exceed the initial sulphur content of most marine photosynthetic biomass (Francois, 1987). Higher S:C ratios require highly functionalized and therefore relatively young organic precursors prior to sulphurization (Brassell, 1985). This
885 early sulphurization, prior to burial, may impact a relatively large pool of functionalized organic matter (Raven et al., 2019). Subsequently, sulphurization over thousand-year timescales can continue to impact free lipid biomarkers such as tricyclic triterpenoids and steroids (Shawar, 2021; Werne et al., 2000; Kok et al., 2000). Different sulphurization products and biogenic organic S can be distinguished through spectroscopy, especially synchrotron x-ray absorption spectroscopy (Kohnen 1989; Amrani 2004; Vairavamurthy 1998; Raven 2021b), or by using stable isotopes. Organic sulphur in biomass from oxic systems
890 generally has an isotopic composition similar to that of sulphate in the environment (Kaplan and Rittenburg, 1964; Trust and Fry, 1992), while organic S from sulphurization typically has variable but broadly more ³⁴S-depleted isotopic values (Anderson and Pratt 1995; Canfield 2001). In detail, individual organic sulphur compounds have a wide range of stable sulphur isotope ($\delta^{34}\text{S}$) values (up to tens of ‰) and may preserve additional layers of information about the lipid pool during early diagenesis (Amrani et al., 2005; Raven et al., 2015; Rosenberg et al., 2017; Shawar et al., 2020). Sulphurization indicators can thus
895 complement multi-proxy reconstructions of redox conditions at the same time that they provide insights into taphonomic bias and organic matter burial.

6.3 Biomarkers of microbial processes associated with oxygen deficiency

Biomarkers provide chemotaxonomic and metabolic information of source organisms inhabiting water columns and/or
900 sediments impacted by a wide range of redox conditions and electron acceptors. This is particularly important for biomarkers from organisms associated with the cycling of nitrogen (e.g., anammox, ammonia oxidation, nitrogen fixation), sulphur (sulphate reduction, sulphide oxidation), and carbon (methanogenesis and methanotrophy), as well as from those organisms feeding on them. Thus, biomarkers provide qualitative redox information that ranges from fully oxygenated conditions to oxygen-deficient, anoxic non-sulphidic, and anoxic sulphidic/euxinic conditions (both within and below the photic zone). We refer to Tab. S1 for a tabularized summary of biomarkers described in the following sections (6.3.1 to 6.3.2).

905 6.3.1 Biomarkers for Nitrogen Cycling in ODZs

Oxygen-deficient environments are hotspots for microbial processes involved in the removal of fixed nitrogen, such as denitrification and other dissimilatory nitrogen transformations, anaerobic ammonium oxidation (anammox) coupled to nitrite

reduction, and nitrite-dependent anaerobic methane oxidation (n-damo) (Lam and Kuypers, 2011; Thamdrup, 2012). Accordingly, the presence of lipids synthesized by bacteria with these anaerobic metabolisms can be used to infer hypoxic or anoxic conditions in the past. For detailed reviews on the use of biomarkers for nitrogen cycling, we recommend the recent work by Rush and Sinninghe Damsté (2017) and Kusch and Rush (2022).

6.3.1.1 Anammox

Anammox, the anaerobic oxidation of NH_4^+ to N_2 using NO_2^- , is the only nitrogen loss process for which several specific biomarkers have been identified. Ladderanes are highly unusual lipids with moieties consisting of cyclobutane rings (Sinninghe Damsté et al., 2002a). They make up the cell membrane of the anammoxosome, the specialized organelle in which the anammox process takes place, and substantially reduce proton permeability (Moss et al., 2018). A suite of ladderane fatty acids and their short chain oxic degradation products are available to trace anammox. However, ladderanes do not preserve well (Rush et al., 2011) and, thus far, the oldest sedimentary record containing ladderanes extends only 140 kyr (Jaeschke et al., 2009). More recently, a unique bacteriohopanepolyol (BHP) biomarker for marine anammox ‘*Candidatus Scalindua profunda*’ was identified (Schwartz-Narbonne et al., 2020): a bacteriohopanetetrol (BHT) isomer with unknown stereochemistry, BHT-x (Rush et al., 2014; Schwartz-Narbonne et al., 2020), has strongly depleted $\delta^{13}\text{C}$ values in sediments consistent with fractionation associated with the reductive acetyl-CoA pathway used by anammox (Hemingway et al., 2018; Lengger et al., 2019), and has a distinct niche in the nitrite maximum of stratified water column settings (e.g., Kusch et al., 2022; Matys et al., 2017). In comparison to ladderanes, BHPs preserve well and BHT has been detected in samples as old as ca. 50–55 Myr (van Dongen et al., 2006; Talbot et al., 2016). In older rocks, BHPs may survive as hydrocarbons after the loss of hydroxyl functionalities due to reducing processes, or after decarboxylation reactions that also shorten the hopanoid side chain. The diagnostic value of these resulting hopenes and hopanes is reduced in comparison to the original lipid. So far, BHT-x has been successfully used to trace OMZ conditions in (non-dated) sediment records in the Benguela Upwelling system (van Kemenade et al., 2022), during the last Glacial in the Gulf of Alaska (Zindorf et al., 2020), and during Pliocene/Quaternary sapropel formation in the Mediterranean (Rush et al., 2019; Elling et al., 2021). For paleoceanographic purposes, sedimentary ladderanes and BHT-x should primarily capture the water column anammox signal (nitrite maximum), which can be orders of magnitudes higher than the benthic background signal (Rush et al., 2012).

6.3.1.2 Nitrite-dependent anaerobic methane oxidation (n-damo)

More recently, bacteria performing anaerobic methanotrophy have been detected. ‘*Ca. Methylomirabilis oxyfera*’ is an exceptional methanotroph that produces its own oxygen via the production of NO by NO_2^- reduction (Ettwig et al., 2010), also known as n-damo. Biomarkers of n-damo include bacteriohopanehexol, 3Me-bacteriohopanehexol, and 3Me-bacteriohopanepentol (Kool et al., 2014) as well as the novel demethylated hopanoids 22,29,30-trisnorhopan-21-ol, 3Me-22,29,30-trisnorhopan-21-ol, and 3Me-22,29,30-trisnorhopan-21-one (Smit et al., 2019). Although not common,

940 bacteriohopanehexol is also produced by thermophilic *Alicyclobacillus acidoterrestris* (Řezanka et al., 2011) and the bacterial
symbiont of a marine *Petrosia* sponge (Shatz et al., 2000). Thus, the C-3 homologs of bacteriohopanehexol and
bacteriohopanepentol as well as the trisnorhopanes may be better indicators for the presence of ‘*Ca. Methyloirabilis oxyfera*’
and n-damo. Although there seem to be several n-damo biomarkers, it should be noted that the role of n-damo bacteria (NC10
945 phylum) in marine ODZs is still not well constrained (e.g., Padilla et al., 2016). However, to date the presence of the above-
mentioned biomarkers in marine sediments can likely be interpreted to indicate anoxia.

6.3.1.2 Feedback mechanisms to nitrogen loss

Removal of nitrogen in OMZ settings causes imbalances in N:P ratios that can promote/intensify aerobic processes involved
in the nitrogen cycle. For instance, in the geologic record, enhanced diazotrophy, the primary source of bioavailable nitrogen
in the ocean (Hutchins et al., 2008), has been invoked to have sustained biological productivity during times of intensified
950 ocean deoxygenation and consequent fixed nitrogen loss (e.g., Kuypers et al., 2004). Accordingly, biomarker evidence for
important feedback mechanisms to nitrogen loss (e.g., diazotrophy and nitrification), can provide context for
paleoceanographic data and shed light on past OMZ-related biogeochemical cycles.

Biomarkers for reconstructing nitrogen fixation have been long sought after. To date, there are no known biomarkers
commonly produced by cyanobacteria, or the subset of cyanobacteria that can fix nitrogen and are the major diazotrophs in
955 the ocean (e.g., Talbot et al., 2008; Saenz et al., 2012). Therefore, molecular evidence for N₂-fixation and denitrification has
been mostly based on the characteristic kinetic isotope fractionation effects (e.g., Sigman, 2009) preserved in the $\delta^{15}\text{N}$ values
of nitrogen-containing organics such as pigments and proteins (e.g., Sachs et al., 1999; Ohkouchi et al., 2006; Higgins et al.,
2010, 2012; Junium et al., 2015). For example, the consistent observation of low $\delta^{15}\text{N}$ values of chlorophyll-derived
tetrapyrroles in ancient sediments deposited under wide-spread anoxic and euxinic conditions (e.g., OAEs) and the abundance
960 of chlorophyll-derived degradation products suggest a direct link between surface water N₂-fixation and water column N-loss
processes (e.g., Junium and Arthur, 2007; Ohkouchi et al., 2006). Recent studies also suggest that $\delta^{15}\text{N}$ values of amino acids
($\delta^{15}\text{N}_{\text{AA}}$) may be useful tools to study water column nitrogen dynamics (McCarthy et al., 2013; Batista et al., 2014) since
phenylalanine $\delta^{15}\text{N}$ values show a good relationship with established $\delta^{15}\text{N}$ proxies such as bulk sediment and foraminifera-
bound N (Li et al., 2019) (see also Section 7; nitrogen isotopes). However, for a subset of diazotrophic cyanobacteria, so-called
965 heterocystous cyanobacteria, specific heterocyst glycolipids (HGs) with C5 and C6 sugar head groups have now been identified
(Bauersachs et al., 2009a,b; Bauersachs et al., 2010). HGs comprise the innermost laminated layer of the heterocysts, forming
a protective envelope for the oxygen-sensitive nitrogenase enzyme (e.g., Gambacorta et al., 1998). C5 sugar HGs are proposed
to be specific biomarkers for marine endosymbiotic heterocystous cyanobacteria while C6 sugar HGs occur in free-living
heterocystous cyanobacteria (Schouten et al., 2013b; Bale et al., 2015). Enhanced deposition of C5 and C6 HGs in the
970 Mediterranean Sea during Plio-Pleistocene sapropel events has been linked to anoxia, indicating that diazotrophy by
heterocystous cyanobacteria was an important feedback to nitrogen loss (Bale et al., 2019; Elling et al., 2021). Heterocystous
cyanobacteria occur mostly in brackish water bodies (e.g., Baltic Sea), but are rare in the open ocean (except as symbionts of

975 diatoms; Stal et al., 2009; Zehr et al., 2011). However, diazotrophy is also observed in open ocean ODZ systems that are associated with enhanced upwelling and primary production such as the Eastern Tropical Pacific (White et al., 2013; Loescher et al., 2014; Jayakumar et al., 2017). It is unknown whether HGs can also track heterocystous cyanobacteria in these environments in the past or present. Thus, tetrapyrrole $\delta^{15}\text{N}$ values may still provide the most unequivocal evidence for N_2 -fixation in the past. Since they preserve well over long timescales (the oldest tetrapyrroles date to 1.1 Ga; Gueneli et al., 2018), the nitrogen isotopic composition of these molecules or their smaller maleimide fragments (e.g., Grice et al., 1996) can be used to gauge N_2 -fixation over much of Earth's history.

980

Nitrification, the aerobic transformation of ammonia (NH_4^+) to nitrite (NO_3^-), is performed either as a two-step process by ammonia-oxidizing bacteria (AOB), ammonia-oxidizing archaea (AOA) and nitrite-oxidizing bacteria (NOB), or as a one-step process by ammonia-oxidizing bacteria (comammox). Although nitrification is considered an obligately aerobic process, AOA and NOB persist in suboxic and anoxic waters, and two novel *Nitrospina*-like lineages (NOB) have been found and implicated in nitrite oxidation in ODZs (Sun et al., 2019). Thus, for the majority of known AOA and NOB, active nitrification under low-oxygen conditions requires a source of cryptic oxygen, i.e. the presence of short-lived oxygen-bearing intermediates that typically occur below detection limit but provide important substrates (Kappler and Bryce, 2017). For AOA, internal oxygen production has been observed as a response to anoxia (Kraft et al., 2022). AOA are the dominant sources of glycerol dialkyl glycerol tetraethers (GDGTs) to marine sediments and produce the specific biomarker crenarchaeol (Sinninghe Damsté et al., 985 2002b), methoxy archaeol (Elling et al., 2014, 2017), as well as specific quinones (MK_{6:0} & MK_{6:1}; Elling et al., 2016). Crenarchaeol has been shown to track Thaumarchaeota in the suboxic zones of modern (e.g., Wakeham et al., 2007; Sollai et al., 2015; Kusch et al., 2021) and paleo systems, particularly during times of ocean deoxygenation, such as during Mediterranean sapropel deposition (Menzel et al., 2006; Polik et al., 2018). As such, increased deposition of crenarchaeol relative to organic matter may be useful for tracing intensified suboxic-anoxic nitrogen cycling (Rush et al., 2017; Elling et al., 995 al., 2020). The presence of crenarchaeol alone can, however, not be used to infer suboxic conditions. AOB, NOB, and comammox do not seem to synthesize chemotaxonomically specific lipids. Known lipids of AOB include generic BHPs and unsaturated fatty acids (Sakata et al., 2008) and some hopanoids produced by NOB have not previously been found in other bacteria (Rush & Sinninghe Damsté, 2017; Elling et al., 2022).

1000 **6.4 Biomarkers for Sulphur Cycling in ODZs**

In addition to the abiotic sulphurization mechanisms described above, ODZs are characterized by active sulphide oxidation and sulphate reduction mediated by diverse bacteria (e.g., Callbeck et al., 2021; van Vliet, et al., 2021). These sulphur metabolisms are not only present in sulphide-rich anoxic sediments and euxinic water columns, but open ocean ODZs and particle microniches also harbour a cryptic sulphur cycle (Canfield et al., 2010; Raven et al., 2021a). Diverse biomarkers with

1005 high preservation potential have been identified for various sulphide-oxidizing bacteria (SOB) and sulphate-reducing bacteria (SRB) and allow detailed reconstructions of water column stratification in paleoceanographic studies.

6.4.1 Sulphide oxidation

Phototrophic green sulphur bacteria (GSB; Chlorobiaceae) and purple sulphur bacteria (PSB; Chromatiaceae) are the principal microbes metabolizing reduced sulphur species, such as H₂S, whilst fixing carbon through anoxygenic photosynthesis. As such
1010 they occupy anoxic environmental niches with access to light and H₂S, amongst other sulphur species (Summons and Powell, 1987). Apart from benthic microbial mats at shallow water depths, this involves euxinic photic zones of marine water columns. Characteristically, green and purple sulphur bacteria biosynthesize diaromatic carotenoids that function as accessory pigments. Isorenieratene and chlorobactene, as well as their fossilized equivalents isorenieratane and chlorobactane, are commonly used as indicators for the presence and activity of green- (chlorobactane) and brown-pigmented (isorenieratane) species of the
1015 Chlorobiaceae during sediment deposition, providing clues about the depth of the chemocline given that brown pigmented Chlorobiaceae are adapted to lower irradiance than their green-pigmented relatives (Summons and Powell, 1987; Schaeffer et al., 1997; French et al., 2015). In very shallow chemoclines, the relative abundance of anoxygenic phototrophy is typically skewed towards a higher proportion of PSB, which characteristically biosynthesize the monoaromatic carotenoid okenone that can survive in sediments as the fossil equivalent okenane (Brocks and Schaeffer, 2008). All of the saturated C₄₀ carotenoids
1020 can survive for exceedingly long time spans and have been detected in sediments up to 1.64 Ga in age (see review and updated analytical method in French et al., 2015). Once subjected to thermal breakdown during sedimentary burial, the methylation pattern of the remaining arylisoprenoids (2,3,4- vs. 2,3,6- substitution pattern) can still yield clues to the biological precursor, whereas the relative abundance of longer versus shorter aryl isoprenoid chains may allow distinguishing long-lived and persistent euxinia from short-lived and episodic photic zone euxinia (Schwark and Frimmel, 2004). Using the reverse
1025 tricarboxylic acid cycle during carbon fixation, biomass of green sulphur bacteria may also be recognized by their characteristic enrichment in ¹³C compared to that of oxygenic phototrophs, whilst their bacteriochlorophyll-c/d/e pigments can be recognized both intact, as well as after breakdown to maleimides such as 3-isobutyl-4-methylmaleimide (e.g., Grice et al., 1996; Naehler et al., 2013).

6.4.2 Sulphate reduction

1030 Sulphate reduction is a heterotrophic anaerobic bacterial pathway leading to the formation of hydrogen sulphide, which can fuel the cryptic sulphur cycle in offshore ODZs by supplying reactive sulphur species as intermediates for other redox reactions (Callbeck et al., 2021). A group of compounds commonly associated with SRB are non-isoprenoid 1-*O*-monoalkyl or 2-*O*-monoalkyl glycerol ethers (MAGEs) and 1,2-*O*-dialkyl glycerol ethers (DAGEs). They have been identified in hyperthermophilic bacteria and commonly occur in settings influenced by hydro/geothermal activity (e.g., Bradley et al., 2009)
1035 or seep systems hosting consortia of anaerobic methane oxidizing archaea (ANME) and SRB (Niemann & Elvert, 2008). Hernandez-Sanchez et al. (2014) also identified 1-*O*-MAGEs in suspended particulate matter sampled from oxygenated surface

waters and suggested a role of bacteria other than SRB in the production of these lipids. However, recent evidence of sulphate reduction in sinking marine particles (Raven et al., 2021a) can explain the observation of SRB or 1-*O*-MAGEs in oxygenated surface waters and sediments (e.g., Hernandez-Sanchez et al., 2014; Teske et al., 1996). SRB belonging to the
1040 *Desulfosarcina/Desulfococcus* group (syntrophic partners of the ANME-1 and -2 clades, except ANME-2d) and *Desulfobulbus* spp. (syntrophic partner of the ANME-3 clade) also produce characteristic alkanolic acid fingerprints with strong ¹³C-depletion, including C16:1 ω 5 (C_{16:1} Δ^{12}), cy-C17:0 ω 5,6 and C17:1 ω 6 (Niemann and Elvert, 2008). No biomarkers are known for sulphur-disproportionating bacteria, which perform reverse sulphate reduction.

6.5 Biomarkers for Carbon Cycling in ODZs

1045 Oxygen-deficient conditions in the ocean are also intimately linked to the methane cycle via both the generation (methanogenesis) and utilization (methanotrophy) of methane. Methanogenesis and anaerobic methanotrophy are performed by anaerobic archaea using sulphate, nitrate, iron, and manganese as electron acceptors (for a recent overview see Guerrero-Cruz et al., 2021). Methane is also respired by aerobic methane-oxidizing bacteria (MOB). Although these MOB are aerobes, their lipids are useful proxies in paleoceanography since MOB are typically present at oxic-anoxic transitions where both
1050 methane and oxygen are available and can thrive under oxygen-deficient conditions (Guerrero-Cruz et al., 2021). In addition, the utilization of methane is recorded by strongly ¹³C-depleted biomarker signatures irrespective of their chemotaxonomic specificity (e.g., Jahnke et al., 1999).

6.5.1 Methanogenesis

Methane in the ocean is primarily produced in anoxic marine sediments although aerobic sources also exist (Metcalf et al.,
1055 2012; Bižić et al., 2020). In sediments, methanogenesis is performed by strictly anaerobic primarily hydrogenotrophic and acetoclastic Euryarchaeota (Ferry and Lessner, 2008). Methanogenic Euryarchaeota primarily produce isoprenoid tetraethers without cyclic moieties (GDGT-0) and the isoprenoid diether archaeol (Koga et al., 1993, 1998). Ratios >2 of GDGT-0 over the thaumarchaeal isoprenoid tetraether crenarchaeol have been proposed as a proxy for methanogens in the paleo record (Blaga et al., 2009), although these ratios have to be interpreted in the context of the biomarker assemblage due to the presence
1060 of GDGT-0 in many non-methanogenic archaea (Schouten et al., 2013a; Elling et al., 2017).

Likewise, *Methanothermococcus thermolithotrophicus* has been shown to synthesize hydroxylated GDGTs (OH-GDGT) with 0-2 pentacyclic moieties (Liu et al., 2012). Although the lipids mentioned above are not exclusive to methanogens, other sources such as methanotrophic Euryarchaeota or Thaumarchaeota typically have much more diverse GDGT fingerprints (Schouten et al., 2013a; Elling et al. 2017) and also synthesize additional lipids (see below). Since methanogenesis is performed
1065 in situ, for paleoceanographic purposes it is crucial to identify in situ overprints. One approach to distinguish paleo and in situ signals is the screening for biomarkers that imply metabolic activity, such as the functional quinone analogs methanophenazines (Abken et al., 1998; Elling et al., 2016), which (to date) have only been shown to be produced by the order *Methanosarcinales*, or coenzyme F430, the cofactor of methyl coenzyme M reductase possessed by all methanogens (Kaneko

et al., 2021). It should, however, be noted that anaerobic methanotrophic archaea are also suspected to produce these
1070 biomarkers (although direct evidence is still missing).

6.5.2 Methanotrophy

Anaerobic methanotrophy with sulphate (reverse methanogenesis) is performed by ANME archaea in syntrophic consortia
with sulphate-reducing bacteria (Boetius et al., 2000). ANME biomarkers include isoprenoids such as tetramethylhexadecane
(crocetane; ANME-2), pentamethylcosane (PMI) and unsaturated PMIs, archaeol, and *sn2*-hydroxyarchaeol or *sn3*-
1075 hydroxyarchaeol (Koga et al., 1993, 1998; Elvert et al., 1999; Thiel et al., 1999; Hinrichs et al., 2000; 2003). Furthermore,
ANME ecotypes (classified as ANME-1, ANME-2, ANME-3) seem to be discernible by *sn2*-hydroxyarchaeol/archaeol ratios
and the $\delta^{13}\text{C}$ signature of archaeol, the alkanolic acid signature of the SRB partners (Blumenberg et al., 2004; Niemann &
Elvert, 2008), and specific intact polar lipid (IPL) compositions (e.g., Rossel et al., 2011), although the IPL characteristics
might be lost in the paleo record. However, the remaining core lipid GDGT signature may aid the identification of ANME in
1080 the paleo record. GDGT-2/crenarchaeol ratios exceeding the threshold of 0.2 could indicate the presence of ANME (Weijers
et al., 2011). The characteristic depletion in ^{13}C of ANME biomarkers can be traced in the paleo record.

Methane produced under anoxic conditions can also be utilized by aerobic MOB, and their presence in paleoceanographic
records indicates a methane-rich environment. Aerobic MOB synthesize a range of characteristic lipids, including a suite of
amino-functionalized BHPs and their respective unsaturated and C-3 methylated homologs. Aminopentol is considered a
1085 characteristic biomarker for Type I gammaproteobacterial MOB and aminotetrol is commonly produced by Type II
alphaproteobacterial MOB (e.g., Rohmer et al., 1984; Jahnke et al., 1999; Talbot et al., 2001). They also produce structurally
similar methylcarbamate (MC) BHPs (MC-pentol and MC-tetrol), which seem to be much more common in methane-
influenced marine environments that often lack aminopentol (Rush et al., 2016). It should be noted that minor amounts of
aminopentol and aminotetrol are also produced by SRB of the *Desulfovibrio* genus (Blumenberg et al., 2006; 2012), NOB
1090 (Elling et al., 2022), and several terrestrial thermophilic bacterial species (Kolouchová et al., 2021). Likewise, small amounts
of MC-triol have recently been identified in cultures of *Nitrobacter vulgaris* and marine *Nitrococcus mobilis* (Elling et al.,
2022). C-3 methylation of hopanoids alone can no longer unequivocally be linked to AOM unless confirmed by depleted $\delta^{13}\text{C}$
values. The gene for C-3 methylation is not present in all methanotrophs but present in various non-methanotrophic bacteria
(Welander and Summons, 2012), C-3 methylated BHPs accumulate in the euxinic Black Sea water column (Kusch et al.,
1095 2022), and other known sources include the phototrophic purple non-sulphur bacterium *Rhodospira globiformis* (Mayer et al.,
2021). The presence of MOB may, however, also be confirmed by other biomarkers such as alkanolic acids and quinones. Type
I MOB produce methylene-ubiquinone $\text{MQ}_{8:7}$ (Nowicka & Kruk, 2010), which has been observed in the suboxic and anoxic
zones of the Black Sea (Becker et al., 2018), and *Methylococcaceae* synthesize $\text{C}_{16:1}\Delta^{8c}$ (C16:1 ω 8c) and $\text{C}_{16:1}\Delta^{12t}$ (C16:1 ω 5t)
alkanoic acids (e.g., Bodelier et al., 2009). Type II MOB of the *Methylocystaceae* and *Beijerinckiaceae* are characterized by
1100 $\text{C}_{18:1}\Delta^{10c}$ (C18:1 ω 8c) (e.g., Bodelier et al., 2009).

6.6 Non-specific/ orphan biomarkers from oxygen-deficient depositional settings

6.6.1 Redox controlled processes

Independent of their specific biological source, various lipids will undergo diagenetic molecular modifications that are principally controlled by environmental redox chemistry. One of the first established indicators for oxic versus anoxic conditions was the ratio of pristane (Pr) over phytane (Ph) — C₁₉ and C₂₀ isoprenoid hydrocarbons that derive from the phytol sidechain of chlorophyll by oxidative decarboxylation or by reduction, respectively (Rontani et al., 2003). Strongly elevated values (e.g., >4) are observed under oxic conditions whereas values <<1 are found under anoxic conditions, yet the use of the Pr/Ph index is complicated by alternative (non-chlorophyll-derived) sources of both Pr and Ph (e.g., Goossens et al., 1984), as well as by questions of organic matter transport pathways and oxygen exposure (e.g., Ten Haven et al., 1987). A hopanoid-based indicator involving the relative abundance of long chain C₃₁-C₃₅ homohopanes over C₃₀ hopanes (known as the homohopane index) follows a similar rationale and assumes that longer side chains are preferentially preserved in sediments under reducing conditions (Peters et al., 2005). Similarly, phototroph-derived chlorophylls are commonly used as indicators of primary productivity (Carpenter et al., 1986; Harris et al., 1996). However, certain degradation products such as pyropheophytin and steryl chlorin esters are only formed under anoxic conditions (Szymczak-Żyła et al., 2008), and the proportional abundance of these chlorophyll degradation products has been proposed as proxy for bottom water anoxia (e.g., Szymczak-Żyła et al., 2017).

6.6.2 Orphan biomarkers

A range of lipids have been shown to be associated with OMZ settings for which the source organisms are unknown. Although these lipids cannot be linked to specific taxa or metabolisms, these ‘orphan biomarkers’ can still be useful indicators for paleoceanographic purposes. One common orphan biomarker in sediments from anoxic settings is the isoprenoid 19,23,27,31-octamethyldotriacontane (lycopane) for which methanogenic archaeal (Brassell et al., 1981) and phototrophic (Wakeham et al., 1993) origins have been suggested. For paleoceanographic purposes, the lycopane/C₃₁ *n*-alkane ratio has been suggested as a proxy for paleoacidity (Sinninghe Damsté et al., 2003), although it must be applied with caution in areas where plant wax input is large. Derivatives of branched GDGTs such as overly branched GDGTs (OB-GDGTs), are produced in specific patterns in anoxic marine zones (Liu et al., 2014; Xie et al., 2014) and have been interpreted as biomarkers for OMZ presence in the paleo record (Connock et al., 2022). Yet, the sources of these lipids, oxygen thresholds for their production, and potential production in sediments remain unstudied.

6.7 Analyses and resources required

For biomarker analyses, sediments are extracted with organic solvents to recover the total lipid extract (TLE, or bitumen), which is further processed to separate compound classes that are subsequently analysed using mass spectrometry techniques.

For extraction, pure organic solvents or mixtures that contain water and/or buffers are used with ultrasonication, Soxhlet, or automated pressurized systems such as ASE and microwave. Extraction is typically followed by wet-chemical processing to obtain polarity fractions and it may be necessary to remove elemental sulphur to avoid interference during chromatography, or release S-bound organics that would otherwise evade detection (Kohnen et al., 1991).

Small non-polar compounds can be analysed using gas chromatography-mass spectrometry (GC-MS), whereas larger and/or more polar compounds require the use of liquid chromatography-mass spectrometry (LC-MS) techniques, unless they are derivatized and/or cleaved of polar functional groups. Isotope ratio mass spectrometry (GC-IRMS) systems are used to obtain compound-specific stable isotope values ($\delta^{15}\text{N}$, $\delta^{13}\text{C}$, $\delta^2\text{H}$), or compounds are isolated using LC and subsequently analysed using spooling wire micro-combustion IRMS (Pearson et al., 2016) or nano-elemental analyser (EA)-IRMS analysis (e.g., Kusch et al., 2010; Ogawa et al., 2010).

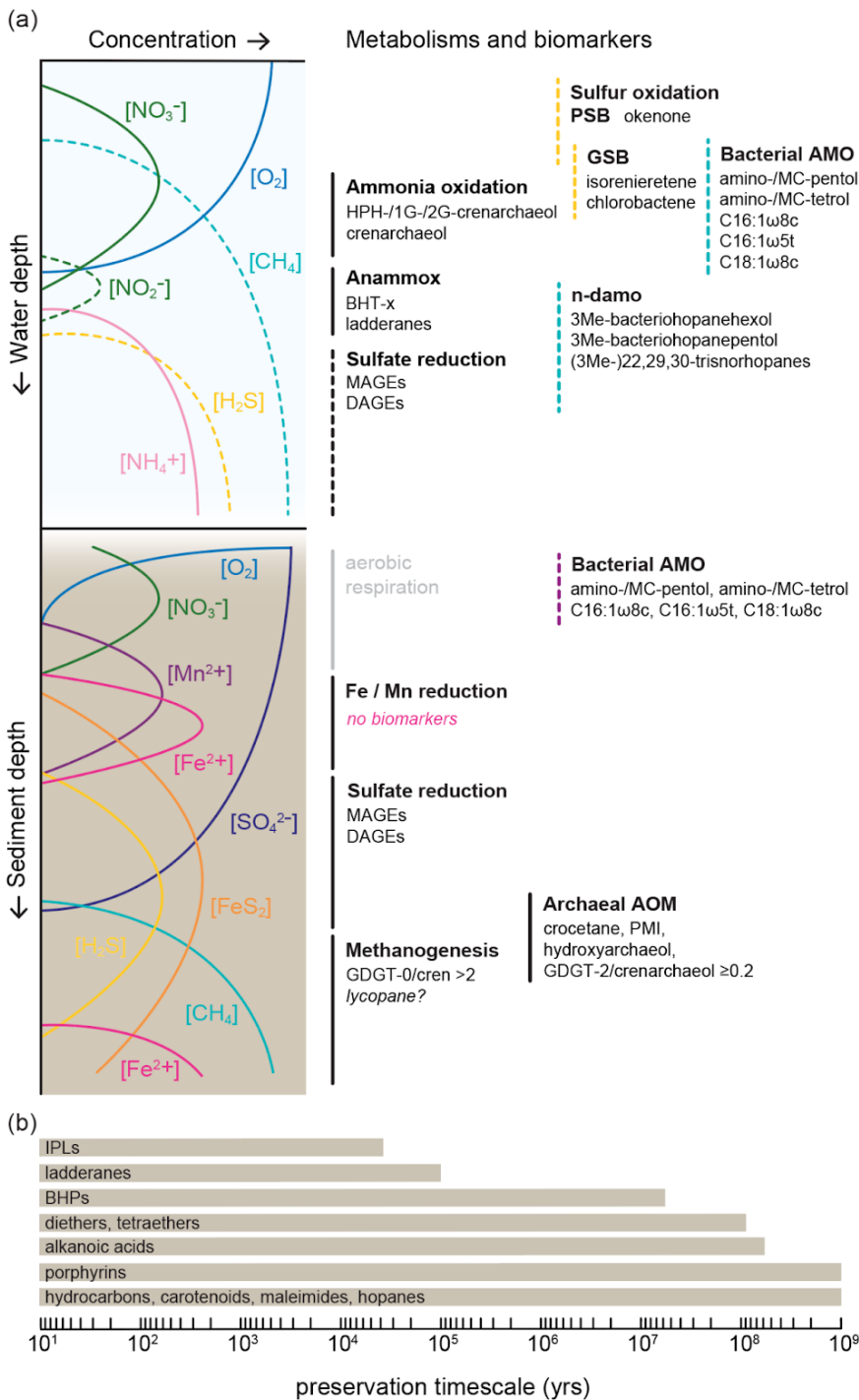
6.8 Major analytical advancements

Major advancements in the field of organic geochemistry have been made since the introduction of high-resolution accurate mass-mass spectrometry (HRAM-MS) techniques, including quadrupole time-of-flight (Q-ToF), Orbitrap, and Fourier transform ion cyclotron resonance (FT-ICR). Paired with ultra-high performance LC systems, improved column materials and chemistries (e.g., core shell, HILIC), Q-ToF and Orbitrap platforms have opened up a new window into lipidomics of environmental samples (e.g., Hopmans et al., 2021; Wörmer et al., 2013). Orbitrap technology specifically offers substantial further analytical potential that includes compound-specific isotope analysis and position-specific isotope analysis (Eiler et al., 2017). Recent analytical advancements have also been made using scanning techniques. Matrix-assisted laser desorption/ionization (MALDI)-FT-ICR-MS allows mapping of spatial biomarker abundances in situ, which facilitates obtaining ultra high-resolution records from sediment cores (e.g., Alfken et al., 2021). For a comprehensive overview of high-resolution analytical organic geochemical methods, we refer to Steen et al. (2020).

6.9 Future prospects

Biomarkers are excellent tools in paleoceanography due to their preservation potential in sediment and their biological and environmental associations. Open ocean ODZs in general are high productivity systems that foster preservation of high amounts of organic matter. Moreover, the high preservation potential of lipids leads not only to high abundances of biomarkers in the paleo record, but also the preservation of a diverse pool of compounds. This structural diversity allows use of comprehensive biomarker assemblage approaches to reconstruct the water column structure (e.g., Connock et al., 2022; Dummann et al., 2021). Biomarkers also preserve well under conditions that lead to the absence of calcareous microfossils or trace metals in sediments, such as carbonate undersaturation or oxygen exposure. Nonetheless, challenges as well as new frontiers remain for the biomarker community. Most profoundly, biomarker proxies have yet to allow the quantitative reconstruction of oxygen concentrations in the past. Indirectly, the half-maximal inhibitory concentration (IC_{50}) of oxygen in specific organisms provides a means to infer maximum oxygen concentrations. For example, anammox bacteria have an upper

oxygen limit of $\sim 20 \mu\text{mol kg}^{-1}$ (Kalvelage et al., 2011) and a recent study suggests that BHT-x ratios (the normalized abundance of BHT-x/[BHT+BHT-x]) of ≥ 0.2 indicate oxygen concentrations $< 50 \mu\text{mol kg}^{-1}$ (van Kemenade et al., 2022). Recently, Kim and Zhang (2023) demonstrated how the methane index can be used to calculate sedimentary methane fluxes. Analogous proxies to reconstruct oxygen are lacking, as a range of lipids are produced in the water column as well as in sediments (e.g., anammox, sulphate reduction), and different biomarkers may sometimes provide divergent paleoenvironmental information (e.g., in settings receiving input from land or affected by lateral input). In addition to making the available biomarker tools more quantitative, efforts of the biomarker community are also focused on exploiting the potential afforded by technological advances to expand the utility of biomarker applications in paleoceanography. New isotope tools, such as compound-specific ^{15}N analysis of amino acids, as well as the discovery of new biomarkers through lipidomics approaches in combination with (meta)genomics offer large potential to trace oxygen limitation in more detail. These new tools may also aid the identification of the sources of orphan biomarkers that accumulate under anoxic conditions. Identifying the source organisms will improve our understanding of the metabolism or ecological niche recorded by these lipids and, ultimately, the paleoenvironmental conclusions drawn from them.



1180 **Figure 6 : A) Idealized water column and sediment redox zonation and associated metabolisms and their biomarker signatures discussed in the text. Dashed lines indicate species and metabolisms that may be present in specific settings B) Biomarker**

preservation timescale. Solid lines indicate timescales on which distinct compound classes are preserved. Note that observations are less frequent where the scale extends to the oldest known record.

7 Nitrogen isotopes

7.1 Introduction

1185 Nitrogen (N) has two stable isotopes, ^{14}N and ^{15}N . The lighter isotope, ^{14}N , comprises $99.63 \pm 0.02\%$ of the N found on Earth. Natural processes in the ocean discriminate between the two isotopes leading to subtle changes in the $^{15}\text{N}/^{14}\text{N}$ ratio of different nitrogen compounds. This is reported in delta notation, with atmospheric N_2 as the reference material:

$$\delta^{15}\text{N} (\% \text{ vs. Air}) = \left(\frac{(^{15}\text{N}/^{14}\text{N})_{\text{Sample}}}{(^{15}\text{N}/^{14}\text{N})_{\text{Air}}} - 1 \right) \cdot 1000$$

1190

The most widely used technique for N isotopic analysis relies on online combustion of samples to N_2 using an elemental analyzer (EA) coupled with isotope ratio mass spectrometry (IRMS). This method requires a typical sample size of 1–2 mmol N per analysis, with analytical precision near 0.1% (1 standard deviation) and has mostly been applied to bulk sedimentary N (Robinson et al., 2012; Tesdal et al., 2013). Ongoing innovations, for example through cryo-focusing of the resulting N_2 sample gas, allows for much reduced sample sizes (~25–40 nmol N) (Polissar et al., 2009). Specific organic compounds, amino acids and other polar compounds, typically require a derivatization process for gas chromatograph-based analysis. Amino acids can also be isolated using liquid chromatography followed by micro-combustion to N_2 , which is commonly applied prior to the IRMS analysis of the resulting N_2 (Ohkouchi et al., 2017; Ishikawa et al., 2022).

1195

In addition to N_2 , N_2O can be analysed by IRMS for N isotopic analysis. As N_2O has a much lower atmospheric background relative to N_2 , the sample size requirement can be further reduced when N_2O is the final analyte. Methods have been developed for the conversion of nitrate (NO_3^-) and nitrite (NO_2^-) to N_2O , preceded by chemical procedures to convert different N forms to $\text{NO}_3^-/\text{NO}_2^-$ (Sigman et al., 2001; McIlvin and Altabet, 2005; Weigand et al., 2016). The N_2O -based method, using denitrifying bacteria, has a typical sample size requirement of 2–5 nmol N, with analytical precision better than 0.2‰ (Weigand et al., 2016). This technique has expanded the range of sample types accessible to isotopic analyses and has successfully been applied to a range of fossil-bound N, including diatoms, foraminifera, corals, among others.

1200

1205

Nitrogen cycling is closely linked to the dissolved oxygen content in the ocean. In ODZs, where water column oxygen concentrations are lower than roughly $5 \mu\text{mol kg}^{-1}$, the bacterial reduction of NO_3^- to N_2 , also known as denitrification, removes NO_3^- from the ocean (Sigman et al., 2009b). Denitrification strongly discriminates against the heavier isotope, progressively increasing the $\delta^{15}\text{N}$ of the remaining NO_3^- pool. Culture and field studies show an isotope effect between 15‰ and 25‰ for denitrification (Sigman and Fripiat, 2019). Recent work suggests that anaerobic ammonium oxidation (anammox), where NO_2^- is used to oxidize ammonium (NH_4^+) to N_2 , could also lead to an increase in the N isotope composition of NO_3^- ($\delta^{15}\text{N}_{\text{nitrate}}$)

1210

from suboxic environments, where extensive NO_2^- oxidation co-occurs with anammox (Brunner et al., 2013; Casciotti, 2016). Multiple factors influencing the net-effect of anammox on $\delta^{15}\text{N}$ are still under investigation (Kobayashi et al., 2019). However, since denitrification and anammox typically coexist in suboxic environments, isotope effects estimated from previous field studies should include both processes. For the purpose of this review, we will only refer to denitrification, but note that denitrification likely coexists with anammox. Because of the low-oxygen threshold for denitrification and anammox, the two processes only occur in ODZs, which represent the most oxygen-depleted areas within the broader low-oxygen zones (OMZs). In contrast to water column denitrification, sedimentary denitrification leads to little increase in the $\delta^{15}\text{N}_{\text{nitrate}}$ in the overlying water column, because the isotopic discrimination is minimized by nearly complete consumption of NO_3^- at the site of denitrification within sediment pore waters, leading to a small overall isotope effect (less than 3‰) (Sigman and Fripiat, 2019). In highly productive ocean margin environments such as subarctic and Arctic shelves, sedimentary denitrification has been reported to have a somewhat greater effect (up to 8‰) (Granger et al., 2004), albeit the effect on water column NO_3^- remains small.

In summary, denitrification/anammox leaves a strong imprint on the isotopic composition of the residual NO_3^- in the water column of ODZs (Cline and Kaplan, 1975; Liu and Kaplan, 1989). In those regions, isotopically enriched NO_3^- can be upwelled and taken up by primary producers. The organic N produced in the surface ocean is exported, part of which is remineralized below the euphotic zone, spreading the high $\delta^{15}\text{N}$ signal of denitrification/anammox further away from the ODZs and suboxic environments through lateral transport (Sigman et al., 2009a, b). The organic N that is not respired can carry the resulting isotopic enrichment into the underlying sediment and, if preserved well during sinking and burial, can be used as a recorder for changes in $\delta^{15}\text{N}_{\text{nitrate}}$ and thus changes in the extent of ODZs in the past (Altabet et al., 1995; Ganeshram et al., 1995).

The $\delta^{15}\text{N}$ of sedimentary archives is a semi-quantitative proxy for oxygen content in the water column. Several challenges must be overcome to quantitatively calibrate the proxy. This will require understanding of (i) uncertainties in the denitrification/anammox isotope effect, (ii) controls on denitrification rates, and (iii) influences of other processes such as NO_3^- consumption and N_2 fixation on $\delta^{15}\text{N}_{\text{nitrate}}$. First, the current estimate of the isotope effect associated with denitrification/anammox has a large range. Earlier field-based estimates for the isotope effect often led to overestimation by comparing NO_3^- from dysoxic environments with deep ocean NO_3^- (Marconi et al., 2017). This can be improved with new analyses with the assistance of modelling and culture studies. Second, controls on the overall rate of denitrification in dysoxic environments are not fully constrained, although it is most likely tied to organic carbon supply (Ward et al., 2008). Field and modelling studies are needed to understand the relationship between the rate of denitrification/anammox, the size of the ODZs, and the oxygen content in the OMZ. Third, other biological processes occurring in the upper water column, especially NO_3^- consumption and N_2 fixation, can affect $\delta^{15}\text{N}_{\text{nitrate}}$ when it is upwelled from dysoxic waters to the surface ocean (e.g., Farrell et al., 1995). The three major modern OMZs in the Eastern Tropical North and South Pacific, and the Arabian Sea are all currently characterized by strong upwelling, high productivity, and in many cases, incomplete NO_3^- utilization in the surface

ocean. Because phytoplankton preferentially assimilate ^{14}N relative to ^{15}N , incomplete utilization of surface NO_3^- would elevate surface $\delta^{15}\text{N}_{\text{nitrate}}$ independent of changes associated with denitrification (e.g., Studer et al., 2021). In addition, upwelled waters from dysoxic environments have lower N:P ratios due to N loss from denitrification. This may encourage biological N_2 fixation in the surface ocean, which brings in newly fixed N with lower $\delta^{15}\text{N}$ values (-1 to 1‰) (Sigman et al., 2009; Ryabenko, 2013). These processes could modify the $\delta^{15}\text{N}$ of nitrate upwelled from dysoxic waters, especially in regions above and downstream of ODZ cores (e.g., Knapp et al., 2016; Wang et al., 2019). Careful selection of paleoceanographic study sites and modelling studies constrained by analyses of modern $\delta^{15}\text{N}_{\text{nitrate}}$ from dysoxic environments are needed to separate influences from NO_3^- consumption and N_2 fixation. Finally, various processes can influence the incorporation of the $\delta^{15}\text{N}$ signal into different organic N pools in the surface ocean and its preservation during sinking and burial. These processes are specific for each N archive and will be discussed in the following sections.

7.2 Bulk sedimentary N isotopes

There is generally a good correlation between the upper ocean $\delta^{15}\text{N}_{\text{nitrate}}$, sinking particulate $\delta^{15}\text{N}$, and surface sediment $\delta^{15}\text{N}$ ($\delta^{15}\text{N}_{\text{bulk}}$) in or near ODZs (Tesdal et al., 2013). As a result, $\delta^{15}\text{N}_{\text{bulk}}$ in marine sediments at or near an ODZ has been used to reconstruct changes in past water column denitrification and oxygen content, with most applications during the recent glacial/interglacial cycles (e.g., Altabet et al., 1995; Ganeshram et al., 1995; Galbraith et al., 2008; Galbraith, et al., 2013). Interpretations of $\delta^{15}\text{N}_{\text{bulk}}$ records rely on the assumption that the total N preserved in the sediments represent the total N generated and exported out of the surface ocean. This assumption has been challenged in two main aspects (Robinson et al., 2012 and references therein). First, it has been widely observed that $\delta^{15}\text{N}_{\text{bulk}}$ is modified during sinking and incorporation into marine sediments. Sinking particles collected in the water column often show decreasing $\delta^{15}\text{N}$ with water depth (Altabet et al., 1991), which may be due to disaggregation of large particles into smaller particles, and thus infers a preferential loss of isotopically heavy N forms. Upon burial, microbial degradation processes may increase $\delta^{15}\text{N}_{\text{bulk}}$ in surface sediments with respect to sinking particles (by 2-5‰) (Altabet and Francois, 1994). Diagenetic effects on $\delta^{15}\text{N}_{\text{bulk}}$ have been considered small in ODZs, because of low-oxygen content and high sedimentation rates, but this requires further validation. Second, $\delta^{15}\text{N}_{\text{bulk}}$ integrates the $\delta^{15}\text{N}$ signal of different N compounds in marine/terrestrial organic matter and clay-bound inorganic nitrogen. As such, it can be biased by the contribution of organic and inorganic N derived from terrestrial or distal marine (e.g., shelf) sources (Schubert and Calvert, 2001; Meckler et al., 2011). Thus, $\delta^{15}\text{N}_{\text{bulk}}$ is often used in combination with the total N content, carbon (C) to N ratio, and organic carbon isotope composition ($\delta^{13}\text{C}_{\text{org}}$) to quantify different endmember contributions using a simple mixing model. However, uncertainties using these calculations can be significant. Other efforts have been made to measure the $\delta^{15}\text{N}$ of total sedimentary N and clay-bound inorganic N separately to calculate the $\delta^{15}\text{N}$ value of the organic N ($\delta^{15}\text{N}_{\text{org}}$) (e.g., Schubert and Calvert, 2001). Despite these challenges in applying and interpreting $\delta^{15}\text{N}_{\text{bulk}}$, it remains one of the most used $\delta^{15}\text{N}$ archives in ODZs, especially in sediment cores with lower carbonate content. It can be analysed relatively quickly and easily, and at a lower cost compared to other $\delta^{15}\text{N}$ archives.

7.3 Foraminiferal calcite-bound N isotopes

1280 N isotopes in planktic foraminifera (FB- $\delta^{15}\text{N}$) have emerged as a novel approach to reconstruct past ocean oxygenation (Ren
et al., 2009; Kast et al., 2019; Studer et al., 2021; Auderset et al., 2022; Wang et al., 2022). When Rotaliid foraminifera build
their chambers, they first produce an organic layer, upon which the calcite is precipitated (Branson et al., 2016). These organic
sheets are mainly composed of proteins and polysaccharides, which are encased within the shells after calcification (Hemleben
et al. 1989; Paoloni et al., 2023). Thus, foraminiferal-bound organic matter is protected by the calcite shells and less prone to
1285 diagenesis than bulk sediments. The amino-acid composition of the foraminiferal-bound organics of modern foraminifera
appears to be very similar to that of fossil foraminifera from millions of years ago (King and Hare, 1972; Kast et al., 2019),
suggesting there is little breakdown of more labile amino acids. Laboratory experiments have also shown that neither the N
content nor its $\delta^{15}\text{N}$ vary with oxidative degradation, fossil dissolution, and thermal alteration, confirming the robustness of
FB- $\delta^{15}\text{N}$ with respect to diagenesis (Martínez-García et al., 2022).

1290 Planktic foraminifera incorporate N primarily by feeding on primary producers and zooplankton (Hemleben et al., 1989).
Assimilation of NO_3^- and NH_4^+ from the environment by photosynthesizing symbionts hosted in foraminifera could occur,
but this is considered to be negligible in much of the oligotrophic oceans where the concentrations of both dissolved inorganic
nitrogen (DIN) forms are low (Ren et al., 2012a, b). However, the symbionts could contribute to the internal N cycle by
assimilating the recycled NH_4^+ excreted by the foraminiferal host. This process may reduce the overall ammonium leakage
1295 and lower the expected trophic enrichment associated with it (Ren et al., 2012a, b). These processes propagate the $\delta^{15}\text{N}_{\text{nitrate}}$
signal through the food web into the biomass of foraminifera. It has been shown that modern planktic FB- $\delta^{15}\text{N}$ provide a robust
record of $\delta^{15}\text{N}_{\text{nitrate}}$ in thermocline waters (e.g., Ren et al., 2009, 2012a), which allows use of foraminifera from ODZ-influenced
regions for the reconstruction of past ocean suboxia (e.g., Kast et al., 2019; Studer et al., 2021; Auderset et al., 2022; Wang et
al., 2022).

1300 7.4 Other potential archives for N isotopes in dysoxic environments

Diatom-bound $\delta^{15}\text{N}$ ($\delta^{15}\text{N}_{\text{db}}$) is a potential, yet unexplored, proxy for past ocean oxygenation. Diatoms are siliceous
phytoplankton that assimilate NO_3^- as their main N source with an isotopic offset of roughly 5‰ (Waser et al., 1998). During
biomineralization, a fraction of that biomass is incorporated into their silica shell, termed frustule, which is thought to protect
the organic matter from bacterial degradation and diagenetic alteration during sinking and burial in the water column and the
1305 sediment (Sigman et al., 1999). While the exact controls on the isotopic fractionation between diatom biomass N and frustule-
bound N are not yet fully explored, $\delta^{15}\text{N}_{\text{db}}$ has been shown to correlate with the $\delta^{15}\text{N}$ of the NO_3^- source to the diatoms (Horn
et al., 2011; Jones et al., 2022). Since diatoms thrive in areas of high nutrient supply, most paleoceanographic applications of
the $\delta^{15}\text{N}_{\text{db}}$ proxy have so far focused on the Southern Ocean and the Subarctic/Arctic oceans (Robinson and Sigman, 2008;
Studer et al., 2012, 2015). While diatom opal also accumulates in the EEP upwelling region, diatoms are difficult to separate
1310 from radiolarians in those sediments, which can bias the $\delta^{15}\text{N}_{\text{db}}$ signal (Studer et al., 2013; Robinson et al., 2015). Furthermore,

incomplete NO_3^- consumption in EEP surface waters complicates the interpretation of $\delta^{15}\text{N}_{\text{db}}$ as an oxygen proxy, as it is influenced by both changes in denitrification and NO_3^- assimilation. As such, $\delta^{15}\text{N}_{\text{db}}$ has the potential to record past ocean oxygenation only in regions of complete surface NO_3^- consumption. Often, these oligotrophic environments are not hot-spots for diatom accumulation on the seafloor. Nonetheless, a recent global compilation of opal flux records indicates that sedimentary opal concentrations reach >10% in the northeastern Atlantic and equatorial Indian Ocean (Hayes et al., 2021). Those areas could be potential targets for future studies investigating past ocean oxygenation using diatom-bound N isotopes. Most deep-water marine sediment records do not have the temporal resolution to capture the seasonal, annual or decadal climate variability required for direct comparison with historical observations. In contrast, reef-building, scleractinian corals are unique environmental archives that have been used extensively to reconstruct climate variability during past centuries at high resolution (Wang et al., 2016). Typical growth rates in most coral species used in paleoclimatic reconstructions are in the range of ~1–2 cm per year, allowing monthly sampling resolution in most cases. Methods have been developed to analyse the $\delta^{15}\text{N}$ of coral skeleton-bound organic matter (CS- $\delta^{15}\text{N}$) requiring as little as 5 mg of coral carbonate (Wang et al., 2015). Modern ground-truthing has demonstrated that CS- $\delta^{15}\text{N}$ follows that of the NO_3^- assimilated across a wide range of isotopic compositions and environmental settings (Wang et al., 2014, 2016). As a result, corals living close to the major ODZs are ideal candidates to study past changes in water column denitrification and ocean oxygenation at high temporal resolution. For example, a monthly-resolved CS- $\delta^{15}\text{N}$ record from the Oman margin shows values as high as 10-11‰, apparently recording the ODZs-sourced NO_3^- signal in the Arabian Sea (Wang et al., 2016). Despite their slower growth rates, deep-sea corals (both scleractinian and proteinaceous) can also be used to investigate the marine N cycle and ocean deoxygenation in the past (McMahon et al., 2015; Sherwood et al., 2014; Wang et al., 2014).

1330 **7.5 Case study: N-isotopes in the Eastern Tropical Pacific**

An increase in overall denitrification rate may be expected to result from an increase in anoxic water volume, as a result of global warming and decline in the whole ocean oxygen concentration. Sedimentary $\delta^{15}\text{N}$ records could help constrain the various factors governing changes in water column denitrification rates and the oxygen content in the ocean. Below we discuss a nitrogen isotope case study, focusing on the dynamics of the Eastern Tropical Pacific ODZ across different time intervals and climatic backgrounds.

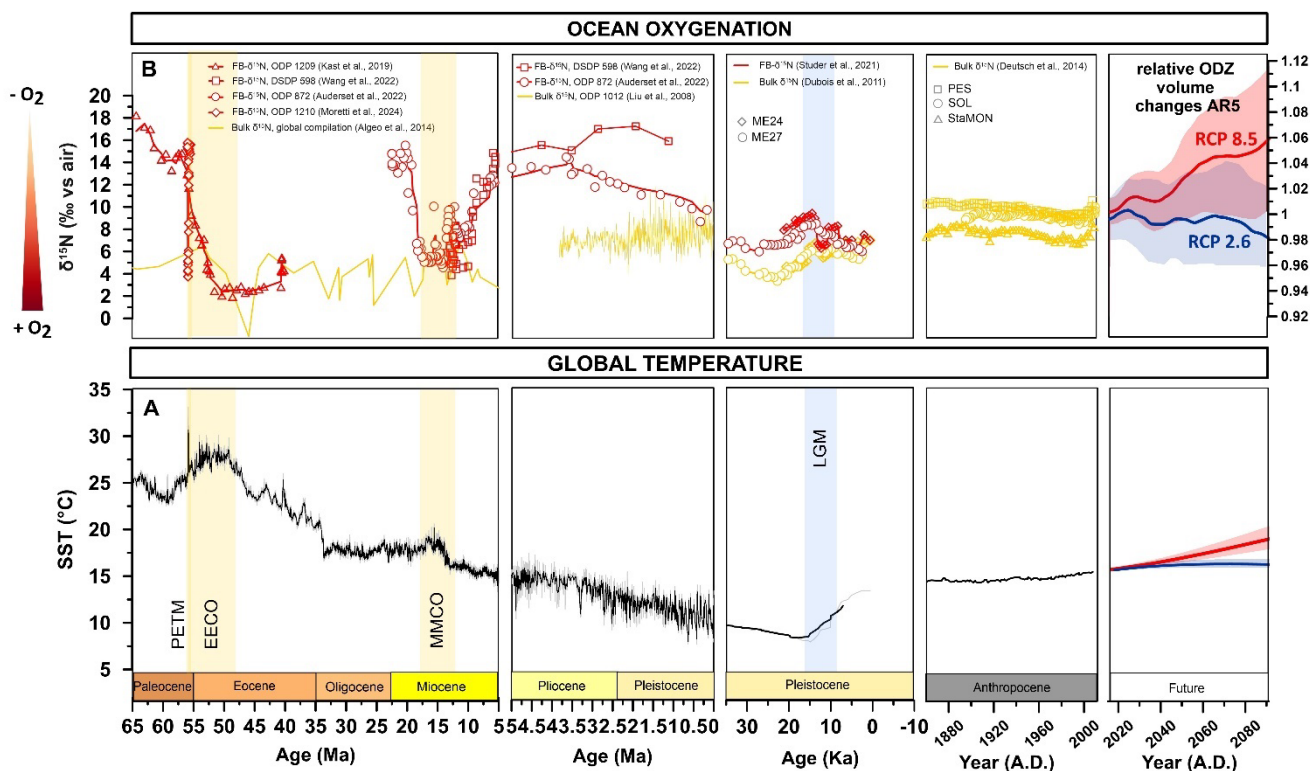
1335 While previous Cenozoic records using $\delta^{15}\text{N}_{\text{bulk}}$ show nearly no changes (Algeo et al., 2014), Auderset et al. (2022) and Kast et al. (2019) found a decline in FB- $\delta^{15}\text{N}$ during prolonged warm periods indicating a reduction in water column denitrification and better ventilation of the Pacific ODZs (Fig. 7). Two possible mechanisms are proposed to explain the FB- $\delta^{15}\text{N}$ trend: (i) a reduction of equatorial upwelling as a result of a reduced atmospheric pressure gradient during the warm periods and/or 2) a decline in the biological pump efficiency resulting in less regenerated nutrients in the deep ocean. Both processes would lead to a better ventilated EEP and reduction of the ODZs.

1340 In addition, a FB- $\delta^{15}\text{N}$ record from the Eastern Tropical South Pacific (Wang et al., 2022) showed a significant long-term increase in $\delta^{15}\text{N}$ since the Miocene (Fig. 7). A $\delta^{15}\text{N}_{\text{bulk}}$ record from the California margin (Liu et al., 2008) also showed an

increase since ~2.1 Ma. These records indicate expansion of the ODZs in the Eastern Tropical Pacific, when global climate
1345 was cooling since the mid-Miocene (Herbert et al., 2016; Westerhold et al., 2020). Although decreasing sea surface
temperatures may have supplied more oxygen to the surface ocean since the late Miocene, Wang et al., (2022) argue that the
rising oceanic nutrient content and resulting higher productivity appear to have overwhelmed the solubility effect and driven
ocean deoxygenation over the past 8 Myrs.

On glacial/interglacial timescales, most published $\delta^{15}\text{N}_{\text{bulk}}$ records from the Eastern Tropical Pacific generally show lower
1350 $\delta^{15}\text{N}_{\text{bulk}}$ values during the last ice age compared to the Holocene warm period, which has been interpreted as lower water
column denitrification and thus, higher oxygen content in the water column (Ganeshram et al., 1995; Galbraith et al., 2004;
Dubois et al., 2011). However, two recent FB- $\delta^{15}\text{N}$ records from the EEP show similar $\delta^{15}\text{N}$ values during the LGM and the
Holocene, indicating comparable water column oxygen content during those periods (Studer et al., 2021) (Fig. 7). The
difference between FB- $\delta^{15}\text{N}$ and $\delta^{15}\text{N}_{\text{bulk}}$ may be attributed to lower diagenetic alteration and/or higher foreign N input during
1355 ice ages which may have altered the $\delta^{15}\text{N}_{\text{bulk}}$ signal (Robinson et al., 2012; Studer et al., 2021). Using a box model, Studer et
al. (2021) argue that multiple processes may have stabilized the oxygen content. A glacial shoaling of the Atlantic meridional
overturning circulation, enhanced iron fertilization in the Subantarctic, and global cooling would have raised mid-depth oxygen
content, whereas a more efficient biological pump would have led to an accumulation of regenerated nutrients and thus a
decrease in deep Pacific oxygen content. This signal would have been mixed/upwelled into the mid-depth Pacific, leading to
1360 little net LGM-to-Holocene change in the Eastern Tropical Pacific ODZ extent (Hain et al., 2010; Studer et al., 2021). The FB-
 $\delta^{15}\text{N}$ data are supported by the independent oxygen proxy I/Ca on planktic foraminifera (Hoogakker et al., 2018, Section 8)
and challenges the previous views on reduced Eastern Tropical Pacific water column denitrification during ice ages based on
 $\delta^{15}\text{N}_{\text{bulk}}$ (Ganeshram et al., 1995; Galbraith et al., 2004).

By combining different $\delta^{15}\text{N}$ records from the Eastern Tropical Pacific across various time scales, a novel hypothesis has
1365 emerged that temperature-driven changes in mid-ocean oxygen content may not be the dominant control for ODZ evolution
and changes in water column denitrification rate. Instead, ocean circulation and biological activity are important additional
controls (e.g., Robinson et al., 2014). These findings highlight the need for multiple N proxy applications in the same region
or even the same sedimentary record, in combination with other oxygen proxies. In particular, we note an interesting recurring
pattern that $\delta^{15}\text{N}_{\text{bulk}}$ records tend to be similar to the FB- $\delta^{15}\text{N}$ when $\delta^{15}\text{N}$ and denitrification rate increase, but they often fail to
1370 record $\delta^{15}\text{N}$ decreases across a climate event (Fig. 7 and references therein). As we generally assume better preservation
conditions under low-oxygen conditions, the high $\delta^{15}\text{N}$ values recorded by the bulk sediment during intervals of decreased FB-
 $\delta^{15}\text{N}$ and increases in water column oxygen content could then be due to an increase in the diagenetic effect on $\delta^{15}\text{N}_{\text{bulk}}$
(Robinson et al., 2012). The $\delta^{15}\text{N}$ difference between bulk sediment and fossil-bound N may in turn hold interesting
information on past changes in oxygen content in the water column and sediments. Finally, as physical and biological processes
1375 are both important in understanding the history of the ODZs, an oxygen-realistic biogeochemical model embedded with
nitrogen isotopes would be important to advance our interpretation of these $\delta^{15}\text{N}$ records.



1380 **Figure 7: Compilation of proxy-reconstructions of Equatorial Pacific anoxia from (FB-) $\delta^{15}\text{N}$.** From left to right for the timespan
 65–5 Ma, 5–0 Ma, 35–0 ka, 1860–2010 CE and simulated global ODZ volume for RCP2.6 and RCP8.5 projections 2020–2100 from
 IPCC AR5 (Bindoff et al., 2019). A) Sea surface temperature compilation by Hansen et al. (2013). B) Analyses of $\delta^{15}\text{N}$ in bulk
 1385 sediment (yellow) and foraminifera-bound organics (FB; pink) in Pacific sedimentary archives. $\delta^{15}\text{N}$ is used as a qualitative oxygen-
 sensitive proxy due to the strong isotopic fractions of denitrification by ODZ dwelling bacteria. Data compiled from the following
 sources: ODP 1209 (Kast et al., 2019); DSDP 598 (Wang et al., 2022); ODP 872 (Auderset et al., 2022); ODP 1012 (Liu et al., 2008);
 ME24 and ME27 (Studer et al., 2021; Dubois et al., 2011); PES, SOL, StaMON (Deutsch et al., 2014); global Paleocene-Miocene
 compilation from Algeo et al. (2014); PETM (Moretti et al., 2024).

8 Foraminiferal trace elements

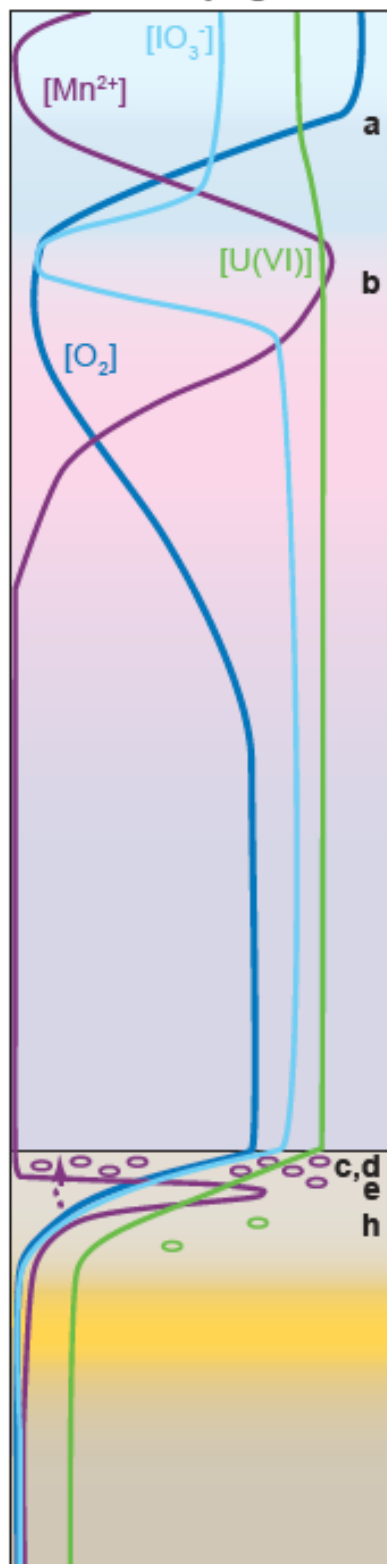
1390 8.1 Introduction to proxy/geochemical system

In addition to sedimentary trace elements, foraminiferal trace elements can provide information about environmental redox conditions. In this section we will focus on foraminiferal I/Ca, Mn/Ca, and U/Ca, which are commonly used proxies to track seawater redox conditions and relative dissolved oxygen concentrations. Specifically, these proxies are thought to track dissolved iodate (IO_3^-), manganese (Mn(II)), and uranium (U(VI)), respectively. One frontier of the carbonate lattice-based
 1395 proxies lies with determining the potential for their differential application to benthic and planktic foraminifera to quantify

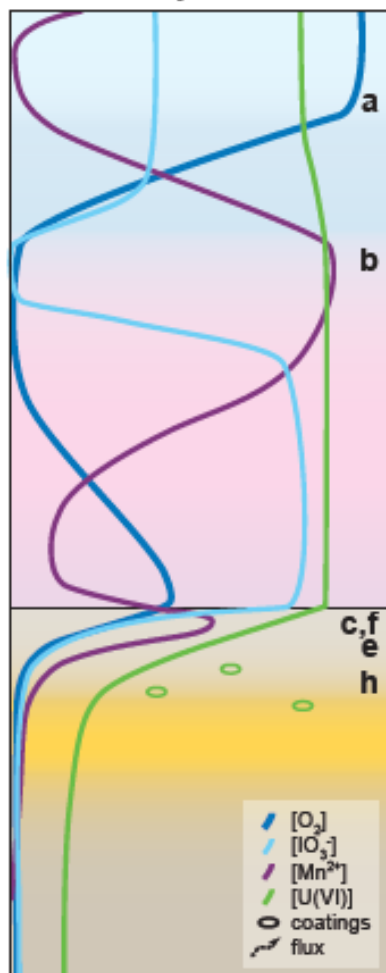
depth gradients in the water column. We discuss the proxy sensitivities within the context of the redox ladder, to avoid confusion with nomenclature (e.g., Canfield and Thamdrup, 2009). Below we discuss the distribution of IO_3^- , Mn(II) , and U(VI) in the water column and pore waters, their incorporation into foraminiferal calcite, and evaluate their potential use as proxies for dissolved oxygen concentrations and seawater redox conditions (Fig. 8).

1400

(a) Deep-ocean site with overlying ODZ



(b) Intermediate-depth ODZ-adjacent site



water column
 mixed layer
 thermocline
 ODZ
 deep ocean
 sediments
 above sulfidic zone
 sulfidic zone
 below sulfidic zone

(c) Shallow-water site with sediments in the ODZ



- a: IO_3^- incorporated in planktonic foraminifera. I^- oxidation is relatively slow in ODZ waters mixing upwards, lower $[\text{IO}_3^-]$ above ODZ than in deep ocean
- b: IO_3^- reduction to I^- in the upper ODZ
- c: IO_3^- reduction to I^- in anoxic pore waters
- d: Mn^{2+} oxidation to Mn-Fe-(oxy)hydroxides, precipitation of Mn-carbonate coatings
- e: Mn reduction to soluble Mn^{2+} , deep infaunal foraminifera incorporate Mn
- f: Shallow O_2 penetration, shallower Mn^{2+} front than in open ocean, deep and intermediate infaunal foraminifera incorporate Mn
- g: Low- $[\text{O}_2]_{\text{bottom water}}$ allows Mn^{2+} to escape sediments, less Mn for foraminifera to incorporate
- h: U filtering in from overlying water column precipitates gradually in areas with deeper O_2 penetration
- i: U filtering in from overlying water column precipitates rapidly in Fe-reduction zone

1405 **Figure 8: Illustration of chemical profiles and key processes (a-i) affecting the I/Ca, Mn/Ca, and U/Ca in foraminifera oxygenation proxies in a theoretical transect through an ODZ from A) a deep ocean site with overlying ODZ to B) an intermediate-depth ODZ-adjacent site to C) a shallow-water site with sediments in the ODZ. Based on data and concepts from Anderson et al. (1989), Thamdrup et al. (1994), Morford et al. (2009), Singh et al. (2011), Koho et al. (2015), Mariyasu et al. (2020), and Singh et al. (2023). Note that when we refer to shallow water we refer to the continental shelf; for intermediate waters the continental slope, and for deep water the abyssal plain.**

8.1.1 Seawater elemental cycling tracked via paleoredox proxies

1410 Multiple published seawater transects from the Eastern Tropical North and South Pacific document the geochemistry of Mn and I (Rue et al., 1997; Cutter et al., 2018; Rapp et al., 2020; Moriyasu et al., 2020, 2023). These studies demonstrate similarities and differences in seawater I and Mn speciation that can be exploited for defining water column redox conditions. For example, redox thresholds for IO_3^- and Mn-oxide reduction overlap (Fig. 8), and both display potentially rapid reduction kinetics, sluggish oxidation kinetics, and an important benthic component of accumulation within ODZs (Cutter et al., 2018; Rue et al., 1997). Specifically, in ODZs, dissolved iodate (IO_3^-) is reduced to dissolved iodide (I^-) at and below the oxycline (Fig 8 areas labelled b). Estimates of the iodate oxygen reduction threshold range from up to $50 \mu\text{mol kg}^{-1}$ (Lu et al., 2020) to potentially less than $1 \mu\text{mol kg}^{-1}$ (Hardisty et al., 2021). Thresholds less than $1 \mu\text{mol kg}^{-1}$ may be possible, but iodine cycling has yet to be evaluated alongside oxygen sensors with sub- μM detection limits (e.g., Thamdrup et al., 2012). Regardless, the lowest IO_3^- has been demonstrated to nearly exclusively occur in low-oxygen waters, thus, defining a threshold for ‘iodinous’ conditions (Fig. 8) (Hardisty et al., 2021).

At similar water column depths to where IO_3^- reduction occurs in ODZ cores (i.e. oxygen minima), dissolved Mn(II) also begins to accumulate (Fig. 8). Mn(II) is formed through the reduction of suspended manganese oxyhydroxides (III, IV) minerals driven by organic matter mineralisation and/or oxidation of reduced components (e.g., dissolved iron, sulphides, and ammonium, Burdige, 1993; Thamdrup et al., 1994a, 1994b; Kristiansen et al., 2002). Potential oxygen thresholds for Mn accumulation have been evaluated using Switchable Trace Oxygen Sensor (STOX) microsensors, which indicate that Mn(II) may be re-oxidized at oxygen levels as low as 100 nM (Clement et al., 2009). Ultimately, the accumulation of both Mn(II) and I^- are well-defined features in ODZs, and these are increasingly used alongside NO_2^- (product of nitrate reduction) maxima to define ODZ cores and so-called ‘functional anoxia’, which are zones where these and potentially more reducing metabolisms such as SO_4^{2-} reduction may occur within micro-niches (e.g., Canfield et al., 2010; Raven et al., 2018).

1430 Uranium cycling is a useful comparison to I and Mn cycling in that it is sensitive to more reducing ferruginous conditions (Fig. 1). U(VI) is dissolved in oxygenated seawater as uranyl carbonate (U(VI)) complexes and behaves conservatively (Ku et al., 1977; Chen et al., 1986; Dunk et al., 2002; Not et al., 2012). Uranium has a long residence time in seawater (~ 400 kyr), and therefore its concentration is homogenous and relatively constant on timescales of 10^5 yrs (Dunk et al., 2002). While uranium exhibits conservative behaviour in oxic settings, in oxygen-deficient/ ferruginous seawater conditions, characteristic of some ODZ bottom waters, U(VI) is reduced to insoluble U(IV) and may precipitate on settling marine particles. Some of these U-containing particles ultimately reach the sediment to either be scavenged or re-oxidized to a soluble uranyl-carbonate complex

at the sediment/water interface (Anderson et al., 1989). Under sufficiently reducing bottom- and pore water redox conditions (dysoxic to anoxic), U will precipitate in the sediments as uraninite ($\text{U(IV)O}_{2(s)}$; Fig. 8 areas labelled i).

Reduction of IO_3^- , Mn-oxide, and U(VI) takes place through bacterial catalysation. Reduction of IO_3^- has been associated with
1440 IdRA genes (Uyamas et al., 2021). Soluble U(VI) is most likely reduced to insoluble uraninite U(IV) by iron-reducing bacteria
(e.g., Lovley et al., 1991). Abiotic reduction is important as well. I and Mn are rapidly reduced via abiotic reactions with Fe
and sulphide (Luther et al., 2023). Because ferruginous and sulphidic conditions are common in modern sediments, rapid
reduction of IO_3^- , Mn-oxides, and U(VI) creates large gradients that can control diffusive fluxes to and from seawater. For IO_3^-
and Mn-oxides in sediments, rapid reduction creates elevated $[\text{I}^-]$ and $[\text{Mn(II)}]$ —which can be further exacerbated for $[\text{I}^-]$ due
1445 to organic matter remineralization (Kennedy and Elderfield, 1987a; 1987b) —that drives benthic fluxes into the overlying
seawater (Fig. 8 areas labelled c and g). These fluxes are large within ODZ water columns, where low-oxygen concentrations
enable the persistence of the reduced I^- (e.g., Cutter et al., 2018; Moriyasu et al., 2020) and Mn(II) (e.g., Froelich et al., 1979;
Sundby and Silverberg, 1985; Metzger et al., 2007; Mouret et al., 2009) (Fig. 8). U behaves the opposite, where the formation
of insoluble U(IV) under ferruginous conditions removes U from pore waters. This causes a concentration gradient to form
1450 between high $[\text{U}]$ overlying bottom waters and low $[\text{U}]$ pore waters and leads to a diffusive flux of seawater U into the
sediments (Barnes and Cochran, 1990; Klinkhammer and Palmer, 1991), causing sediment authigenic U (aU) enrichment, at
a rate established by the diffusive flux (Fig. 8 area labelled i).

8.1.2 Incorporation: how, when, and where are elements incorporated?

The I/Ca, Mn/Ca, and U/Ca proxies track iodinous, manganous, and ferruginous conditions respectively (Fig. 8). Below we
1455 consider what is known for each proxy. Importantly, recent studies indicate that, whether applied to planktic or benthic
foraminifera, each proxy may, at least in part, reflect the geochemistry of bottom waters, but more work is needed.

It has been demonstrated that only the oxidized I species, IO_3^- , can be incorporated into both abiotic calcite (Lu et al., 2010;
Zhou et al., 2014; Podder et al., 2017; Kerisit et al., 2018) and dolomite (Hashim et al., 2022) (Fig. 8 inset labelled a). Therefore,
the I/Ca of planktic and benthic foraminiferal calcite has traditionally been used to infer $[\text{IO}_3^-]$ as a proxy for changes in
1460 subsurface and bottom water oxygen concentrations, respectively (Glock et al., 2014; 2016; Hardisty et al., 2014; 2017;
Hoogakker et al., 2018; Lu et al., 2010; 2016; 2020; Zhou et al., 2014; 2016). However, the incorporation of IO_3^- has not been
directly tested within foraminifera, which may include vital effects not currently recognized. A recent study found that I/Ca
values of planktic foraminifera sampled from plankton tows showed little-to-no relationship with the dissolved $[\text{IO}_3^-]$ of
ambient seawater (Winkelbauer et al., 2023). In fact, this work showed that planktic foraminiferal I/Ca was about ten times
1465 lower in plankton tows compared to that in sediment core-tops and as would have been expected from abiotic calcite
precipitation experiments (Winkelbauer et al., 2023). Winkelbauer et al. (2023) suggest that planktic foraminifera may gain
iodine during gametogenesis or post-mortem, either when falling through the water column, or through burial. Lu et al., (2023)
confirm that proxy data from plankton tows and sediment core top samples may not agree because of the complexity of
foraminiferal calcification and post depositional overprints in marine surface sediments. Thus, core-top and downcore planktic

1470 foraminiferal I/Ca may be representative of an integrated IO_3^- signal from across the water column and sediment, instead of the depth that they occupy during their life cycle.

While both benthic and planktic foraminiferal I/Ca data from core-top samples support a relationship with bottom and subsurface water dissolved oxygen (Fig. 9a), the species-specific and/or mineralogical controls for incorporation of IO_3^- into biogenic carbonates are still not well-understood. Globally, the highest core-top I/Ca values are found to be $\sim 9 \mu\text{mol mol}^{-1}$ for planktic foraminifera in the Walvis Ridge region (Lu et al., 2020) and $\sim 22 \mu\text{mol mol}^{-1}$ for benthic foraminifera in Little Bahamas Bank region (Lu et al., 2022), both from well-oxygenated environments. Assuming the IO_3^- concentrations in these oxic waters range between 0.5 and 0.65 $\mu\text{mol L}^{-1}$, the partition coefficient (Kd) for IO_3^- incorporation ($\text{Kd} = [\text{I/Ca}]_{\text{foram}} / [\text{IO}_3^-]_{\text{sw}}$, with a unit of $[\mu\text{mol mol}^{-1}]/[\mu\text{mol L}^{-1}]$) can range from 14 to 44, or even higher if the seawater IO_3^- concentration is lower than 0.5 μmol . These Kd estimates are much higher than those reported in abiotic calcite synthesis experiments (~ 10) (Lu et al., 2010), suggesting a potential biological control on the I incorporation in the calcite. The strong association of iodine with organic heterogeneities in the calcite of benthic foraminifera might be another challenge to consider within future studies on foraminiferal I/Ca (Glock et al., 2019).

Interpretations of redox-conditions based on the foraminiferal Mn/Ca proxy may be derived from calcite lattice-bound Mn ($\text{Mn/Ca}_{\text{foram}}$) and Mn bound in post-depositional authigenic coatings of foraminifera tests (e.g., Barras et al., 2017; Chen et al., 2017). Foraminifera can incorporate soluble Mn(II) into their calcite tests (Fig. 8 inset labelled e). Barras et al. (2018) observed a linear correlation between Mn/Ca_{sw} and $\text{Mn/Ca}_{\text{foram}}$ for two different species (*Ammonia* T6 and *Bulimina marginata*) of benthic foraminifera in controlled laboratory conditions. That said, it seems that the partition coefficient increases when concentrations are lower than $\sim 10 \mu\text{mol L}^{-1}$ of Mn_{sw} . The genus *Ammonia* is a shallow water taxon (inner neritic – intertidal) and it unclear if its biology is relevant to deep water taxa. Because of the link between Mn(II) and ODZs, Mn/Ca in benthic foraminifera has been linked to dissolved oxygen in the bottom and/or pore waters of their microhabitat (e.g., Klinkhammer et al., 2009; Koho et al., 2015). Concentrations of benthic foraminiferal (lattice-bound) Mn/Ca from low-oxygen environments and culture experiments can range from 0.1 to $>150 \mu\text{mol mol}^{-1}$ (Lea, 2003; Glock et al., 2012; Koho et al., 2017; Barras et al., 2018; Brinkmann et al., 2021) depending on oxygen in bottom/pore waters. Planktic foraminiferal (lattice-bound) Mn/Ca ratios from plankton tows and sediment traps also seem to be linked to seawater oxygen, with higher Mn/Ca relating to lower oxygen (Steinhardt et al., 2014; Davis et al., 2023). The advantage of foraminiferal calcite-bound Mn/Ca ratios compared to a bulk sediment proxy such as Mn/Al is that once precipitated, the Mn concentration remains fixed in the foraminiferal shell and should not be subject to diagenetic reduction or oxidation (Koho et al., 2015; McKay et al., 2015).

Nevertheless, in the case of fossil tests, post-mortem Mn-rich contaminant secondary coatings (e.g., Mn oxides or Mn carbonate; Fig. 8 inset labelled d) may obscure the Mn/Ca signal of the pristine calcite signal (Barker et al., 2003; Ni et al., 2020). Authigenic Mn mineral formation can occur on the outside and/or inside of the foraminiferal tests and pores. Recrystallization or banding within foraminiferal test laminae can interfere with the application of this proxy for reconstructing redox conditions when the foraminifera were formed (e.g., Detlef et al., 2020; Ni et al., 2020). In addition to the primary foraminiferal Mn proxy, several studies suggest authigenic foraminiferal U/Mn in coatings as a proxy for sedimentary post-

deposit redox conditions (Gottschalk et al., 2016; Chen et al., 2017; Detlef et al., 2020). The formation of Mn-rich authigenic carbonates potentially responds to the microbial activity in the pore water which is linked to the sedimentary redox environment (Detlef et al., 2020; Ni et al., 2020).

The U/Ca proxy does not target carbonate lattice-bound U. Instead, this utilizes the formation of aU which precipitates onto foraminifera tests buried in marine sediments, forming a U-rich (post-depositional) coating on their carbonate tests (Boiteau et al., 2012) (Fig. 8 area labelled i). The rate of authigenic enrichment is established by the U diffusive flux between overlying bottom waters and pore waters and follows similar dynamics to aU precipitation in bulk sediments (Boiteau et al., 2012). The diffusive flux, in turn, depends on how reducing the conditions are within the sediments (Barnes and Cochran, 1990; Klinkhammer and Palmer, 1991). Therefore, higher U/Ca concentrations are indicative of reducing oceanic bottom water conditions.

Concentrations of foraminiferal U/Ca can reach 300-700 nmol mol⁻¹ (Boiteau et al., 2012; Gottschalk et al., 2016; 2020; Skinner et al., 2019; Chen et al., 2017). This exceeds the foraminiferal lattice-bound [U], with shell matrix U/Ca ranging from ~1-23 nmol mol⁻¹ (Russell et al., 1994; Raitzsch et al., 2011; Boiteau et al., 2012; Yu et al., 2008; Chen et al., 2017). Therefore, lattice-bound U has a negligible impact on the measured U/Ca values of a diagenetically altered shell. Furthermore, the post-depositional accumulation of aU as foraminiferal authigenic coating means that any species can be measured, including planktic foraminifera which tend to be much more abundant in open ocean settings.

1520 **8.1.3 Additional impacts on proxy values**

Preservation and diagenetic effects on I/Ca ratios from biogenic calcite in sediments are currently unexplored, although it is well-known that I/Ca in bulk carbonate is susceptible to diagenetic alterations, specifically declining values due to diagenesis in reducing IO₃⁻ free pore waters (Hardisty et al., 2017; Lau and Hardisty, 2022). Diagenetic impacts on local IO₃⁻ availability in pore fluids relative to overlying seawater may also make benthic foraminiferal signals particularly susceptible to recording diagenetic conditions. Specifically, a combination of excess I, related to I input from organic remineralization, and reducing conditions which can impact IO₃⁻ availability, are possible. For example, I/Ca values as high as 20 μmol mol⁻¹ have been observed in infaunal foraminifera from the PETM. This may be due to higher IO₃⁻ near the sediment-water interface driven by oxic organic remineralization (Zhou et al., 2016; Kennedy and Elderfield, 1987a,b), or higher-than-modern total iodine concentrations in the seawater during the PETM. In the modern Peruvian OMZ, shallow infaunal species (*Uvigerina striata* and *U. peregrina*) show I/Ca values ~1 μmol mol⁻¹ lower than epifaunal species (*Planulina limbata*) (Glock et al., 2014). If oxygen was the only control on pore water IO₃⁻, these lower I/Ca values in modern infaunal species would reflect lower IO₃⁻ concentrations in pore water, linking to rapid oxygen decrease within a few centimetres or millimetres of sediments. Thus, it remains unclear how pore water IO₃⁻ may influence I/Ca of infaunal foraminifera. Attention should be given to possible contamination through organic bound iodine in foraminiferal calcite (Glock et al., 2016, 2019), which might significantly impact measured I/Ca ratios, thus requiring intense oxidative cleaning. Additional oxidative cleaning steps can result in considerably lower I/Ca ratios (Winkelbauer et al., 2021, 2023; see also Fig. 9a).

1540 Like many other foraminiferal trace element proxies, several additional environmental parameters (e.g., temperature, salinity, and carbonate ion concentrations) may impact the elemental incorporation as well. In the Little Bahama Bank region where bottom-water oxygen concentrations are similarly high between 150 and 200 $\mu\text{mol kg}^{-1}$, seawater temperature, salinity, and carbonate ion concentration show negative correlation with benthic foraminiferal I/Ca (Lu et al., 2022). It is thus speculated that benthic foraminifera may preferentially incorporate IO_3^- at lower temperature and/or lower salinity. Additionally, or alternatively, when ambient seawater has less carbonate ion availability, IO_3^- may be used as an alternative substitute for calcite structure by foraminifera. It is not clear whether the negative correlation between I/Ca and temperature could still be found under lower bottom water oxygen conditions, as bottom water oxygen is often anti-correlated with temperature. Further studies are needed to disentangle such effects. Lastly, one epifaunal species, aragonitic *Hoeglundina elegans*, shows lower I/Ca values than observed in other benthic foraminifera (*Planulina limbata*, *Uvigerina peregrina* and *Uvigerina striata*, Glock et al., 2014), suggesting different IO_3^- incorporation mechanisms for differing mineralogies (e.g. aragonite versus calcite), or an effect of different microhabitat preferences. Future work is needed to clarify these differences.

1550 Factors such as carbonate chemistry, metabolic effects, ontogenetic effects, and species-specific effects could also have potential impacts on Mn incorporation into the foraminiferal test. Culture experiments with different partial pressure of carbon dioxide ($p\text{CO}_2$) levels show Mn/Ca of larger benthic foraminifera increased under high $p\text{CO}_2$ conditions, which can be mainly ascribed to Mn speciation changes in seawater for Mn incorporation (van Dijk et al., 2020). Mn incorporation can also be affected by Mg incorporation in hyaline species. Mg and Mn are coupled during foraminiferal calcification and are correlated on specimen and species level (van Dijk et al., 2020). In the case of symbiont-bearing species grown under low-oxygen conditions, Mn mapping using electron probe microanalysis (EPMA) on the cross-section of the test highlighted that layers of calcite are enriched with Mn compared to ones grown under high-oxygen conditions (van Dijk et al., 2019). This may be caused by the influence of the day/night (light/dark) cycles, meaning that symbiont activity (photosynthesis/respiration) or other diel shifts in physiology may directly or indirectly impact Mn concentration/speciation at the site of calcification. Different chamber-to-chamber trends (such as between proloculus and last chambers) for *Ammonia* and *Bulimina* species show ontogenetic effects (Barras et al, 2018, Brinkmann et al., 2023). Ontogeny-driven (life strategy) preferences may influence Mn/Ca in initial chambers (incl. proloculus) of *Bulimina*, as indicated by in-field observations (Brinkmann et al., 2023). Species-specific biomineralization processes and microhabitat effects could also impact Mn incorporation in small benthic foraminifera (Koho et al., 2015; Barras et al, 2018, Brinkmann et al., 2023, Groeneveld and Filipsson, 2013; Groeneveld et al., 2018). Culture experiments demonstrate species-specific ontogenetic effects on Mn/Ca with opposite chamber-to-chamber trends in the last three chambers of *Ammonia* and *Bulimina* species (Barras et al., 2018). Diagenetic effects, including secondary mineral coatings, can significantly interfere with the Mn/Ca measurements of primary calcite under hypoxic/anoxic burial conditions (e.g., Detlef et al., 2020; Ni et al., 2020). The formation of inorganic carbonates with highly elevated Mn on the internal and external surfaces of foraminiferal tests, and especially in the pores, is difficult to eliminate through standard foraminiferal trace element cleaning procedures (Ni et al., 2020).

1570

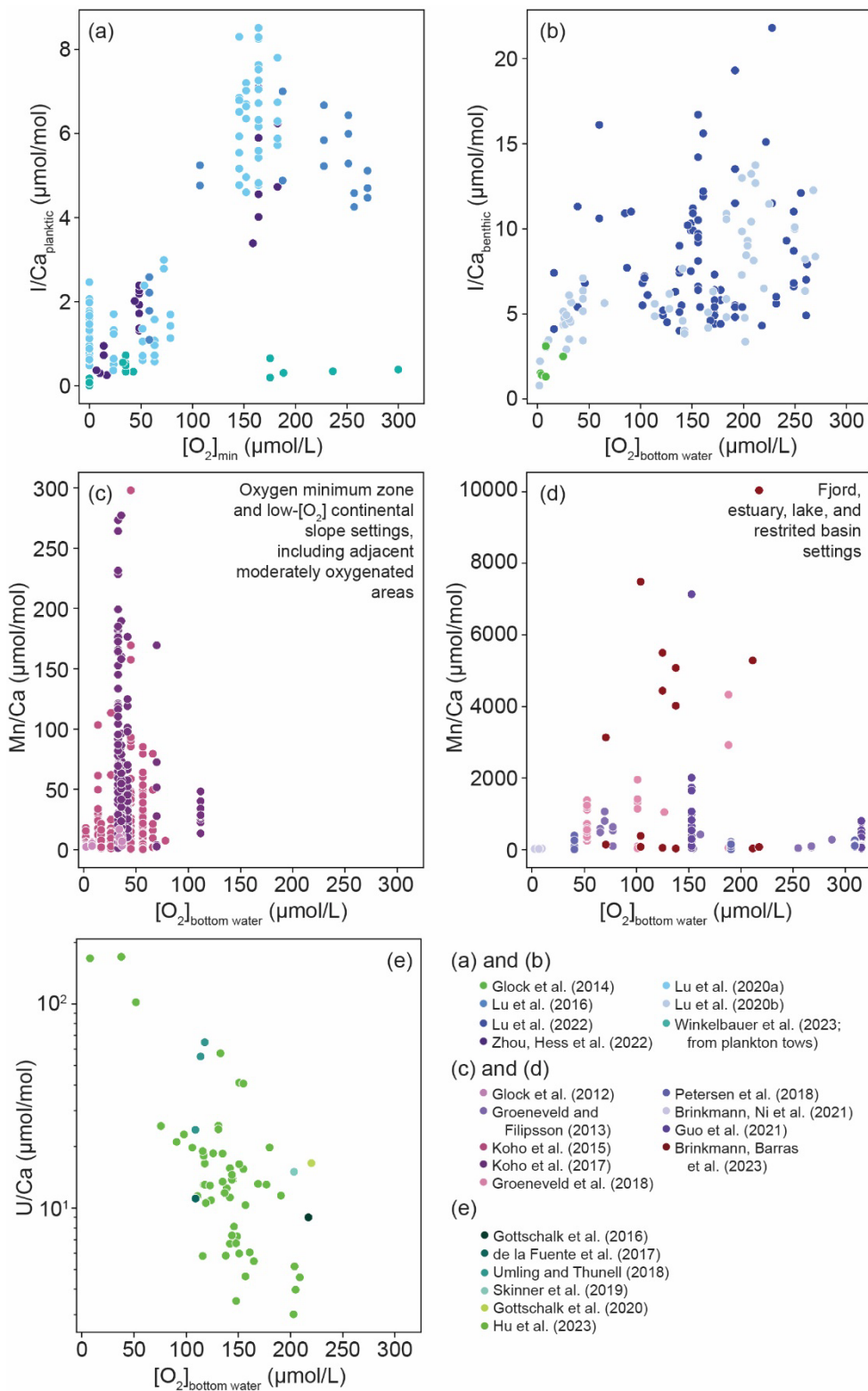
By contrast, post-depositional alterations form the basis of the U/Ca proxy. Authigenic U accumulated in sediments may be remobilized, due to a deepening of the anoxic boundary, driven by an increase in bottom water oxygen, decreased C_{org} flux, or bioturbation (McManus et al., 2005; Zheng et al., 2002). Such a change in oxygen penetration depth could lead to a reversed pore-to-bottom water [U] gradient, causing an efflux (remobilization) of dissolved U from the sediments back into the overlying bottom water, therefore eliminating the primary U signal (McManus et al., 2005; Zheng et al., 2002). It has been suggested that the U/Ca of foraminiferal coatings from marine sediment cores with high sedimentation rates ultimately record aU formed in steady state with bottom water, and that the diagenetic aU loss is minimal (Gottschalk et al., 2020; Jacobel et al., 2020).

8.2 How does the proxy relate back to oxygen?

Quantitatively relating proxies to oxygen content is an important goal for understanding paleo-redox evolution. This is extremely challenging because each proxy has variable oxygen thresholds and vital, mineralogical, and diagenetic effects that can distort its signal in the geologic record. Empirical comparisons of plankton tow and core-top proxy values to subsurface or bottom water oxygen can provide important constraints on proxy-oxygen relationships applicable to the geologic record. Toward this goal, Figure 9 provides proxy-oxygen syntheses, and below we provide both mechanistic and empirical discussions for relating proxy records back to specific oxygen levels. For each of the proxies this means understanding at least two tiers of oxygen relationships: oxygen values allowing for an initial change in the proxy from baseline conditions and subsequent scaling of changing proxy values to dynamic oxygen conditions.

I/Ca values recorded in planktic and benthic foraminifera are lower in areas with lower subsurface and bottom-water oxygen, respectively (Fig. 9 and references therein). Of the three foraminiferal proxies discussed here, I/Ca has the best empirical constraints on oxygen thresholds, but at the same time the mechanistic understanding of factors driving these relationships remains unclear (see Section 8.1). Recent studies provide two ways to interpret I/Ca relative to oxygen content or redox conditions. The first is the simple presence/absence of carbonate-associated iodine, and hence the presence/absence of IO_3^- . Iodide (I^-) and IO_3^- have a similar redox potential and thus IO_3^- is quantitatively reduced to I^- in productive anoxic settings. This implies that the simple presence of IO_3^- or carbonate-associated iodine may be indicative of oxygen at some level (e.g., Hardisty et al., 2014). We note that a global compilation of IO_3^- in ODZs demonstrates that IO_3^- may persist when oxygen is below detection; however, this is interpreted to reflect sluggish reduction of IO_3^- , not in situ IO_3^- production (Hardisty et al., 2021; Moriyasu et al., 2020; Cutter et al., 2018). Also, as discussed earlier, the CTD oxygen sensor detection limits, which are typically near $1 \mu\text{mol kg}^{-1}$, are currently a limitation for understanding IO_3^- -oxygen thresholds, as nmol kg^{-1} oxygen levels may support active I redox cycles, as has been demonstrated for N and Mn (Clement et al., 2009; Thamdrup et al., 2012).

1600



1605 **Figure 9: Element/Ca from core-top (top 10 cm) compared to oxygenation. from core-top (top 10 cm) and plankton tow foraminifera**
a) I/Ca in core-top and plankton tow planktic foraminifera versus minimum oxygen concentration in the water column. Zhou et al.
(2023) data were corrected for reductive cleaning. b) I/Ca in epifaunal and infaunal benthic foraminifera versus bottom water oxygen
1610 concentration. C and D: Mn/Ca data from core-top benthic foraminifera compared to oxygenation in different settings. Note the
differences in scale between c and d. c) OMZ and low-oxygen continental slope and d) fjord, estuary, lake, and restricted basin
settings. Note two-tailed distribution from right to left, with (1) low Mn/Ca values where a deeper oxycline in pore waters results in
less Mn²⁺ available at foraminiferal depth habitats, (2) high Mn/Ca values where low-oxygen bottom water prevents Mn²⁺ from
leaving pore waters, and (3) low Mn/Ca where Mn²⁺ is lost to water column with low-oxygen bottom water or precipitated as Mn-
carbonate. E: U/Ca from planktic foraminifera deposited in sediments <10 ka BP compared to current bottom-water oxygenation
from World Ocean Atlas 18. Modified from Hu et al. (2023).

1615 A major challenge in interpreting I/Ca data quantitatively is that the oxidant(s) responsible for I⁻ oxidation to IO₃⁻ is unknown.
Indeed, unambiguous *in situ* IO₃⁻ production has not been observed under normal marine conditions. Oxygen is not directly
responsible for IO₃⁻ formation, at least abiotically, as demonstrated by the long residence time - estimated to range from 40 to
<0.5 yrs - of I⁻ in oxygenated seawater (Chance et al., 2014). Some recent culture studies propose that superoxide or ammonia-
oxidizing bacteria may be responsible for catalysing IO₃⁻ production, but results have yet to be confirmed in natural marine
1620 settings or in cultures without iodine in excess of seawater (Hughes et al., 2021; Li et al., 2014). While I⁻ oxidation is a
limitation for models used to interpret mechanisms and distributions of ancient IO₃⁻, constrained via I/Ca (e.g., Lu et al., 2018),
IO₃⁻ reduction is clearly linked to declining oxygen, thus bolstering proxy applications.

Beyond presence/absence, I/Ca values above and below a threshold range may be used to define 'iodinous' conditions typical
of ODZs. The 'iodinous' framework allows for I/Ca interpretations in the context of the redox ladder alongside other proxies
1625 reflecting specific reduction potentials (Canfield and Thamdrup, 2009; Lau and Hardisty, 2022; Algeo and Li, 2020) (Fig. 1).
I/Ca < 3 μmol mol⁻¹ can be related back to the IO₃⁻ range <300 nM common to ODZ settings (Lu et al., 2016; Hardisty et al.,
2021; Lu et al., 2022). Lastly, specific oxygen thresholds have been recommended for the recognition of 'iodinous' conditions.
I/Ca values <3 μmol mol⁻¹ have been demonstrated in benthic foraminifera with a bottom water oxygen concentration <50
μmol kg⁻¹ (Fig. 8; Lu et al., 2022). I/Ca variations >3 μmol mol⁻¹ are unlikely directly related to oxygen, but instead likely
1630 reflect combinations of biologically mediated transformations during primary production and physical mixing and advection
processes (Chance et al., 2014; Campos et al., 1996; Truesdale, 2000; Hepach et al., 2020).

The application of Mn/Ca is mainly limited to environmental conditions characterized by trace amounts of bottom-water
oxygen. Whilst water column Mn cycling systematics are well understood, the direct relationship of Mn/Ca values to specific
oxygen levels is restricted in comparison to I. Fundamentally, the highest Mn/Ca values are found in benthic foraminifera from
1635 manganese environments, allowing for high dissolved Mn²⁺ beneath intermediately oxic water columns that limit benthic Mn
fluxes out of the sediments (Fig. 9c&d). This is because Mn/Ca tracks the reduced Mn endmember, contrarily to I/Ca, and
because abiotic and benthic cycling can contribute to Mn(II) accumulation. For Mn, the diffusion of dissolved Mn from pore
waters into bottom water, under prolonged anoxic conditions, prevents a linear relationship between Mn/Ca in foraminiferal
calcite and bottom water oxygen concentrations (Koho et al., 2015). Recently, Brinkmann et al. (2023) found that an upper
1640 limit of around 130 μmol L⁻¹ exists in a fjord setting above which the linear correlation between foraminiferal Mn/Ca and

bottom water oxygen no longer exists, confirming earlier work by Guo et al. (2019) from the Yangtze River Estuary. This proxy would also be difficult to apply in environments with very low dissolved Mn content, as is the case, for example in the Santa Barbara Basin (Brinkmann et al., 2021). In the case of a depleted Mn pool in the sediment, the changes in Mn speciation according to oxygen concentrations would not be significant enough to be recorded in the foraminiferal shell. On the other
1645 hand, the vicinity of continental inputs or other sources of Mn into the sediment, independent from oxygen conditions, could also hamper the proxy robustness (Klinkhammer et al., 2009).

The Mn/Ca proxy is best related to relative oxygen levels, with highest Mn/Ca encountered under hypoxic conditions. The Mn/Ca proxy will reflect the oxygen conditions in the microenvironment surrounding the foraminifera during calcification,
1650 i.e. bottom water, pore water, or water column conditions in the case of planktic foraminifera. Benthic foraminiferal species considered as epifaunal or shallow infaunal should therefore better record bottom water conditions than intermediate and deep infaunal taxa. Moreover, under oxic conditions epifaunal species would incorporate less Mn. With decreasing bottom water oxygen concentrations, the redox boundary would migrate towards the sediment water interface and Mn incorporation would increase for the shallow infaunal species. However, under anoxic/hypoxic bottom water conditions, dissolved Mn diffuses out
1655 of the sediment resulting in less free Mn available for incorporation in the foraminiferal shell (e.g., Groeneveld et al., 2018). Intermediate and deep infaunal taxa are already living at or below the redox boundary and could migrate in the sediment accordingly, potentially changing their microhabitat.

Similar to Mn/Ca, the U/Ca proxy is best related to relative increases/decreases in oxygen, rather than absolute oxygen values. Higher U/Ca concentrations in foraminifera indicate more reducing sedimentary conditions, which are driven by low-oxygen
1660 concentrations in bottom and pore waters (Fig. 9e). However, these are driven by multiple processes of physical or biological nature. Specifically, high organic C fluxes can lead to low-oxygen environments in pore waters and bottom waters, which ultimately causes the in-situ precipitation of aU as foraminiferal coatings.

8.3 Description of analyses and resources required

1665 Foraminiferal elemental analyses require careful species selection, preparation and cleaning, and analytical procedures, which can vary from element to element. For example, as outlined in Table 3, the I/Ca and Mn/Ca paleo-redox proxies specifically target lattice-bound I and Mn, while the U/Ca paleo-redox proxy targets aU, meaning differential cleaning procedures are required. In addition, while recent advances have been made (Zhou et al., 2022; Cook et al., 2022), the matrices used for analyses can vary between elements, thus requiring careful consideration and in some cases inhibiting multi-elemental
1670 analyses. Below, we provide an overview of cleaning and analytical procedures for I/Ca, Mn/Ca, and U/Ca.

The foraminiferal cleaning procedures for both I/Ca and (calcite-bound) Mn/Ca are adapted from Mg/Ca protocols (Boyle and Keigwin, 1985; Barker et al., 2003). Samples are first gently crushed with cleaned glass slides to open all chambers, then cleaned by ultrasonication in deionized water to remove clays, followed by a 10-20 min boiling-water bath in NaOH-buffered

1% H₂O₂ solutions to remove organic matter, and lastly rinsed thoroughly with deionized water. It is recommended that samples with high organic matter should use additional oxidative cleaning steps (Glock et al., 2016; Winkelbauer et al., 2021). However, Mn and I analyses differ in that a reductive cleaning step is required for targeting lattice-bound Mn, as it is needed to remove authigenic Mn-oxide coatings on the exterior of the test. For I/Ca, the reductive cleaning step is not required as the iodine content in Mn/Fe oxides is minimal (Zhou et al., 2014). Further, the reductive cleaning step has been demonstrated to cause a systematic offset in I/Ca values, and perhaps even Mn/Ca (Fritz-Endres and Fehrenbacher, 2021), so is not recommended (Zhou et al., 2022). Notably, Mn-carbonate coatings are formed under reducing conditions and cannot be removed with the existing cleaning techniques. Accordingly, increased Mn/Ca values in foraminiferal calcite may either be part of the test calcite itself or present as a coating. Diagenetic contamination on the outer or inner surface of foraminiferal tests like Mn carbonates and Mn-rich oxyhydroxides can be identified with LA-ICP-MS, EMP and XRF mapping. However, Mn overgrowth inside foraminiferal pores is difficult to eliminate using LA-ICP-MS (Ni et al., 2020) due to the material inside the pores being ablated through the whole depth profile. We also need to consider that the Mn oxides can be removed through a reductive cleaning step whereas authigenic Mn carbonates cannot be eliminated using standard solution-based cleaning methods including the reductive cleaning step (Boyle and Keigwin, 1985).

In order to preserve authigenic foraminiferal coatings, only a ‘weak chemical cleaning’ protocol is used for U/Ca foraminiferal analysis, whereby only the first step of clay cleaning from the standard cleaning protocol from Barker et al. (2003) is carried out. Cleaning experiments have shown that the ‘Mg-protocol’ cleaning method (i.e. the addition of oxidative cleaning) removes the authigenic coating and therefore produces systematically lower U/Ca offsets, in comparison to clay cleaning only (Boiteau et al., 2012; Chen et al., 2017).

While I/Ca, Mn/Ca and U/Ca are all commonly measured via solution-based ICP-MS or ICP-OES, for the most accurate I/Ca results, it is best to analyse samples in a mildly basic solution (Cook et al., 2022). For example, while carbonate dissolution via 1-3% nitric acid (HNO₃) is suitable for other trace elements/Ca ratios, samples for I/Ca measurements are typically diluted in a 0.1% or 0.5% tertiary amine, tetramethylammonium hydroxide (TMAH), or ammonium hydroxide matrix to stabilize iodine in solution before analyses (Winkelbauer et al., 2021). Other trace elements are commonly diluted in a 2% HNO₃ matrix for analysis, which may be advantageous if the goal is to compare elemental data from the same foraminifera or to reduce the required sample mass and time/resources needed to separately pick, clean, and measure two sets of foraminifera in order to get separate I/Ca data. Importantly, a recent study calibrated a TMAH-nitric based matrix that allows for simultaneous measurement of I/Ca, Mn/Ca, U/Ca, and a suite of other trace elements (e.g., Li, B, Na, Mg, Al, Mn, Fe, Zn, Sr, Cd, Ba, U, and Ca) (Cook et al., 2022). The drawback of simultaneously measuring a large suite of trace elements is that the ideal cleaning and analysis procedures may vary from element to element and thus, some elements may be measured under less-than-ideal circumstances. Differences in cleaning or analytical procedure may also make comparison between datasets measured using different protocols difficult.

The most commonly used reference material for I/Ca analyses is coral JCP-1 with reported values ranging between 3.70 ± 0.27 $\mu\text{mol mol}^{-1}$, but with values as high as 4.33 ± 0.36 $\mu\text{mol mol}^{-1}$ (compiled in Lu et al., 2020), suggesting the potential for some

1710 heterogeneity and/or the need for a multi-lab intercalibration. A limestone standard (ECRM752-1) that is commonly used for Mg/Ca for inter-laboratory comparison may have a similar potential for Mn/Ca, although extensive datasets are still missing (Greaves et al., 2008).

1715 Techniques with higher spatial resolution, such as nanoSIMS and SIMS, have also been used to understand I/Ca distribution in foraminiferal tests (Glock et al., 2019; Glock et al., 2016), but there has been limited subsequent application. For Mn, in situ measurements include laser ablation (LA)-ICP-MS and SIMS for quantitative measurements, while μ XRF and conventional EPMA are usually used as semi-quantitative or relative measurements. For such high spatial resolution measurements, cleaning processes are minimal. Ca^{43} is used as the internal standard and NIST SRM 610 glass standard as the external calibration material (using established values from Jochum et al., 2011) for LA-ICP-MS. NIST SRM 612 glass (Jochum et al., 2011) and calcium carbonate pellets of MACS-3 (Jochum et al., 2012), JCp1, Jct1 and now NFHS (Boer et al., 2022) can be used as quality control material. For U, Skinner et al. (2019) showed that core-top and downcore measurements of U/Ca using LA-ICP-MS are also possible. We note that high resolution ICP-MS is not required, and a more accessible quadrupole ICP-MS may also be used. However, due to the low concentration of uranium in foraminiferal coatings (compared to, for example, Mg or Sr), ICP-OES is not sensitive enough to carry out U/Ca measurements.

Table 3. Summary of cleaning methods and analytical techniques for foraminifera I/Ca, Mn/C and U/Ca analyses.

Trace Element	Cleaning Method	Instrument for measurement	Lattice Bound/ Coating	References
I/Ca	Clay and organic matter	Solution ICP-MS	Lattice bound	Lu et al, 2010; Glock et al., 2014; Winkelbauer et al., 2021; Cook et al., 2022; Zhou, Hess et al., 2023
Mn/Ca	Clay and organic matter	Solution ICP-MS/ICP-OES LA-ICP-MS	Lattice bound	Boyle and Keigwin, 1985; Groeneveld & Filipsson 2013; Ni et al., 2020; Brinkmann et al 2023
U/Ca (Mn/Ca) (U/Mn)	Clay clean only	Solution ICP-MS/ LA-ICP-MS (coatings)	Coating	Boiteau et al., 2012, Gottschalk et al., 2016; 2020, Skinner et al., 2019; Chen et al., 2017; Umling and Thunell, 2018

1725

8.4 Future directions

There are important knowledge gaps for each of the proxies discussed above. Addressing these gaps requires an overview of water column and pore water geochemistry obtained through oceanographic and sediment and pore water sampling. Though

multi-element applications show potential (Hu et al., 2023), cross proxy calibration comparisons of I, Mn, and U in sediments or water column transects are currently lacking. We also note that there are gaps in the calibration of the various element/Ca ratios relative to oxygen. For planktic and benthic foraminifera, I/Ca ratio gaps are found around oxygen levels between 80 and 140 $\mu\text{mol kg}^{-1}$ respectively (Fig. 9). Mn/Ca measurements from oceanic settings are concentrated at oxygen levels below 70 $\mu\text{mol kg}^{-1}$ (Fig. 9c & d). The U/Ca proxy is specific to coatings, and thus is bottom water specific, but there are only a few calibrations in low-oxygen environments (Fig. 9e). Finally, the application of Mn/Ca to planktic foraminifera has hardly been explored, but some recent studies show promise that the Mn/Ca could record redox conditions in OMZs (Vedamati et al., 2015, Davis et al., 2023).

It is important to understand the impacts that vital effects may exert on element/Ca ratios. Controlled culture experiments allow the assessment of direct relationships between foraminiferal element/Ca (e.g., I/Ca and Mn/Ca) and ambient sea- and pore water elemental concentrations. Planktic foraminifera migrate through the water column during their life cycle (Schiebel and Hemleben, 2017). As such, the element/Ca signal represents an integrated signal from environments with potentially variable elemental compositions. In order to constrain pathways of element incorporation into planktic foraminiferal calcite, we need to study the life cycle of living planktic foraminifera (i.e. from plankton tows), as well as settling dead planktic foraminifera (i.e. from sediment traps), and planktic foraminifera in sediments (e.g., from core-top samples), all across the variable ambient element concentrations. This integrated framework allows us to track the proxy from seawater elemental values to the fossil record, thus integrating vital effects and diagenesis. Benthic foraminifera can actively migrate between the top of sediments and different redox zones within the sediments. To monitor the effect of their migratory behaviour on element incorporation, controlled culture experiments are needed, tracking benthic foraminifera depth habitat, calcification and bottom- and pore-water chemistry.

On a final note, analysis of successive chambers from single foraminiferal shells has shown promise for Mn/Ca when using high resolution techniques such as LA-ICP-MS (Guo et al., 2019; Petersen et al., 2018; Brinkmann et al., 2023). This approach may be further developed for I/Ca, U/Ca and other redox proxies to reconstruct short-term (seasonal to annual, since foraminifera can live up to 1-2 years) variations in paleo-records.

9 Foraminiferal assemblages

1755 9.1 Introduction

Like all organisms, foraminifera thrive when environmental conditions match their requirements. Among the environmental parameters that drive benthic foraminifera species presence and abundance, the most important are export productivity (supply of nutrients to the seafloor) and bottom water oxygenation (Jorissen et al., 1995). The tolerance of specific species to different oxygen levels has made benthic foraminifera assemblages an especially useful tool for qualitative and quantitative reconstructions of past bottom water oxygenation variability with planktic foraminifera also emerging as a tool with

understanding water column oxygenation (Sen Gupta and Machain-Castillo, 1993; Kaiho, 1994; Alve and Bernhard, 1995; Bernhard et al., 1997; Baas et al., 1998; Nordberg et al., 2000; Jannink, 2001; Schmiedl et al., 2003; Leiter and Altenbach, 2010; Ohkushi et al., 2013; Tetard et al., 2017; Sharon et al., 2021; Erdem et al., 2020; Tetard et al., 2021; Tetard et al., 2024).

9.2 Historical perspective on foraminifera assemblages

1765 The use of benthic foraminiferal assemblages as indicators of environmental conditions began with their application as proxies
for paleobathymetry (Bandy, 1953). Since then, numerous studies have established connections between the distribution of
benthic foraminifera and various environmental parameters, with particular emphasis on oxygenation in open ocean settings
(e.g., Phleger and Soutar, 1973; Lutze and Coulbourne, 1984; Mackensen and Douglas, 1989; Sen Gupta and Machain-Castillo,
1993; Bernhard et al., 1997; den Dulk et al., 1998; Jannink et al., 1998; Levin et al., 2002; Schumacher et al., 2007; Cardich
1770 et al., 2012, 2015; Mallon et al., 2012; Cauille et al., 2014). Certain species inhabit regions characterized by sustained low-
oxygen concentrations, such as the OMZs in the Pacific Ocean (Smith, 1964; Bernhard et al., 1997; Bernhard and Sep Gupta,
1999; Cardich et al., 2012; 2015; Mallon et al., 2012; Erdem et al., 2020; Castillo et al., 2021; Tavera Martínez et al., 2022),
and Arabian Sea (Hermelin and Shimmield, 1990; Cauille et al., 2015; Gooday et al., 2000; Jannink et al., 1998), as well as in
restricted basins and fjords (Bernhard and Alve, 1996; Leiter and Altenbach, 2010; Nordberg et al., 2000; Bouchet et al., 2012;
1775 Fontanier et al., 2014). Culture studies have confirmed the ability of certain species of both benthic and planktic foraminifera
to survive (Alve and Bernhard, 1995; Moodley and Hess, 1992; Moodley et al., 1997; Geslin et al., 2004, 2014; Bernhard and
Alve, 1996), calcify (Kuroyanagi et al., 2013; Nardelli et al., 2014), and thrive (Bernhard, 1993; Enge et al., 2016; Orsi et al.,
2020) under very low-oxygen and even euxinic conditions (Fig. 10).

Oxygen-depleted marine environments are often characterized by a high organic carbon rain rate, and these two factors together
1780 influence the habitat depth, abundance, and assemblage composition of benthic foraminifera (e.g., Lutze and Coulbourn, 1984;
Corliss and Emerson, 1990; Loubere, 1994; Altenbach et al., 1999; Gooday and Rathburn, 1999; Geslin et al., 2004). The
Trophic-Oxygen, or TROX, model which was the first to consider food and oxygen availability as key factors in determining
benthic foraminiferal assemblages and microhabitat (Barmawidjaja et al., 1995; Jorissen et al., 1995), though other
considerations such as food quality and nitrate concentrations are also predictive (Jorissen et al., 2022). The oxygen
1785 concentration in pore water is influenced not only by bottom-water oxygen concentration but also by respiration in pore waters,
which relates to the organic matter content in the sediments. Thus, bottom-water oxygen concentration is a key driver for
infaunal foraminifera living deeper in the sediments (Jorissen et al., 1995), particularly because several infaunal species have
been shown to denitrify (a form of respiration without of oxygen; Risgaard-Petersen et al., 2006). A more detailed discussion
of this phenomenon will follow.

1790

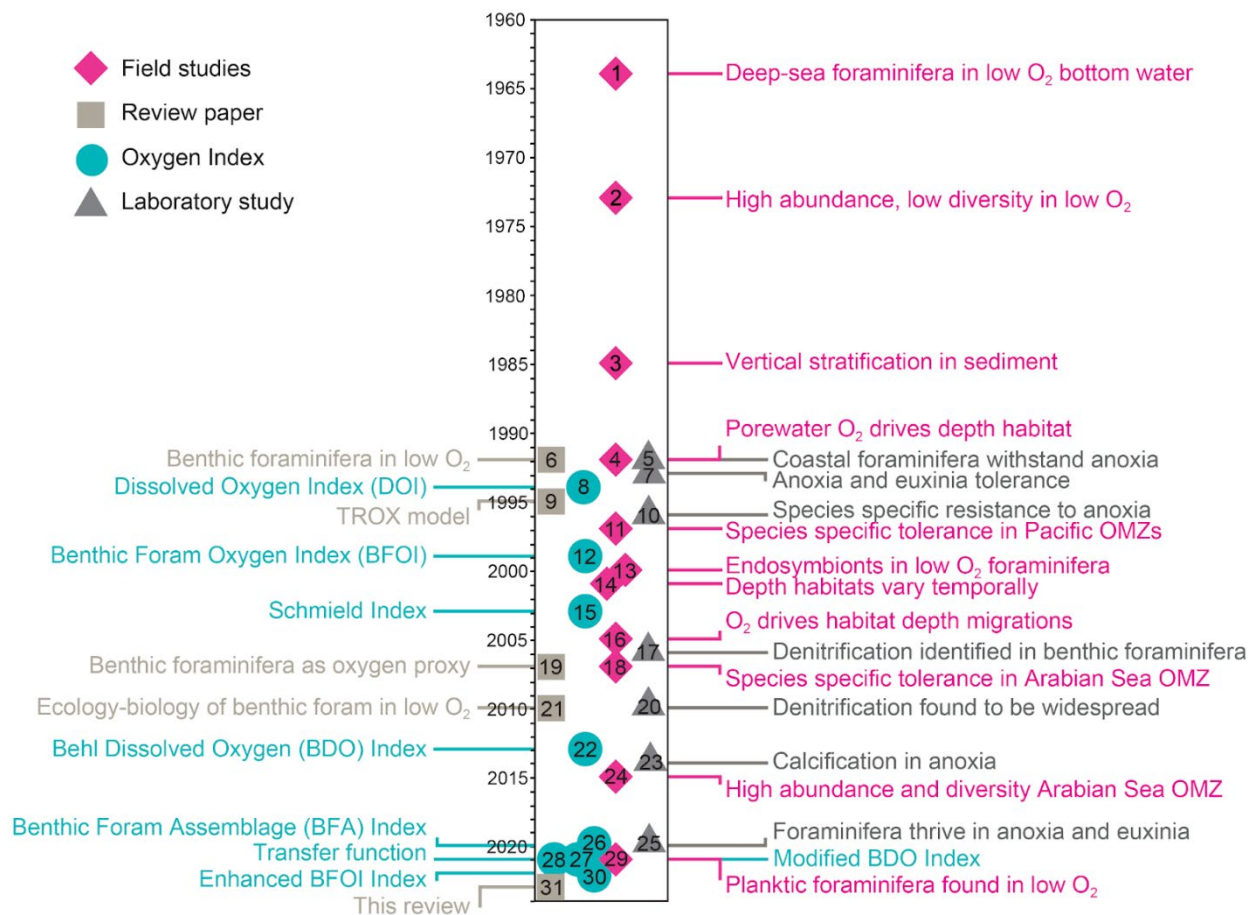


Figure 10: Timeline of key discoveries and advances regarding physiology, ecology and proxy development based on benthic and planktic foraminifera since the 1960's including field and laboratory studies, oxygen indices and review papers. 1. Smith (1964), 2. Phleger and Soutar (1973), 3. Corliss (1985), 4. Bernhard (1992), 5. Moodley and Hess (1992), 6. Sen Gupta and Machain-Castillo (1993), 7. Bernhard (1993), 8. Kaiho (1994), 9. Jorissen et al. (1995), 10. Bernhard and Alve (1996), 11. Bernhard et al. (1997), 12. Kaiho (1999), 13. Bernhard et al. (2000), 14. Alve and Murray (2001), 15. Schmieidl et al. (2003), 16. Fontanier et al. (2005), 17. Risgaard-Petersen et al. (2006), 18. Schumacher et al. (2007), 19. Jorissen et al. (2007), 20. Piña-Ochoa et al. (2010a), 21. Koho and Piña-Ochoa (2010), 22. Ohkushi et al. (2013), 23. Nardelli et al. (2014), 24. Caille et al. (2015), 25. Orsi et al. (2020), 26. Erdem et al. (2020), 27. Sharon et al. (2021), 28. Tetard et al. (2021a,b), 29. Davis et al. (2021), 30. Kranner et al. (2022), 31. This review.

1795

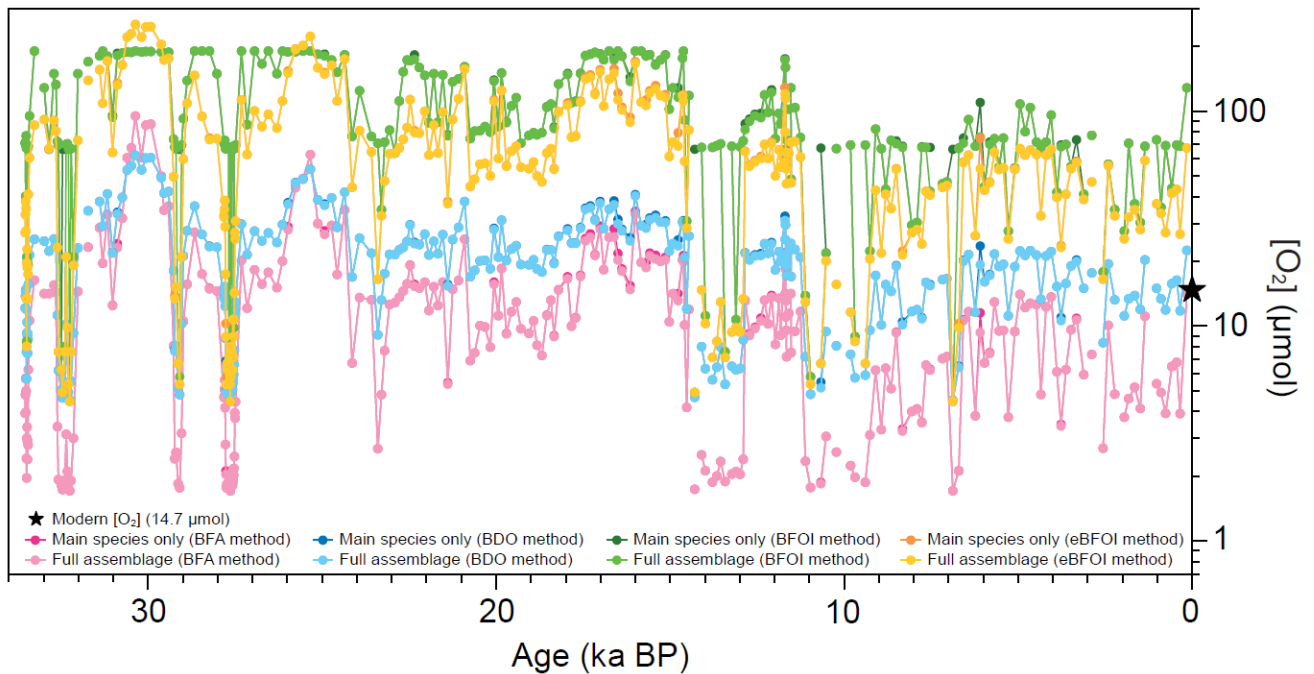
1800

Ecological studies have identified benthic foraminiferal species that can serve as indicator taxa for low-oxygen conditions, and the association of specific species with quantitative ranges of bottom water oxygen. Several studies have developed indices to reconstruct paleo-oxygen levels based on benthic foraminiferal assemblages (e.g., Kaiho, 1994, 1999; Jannink, 2001; Schmieidl et al., 2003, review in Jorissen et al., 2007; Ohkushi et al., 2013; Tetard et al., 2017; Sharon et al., 2021; Erdem et al., 2020; Tetard et al., 2021, Kranner et al., 2022, Tetard et al., 2024), which are summarized here (Fig. 10). The benthic foraminiferal oxygen index (BFOI) developed by Kaiho (1994, 1999) considers the relative proportion of taxa indicative of low bottom or pore water oxygen conditions compared to the total fauna. Another index developed by Jannink (2001) focuses on the presence of oxyphilic species, which consistently inhabit the top centimetre of sediment. Schmieidl et al. (2003) proposed a method

1805

based on a combination of the relative proportion of low-oxygen tolerant species and a diversity index. Ohkushi et al. (2013) developed a new index using thresholds of oxygen tolerance for different species and paleoenvironment assessments through principal component analysis (PCA) of assemblages. Tetard et al. (2017, 2021a) also used PCA and calibrated transfer functions to semi-quantitatively reconstruct benthic oxygen offshore California during the last 80 kyrs. Sharon et al. (2021) presented downcore applications using a modification of the Ohkushi et al. (2013) index, updated through comparison with modern assemblages from core-top studies and cross-checked with redox-sensitive trace metals. Erdem et al. (2020) employed a transfer function approach, using living Rose Bengal-stained benthic assemblages and prevailing oxygen concentrations as a regional analogue for downcore environments. More recently, Tetard et al. (2021) proposed the use of the relative abundance of *Eubuliminella exilis* (*Buliminella tenuata*) as a proxy, calibrated with average bottom-water oxygenation and core-top samples predominantly from the Pacific Ocean. A recent attempt to quantify paleo oxygen updates the original BFOI from Kaiho (Kraner et al., 2022). The enhanced BFOI (EBFOI) considers multiple indicator species and transfer functions for both bottom water and pore water oxygen concentrations. Finally, Tetard et al. (2024) published an update of the BFA index, the BFAex, which extends its range of applicability, based on the compilation of census data of over 1500 benthic foraminifera species from ~ 1700 samples recovered from the BENFEP database (Diz et al., 2023). Continued improvement and implementation of these approaches are active areas of research.

All assemblage-based proxies are empirical with weaknesses identified by several authors (e.g. Buzas et al., 1993; Gooday, 2003 and Jorissen et al., 2007). Buzas et al. (1993) identified a lack of replicate observations prior to assignment of species to a microhabitat preference, while Gooday (2003) and Jorissen et al. (2007) note that the availability of food might be as important for the distribution of foraminifera as oxygen. Furthermore, when applied to extinct foraminifera species, they will lack any observation of microhabitat. In such cases microhabitat assignment is based on the morphology (i.e. size and shape) (e.g. Kaiho, 1994), though violations of morphologically-based assumptions are known even in modern foraminiferal species. For example, while large trochospiral forms are used as indicators for oxic conditions (Kaiho, 1994), several *Ammonia* species match this morphology but thrive in anoxic shallow water environments (e.g. *Ammonia confertitesta*, see Richirt et al., 2022). Further refinement of indices and calibrations will increase reliability of these proxies, while careful consideration of limitations, depositional environment, and specific question can improve applications.



1835

Figure 11: Comparison of past oxygen reconstructions for core site MD02-2503 (Okhushi et al., 2013) comparing main species (determined by a PCA on the census data, usually corresponding to species with an averaged relative abundance >5%) with the complete assemblage. This comparison was performed using 4 dissolved oxygen estimation methods: the BFOI (Kaiho, 1994), the BDO (Okhushi et al., 2013), the BFA (Tetard et al., 2021), and the eBFOI (Kranmer et al., 2022). Black star shows the modern oxygen value at the core site. Note that there is significant overlap between the “Main species only” and “Full assemblage” approaches in all four methods, which makes the curves hard to distinguish.

1840

Identifying where whole assemblages or indicator taxa are most useful will also improve reconstructions. There is active debate whether it is advantageous to use full assemblages (e.g., Sharon et al., 2021), only the dominant species (e.g., Tetard et al., 2017), or only indicator species (see also Fig. 11). For example, a comparison of indices applied to a sediment core from the Californian Margin demonstrates that while different indices follow the same trends, large offsets exist in quantitative oxygen reconstructions (Fig. 11). It is likely that different approaches are appropriate for different environments and questions. For example, in environments with a high degree of temporal or spatial averaging, use of indicator species may be more successful in positively identifying low-oxygen events. However, use of indicator species alone may limit the range of oxygen conditions reconstructed. These hypotheses deserve more rigorous testing.

1850

Planktic foraminifera inhabit the water column above the seafloor. As most species occupy a near-surface habitat, planktic foraminiferal assemblages have primarily been used to reconstruct sea surface or mixed layer temperature and, to a lesser extent, conditions such as productivity, salinity, and stratification (e.g., Imbrie & Kipp et al., 1971; Kipp, 1976; Cayre et al., 1999; Kucera et al., 2005; Morey et al., 2005; Kucera, 2007; Sicca et al., 2009). However, certain extant species of planktic foraminifera, including *Hastigerinella digitata* and *Globorotaloides hexagonus* have been observed in low-oxygen pelagic environments (Hull et al., 2011, Davis et al., 2021), with the latter taxon subsequently used to infer past distribution of low-

1855

oxygen water in the open ocean (Davis et al., 2023). Some extinct species of planktic foraminifera, particularly those with digitate morphologies such as the clavigerinellids, have also been associated with low-oxygen environments (reviewed in Coxall et al., 2007). As planktic foraminiferal assemblages integrate across multiple distinct depth habitats, the use of indicator species rather than relative abundance is generally more appropriate for interpreting paleo-oxygenation. A notable example is the use of biserial chiloguembelinids, interpreted as OMZs-dwellers based on isotope records (Boersma et al., 1987, Boersma and Premoli Silva, 1989, Luciani et al., 2020). The presence of their shells has been used to infer the presence of a pelagic OMZ in Paleocene to Oligocene sediments (e.g., Corfield & Shackleton, 1988; Pardo et al., 1997; Luciani et al., 2020).

9.3 Analyses and Required Resources

The majority of foraminiferal assemblages relevant to Cenozoic oxygen reconstructions are obtained from sedimentary records, with a smaller portion coming from lithified outcrops. For the purposes of this review, we will focus on the sedimentary records. Collecting samples from subtidal stations, ranging from coastal to abyssal environments, often requires the use of seagoing vessels. However, the study of foraminiferal assemblages is relatively inexpensive once sediment samples have been collected. Prior to analysing assemblages, sediment samples typically undergo various laboratory treatments. These may include disaggregation using hexametaphosphate, wet or dry sieving to separate different size fractions, and sample splitting. Standard size fractions include 63, 125, or 150 μm , and sometimes 32 or 250 μm , with choice of size influencing the composition of the represented assemblage such that careful attention needs to be paid that these match size fractions used by a transfer function, if applicable. The subsequent steps involve ‘picking’, isolating and sorting foraminiferal tests using a fine brush and black tray, and gathering the specimens in micropaleontological slides. Standard collection and counting procedures have been reviewed by Schönfeld (2012).

It is important to highlight that conducting robust counts requires an even split of the sample. Typically, a split containing 200–300 specimens is considered sufficient for evaluating species assemblages with a reasonable degree of accuracy (Patterson & Fishbein, 1989). This number could be lower if only the most abundant species are being considered, but may be insufficient if rare species are important to the analyses (Fatela & Taborda, 2002). This work is carried out using an optical stereomicroscope equipped with a light source. Best practices also require documenting taxonomic attribution using either a high-resolution camera or a Scanning Electron Microscope (SEM). Ultimately, the most crucial resource needed for these analyses is a trained researcher or technician, skilled in taxonomic identification of foraminiferal species. It is worth noting that acquiring such ability is relatively accessible compared to the taxonomy of macrofauna.

9.4 Recent Advances

Several recent advances in analytical methods have shown promise in automating labour-intensive aspects of foraminiferal assemblage analysis. This is exemplified by the utilization of high through-put imaging and artificial intelligence (AI) neural networks to generate species-level identifications (Mitra et al., 2019; Hsiang et al., 2019; Marchant et al., 2020). These methods have been combined with mechanical shell sorting to further enhance efficiency (Mitra et al., 2019; Richmond et al., 2022).

1890 While the current applications of automatization techniques have been primarily focused on planktic foraminifera, Marchant et al. (2020) have also included a few benthic taxa. Although these approaches are still in their early stages, the use of AI to generate assemblages holds tremendous potential, especially as models can be trained on an increasing number of species. Another important advancement is the increased availability of imaging technology. This includes the use of high-resolution digital cameras, enabling high-quality, true-colour imaging (e.g., Erdem and Schonfeld, 2017; Wilfert et al., 2015), as well as the growing popularity of desktop or environmental SEMs. Both approaches enhance the speed and cost-effectiveness of
1895 generating and sharing assemblage data. Alongside improved data storage capabilities, both internally and in online repositories, the sharing of images can and should continue to increase the transparency and reproducibility of assemblage work. The best practice for assemblage work is that all, or at least a representative subset, of images should be published alongside manuscripts. Furthermore, efforts should be made to ensure that images are uploaded to publicly available archives or repositories and stored as supplementary media whenever permitted by journals. The inclusion of images in publications
1900 and their archival in digital repositories offer several benefits to the scientific community. Firstly, it increases reproducibility, as other researchers can refer to the images for verification, validation, and comparison. Secondly, it facilitates resolution of taxonomic and nomenclature issues related to key indicator species. This is particularly important considering as taxonomic revision is ongoing.

9.5 Environmental influences

1905 Most benthic foraminifera have the ability to survive at relatively low oxygen concentrations of around 1-2 ml L⁻¹ or 44.6 - 89.3 μmol kg⁻¹ (Jorissen et al., 1995; Bernhard et al., 1997; Van der Zwaan et al., 1999; Levin et al., 2001; Murray, 2001; Geslin et al., 2011). Some species are even able to survive, calcify and reproduce under anoxia (Langlet et al., 2013 & Nardelli et al., 2014) possessing diverse adaptations and survival strategies to oxygen depleted conditions (reviewed in Glock 2013). Thus, it is only below this threshold that oxygen is expected to be a key driver of assemblage composition and robustly
1910 quantifiable. While oxygen concentrations and the tolerance of individual species are important factors, designating species as low-oxygen indicators is an ecological oversimplification, but a useful one. Other factors such as food supply, biogeography, differing metabolic strategies, habitat depth, and other environmental gradients including temperature and salinity, all contribute to defining ecological ranges. Some species may be opportunistic rather than specifically adapted to low-oxygen conditions. Other species may possess a unique tolerance to very low-oxygen or have metabolic adaptations that allow them
1915 to utilize alternate electron receptors. Although low-oxygen adapted species may survive in oxic environments, their relative abundance increases when oxygen becomes a limiting factor and competition with other species decreases. Tetard et al. (2024) detail dissolved oxygen affinities and ranges of 200 common occurring species from the Pacific.

There is a particularly complex interplay between organic matter flux and oxygenation of bottom and pore waters. In general, higher organic matter content leads to higher remineralization rates, i.e. through decomposition of organic material, and
1920 subsequent oxygen consumption, resulting in lower dissolved oxygen concentrations in pore waters. This covariation can make it challenging or impossible to differentiate between the two drivers. Indeed, many indicator species can be viewed as

specialists adapted to high productivity that also happen to tolerate low-oxygen conditions. This is likely the case for taxa such as *Bulimina*, *Bolivina*, and *Nonionella* (Margreth et al., 2009), which are rare in oligotrophic low-oxygen conditions, but found in highly productive, yet oxic, regions.

1925 Discrepancies can also be observed between geographical areas with similar bottom water oxygenation, particularly in defining specific indicator taxa. For example, *Uvigerina peregrina* is typical of OMZ environments in the Pacific and Arabian Sea, where it can be used in oxygen reconstructions (e.g., Moffitt et al., 2014; Schumacher et al., 2007). However, the same species is considered a high productivity indicator in the relatively well oxygenated waters of the Northeast Atlantic (e.g., Lutze and Coulbourn, 2984; Fontanier et al., 2005; Mojtahid et al., 2017). Similar observations apply to *Nonionella stella* (Moffitt et al., 1930 2014; Diz and Francés, 2008). In some cases, these geographic differences may highlight the complexity of food and oxygen as co-drivers, or they may suggest the presence of unknown environmental drivers, cryptic species, or adaptive differences between populations.

Benthic foraminifera are distributed throughout the upper centimetres of the sediment column, and their depth habitat is influenced by the availability of food, oxygen, ecosystem stability, bioturbation, and competition for resources (Jorissen et al., 1935 2007 and references therein). In oligotrophic conditions, particularly open ocean settings, most species tend to occupy the uppermost sediment levels to maximize access to food exported from the photic zone (Linke and Lutze 1993). However, other factors such as the quality of food, with fresh phytodetritus sometimes preferred, can also have an impact (Smart et al., 1994; Gooday & Hughes, 2002). In eutrophic conditions, where oxygen levels are low, the depth habitat of benthic foraminifera is determined by the capability of the species or assemblage to tolerate low-oxygen (Jorissen et al., 1995). A key consequence of 1940 variability in habitat depth is that not all benthic foraminifera at a particular site will experience the same environmental conditions (Tetard et al., 2021a). This variability in sediment depth habitat not only impacts assemblage composition, but also plays a fundamental role in other oxygen proxies such as $\Delta\delta^{13}\text{C}$ (Section 11) and determines the chemical microenvironment that is recorded by trace metal proxies (Section 8).

While oxygen concentration may be limiting for many species, certain adaptations, including anaerobic metabolisms like 1945 denitrification, enable some foraminifera to persist even in euxinic conditions (Orsi et al., 2020). Deep-infaunal *Globobulimina* spp. (i.e. *G. turgida*, *G. pacifica*, *G. affinis*), and *Chilostomella* spp. (i.e. *C. ovoidea*, *C. oolina*) inhabit anoxic sediments below the oxygen and nitrate penetration depth (e.g., Jorissen et al. 1998; Schönfeld 2001; Fontanier et al. 2002, 2003, 2005; Koho et al. 2007, 2008a; Glud et al. 2009). These species are capable of storing nitrate and as well as respiring nitrate in absence of oxygen (Risgaard-Petersen et al., 2006; Piña-Ochoa et al., 2010a, b; Koho and Pina-Ochoa, 2012). They can be considered 1950 facultative (an)aerobes. The foraminiferal denitrification pathway is a rare example of eukaryotic denitrification (Woehle et al., 2018; Gomaa et al., 2021), and while foraminifera appear to perform only incomplete denitrification, the missing steps are likely completed by bacterial symbionts (Bernhard et al., 2010; Woehle et al., 2022). Intracellular nitrate accumulation has been found in species including *Nonionella cf. stella*, *Uvigerina akitaensis*, and *Bolivina spissa* (Høgslund et al., 2008; Glud et al. 2009). Some species even exhibit a metabolic preference for nitrate over oxygen with nitrate concentrations rather than 1955 oxygen concentrations being limiting (Glock et al., 2019; Suokhrie et al., 2020). Dormancy has also been identified as an

adaptive response to short-term oxygen depletion (LeKieffre et al., 2017; Ross and Hallock, 2017). A comprehensive review about the survival strategies of foraminifera under low-oxygen conditions is given in Glock (2023). However, due to the limited number of species that have evolved these adaptations, oxygen-depleted conditions are characterized by lower species diversity and higher dominance compared to oxygenated settings (Phleger and Soutar, 1973; Sen Gupta and Machain-Castillo, 1993; Gooday et al., 2000, Levin, 2003; Koho and Ochoa, 2011).

The role of oxygen as a driver of planktic foraminiferal abundances is not as well-established as in benthic foraminifera, however it is likely that the key environmental drivers in low-oxygen environments are similar. A combination of drivers including accessibility of food, and either tolerance of or adaptations to low-oxygen are probable. Some planktic low-oxygen specialists, such as *H. digitata* and *G. hexagonus*, do not seem to occur in oxic environments, and may possess special adaptations to low-oxygen. It remains unknown whether more widely distributed deep-dwelling species such as *Globorotalia scitula* or *Globorotalia truncatulinoides*, whose habitat intersects low-oxygen waters, can opportunistically persist across both oxic and low-oxygen environments.

9.6 Marine archives and limitations

Reconstructions based on foraminiferal assemblages can be applied in any marine environment where foraminiferal shells are deposited and preserved in relatively undisturbed sediments. This includes fjord, estuarine, supratidal shelf, and deep-sea (including continental shelf) environments above the lysocline. While foraminiferal archives are widely available, they are most useful as oxygen indicators in low-oxygen environments, where oxygen limitation is a meaningful driver of assemblage composition. The use of foraminiferal assemblages may be more limited in settings where it is more difficult to deconvolve oxygen and productivity as drivers.

Low carbonate saturation state environments also pose a limitation, where living calcareous species are rare or absent due to unfavourable conditions (Bernhard et al., 2009; Dias et al., 2010; Petit et al., 2013; Martinez et al., 2018). Taphonomic processes in such environments can further complicate interpretations. Corrosive bottom or pore waters can lead to preferential dissolution of small, thin-walled species, or those with a spiral arrangement of chambers (Berger, 1973; Hecht et al., 1975; Nguyen et al., 2009, 2011, 2014), or even lead to the complete loss of calcareous foraminifera (Gutiérrez et al., 2009), potentially altering the preserved assemblage. Thus, while dissolution could impact different methods differently (i.e. use of only indicator species vs diversity metrics), it should always be considered. Dissolution can pose limitations, particularly in very low-oxygen or high productivity sites where high respiration rates can result in both low carbonate saturation states and oxygen-depleted conditions.

Fossil assemblages contain individuals that lived over a period of time, depending on factors such as sedimentation rate and degree of sediment mixing. Within a single centimetre of sediment, it is possible to find foraminiferal species that lived contemporaneously or thousands of years apart (e.g. Hupp et al., 2019, 2022; Hupp and Kelly, 2020). This complication is common to all marine sedimentary records, but it poses specific concerns for foraminifera. One important factor to consider is the vertical migration of infaunal species within the sediment column, which can occur over several centimetres (Alve and

Murray, 2001; Jorissen et al., 1995; Duijnsteet al., 2003). As a result, older fossil epibenthic foraminifera can be recovered alongside younger infaunal specimens. This vertical movement of species contributes to the phenomenon of time-averaging in fossil assemblages. In environments with seasonal or short-term variation in oxygen levels, the presence of both oxic and low-oxygen taxa as part of the same death assemblage can limit high temporal resolution reconstructions using foraminiferal assemblages, rather than indicator taxa. However, this time-averaging effect can also offer opportunities to investigate seasonal contrasts. For instance, when species from contrasting environmental settings occur together in the same samples, it could indicate large seasonal (e.g. Stassen et al., 2015; Wagner et al., 2022), or other short-term differences in oxygenation at the site. Foraminifera populations can fluctuate over inter-annual and seasonal time scales even in the deep sea (Heinz and Hemleben, 2003, Goineau and Gooday, 2019). Due to these temporal variabilities and the spatial variations (patchiness) within the foraminiferal assemblages, replicate samples might be required to provide a realistic assessment of the species-level composition of modern assemblages. Nevertheless, in intertidal to nearshore environments, log-normal distributions of foraminiferal standing stocks appear to be a pervasive feature (Schönfeld et al., 2023) and internal reproducibility of the analysis of foraminiferal assemblage compositions has been shown to be within ~2% (Schönfeld et al., 2013).

Another challenge in interpreting foraminiferal assemblages is the occurrence of “no-analogue” fauna, where taxa that are not observed together in modern environments coexist in the sediment record. This poses a potential limitation as most identification and quantification of relationships between assemblages or indicator species and oxygenation are based on observations in the modern ocean. The presence of no-analogue fauna can have different explanations. Time-averaging can create assemblages that do not reflect the present-day co-occurrence patterns. In other cases, the limited range of modern sites used for calibration may not capture the full spectrum of environmental conditions that have existed throughout space and time. Consequently, there may be gaps in our understanding of the relationships between foraminiferal assemblages and oxygenation in certain environments. This highlights the need for further research and a broader spatial and temporal sampling of modern environments to improve our understanding of foraminiferal assemblage dynamics and their relationship with oxygenation.

9.7 Future Directions

Open Questions

To improve reconstructions of past oxygen levels based on foraminiferal assemblages, it is crucial to enhance our understanding of foraminiferal ecology. By doing so, we can distinguish between opportunistic species driven by food availability and true low-oxygen specialists. Exploring ecological questions related to seasonality and physiological oxygen tolerances in key species is also important. Understanding the constraints and variations in seasonality can provide insights in the temporal dynamics of foraminiferal assemblages and their response to changing oxygen conditions. Investigating the physiological oxygen tolerances of different species, while considering interactions between oxygen, food availability, and carbonate chemistry stresses, will contribute to a more comprehensive understanding of their ecological responses.

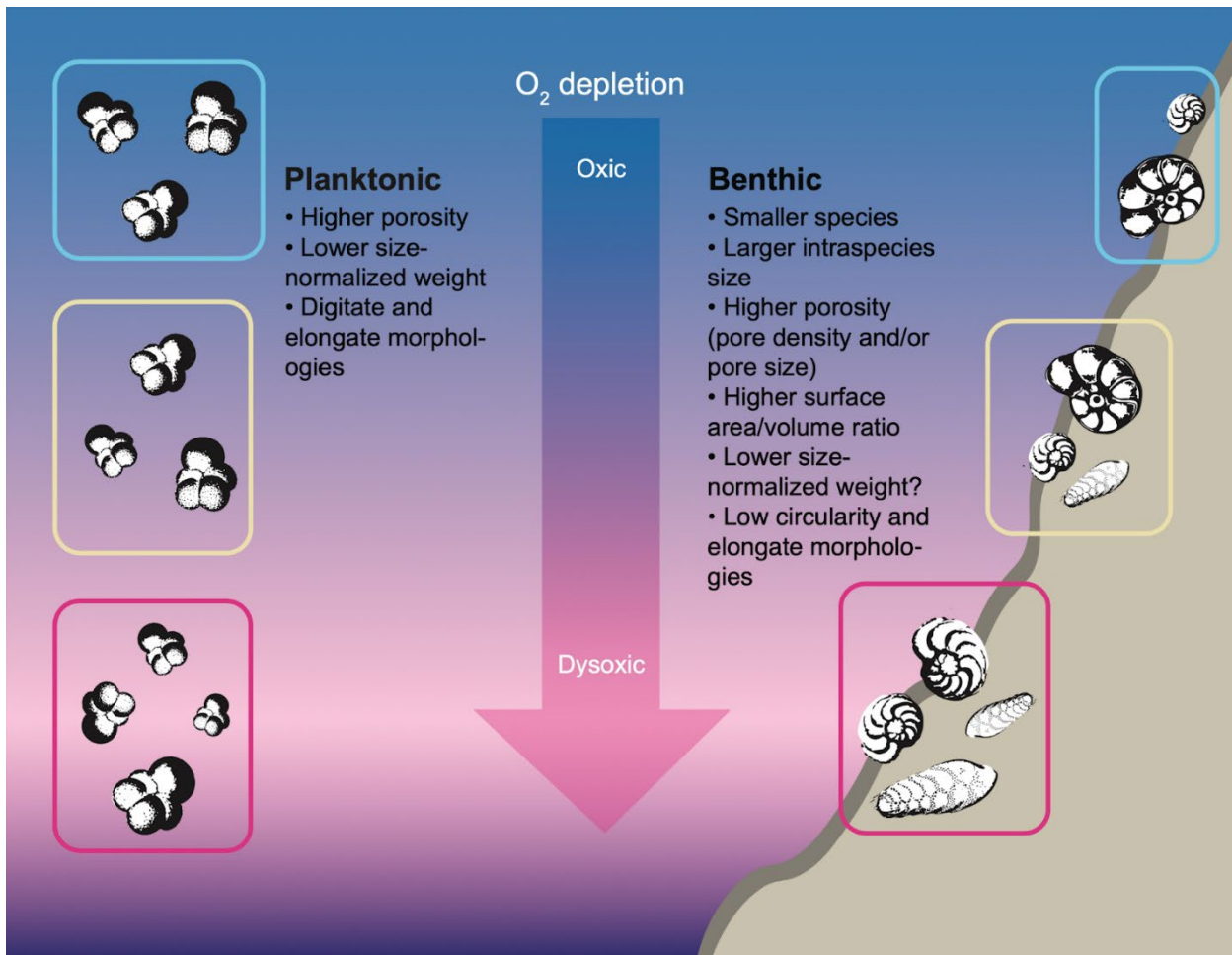
The exploration of metabolic adaptations and the role of oxygen and nitrogen respiration in different species and environments is another avenue of research. New technologies, such as the increasing availability of genetics and genomics' analyses hold promise for addressing these metabolic questions (Woehle et al. 2018; Orsi et al., 2020; Gomaa et al., 2021) and explaining the variations in optimal oxygen ranges observed among geographically disparate populations. These advanced techniques can provide valuable insights into the underlying mechanisms and adaptations that allow foraminifera to thrive in low-oxygen environments. It is important to note that while this discussion has focused primarily on benthic foraminifera, addressing the same suite of questions for planktic foraminifera is equally important and will improve the use of planktic assemblages for reconstructing pelagic oxygenation. Environmental DNA metabarcoding (eDNA) of foraminifera is another evolving method that might even be applied to paleoreconstructions of foraminiferal assemblages in environments, where ancient DNA can be preserved in sediments (Pawlowska et al., 2022, Barrenechea Angeles et al., 2023). Continued focus on foraminiferal ecology can facilitate the integration of “traditional” assemblage-based proxies with emergent proxies, leading to more comprehensive reconstructions. Understanding the ecological and physiologic drivers of foraminiferal oxygen tolerance can help researchers to determine where regionally-specific or global calibrations are appropriate and which species should be considered. This will be crucial when applying calibrations developed in specific times and regions, such as the modern Pacific, to other times and places. It is especially relevant when comparing restricted basins and fjord environments to open ocean OMZs. Understanding the species-specific responses to varying oxygen content and co-stressors can be achieved through advances in culturing techniques, enabling analyses of assemblage-level changes (Bernhard et al., 2021). Furthermore, denitrifying species capable of living across large oxygen gradients can serve as target species for complementary proxy approaches, such as foraminiferal morphometrics and geochemistry. These approaches can provide additional insights into environmental conditions and further enhance our ability to reconstruct past oxygen levels.

While foraminiferal assemblages form the basis of some of the more established approaches for constraining marine oxygenation, a lack of sensitivity to oxygen higher than 1-2 ml L⁻¹ (45-89 μmol kg⁻¹) remains a key limitation. The inclusion of other fossilizing organisms in addition to foraminifera is one solution for extending oxygen reconstructions into more oxic conditions. This potential is reviewed briefly in Gooday et al., (2009) and discussed in Myhre et al. (2017). By incorporating groups such as brachiopods, mollusks, ostracods, brittle stars, sponges and other organisms with hard parts recoverable in marine sediments, a composite index could be developed that is sensitive to intermediate oxygen concentrations. This expanded approach would provide a more comprehensive understanding of past oxygen levels.

The use of foraminiferal assemblages for reconstructing oxygenation has a robust, decades-long history. Due to the time consuming nature of this approach and recent advances in genetic methods, traditional morphology-based taxonomists are getting rarer, though distinction of morphologically similar species is often crucial also for geochemical approaches. However, studying foraminiferal assemblages remains an area of active research. Advancements in both knowledge and technological applications continue to expand the utility of foraminiferal assemblages as an oxygen proxy. Lessons from this approach have already and will continue to inform other foraminifera-based proxies and it is likely that it will remain in the toolkit of paleoceanographers for years to come.

10.1 Introduction

The principles behind the use of foraminiferal assemblages have sometimes been distilled into a few morphological traits, primarily size and shape. Most extant low-oxygen tolerant species share several features. The calcareous hyaline foraminifera, often have thin, porous test walls such as those seen in *Bolivina* and *Globobulimina* species (e.g., Kaiho, 1994; Sen Gupta & Machain-Castillo, 1993; Bernhard & Sen Gupta, 2003; Gooday, 2003; Boltovskoy et al., 1991; Caille et al., 2014). Conversely, larger Nodoriiidae species like *Dentalina*, *Lagena*, and *Nodosaria* species are associated with well-oxygenated conditions in modern settings. In terms of shape, more circular epifaunal species like *Cibicides* and *Planulina* species dominate during oxygenated conditions, while elongated infaunal species like *Eubulimina*, *Bolivina*, and *Brizalina* species migrate to the water-sediment interface, and dominate the benthic foraminiferal record during oxygen-impooverished periods (Jorissen et al., 1995, 2007; Palmer et al., 2020). These observations of size and shape have been crucial to the development of indices, based on test morphology and individual size. Today, the morphology of foraminiferal shells, both within and across species, is widely understood to reflect environmental conditions, including oxygenation (Fig. 12 and Tab. 4). Specific features include those influenced by in situ calcification environment, such as shell porosity, size, ornamentation features (e.g., spines, costae and keels), shape, and coiling direction. It also includes features influenced by the carbonate saturation state of the depositional environment where the shells are deposited. These can manifest as shell density changes, pitting or other dissolution features. Some features like shell thickness or size-normalized weight can be affected by both growth and depositional environments. Out of these metrics, porosity (percentage of pore area of total shell surface) and pore density (number of pores per surface area) have received particular attention as proxies for redox conditions and they will be the primary focus of this section (Petersen et al., 2016; Rathburn et al., 2018; Glock et al., 2011, 2018 & 2022; Tetard et al., 2017; Richirt et al., 2019; Lu et al., 2022). Shell size and circularity, especially within the context of the Major Axis and Roundness INdex (MARIN; Tetard et al., 2021), will be discussed as well.



2080 **Figure 12: Cartoon showing the response of different foraminiferal morphometrics to changes in oxygen concentrations. Typical conditions at a continental margin OMZ are used as an example. For an overview of methods, see Tables 4 and 5.**

10.2 Historical Perspective

10.2.1 Porosity and Pore Density

2085 Porosity is defined as the percentage of pore area relative to the surface area of the foraminiferal shell. Pore density is defined as the number of pores per surface area. The two measures are distinct, but tightly linked: larger pores at constant pore density result in a higher porosity. A detailed review of pores as an oxygen proxy in foraminifera can be found in Glock et al. (2012), and is summarized here. The first studies of the morphology and fine structure of pores in foraminiferal tests go back to the middle of the 20th century. Advances in electron microscopy during this period allowed scientists to describe “pore plates” or “sieve plates” that cover the pores of many benthic foraminiferal species (Le Calvez, 1947; Jahn, 1953; Arnold 1954; Angell
2090 1967; Sliter, 1974; Berthold, 1976, Leutenegger, 1977). There was also early evidence for strong environmental influences on

2095 pore density and other morphological features in *Bolivina spissa* and other closely related bolivinids (Lutze, 1962; Harmann, 1964). In the 1980s and 1990s more studies described the correlation between pore size and pore density in benthic foraminifera and ambient oxygen concentrations and species with higher porosity having been suggested as indicators for oxygen-depleted conditions (Bernhard, 1986; Perez-Cruz and Machain-Castillo, 1990; Moodley and Hess, 1992; Sen-Gupta and Machain-Castillo, 1993; Kaiho, 1994). Since then, several studies have shown that in some species of benthic foraminifera, individuals living in oxygen-depleted environments have higher pore density and porosity than conspecifics in well-oxygenated conditions (Glock et al., 2011; Kuhnt et al., 2013, Petersen et al., 2016, Rathburn et al., 2018; Richirt et al., 2019, Lu et al., 2022). Over the past decade, the porosity and pore density of foraminifera has evolved from a qualitative indicator for redox conditions towards a quantitative proxy.

2100 Shell porosity as an oxygen proxy has received less attention in planktic foraminifera. Bé (1968) initially interpreted the porosity of planktic foraminifera as a potential temperature proxy due to a significant correlation between the porosity and latitudinal temperature gradients. A correlation between temperature and porosity was more recently validated in culture, with higher porosity interpreted as the result of the increase in metabolic rates with increasing temperature (Burke et al., 2018). Differences in porosity have also been observed with oxygen (Kuroyanagi et al., 2013; Davis et al., 2021). Notably, Kuroyanagi et al. (2013) report smaller pores in the final spherical chamber of the shallow, symbiont-bearing foraminifer *Orbulina universa* cultured under low-oxygen conditions. Davis et al. (2021) report higher porosities in the youngest chambers of deep-dwelling, low-oxygen affiliated species *Globorotaloides hexagonus*. The differences in these observations could reflect either inter-species variability, ecological specificity, or a difference in the metric (pore size vs porosity) used.

2110 **Table 4 Foraminiferal morphometrics that can be assessed to estimate past oxygen concentrations. Morphometrics are divided by benthic and planktic foraminifera. The column “Low-oxygen conditions” refers to the response of the correspondent morphometric under low-oxygen concentrations. “Other controlling factors” list other environmental parameters that might influence the morphometric.**

Morphometric	Low-oxygen conditions	Other controlling factors	Example species
BENTHIC			

Test Pore Density/ Porosity	High	Temperature (affecting metabolic rates); nitrate availability; age (decrease with older chambers)	Infaunal: <i>Bolivina spissa</i> , <i>Bolivina seminuda</i> , (Glock et al., 2011); Epifaunal: <i>Cibicidoidea</i> and <i>Planulina</i> spp. (Rathburn et al., 2018; Lu et al., 2022)
Test Size	Small (between different species); small or large (within same species) - respondent but variable direction of effect	Nitrate and food availability; depth in sediment (increase with depth)	The small <i>Nonionella stella</i> dominate low-oxygen sediments of the Santa Barbara Basin (Bernhard et al., 1997); <i>Bolivina spissa</i> adults (larger size) tolerate lower oxygen concentrations deeper in Peruvian margin sediment than juveniles (smaller size) (Glock et al., 2011). <i>Bolivina (seminuda, spissa, argentea, subadvena)</i> , <i>Takayanagia delicata</i> , off California (Tetard et al., 2017; Moffitt et al., 2014; Ohkushi et al., 2013)
Test Circularity	Size and circularity used for MARIN index to reconstruct oxygen: Low-oxygen: small size and elongated specimen (low MARIN); High-oxygen: big size and round specimen (high MARIN).		Low-oxygen: elongated specimen (bolivinids, buliminids); high-oxygen: Cibicidids, planulinids...(Tetard et al., 2021)
Test Surface Area:Volume Ratio	High or low - respondent but variable direction of effect	Age (increase with older chambers) Pollution	<i>U. peregrina</i> , <i>B. tunata</i> , and <i>L. psuedobeyrichii</i> have lower SA:V during low-oxygen period in Gulf of Alaska (Belanger, 2022)
Sest Size-Normalized Weight	Uncertain		
Test Thickness	Unknown	acidification	<i>Elphidium clavatum</i> (Choquel et al., 2023)
PLANKTIC			

Test Pore Density/ Porosity	High or low - respondent but variable direction of effect	Temperature (affecting metabolic rates)	Low in <i>Orbulina universa</i> (Kuroyanagi et al., 2013); High in <i>Globorotaloides hexagonus</i> (Davis et al., 2021)
Test Size	Small or large (within same species) - respondent but variable direction of effect		
Test Circularity	Unknown		
Test Surface Area:Volume Ratio	High or low - respondent but variable direction of effect		Lower for <i>G. hexagonus</i> in lowest oxygen conditions of eastern tropical North Pacific (Davis et al., 2021)
Test Size- Normalized Weight	Low (high dissolution)	Mainly controlled by carbonate chemistry	<i>G. sacculifer</i> , <i>P. obliquiloculata</i> , and <i>N. dutertrei</i> (Broecker and Clark, 2001)
Test Thickness	Unknown		

2115 Several equations are available to calculate environmental oxygen and $[\text{NO}_3^-]$ concentrations, using the porosity or pore density of benthic foraminifera. Rathburn et al. (2018) found that the porosity of *Cibicides* spp. and *Planulina* spp. within a $5000 \mu\text{m}^2$ window at the centre of the ultimate or penultimate chamber can be used to calculate bottom water oxygen concentrations ($[\text{O}_2]_{\text{BW}}$) according to equation 10.1:

$$\text{Equation 10.1.: } [\text{O}_2]_{\text{BW}} = e^{((\text{Pore}\% - 47.237)/(-8.426))}$$

2120 In the same way the pore density (pores per μm^2) of *Cibicides* spp. and *Planulina* spp. within a $5000 \mu\text{m}^2$ window at the centre of the ultimate or penultimate chamber on the spiral side can be used with slightly lower accuracy (see Eq. 10.2; Glock et al., 2022):

$$\text{Equation 10.2.: } [\text{O}_2]_{\text{BW}} = e^{((\text{PD} - 0.008[+/-0.0002])/(-0.00142[+/-0.00006]))}$$

Within a limited $[\text{O}_2]_{\text{BW}}$ range of 2 - 14 $\mu\text{mol kg}^{-1}$, the PD of *Planulina limbata* on a size normalized area of the older part on the spiral side can be used to calculate $[\text{O}_2]_{\text{BW}}$ with higher accuracy according to eq. 10.3 (Glock et al. 2022):

2125 $\text{Equation 10.3: } [\text{O}_2]_{\text{BW}} = -6027[+/-652] \cdot \text{PD} + 22.0[+/-1.7]$

Glock et al. 2011 & 2018 found that the pore density of some denitrifying benthic foraminifera can be used to calculate bottom water NO_3^- concentrations ($[\text{NO}_3^-]_{\text{BW}}$). The most recent equations to reconstruct $[\text{NO}_3^-]_{\text{BW}}$ have been found for *Bolivina spissa* and *Bolivina subadvena* (Govindankutty-Menon et al., 2023). $[\text{NO}_3^-]_{\text{BW}}$ can be calculated using the pore density from a size-normalized area that includes the ~10 oldest chambers according to eq. 10.4:

2130 Equation 10.4: $[\text{NO}_3^-]_{\text{BW}} = -3896[+/-350] \cdot \text{PD} + 61[+/-1]$

10.2.2 Size and Morphotype

A predominance of smaller benthic foraminifera species in low-oxygen environments has frequently been observed (Bernhard, 1986; Sen Gupta & Machain-Castillo, 1993; Bernhard & Sen Gupta, 1994). From the perspective of gas exchange, a decrease in size is an efficient way to increase shell surface area/volume ratio and thus, maximize the relative surface available for gas
2135 diffusion. However, this trend is not universally observed within species. Some studies report no consistent relationships between specimen size and oxygen levels (Keating-Bitonti & Payne et al., 2017). Some low-oxygen adapted species, such as *Uvigerina peregrina* and *Buliminella tenuata* even seem to increase in size and decrease in surface area/volume ratios in lower oxygen settings (Keating-Bitonti & Payne et al., 2017; Davis et al., 2021; Belanger, 2022). This counter-intuitive observation may be explained by reliance on nitrogen rather than oxygen for respiration (Glock et al., 2019), or the influence of high food
2140 availability (Belanger, 2022). Starting in the 1990s, multiple authors mention the relationship between test morphotype or shape of benthic foraminiferal tests and environmental parameters such as bottom water oxygenation (e.g., Corliss, 1991; Kaiho, 1994; Kaiho et al., 2006). These observations were combined with size metrics to develop the Major Axis and Roundness INdex (MARIN; Equation 10.5 ; Tetard et al., 2021).

2145 Equation 10.5: $\text{MARIN} = \text{Major Axis} \times \text{Roundness}$

The “Major Axis” corresponds to the primary axis of the best fitting ellipse. The Roundness can be calculated according to Eq. 10.6:

2150 Equation 10.6: $\text{Roundness} = 4 \times \text{Area} \times \pi^{-1} \times \text{Major Axis}^{-2}$

Tetard et al. (2021) calibrated the MARIN as an oxygen proxy for the Eastern North Pacific according to Eq. 10.7:

2155 Equation 10.7: $[\text{O}_2]_{\text{BW}} = 0.0000266 \times \exp^{0.0354 \times \text{MARIN}}$

Thus by measuring size and shape using image analysis software, such as ImageJ (<https://imagej.nih.gov/ij/download.html> and <https://doi.org/10.5281/zenodo.4740079>), past oxygen values for OMZ conditions can be estimated without the need for species-level identification. An assemblage characterized by small, elongated tests would indicate low bottom water oxygen

conditions, while an assemblage dominated by large, spirally-arranged tests would indicate well-oxygenated conditions. The impact of changing oxygen conditions on foraminiferal morphology is discussed in more detail in the next section.

10.2.3 Size-Normalized Weight and Dissolution

Size-normalized weight (SNW) is a metric derived from normalizing the weight of individual or pooled shells by their length, area, or volume. It serves as a measure of how heavily calcified a foraminifera is and has been frequently linked to carbonate ion concentration in both pelagic and benthic environments. High input of organic matter results in higher oxygen consumption and release of dissolved inorganic carbon (DIC) by remineralization. This resulting coupling between oxygen and the carbonate system in many marine environments makes SNW worth mentioning here. While the direct driver of SNW (and shell dissolution) is likely carbonate chemistry, it could act as a viable supporting proxy. Lohmann (1995), followed by Broecker & Clark (2001), proposed the use of planktic foraminiferal shell weights to assess dissolution, and therefore bottom water carbonate chemistry. The use of shell weights as a carbonate chemistry (and, indirectly, oxygen) proxy, however, was rapidly complicated by evidence which shows that carbonate ion concentration influences SNW of planktic foraminifera during growth as well (e.g., Bijma et al., 1999; Barker and Elderfield, 2002; de Moel et al., 2009; Moy et al., 2009; Manno et al., 2012; Marshall et al., 2013). Results from size-normalized weight studies in foraminifera from low-oxygen, high-carbon environments have been equivocal in benthic foraminifera (Davis et al., 2016), but show some promise when applied to planktic foraminifera (Davis et al., 2021). Use of micro-CT to differentiate dissolution from calcification (Iwasaki et al., 2019) may make the application of SNW as an indirect proxy for oxygen more feasible in the future.

10.3 Analyses and Required Resources

Sample preparation is normally as described for foraminiferal assemblages (see Section 9). Morphometric analyses then proceed using one of several microscope and imaging approaches. In most cases, analyses of basic morphology (size, circularity, ornamentation, and sometimes porosity, pore size and pore density) can be carried out using a stereo microscope, equipped with a camera and/or micrometer. This approach can also be automated, using a motorized microscope stage and image acquisition and processing software (e.g., NI Vision software, ImageJ, the R package *forImage*, Freitas et al., 2021) for automatically reconstructing and measuring pore density, pore surface area, volume and various test measurements (e.g., ImageJ, the MorFo_ .ijm plugin available at <https://doi.org/10.5281/zenodo.4740079> (Tetard et al., 2021; Freitas et al., 2021)). Higher resolution analyses, or precise measurements of small features such as pores, sometimes require SEM imaging. The SEM images usually include the entire specimen, and in some processing methods, also need to include higher magnification images of a specific chamber. Processing the SEM images can be performed using open-source software ImageJ (<https://imagej.nih.gov/ij/download.html>) (Petersen et al., 2016) or Adobe Photoshop and ArcGIS software (Rathburn et al., 2018). A detailed manual for semi-automated pore measurements of benthic foraminifera can be found in Petersen et al. (2016).

2190 These analyses are relatively low-cost and highly accessible. In addition, because most SEM analyses are non-destructive, specimens can be re-used in geochemical analyses, which provides potential for a multi-proxy approach to paleo-oxygen reconstruction.

10.4 Recent Advances

2195 While interest in studying foraminiferal morphology in 3D emerged in the mid-20th century (Bé et al., 1969; Schmidt, 1952), quantifications and paleoclimatic reconstructions using such methods have become possible only recently. Since the pioneering μ CT work of Speijer et al. (2008), the number of studies dealing with 3D reconstructions of foraminiferal tests is increasing towards a variety of ends such as taxonomy and ontogeny (e.g., Briguglio et al., 2010, Görög et al., 2012, Schmidt et al., 2013, Caromel et al., 2016, 2017; Burke et al., 2020), ocean acidification and test dissolution processes (e.g., Johnstone et al., 2010, 2011, Iwasaki et al., 2015, 2019, Prazeres et al., 2015, Ofstad et al., 2021, Kuroyanagi et al., 2021, Charrieau et al., 2022, 2200 Choquel et al., 2023), effects of temperature (e.g., Kinoshita et al., 2021, Titelboim et al., 2021), and paleoclimate reconstruction (e.g., Fox et al., 2020, Zarkogiannis et al., 2021, Todd et al., 2020, Schmidt et al., 2018).

Foraminiferal 3D reconstruction is a promising, non-destructive approach for accessing the morphology of the entire shell (inner and outer walls). However, it remains technically and methodologically challenging as well as costly to scan a large number of shells, with high resolution ($< 1\mu\text{m}$). To date “conventional” μ CT scanners have primarily been used, supplemented 2205 with particle accelerator facilities, and Atomic Force Microscopy (AFM). Studies using 3D foraminifera constructions with scanner-based or synchrotron light-based μ CT were reviewed in Choquel et al. (2023). Most studies reconstructing foraminifera in 3D are performed with costly software such as Avizo (e.g., Fox et al., 2020), Amira (e.g., Schmidt et al., 2013), Molcer Plus and ConeCT express (e.g., Iwasaki et al., 2015). These software packages are adapted to the problems of test reconstruction but also can induce limitations on access to data processing and lack guidelines on how to analyse test 2210 morphometrics. Some authors are developing 3D post-data analyses with free software such as ImageJ/Fiji (Belanger et al., 2022), Meshlab (Choquel et al., 2023) or Gwyddion (Giordano et al., 2019).

Reconstruction of pore patterns in 3D is challenging. Few studies have addressed porosity from μ CT images and only from planktic foraminifera (Burke et al., 2018; Davis et al., 2021). Davis et al. (2021) demonstrated that in *Globorotaloides hexagonus* the porosity of the most recent chamber measured by μ CT scans and light microscope images capture the same 2215 trend, however the porosity from μ CT images is higher. This difference could be due to the accuracy of the pore segmentation (the delineation of the automatic pore contour) and the lower resolution of the μ CT images compared to conventional microscopy. Many efforts have been made in the last decade to automate or semi-automate the acquisition of pore measurements (number of pores, pore density, and porosity). Automated pore measurements have the advantage of acquiring data rapidly, facilitating the production of a large amount of representative data (Kuhnt et al., 2014). These automatic methods 2220 are often made from SEM images of a small part, or fragments of the test, to limit the pore deformation linked to the test curvature. The difficulty lies in standardizing pore measurements between individuals of the same species, e.g., *Ammonia tepida* (Petersen et al., 2016; Giordano et al., 2019), *Orbulina universa* (Morard et al., 2009), or *Bolivina seminuda* (Tetard et

al., 2017). The pores are mainly studied with a 2D view but 3D analyses allow access to more parameters such as pore depth and roughness (Giordano et al., 2019). Interest in studying 3D pore patterns from μ CT scans is increasing (Burke et al., 2018; 2225 Davis et al., 2021). Indeed, the 3D reconstruction of the test is a promising tool that could give us access to the pore patterns chamber by chamber, and especially be adaptable to different shapes of the tests.

10.5 Proxy drivers

While porosity and/or pore density are empirically useful proxies in some species of foraminifera, understanding the parameters that directly drive this correlation is a work in progress. Several authors have hypothesized that larger pores act to 2230 facilitate increased gas exchange across the shell in low-oxygen environments (Leutenegger and Hansen, 1979; Corliss, 1985). A clustering of mitochondria behind the pores and the exchange of labelled CO_2 through pores suggest that pores are involved in respiratory processes in several species (Leutenegger and Hansen, 1979; Bernhard et al., 2010). Leutenegger & Hansen (1979) argues that the clustering of mitochondria below the pores will create a deficiency of oxygen, and thereby a diffusion gradient across the pores. *Patellina corrugata* has been shown to actively pump dissolved organic dyes through its pores into 2235 the cytoplasm (Berthold, 1976). Moreover, pores have been found adequate for the exchange of gasses in both low and high oxygen conditions (Moodley & Hess, 1992). A gas exchange function would lead to a prediction of increased porosity and/or pore density under conditions of increased demand for oxygen diffusion due either to increased metabolic demand or decreased oxygen.

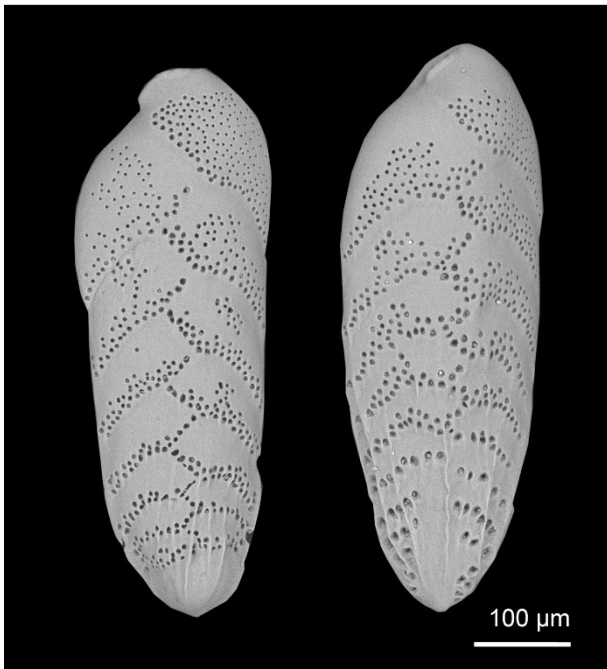
Studies reviewed above (Section 9.5) show that some foraminifera are able to denitrify and complicate this interpretation. 2240 Some denitrifying foraminifera such as *Bolivina spissa* most likely take up nitrate through pores. The pore density of denitrifying species is more strongly related to nitrate rather than oxygen, suggesting it can be used as a paleoproxy for nitrate (Glock et al., 2011; 2018; 2019). Other potential functions of surface pores include taking up dissolved organic matter as food resources and releasing metabolic CO_2 (Glock et al., 2012).

Direct drivers of porosity may therefore be species and environment specific. For example, epifaunal or very shallow infaunal 2245 species such as *Cibicidoides* and *Planulina* spp. do not live or migrate to anoxic pore waters and no studies have suggested their use of nitrate for respiration. Thus, it can be inferred that bottom water nitrate does not influence the porosity of these species (Rathburn et al., 2018). However, there is a possibility that some *Cibicides* spp. might be able to denitrify under severe oxygen depletion, since they cluster next to the known denitrifiers within their phylogenetic tree (Woehle et al., 2022). Another recent study from the Arabian Sea found no significant correlation between surface porosity of *Cibicidoides* spp., dissolved 2250 organic carbon, and CO_2 concentrations in the seawater, suggesting that bottom water oxygen is likely the major control on surface porosity for *Cibicidoides* spp. (Lu et al., 2022).

10.6 Influence of temperature, ontogeny, and dimorphism on morphological characteristics

There are several other parameters, in addition to oxygen and nitrate, that can influence porosity of foraminifera. This includes temperature (Bé, 1968, Glock et al., 2011, Kuhnt et al., 2013, Burke et al., 2018) which might influence porosity via changes

2255 to metabolic rates and oxygen solubility in the environment. Since these parameters often co-vary, it can be difficult to unravel
the main factors that control porosity. Ontogeny can also influence foraminiferal morphology in various ways. Usually, surface
to volume ratios decrease as foraminifera grow. This results in an increase of pore density and porosity in the youngest
chambers, as the organism compensates for decreased surface to volume ratio (Glock et al., 2011). During ontogeny, benthic
foraminifera can migrate in the sediment (Glock et al. 2011) and planktic foraminifera in the water column (Hemleben et al.,
2260 1989; Schiebel and Hemleben, 2017; Meiland et al., 2021), though this appears to be species-specific. For example, the size
(and likely age) of living *Bolivina spissa* from the Peruvian OMZ increases with sediment depth (Glock et al., 2011). By
contrast, there is no significant correlation between pore density in congener *Bolivina pacifica* and its depth in sediments from
the Arabian Sea, indicating minimal ontogenetic effects on the living depth of this species (Kuhnt et al., 2013). the latter study
also focused on analyzing porosity in small areas of the shell, which may reduce ontogenetic effects, if parts of the test from a
2265 similar ontogenetic state are analyzed (Kuhnt et al., 2013). Generational dimorphism may also impact porosity. At least in
some species there are systematic differences in the pore patterns between megalospheric and microspheric specimens (Fig.
13), and some studies exclusively focused on megalospheric specimens (Glock et al., 2011, 2018). One final consideration
when analysing foraminiferal porosity is shell stability (Richirt et al., 2019). As porosity increases ontogenetically (Glock et
al., 2011), the last chamber usually shows the highest porosity. The last chamber is also usually the thinnest, due to the laminar
2270 calcification mechanism in rotaliid species (Erez, 2009), and may be broken in many fossil specimens. There might be different
strategies to preserve stability while at the same time increasing porosity. One strategy is to build larger but fewer pores (Richirt
et al., 2019). Another strategy might be to increase wall thickness.



2275

Figure 13: Comparison of the pore patterns of a megalospheric (left) and microspheric (right) specimen of *Bolivina spissa*. Note the larger but fewer pores in the old parts of the test of the microspheric specimen (bottom part of the image, close to the proloculus). Location: Mexican Margin. Image taken on a Hitachi Tabletop SEM TM4000 series at Hamburg University.

2280 10.7 Marine archives and limitations

Similar to oxygen assessments based on benthic foraminiferal assemblages, morphometrics can potentially be used wherever marine carbonates are preserved. Features such as size and test morphology should be robust to minor dissolution, and image analyses typically should reveal if extensive dissolution has occurred. Corrosive environments could lead to preferential dissolution of smaller tests and/or enlargement of pores, but this has yet to be directly tested in the context of low-oxygen proxies; proxies such as porosity, pore density and MARIN.

The correlation between pore density/porosity and oxygen concentrations or other environmental parameters is species specific (Kuhnt et al., 2013; 2014; Glock et al., 2011; 2022). The distribution of foraminiferal species is often restricted to a certain oxygen range and thus, the species specific calibrations often cover only a limited oxygen range (Kuhnt et al., 2013; 2014; Tetard et al., 2017, Glock et al., 2011; 2022; Section 9.2). One potential solution to this limitation is a multi-species pore density/porosity calibration. For example, the global multi-species calibration of *Cibicidoides* and *Planulina* spp. suggests a strong negative logarithmic relationship between porosity and bottom water oxygen from oxygen concentrations as low as 2 $\mu\text{mol kg}^{-1}$ to completely oxygenated environments but the correlation is very flat at oxygen concentrations $>100 \mu\text{mol kg}^{-1}$ (Rathburn et al., 2018; Lu et al., 2022). The porosity of these species is usually $>10\%$ when bottom water oxygen is < 100

2295 $\mu\text{mol kg}^{-1}$. In oxic environments, few or no pores are found on the surface (Rathburn et al., 2018). The porosity proxy thus is most useful to indicate low bottom water oxygen conditions (Fig. 1).

The porosity of *Bolivina seminuda* has been suggested as an oxygen proxy for lower oxygen environments (~ 1 to $45 \mu\text{mol}$; Tetard et al., 2017, 2021). Though, *B. seminuda* is a denitrifying species and it is possible that differences in oxygen concentrations play only a minor role regarding its porosity (Piná-Ochoa et al., 2010; Glock et al., 2019). Multiple environmental parameters that have been shown to correlate with porosity or pore density of foraminifera such as oxygen, 2300 nitrate and temperature often covary. This can result in significant correlation of the pore characteristics with multiple parameters (Glock et al., 2011; Kuhnt et al., 2013). Oxygen and nitrate are coupled to both denitrification and remineralization. Nitrate loss through denitrification is increased when oxygen is depleted, while remineralization consumes oxygen and increases nitrate concentrations (Andersen and Sarmiento, 1994; Johnson et al., 2019). Similar opposing trends are found for the correlation between oxygen and temperature. Oxygen solubility decreases with increasing temperatures and both 2305 parameters often covary with water depth (Keeling & Garcia, 2002; Schmidtko et al., 2017). In addition, temperature has an influence on metabolic rates, which might be a factor influencing foraminiferal porosity (Burke et al., 2018). For now the covariation of all these parameters limits interpretation of porosity proxies but future studies using controlled laboratory cultures might unravel their specific influences.

10.8 Future Directions

2310 10.8.1 Emerging Developments

High-throughput imaging and other forms of automation are rapidly increasing the scope of what can be done with morphological proxies but bring new challenges as well. Automation reduces historically intensive work. This means that larger sample sizes, higher-resolution records, and attention to an increasing number of species and environments are becoming more feasible. However, key questions remain, such as how automated analyses compare to manual analyses, and what trade- 2315 offs are associated with high throughput versus accuracy. One concern is that the accuracy of high-throughput automated image analyses may suffer due to a decrease in human oversight, though this might improve with further development of algorithms. High-throughput methods and use of traditional equipment, such as optical microscopy, may also provide different benefits, with the former saving labour while the latter saving instrumental cost.

Other directions include wider application of existing methods and ground-truthing through laboratory culture. Application of 2320 morphological methods developed in benthic foraminifera to other organisms would also increase the number of environments from which oxygen can be constrained. This most readily applies to planktic foraminifera, which would expand proxies into the pelagic realm, but may also apply to other hard-bodied organisms such as ostracods, in which morphology has been linked to environmental parameters including oxygen (e.g., McKenzie et al., 1989).

As mentioned above, the stability of tests is an important factor when studying foraminiferal porosity and pore density (Richirt 2325 et al., 2019). One factor, related to test stability, that is not analyzed yet, is the thickness of the walls. The effects of mechanical

stress on the morphological characteristics such as porosity and wall thickness are currently unknown. Other factors to be considered in future studies include variations in mechanical stresses in the environment induced by varying sediment grain size, bioturbation and the intensity of bottom water currents. Future directions could include culturing experiments to isolate the influence of different environmental parameters on the pore density/porosity of both benthic and planktic species, including both denitrifying and oxygen-respiring species. Previous culture studies have demonstrated pore plasticity responding to environmental conditions within the lifespan of a single individual in multiple benthic (Sliter, 1970; Moodley and Hess, 1992) and planktic (Bijma et al., 1990; Allen et al., 2008; Kuroyanagi et al., 2013; Burke et al., 2018) species. Porosity changes during a foraminifera lifetime is a potential metabolic response to environmental drivers (Kuroyanagi et al., 2013; Burke et al., 2018).

2335 The evolution of 3D methods such as micro-computed tomography (μ CT) provides access to morphological features of the full test. However, the resulting datasets are very large. This can be problematic, since full datasets cannot be easily shared or published and storage space can be a limited resource. Further work is needed to automate and streamline some data handling and processing.

2340 Finally, little attention has been given to studying ecophenotypic variability, or the potential for adaptive responses to environmental forcing, in the frequency of ornamentations and test deformations in response to oxygen depletion. Lutze (1964) and Harman (1964) showed that bolivinids from lower oxygen sites in the Santa Barbara Basin typically have less ornamentations such as spines, costae and keels. In addition, growth disruption and test deformation can appear under unfavorable environmental conditions (Lutze, 1964). Future research might address this issue and include systematic studies on the frequency and size of ornamentations and test deformation under variable oxygen concentrations.

2345 **10.8.2 Open Questions: Resolving methodological differences**

The literature includes many methods for determining foraminiferal pore characteristics, such as porosity, pore size and pore density. A relatively widespread method is focusing on the centre of the ultimate or penultimate chambers and using a small window to approximate a flat surface (Kuhnt et al. 2013 & 2014; Petersen et al., 2016; Rathburn et al., 2018; Richirt et al., 2019; Glock et al., 2022). An alternative method suggests using a larger size-normalized part of the older chambers (Glock et al., 2011, 2018, 2022). Another approach is automated image acquisition and analysis of shards after cracking open the shell, in order to investigate penultimate chamber vs whole test porosity (Tetard et al., 2017). Finally, one study used atomic force microscopy to automatically analyze foraminiferal morphometrics (Giordano et al., 2019). Each method has advantages and disadvantages (see 10.2). A recent study on the pore density of epifaunal *Planulina limbata* found the best correlation between oxygen and pore density by using a size-normalized area on the older parts of the spiral side (Glock et al., 2022). In other epifaunal foraminifera, Rathburn et al. (2018) found that there is a better correlation between porosity and oxygen than between the pore density and oxygen. Finally, to minimize problems through dissolution effects or overgrown pores of planktic foraminifera, Constandache et al. (2013) suggested breaking the shells and determining the pore characteristics on the inner surface. The wide variability in methods that have been used in existing studies shows a need for the development of a common

2360 approach. The ongoing automation of data acquisition may provide a suitable way to achieve this in future work. Although, the approaches may vary a bit, depending on the shape of the shells (i.e. spatulate, planconvex, elliptic etc.).

Table 5 Different methods to determine pore characteristics (e.g., shell porosity and pore density) of foraminifera with a list of different advantages and disadvantages of those methods.

Description of method	Advantages	Disadvantages	References
Focusing on small window with smooth surface in center of ultimate/penultimate chamber	Relatively fast; Minimizes artifacts due to curvature of the specimens; Normalizes regarding ontogenetic stage; Negates problems with overgrown pores	Dataset is limited due to small window size; Ultimate and penultimate chambers usually have highest porosity, which can reduce test stability	Kuhnt et al., 2013 & 2014; Petersen et al., 2016; Rathburn et al., 2018; Richirt et al., 2019; Glock et al., 2022
Using a larger size normalized area on the older parts of the test	Normalization for ontogenetic effects; Larger datasets per specimen; Lower porosity in these parts causes test less stability restrictions and thus porosity might be better adapted to environmental changes	Possible artifacts by overgrown pores and curvature of the test; More effort to acquire the data	Glock et al., 2011, 2018 & 2022
Automated image acquisition and analysis of shards from crushed foraminifera	Large datasets with relatively low effort	Method is “destructive”	Tetard et al., 2017
Automated morphometric analyses using atomic force microscopy	Most metadata of all methods, including depth and 3D shape of the pores	Accessibility of atomic force microscopy	Giordano et al., 2019

Analysis of porosity from the inside after breaking the test	Avoid problems with pores that are overgrown or show evidence for dissolution from the outside	Method is “destructive”	Constandache et al., 2013
3D image of the whole test using x-ray	All pores of the test can be counted and calculated the surface area in 3D and pore sizes	Beamtime is constrained, and mCT can be costly	Burke et al., 2018; Davis et al., 2021; Choquel et al., 2023

11 Benthic foraminiferal carbon isotope offsets

2365 11.1 Theory & proxy driver(s)

The carbon isotopic offset between specific benthic foraminifera species ($\Delta\delta^{13}\text{C}$) can be used to reconstruct bottom water oxygen concentrations. Application of the proxy relies on the principle that oxic remineralization of organic matter releases isotopically light DIC into the pore waters. Within the top few centimetres of the sediment, aerobic respiration of organic matter dominates. This generates a $\delta^{13}\text{C}$ gradient between bottom and pore waters from the sediment-water interface to the anoxic boundary (McCorkle et al., 1985). It is thought that greater aerobic remineralization in pore waters, associated with higher bottom water oxygen concentrations, enhances this $\delta^{13}\text{C}$ gradient, and the availability of oxygen in marine pore waters is set by downward diffusion of bottom water oxygen across the sediment-water interface (McCorkle et al., 1985).

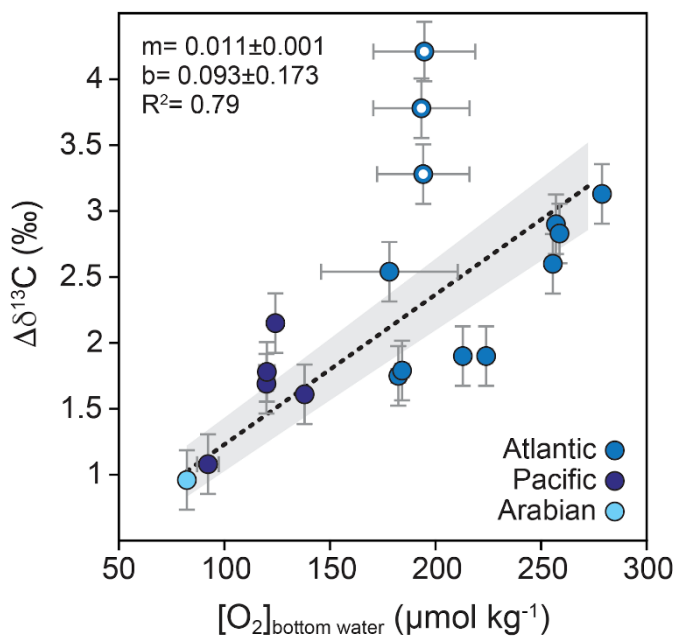
2370 The basis of the $\Delta\delta^{13}\text{C}$ proxy is the difference in $\delta^{13}\text{C}$ between epifaunal and deep infaunal benthic foraminifera species, that theoretically reflect the carbon isotopic composition in their habitats (Eq. 11.1). The carbon isotopic composition of epifaunal foraminifera such as *C. wuellerstorfi* reflects that of DIC in bottom water, and the carbon isotopic composition of deep infaunal foraminifera of the genus *Globobulimina* reflects that of DIC in pore waters near the anoxic boundary (Duplessy et al., 1984; Zahn et al., 1986; Fontanier et al., 2002; Geslin et al., 2004; Schmitter et al., 2017).

Equation 11.1:
$$\Delta\delta^{13}\text{C} = \delta^{13}\text{C}_{C. wuellerstorfi} - \delta^{13}\text{C}_{Globobulimina spp.}$$

2380

Robust quantification of bottom water oxygen concentrations based on the $\Delta\delta^{13}\text{C}$ rests on three fundamental assumptions. First, foraminifera species respectively record the $\delta^{13}\text{C}$ of the DIC of bottom waters and pore waters near the anoxic boundary within subsurface marine sediments. Second, degradation of organic matter above the sedimentary anoxic boundary and associated deviation of pore water $\delta^{13}\text{C}$ of DIC from bottom waters is predominantly driven by aerobic respiration. Lastly, pore water $\delta^{13}\text{C}$ gradients in DIC are largely determined by aerobic respiration of organic matter, which is mediated by the diffusion of dissolved oxygen from bottom waters, and thus directly scales with the availability of dissolved oxygen in bottom waters. If overlying bottom waters are characterized by low-oxygen concentrations, a balance of consumption of oxygen through mainly aerobic respiration and diffusion of oxygen from the overlying bottom waters is reached at shallow sediment depths with small deviations of pore water $\delta^{13}\text{C}$ of DIC at the anoxic boundary from the $\delta^{13}\text{C}$ of DIC in bottom waters. Low $\delta^{13}\text{C}$ gradients are thus associated with low bottom water oxygen levels (Fig. 14). The greater the oxygen concentration in overlying bottom waters, the greater the release of low $\delta^{13}\text{C}$ DIC into pore waters during respiration of organic matter, leading to a larger $\delta^{13}\text{C}$ difference between the DIC at the sediment-water interface and the DIC at the anoxic boundary, and a larger $\delta^{13}\text{C}$ gradient.

There is a strong relationship between $\delta^{13}\text{C}$ of seawater DIC and oxygen in the water column today (Hoogakker et al., 2016). However, epifaunal benthic foraminiferal $\delta^{13}\text{C}$ alone cannot be used to reconstruct past bottom water oxygen due to large uncertainties relating to preformed ^{13}C , air-sea fractionation, mixing with other water masses and terrestrial biomass changes (Lynch-Stieglitz et al., 1995; Schmittner et al., 2013; Gruber et al., 1999; Curry and Oppo, 2005; Oliver et al., 2010). Instead, the carbon isotope gradient pairs epifaunal $\delta^{13}\text{C}$ measurements with those of a deep infaunal species.



2400 **Figure 14: Relationship between $\Delta\delta^{13}\text{C}$ of *C. wuellerstorfi* versus *Globobulimina* (spp.) and bottom water oxygen. White circles represent outliers that were excluded from the regression. Sample details can be found in Supplementary Table S2.**

11.2 History of development and use

McCorkle and Emerson (1988) and McCorkle et al. (1990) first proposed that bottom water oxygen concentrations could be quantified using $\delta^{13}\text{C}$ in benthic foraminifera. They recognized that as remineralization of organic matter in pore waters consumes oxygen and releases isotopically light DIC, in relatively fixed (“Redfield Ratio”) proportions, $\delta^{13}\text{C}$ in pore waters relative to overlying bottom waters will reflect the amount of oxygen consumed in pore waters as a function of bottom water oxygen concentrations. They further suggested that paired specimens of benthic foraminifera that record bottom water and deep pore water carbon isotopes could be used to record this gradient, and thus bottom water oxygen concentrations in the past.

McCorkle et al. (1990) verified that the $\Delta\delta^{13}\text{C}$ of deep infaunal living benthic foraminifera *Globobulimina affinis* and the overlying bottom water is similar to the $\Delta\delta^{13}\text{C}$ between the pore water around the anoxic boundary and overlying bottom waters. Schmiedl and Mackenson (2006) showed that the $\Delta\delta^{13}\text{C}$ between *Globobulimina* species and bottom water DIC correlates well with bottom water oxygen concentrations and applied the derived relationship to reconstruct past bottom water oxygen in the Arabian Sea (Schmiedl and Mackensen, 2006). Hoogakker et al. (2015) used existing (Mackensen and Licari, 2004; Schmiedl and Mackensen, 2006; Fontanier et al., 2008) and new data to show that $\Delta\delta^{13}\text{C}$ of epifaunal *C. wuellerstorfi* and deep infaunal *Globobulimina* species from six locations of the Atlantic, Indian and Pacific Oceans show a similar relationship as $\Delta\delta^{13}\text{C}$ estimates between bottom water and pore water around the anoxic boundary from these basins (but at different locations) (Fig 14). They showed that $\Delta\delta^{13}\text{C}$ between *C. wuellerstorfi* and *Globobulimina* spp. is linearly correlated with bottom water oxygen levels in the range of 50–235 $\mu\text{mol kg}^{-1}$, and used this new calibration to reconstruct bottom water oxygen variations in the North Atlantic. The proxy has been applied in several studies to quantitatively reconstruct past bottom water oxygen concentrations in various ocean regions, with an estimated total error of 17 $\mu\text{mol kg}^{-1}$, including the North Atlantic (Hoogakker et al., 2016; Thomas et al., 2022), South Atlantic (Gottschalk et al., 2016; Gottschalk et al., 2020a), Indian Ocean (Schmiedl and Mackensen 2006; Gottschalk et al., 2020b) and Pacific Ocean (Hoogakker et al., 2018; Umling and Thunell, 2018; Jacobel et al., 2020). Figure 14 shows the most up-to-date core-top calibration between $\Delta\delta^{13}\text{C}$ obtained from *C. wuellerstorfi* and *Globobulimina* spp. and bottom water oxygen, with bottom water oxygen and new data points from Umling and Thunell (2018), Jacobel et al. (2020), and Thomas et al., (2022), as detailed in the supplementary information.

11.3 Description of analyses and resources required

Stable carbon isotope ratios from epifaunal (*Cibicidoides* spp.) and deep infaunal benthic foraminifera (*Globobulimina* spp.) can be measured using a mass spectrometer, commonly a Thermo Kiel V automated preparation device coupled with a Thermo Delta V Plus or Thermo MAT253 Mass Spectrometer. Measurements are calibrated to the international VPDB (Vienna Pee Dee Belemnite) standard. The sample mass required for analysis varies and depends on the mass spectrometer setup. Modern mass spectrometers typically require 40–80 $\mu\text{g CaCO}_3$, but can provide measurements for samples as small as 5 $\mu\text{g CaCO}_3$. Specimen size does not seem to matter for the $\delta^{13}\text{C}$ of *C. wuellerstorfi* (Franco-Fraguas et al., 2011), whereas size effects on

Globobulimina spp. are not yet explored. *Cibicidoides* spp. specimens tend to weigh more compared to *Globobulimina* spp. specimens. Selecting foraminifera from the larger than 250 μm -fraction, about one to four specimens of *Cibicidoides* and two to twenty specimens of *Globobulimina* spp. are needed for stable isotope analysis. Dirty specimens may need some treatment prior to analyses, including crushing, ultrasonication and/or methanol rinses to remove clay particles.

The most commonly used deep infaunal *Globobulimina* species for bottom water oxygen reconstructions via the $\Delta\delta^{13}\text{C}$ proxy is *Globobulimina affinis*. In the absence of *G. affinis*, other *Globobulimina* spp. have been used as mono- or multispecific samples (e.g., Hoogakker et al., 2018), assuming all share a similar deep infaunal depth habitat: *G. pacifica*, *G. turgida*, and *G. auriculata* (Supplementary Fig. S1). A deep infaunal species of the genus *Chilostomella*, a potential candidate to monitor conditions at the anoxic boundary, does not form its test in equilibrium with pore water DIC (McConnaughey et al. 1997; Nomaki et al., 2021). When *C. wuellerstorfi* is absent, other foraminiferal species thought to live epifaunally such as *Cibicides kullenbergi* (synonymously used with *Cibicides mundulus*) have also been used to reconstruct bottom water oxygen levels using the $\Delta\delta^{13}\text{C}$ proxy (e.g., Gottschalk et al., 2016a, 2020; Bunzel et al., 2017; Lu et al., 2022) with some notable caveats for their use (Supplementary Fig. S2).

11.4 Proxy limitations

The infaunal habitat of *Globobulimina* spp. may extend below the depth of sedimentary anoxia in some locations (and/or time periods) (Geslin et al., 2004). This may potentially lead to the incorporation of additional isotopically-light carbon generated at depth via anoxic processes, including denitrification by *Globobulimina* spp. and/or sulphate reduction (McCorkle and Emerson, 1988). Variations in depth habitat are of concern because denitrification and sulphate reduction are known to play a significant role in the remineralization of organic matter, releasing isotopically light carbon to pore waters after oxygen has been consumed. Sulphate reduction and other early diagenetic reactions are of particular concern in margin settings that are shallower than 1500 m (Sarmiento and Gruber, 2006) as, more organic matter is generally deposited in these settings. Sulphate reduction can lead to the shallowing of the early diagenetic zones (Egger et al., 2018) and an increased diffusive flux of DIC into the zone of aerobic respiration. Thus, there may be a variable contribution of anaerobic processes to the pore water DIC from which *Globobulimina* spp. calcify. If one or more of these influences are at play, $\Delta\delta^{13}\text{C}$ is expected to be elevated and the calibration would overestimate bottom water oxygen concentrations.

Recent work has shown that at least four species of *Globobulimina* spp. (including *affinis*, *pacifica*, *turgida* and *pseudospinescens*) concentrate nitrate, for use as an electron acceptor in the absence of oxygen (Risgaard-Petersen et al., 2006; Nomaki et al., 2015; Piña-Ochoa et al., 2010a; Piña-Ochoa et al., 2010b). Metabolic and genetic data corroborates the capability of *Globobulimina* species to denitrify, one of the main reasons they are successful in anoxic settings (Piña-Ochoa et al., 2010b, Woehle et al., 2018 & 2022). These results may imply that *Globobulimina* spp. may thrive and calcify successfully well below the anoxia boundary, meaning they could be influenced by the addition of low- $\delta^{13}\text{C}$ DIC during sulphate and nitrate reduction, although to date there is no direct evidence for this. Furthermore, if *Globobulimina* spp. contribute isotopically-light carbon to the sedimentary pore waters, this could potentially decouple the relationship between bottom water oxygen and $\Delta\delta^{13}\text{C}$. The

influence of shallow denitrification has been invoked to explain observations of inconsistent $\Delta\delta^{13}\text{C}$ between five contemporaneous records of $\Delta\delta^{13}\text{C}$ from the EEP Ocean (Jacobel et al, 2020), and between co-located records of U/Ba and $\Delta\delta^{13}\text{C}$, where U/Ba yields consistently lower estimates of bottom water oxygen concentrations (Costa et al., 2023). Significant inconsistencies between core-top bottom water oxygen concentrations, determined using $\Delta\delta^{13}\text{C}$, and measured bottom water oxygen have also been identified at some equatorial Pacific sites (Jacobel et al, 2020). Separately, higher $\Delta\delta^{13}\text{C}$ values found in the OMZ of the Arabian Sea (Lu et al., 2022) have been attributed to sulphate reduction in sediments. Specifically, $\Delta\delta^{13}\text{C}$ -based bottom water oxygen estimates at these sites are more than $60 \mu\text{mol kg}^{-1}$ higher than reconstructed using other proxies (i.e. benthic surface porosity, benthic I/Ca, and aU) (Lu et al., 2022). Indeed, the three outliers in the updated $\Delta\delta^{13}\text{C}$ - bottom water oxygen relationship in Fig. 14 are from areas where sulphate reduction is known to play an important role (Bradbury et al, 2021, 2024; Thomas et al., 2022).

Another factor that may drive variations in $\Delta\delta^{13}\text{C}$ independent from bottom water oxygen is changes in the carbon isotopic composition of organic material ($\delta^{13}\text{C}_{\text{org}}$) that is remineralized in the pore space of marine sediments (Hoogakker et al., 2015). A decrease in $\delta^{13}\text{C}_{\text{org}}$ would enhance $\Delta\delta^{13}\text{C}$ and cause an apparent increase in reconstructed bottom water oxygen. It is therefore important to assess $\delta^{13}\text{C}_{\text{org}}$ alongside $\Delta\delta^{13}\text{C}$ -based bottom water oxygen quantifications.

Finally, although previous work has shown a generally strong correspondence between $\delta^{13}\text{C}$ of DIC in bottom waters and $\delta^{13}\text{C}$ of *C. wuellerstorfi* (e.g., Schmittner et al., 2017), there is some evidence that seasonal pulses of organic material (the phytodetritus effect) may decrease the $\delta^{13}\text{C}$ of epifaunal species by as much as 0.4‰ (Zarriess and Mackensen, 2011), perhaps due to the development of benthic ‘fluff’ layers in which *C. wuellerstorfi* calcify (Mackensen et al., 1993). This effect has not been found in all locations experiencing seasonally-variable production (Corliss et al., 2006) emphasizing the need for further work to develop the regional and/or time-variant conditions under which these effects develop. Insights into this open question could be derived from core-top samples where organic carbon flux, $\delta^{13}\text{C}_{\text{C. org}}$, $\delta^{13}\text{C}_{\text{C. wuellerstorfi}}$, and bottom water oxygen are directly measured to evaluate and quantify relationships.

11.5 Species relevant for calibration

Application of the $\Delta\delta^{13}\text{C}$ proxy is limited by the availability of epifaunal (*C. wuellerstorfi* or *C. mundulus*) and deep-infaunal (*Globobulimina* spp.) species in the sediment samples. However, some epifaunal species can adopt a shallow infaunal habitat, and can therefore be influenced by the pore water environment (Gottschalk et al., 2016b; Wollenburg et al., 2021). Fig. S2 shows an extended version of Fig.14 including other *Cibicidoides* species. Temporal variations in the $\delta^{13}\text{C}$ offsets of *Cibicides* species and *C. wuellerstorfi* could be an indication of a change in habitat (e.g., Gottschalk et al., 2016b). If there is an indication of temporal variations in this offset, or information about offsets is unavailable, the application of the $\Delta\delta^{13}\text{C}$ proxy based on assumingly shallow infaunal species such as *C. mundulus* may lead to a bias of bottom water oxygen concentrations towards lower values (e.g., Gottschalk et al., 2016a).

Because *Globobulimina* spp. has a deeper habitat compared with *C. wuellerstorfi*, there is the possibility that the measurements are age-offset. Upon death, sediment stirring through benthic organisms will mix the sediments with a bioturbation depth

2500 unique to the sedimentary environment at the time of deposition. It is unlikely that the two species in the fossil record maintain the depth offsets observed in living specimens. The comparison of the stable oxygen isotope records of both species is thus critical for ruling out or determining the appropriate, possibly time-variant, depth offset between species (Hoogakker et al., 2015).

11.6 Future directions and open questions

2505 Direct comparison and correlation between living and dead *C. wuellerstorfi* and *Globobulimina* spp. $\delta^{13}\text{C}$, measurements of bottom and pore water oxygen, and the $\delta^{13}\text{C}$ of bottom and pore water DIC would be ideal for rigorously quantifying calibration uncertainties. The calibration could also be strengthened by quantitative assessment of co-varying environmental parameters such as the flux of organic carbon, the $\delta^{13}\text{C}$ of C_{org} , and the influence of sulphate reduction and denitrification at calibration sites. This could be achieved through coring campaigns and culturing studies following the methods of Wollenburg et al. 2510 (2015).

Several possibilities exist for expanding the use of the $\Delta\delta^{13}\text{C}$ proxy. For example, the improvement of analytical techniques now allows for the analysis of single specimens with respect to oxygen and carbon isotopes (e.g., Ganssen et al., 2011). Analysis of single specimen $\delta^{13}\text{C}$ may provide insights into the natural variability of $\delta^{13}\text{C}$ of communities and improve our interpretation of $\Delta\delta^{13}\text{C}$. Additionally, application of the $\Delta\delta^{13}\text{C}$ proxy could be expanded if other deep infaunal species are 2515 found to record pore water $\delta^{13}\text{C}$ of DIC at the anoxic boundary.

12 Concluding summary statement and future directions

In this review, we summarize the current state-of-knowledge about proxies for reconstructing Cenozoic marine oxygen levels. Sediments are the carriers for all proxies associated with seawater oxygen reconstructions. Sedimentological and other non-destructive methods, as well as presence, relative abundance and potentially trace element compositions of pyrite provide 2520 important information about depositional redox conditions.

Bulk geochemical methods are described that can be used to reconstruct bottom water redox/oxygen conditions, as well as methods that involve fossil foraminiferal abundance, appearance, and geochemistry:

- 1) Redox-sensitive elements that are preserved under various redox potentials have provided key insights into deep ocean oxygenation on a variety of timescales. However, challenges remain and redox element research continues to 2525 refine the interpretations of these proxies by constraining variations of other environmental variables (notably the rain of organic carbon) that affect the redox state of sediments. Recent technical advances have allowed for the development of novel 'non-traditional' stable metal isotope systems, which open new possibilities for more quantitative redox reconstructions and towards globally integrated estimates of ocean oxygenation through time.
- 2) Lipid biomarkers provide a wealth of paleoceanographic information. Their source specificity and excellent 2530 preservation potential allow the detailed and comprehensive reconstruction of water column (and sediment) redox

conditions. Taxonomically specific biomarkers are available for a range of microorganisms thriving in different ecological redox niches, providing insights into past changes in the ocean's carbon, nitrogen, and sulphur cycles. Instrumental advancements and increased resolution continue to widen the analytical window, reveal novel biomarkers, and – in combination with (meta)genomics – aid identification of source organisms. Moreover, biomarker proxies are becoming more and more quantitative and the community strives to develop tools that allow inferring absolute oxygen concentrations.

2535
3) Bulk nitrogen isotopes offer insights into bacterial denitrification processes that are closely linked to water column oxygen concentrations below $<5 \mu\text{mol kg}^{-1}$. The strong isotopic discrimination by denitrifying bacteria can be measured in bulk sediments. Isotopic discrimination by denitrifying bacteria can also be measured in foraminifera-bound $\delta^{15}\text{N}$, and this method shows great promise for understanding dynamics of OMZs. We highlight the need of integrate biogeochemical models in order to refine interpretations of the nitrogen isotopic records.

2540
4) Foraminiferal trace elements, especially I/Ca, Mn/Ca and U/Ca show promise as proxies for reconstructing past oxygen conditions, within the constraints of the complexities arising from various environmental factors and potential interferences. I/Ca values are linked to the presence of IO_3^- and its reduction to I^- in low-oxygen settings. U/Ca utilizes the formation of authigenic U coatings on foraminiferal tests buried in marine sediments. Higher U/Ca concentrations are indicative of reducing oceanic bottom water conditions. Higher Mn/Ca in foraminiferal calcite indicates increased free Mn^{2+} incorporation under low oxygen bottom/pore water conditions. Foraminiferal trace element proxies require careful consideration of carbonate chemistry, variable oxygen thresholds, vital effects, ontogenetic effects, and potential diagenetic effects that can distort the signals in the geologic record. Further work is needed to establish robust calibrations for the relationships between proxies and oxygen conditions in different environmental settings and for different foraminiferal species.

2545
5) Foraminiferal assemblages have a long tradition as paleoproxies. Benthic foraminiferal assemblages are particularly sensitive to changes in bottom water oxygenation due to specific adaptations of some benthic species, including use of anaerobic metabolisms, to survive in O_2 depleted environments. In some cases, it is difficult to decouple changes in bottom water oxygenation from changes in organic matter input. One bottleneck for using foraminiferal assemblages is the high workload for sample processing, including picking foraminifera and taxonomic classification of each sample. The main advantages of this method are the low instrumental and resource requirements for this approach. Future directions include AI-based automation of species recognition, which will greatly reduce the amount of time involved, and the more routine use of planktic foraminiferal assemblages to reconstruct O_2 concentrations in the water column.

2550
2555
2560
6) Various morphological features of foraminiferal shells reflect the environmental conditions in which they grew, including oxygen concentrations. Shell porosity specifically reflects (a) the availability of oxygen for oxygen-respiring species, and (b) nitrate availability for species specialized in denitrification. Although a lot of focus has been placed on morphological features of benthic foraminifera, advances in understanding planktic foraminiferal

2565 morphology opens new windows for oxygen reconstruction within different layers of the water column. The recent
improvement on automated image analysis facilitates the quick generation of large datasets, while non-destructive
methods for image acquisition preserve the analysed specimens for further analyses. In addition, the development of
image acquisition methods and broader availability of μ - and nanoCT techniques allow 3D analyses of specimens to
further provide access to morphological details that were hidden before.

2570 7) There has been significant progress in employing the carbon isotope gradient between epifaunal and infaunal benthic
foraminifera as a proxy to reconstruct bottom water oxygen concentrations. Multi-proxy work has been key in
identifying sources of proxy uncertainty that are currently not well quantified, and in highlighting depositional
environments where $\Delta\delta^{13}\text{C}$ may not work well, specifically areas where sedimentary denitrification and sulphate
reduction are prevalent. Our review emphasizes that $\Delta\delta^{13}\text{C}$ -based reconstructions are likely to provide estimates that
2575 represent an upper bound of past bottom water oxygen concentrations. Further research into uncertainties has the
potential to improve the quantitative nature of the proxy. Specifically, we recommend focusing on the fidelity of
different species in recording the $\delta^{13}\text{C}$ values of bottom and pore waters, the role of carbon isotope composition of
organic carbon, the significance of biases arising from contributions from anaerobic metabolic processes, and how
changes in the rain rate of organic carbon may influence the proxy.

2580

Proxies are by definition indirect measurements, each with their own sources of uncertainty, biases, limitations, and drivers as
detailed in the sections above. For this reason, we recommend applying a multi-proxy approach wherever possible, in which
two or more proxy records are generated in tandem from the sample set. Ideally, the design of a multi-proxy study should
incorporate multiple proxies for the same or related parameters with different sources of uncertainty.

2585 Multi-proxy approaches are particularly appropriate in the field of paleo-oxygenation where most available proxies are semi-
quantitative and cover different ranges of redox chemistries (Fig. 1), and in some cases may have only been recently developed.
They may also differ in their drivers, with some proxies having multiple drivers, which may be independent of oxygen. The
layering of multiple, semi-quantitative proxies can allow researchers to assign more quantitative paleo-oxygen estimates (e.g.,
FB- $\delta^{15}\text{N}$ and planktic foraminiferal I/Ca in Hess et al., 2023), an exercise that may be pivotal in generating paleo-oxygen
2590 reconstructions that can inform models. The rapid development of novel paleo-oxygen proxies, such as the use of biomagnetic
particles (Chang et al., 2023), not discussed here, will continue to benefit the field. However, the limitations and uncertainties
of more recently developed proxies need to be further explored. Multi-proxy approaches can serve to validate these proxies
(e.g., comparing benthic I/Ca, U, and foraminiferal porosity as bottom water oxygen proxies in Lu et al., 2022), and increase
our understanding of their application in the sedimentary record (e.g., $\delta^{13}\text{C}$ and U in Jacobel et al., 2020). Finally, inclusion of
2595 multiple proxies may allow researchers to disentangle multiple drivers in the paleorecord, constraining not only oxygen but
also related environmental factors, such as export productivity or carbon fluxes, redox structure of the water column and
sediment, or depositional settings.

13 Recommendations for data management and transparency

2600 The interdisciplinarity of the communities generating oxygen proxy data and model outputs as well as the presently increasing number of applications make the implementation of FAIR data practices critical. The data availability from publications and data repositories (i.e. PANGAEA, NOAA) for proxy reconstructions (long-term) and validation of benthic and pelagic proxies is increasing rapidly. Moving forward, it is important that data are easily accessible to the wider scientific community using the FAIR (Findability, Accessibility, Interoperability, Reusability) guiding principles (Wilkinson et al., 2016).

2605 Proxy data produced for paleo-oxygen reconstructions are heterogeneous in terms of material (e.g., sediment, calcite, organic matter), methodology, chronology, and data formats. It is important that we standardize oxygen proxy data sets, including qualitatively, semi-quantitatively, and quantitatively, with error margins assessed and reported. As part of the FAIR principles, it is important that meta-data (sample identifier, core name and sections, location, depth, etc.) as well as raw data (original analyses/counts, etc.) are reported. Through networking activities scientists can promote FAIR principles and several institutes and journals have already done so. It is important that this effort is also reflected in the paleo and oceanographic communities. Following FAIR principles in oxygen proxy data management will improve data accessibility for scientists from the same discipline, as well as other disciplines and policy makers.

2610 Below we provide recommendations for data management that follow the guidelines for modern proxy validation data and reconstructions as proposed by Khider et al. (2019), Morrill et al. (2021), Jonkers et al. (2021), Mulitza et al. (2022), Muglia et al. (2023), and Paradis et al. (2023).

1. Organize data and save the file in a format accessible with different operating systems (e.g., linux, windows, iOS). The file needs to be in a format that is accessible and can be edited without altering the order of the data, to adopt the **Interoperability (“I”)** principle. We recommend files in csv (comma separated values). Files with csv format can be easily opened/read by data visualization and statistical software as, e.g., Excel, Rstudio, python, PaleoDataView (PDW), OceanDataView (ODV). Provide auxiliary information (metadata, depth model, age, proxy data) for each site.
2. Organize files following the **findability principle (“F”)** and provide a **unique identifier** for the files (see example in supplementary information).
3. Deposit data files in a public database/ repository to follow the **accessibility principle (“A”)**. The most commonly used data repositories for paleoceanographic data are PANGAEA and NCEI, and Github for code. Recently Zenodo has also emerged as an alternative repository. To make data widely accessible, add the unique repository link. Data can be submitted to repositories at any time prior to paper submission and authors can determine when data becomes available to the public. Data should be made available upon publication of manuscripts.

4. To optimize data use, follow the principle of **reusability (“R”)**. There needs to be a dataset descriptor containing all the necessary details to ensure re-usability and/or replication. The original references should be cited when re-using data.

14 Author contributions

2635 Jorge Cardich, Catherine Davis, Babette Hoogakker, Katrina Nillson-Kerr, and Dharma Reyes Macaya organized the workshop in September 2022 that initiated this review, supported by PAGES. Babette Hoogakker, Catherine Davis, Yi Wang, Stephanie Kusch, Dalton S. Hardisty, Allison Jacobel, Dharma Reyes Macaya, Nicolaas Glock, Sha Ni, Julio Sepúlveda, Abby Ren, Alexandra Auderset, Anya Hess, Katrin Meissner, and Jorge Cardich took the lead of writing various sections of the manuscript, with Babette Hoogakker and Catherine Davis moderating the final text. All further authors (Robert Anderson, 2640 Christine Barras, Chandranath Basak, Harold Bradbury, Inda Brinkmann, Alexis Castillo, Madelyn Cook, Kassandra Costa, Constance Choquel, Paula Diz, Jonas Donnenfeld, Felix Elling, Zeynep Erdem, Helena Filipsson, Sebastian Garrido, Julia Gottschalk, Anjaly Govindankutty Menon, Jeroen Groeneveld, Christian Hallman, Ingrid Hendy, Rick Henneham, Wanyi Lu, Jean Lynch-Stieglitz, Lelia Matos, Alfredo Martínez-García, Giulia Molina, Práxedes Muñoz, Simone Moretti, Jennifer Morford, Sophie Nuber, Svetlana Radionovskaya, Morgan Raven, Christopher Somes, Anja Studer, Kazuyo Tachikawa, Raúl 2645 Tapia, Martin Tetard, Tyler Vollmer, Shuzhuang Wu, Yan Zhang, Xin-Yuan Zheng, and Yuxin Zhou) contributed to the discussions, writing of text and creation of figures.

15 Competing interests

The authors declare that they have no conflict of interest.

2650 16 Acknowledgements

We thank ICP14 and PAGES (<https://pastglobalchanges.org/>) for providing logistic and travel support that facilitated the writing of this manuscript. The manuscript benefitted from discussions with Trinity Ford, Philip Froelich, Zunli Lu, Tim Sweere and Qingchen Wang. Babette Hoogakker acknowledges financial support from a UKRI FLF (MR/S034293/1). Nicolaas Glock would like to thank the Deutsche Forschungsgemeinschaft (DFG) for support via the grants GL 999/3-1 and 2655 GL 999/4-1. Julia Gottschalk acknowledges financial support from Deutsche Forschungsgemeinschaft (DFG) through grant GO 2294/3-1. Felix Elling acknowledges financial support from Deutsche Forschungsgemeinschaft grant 441217575. Alexis Castillo acknowledges financial support from FONDECYT project 11230555. Dalton Hardisty acknowledges an Alfred Sloan Fellowship. Morgan Raven acknowledges financial support from NSF OCE-2143817. Christopher Somes was supported by

the Deutsche Forschungsgemeinschaft (project no. 445549720). Raul Tapia is supported by the National Science and
2660 Technology Council of Taiwan (112-2116-M-002-003, 113-2611-M-002-008, 113-2811-M-002-039). Lelia Matos was
supported by FCT through projects UIDB/04326/2020, UIDP/04326/2020, LA/P/0101/2020 and 2022.05765.PTDC. Simone
Moretti acknowledges support from DFG Grant MO 4402/2-1. Helena Fillipsson, Sha Ni and Ina Brinkman acknowledge
support from the Swedish Research Council VR (Grant #2017-04190).

2665 **References**

- Abken, H. J., Tietze, M., Brodersen, J., Bäumer, S., Beifuss, U., and Deppenmeier, U.: Isolation and characterization of
methanophenazine and function of phenazines in membrane-bound electron transport of *Methanosarcina mazei* Gö1, *J*
Bacteriol, 180, 2027–2032, <https://doi.org/10.1128/jb.180.8.2027-2032.1998>.
- Adam, P., Schneckenburger, P., Schaeffer, P., and Albrecht, P.: Clues to early diagenetic sulfurization processes from mild
2670 chemical cleavage of labile sulfur-rich geomacromolecules, *Geochim. Cosmochim. Ac.*, 64, 3485–3503,
[https://doi.org/10.1016/S0016-7037\(00\)00443-9](https://doi.org/10.1016/S0016-7037(00)00443-9), 2000.
- Ahrens, J., Beck, M., Böning, P., Degenhardt, J., Schnetger, B., and Brumsack, H.: Thallium cycling in pore waters of intertidal
beach sediments, *Geochim. Cosmochim. Ac.*, 306, 321–339, <https://doi.org/10.1016/j.gca.2021.04.009>, 2021.
- Akintomide, O. A., Adebayo, S., Horn, J. D., Kelly, R. P., and Johannesson, K. H.: Geochemistry of the redox-sensitive trace
2675 elements molybdenum, tungsten, and rhenium in the euxinic porewaters and bottom sediments of the Pettaquamscutt River
estuary, Rhode Island, *Chem. Geol.*, 584, 120499, <https://doi.org/10.1016/j.chemgeo.2021.120499>, 2021.
- Alfken, S., Wörmer, L., Lipp, J. S., Napier, T., Elvert, M., Wendt, J., Schimmelmann, A., and Hinrichs, K. -U.: Disrupted
coherence between upwelling strength and redox conditions reflects source water change in Santa Barbara Basin during the
20th century. *Paleoceanography and Paleoclimatology*, 36, e2021PA004354, <https://doi.org/10.1029/2021PA004354>, 2021.
- 2680 Algeo, T.J.: Can marine anoxic events draw down the trace element inventory of seawater? *Geology* 32 (12), 1057-1060, 2004.
- Algeo, T.J. and Maynard, J.B.: Trace-element behaviour and redox facies in core shales of Upper Pennsylvanian Kansas-type
cyclothem. *Chemical Geology* 206 (3), 289-318, 2004.
- Algeo, T. J., & Lyons, T. W. Mo–total organic carbon covariation in modern anoxic marine environments: Implications for
analysis of paleoredox and paleohydrographic conditions. *Paleoceanography*, 21(1), <https://doi.org/10.1029/2004PA001112>,
2685 2006.
- Algeo, T.,J., Tribovillard, N.: Environmental analysis of paleoceanographic systems based on molybdenum-uranium
covariation. *Chemical Geology* 268, 211-225, <https://doi.org/10.1016/j.chemgeo.2009.09.001>, 2009.
- Algeo, T.J. and Rowe, H.: Paleoceanographic applications of trace-metal concentration data. *Chemical Geology* 324 (6) 6-18,
2012. Algeo, T. J., Meyers, P. A., Robinson, R. S., Rowe, H., and Jiang, G. Q.: Icehouse–greenhouse variations in marine
2690 denitrification, *Biogeosciences*, 11, 1273–1295, <https://doi.org/10.5194/bg-11-1273-2014>, 2014.
- Algeo, T. J., Li, C.: Redox classifications and calibration of redox thresholds in sedimentary systems, *Geochim. Cosmochim.*
Ac., 287, 8-26, <https://doi.org/10.1016/j.gca.2020.01.055>, 2020.
- 2695 Alibo, D.S. and Nozaki, Y.: Rare earth elements in seawater: particle association, shale-normalization, and Ce oxidation,
Geochim. Cosmochim. Acta, 63(3-4), 363-372, [https://doi.org/10.1016/S0016-7037\(98\)00279-8](https://doi.org/10.1016/S0016-7037(98)00279-8), 1999.

- Altabet, M. A., Deuser, W. G., and Honjo, S.: Seasonal and depth-related changes in the source of sinking particles in the North Atlantic, *Nature*, 354, 136-139, <https://doi.org/10.1038/354136a0>, 1991.
- Altabet, M. A. and Francois, R.: Sedimentary nitrogen isotopic ratio as a recorder for surface ocean nitrate utilization, *Glob. Biogeochem. Cy.*, 8, 103-116, <https://doi.org/10.1029/93GB03396>, 1994.
- 2700 Altabet, M. A., Francois, R., Murray, D. W., and Prell, W. L.: Climate-related variations in denitrification in the Arabian Sea from sediment 15N/14N ratios, *Nature*, 373, 506-509, <https://doi.org/10.1038/373506a0>, 1995.
- Altenbach, A. V., Pflaumann, U., Schiebel, R., Thies, A., Timm, S., and Trauth, M.: Scaling percentages and distributional patterns of benthic foraminifera with flux rates of organic carbon, *J. Foramin. Res.*, 29, 173-185, 1999.
- Alve, E., and Bernhard, J. M.: Vertical migratory response of benthic foraminifera to controlled oxygen concentrations in an experimental mesocosm. *Mar Ecol Prog Ser*, 116, 137-151, <https://doi.org/10.3354/meps116137>, 1995.
- 2705 Alve, E. and Murray, J. W.: Temporal variability in vertical distributions of live (stained) intertidal foraminifera, Southern England, *J. Foramin. Res.*, 31, 12-24, <https://doi.org/10.2113/0310012>, 2001.
- Amos, C.L., Sutherland, T.F., Radziewicz, B. and Doucette, M.: A rapid technique to determine bulk density of fine-grained sediments by X-ray computed tomography. *Journal of Sedimentary Research*, 66(5), <https://doi.org/10.1306/D4268144-2B26-11D7-8648000102C1865D>, 1996.
- 2710 Amrani, A., and Aizenshtat, Z.: Reaction of polysulfide anions with α,β unsaturated isoprenoid aldehydes in aquatic media: simulation of oceanic conditions. *Org. Geochem.*, 35, 909-21, <https://doi.org/10.1016/j.orggeochem.2004.04.002>, 2004.
- Amrani, A., Said-Ahamed, W., and Aizenshtat, Z.: The $\delta^{34}\text{S}$ values of the early-cleaved sulfur upon low temperature pyrolysis of a synthetic polysulfide cross-linked polymer. *Org. Geochem.*, 36, 971-74, <https://doi.org/10.1016/j.orggeochem.2005.02.002>, 2005.
- 2715 Andersen, M., Romaniello, S., Vance, D., Little, S., Herdman, R., and Lyons, T.: A modern framework for the interpretation of $^{238}\text{U}/^{235}\text{U}$ in studies of ancient ocean redox, *Earth Planet. Sc. Lett.*, 400, 184-194, <https://doi.org/10.1016/j.epsl.2014.05.051>, 2014.
- Andersen, M. B., Stirling, C. H., and Weyer, S.: Uranium isotope fractionation, *Rev. Mineral, Geochem.*, 82, 799-850, <https://doi.org/10.2138/rmg.2017.82.19>, 2017.
- 2720 Andersen, M. B., Matthews, A., Vance, D., Bar-Matthews, M., Archer, C., and de Souza, G.: A 10-fold decline in the deep Eastern Mediterranean thermohaline overturning circulation during the last interglacial period, *Earth Planet. Sc. Lett.*, 503, 58-67, <https://doi.org/10.1016/j.epsl.2018.09.013>, 2018.
- Andersen, M., Matthews, A., Bar-Matthews, M., and Vance, D. Rapid onset of ocean anoxia shown by high U and low Mo isotope compositions of sapropel S1, *Geochem. Perspect. Lett.*, 15, 10-14, <https://doi.org/10.7185/geochemlet.2027>, 2020.
- 2725 Anderson, L. and Sarmiento, J.: Redfield ratios of remineralization determined by nutrient data analysis, *Global Biogeochem. Cy.*, 8, 65-80, <https://doi.org/10.1029/93GB03318>, 1994.
- Anderson, R.F., LeHuray, A.P., Fleisher, M.Q. and Murray, J.W.: Uranium deposition in saanich inlet sediments, vancouver island. *Geochim. Cosmochi. Ac.*, 53(9), pp.2205-2213, [https://doi.org/10.1016/0016-7037\(89\)90344-X](https://doi.org/10.1016/0016-7037(89)90344-X), 1989.
- 2730 Anderson, R. F., Sachs, J. P., Fleisher, M. Q., Allen, K. A., Yu, J., Koutavas, A., and Jaccard S. L.: Deep-Sea Oxygen Depletion and Ocean Carbon Sequestration During the Last Ice Age, *Global Biogeochem. Cy.*, 33, 301-317, <https://doi.org/10.1029/2018GB006049>, 2019.
- Angell, R. W.: The Test Structure of the Foraminifer *Rosalina floridana*, *J. Protozool.*, 14, 299, <https://doi.org/10.1111/j.1550-7408.1967.tb02001.x>, 1967.
- 2735

- Anschutz, P., Jorissen, F.J., Chaillou, G., Abu-Zied, R., and Fontanier, C.: Recent turbidite deposition in the eastern Atlantic: early diagenesis and biotic recovery. *J. Mar. Res.*, 60, 835–854, <https://doi.org/10.1357/002224002321505156>, 2002.
- 2740 Arndt, S., Jørgensen, B. B., LaRowe, D. E., Middelburg, J. J., Pancost, R. D., and Regnier, P.: Quantifying the degradation of organic matter in marine sediments: A review and synthesis, *Earth-Sci. Rev.*, 123(0), 53–86, <https://doi.org/10.1016/j.earscirev.2013.02.008>, 2013.
- Arnold, Z. M.: A Note on Foraminiferan Sieve Plates, *Contrib. Cushman Found. Foramin. Res.*, 5, 77–67, 1954.
- Auderset, A., Moretti, S., Taphorn, B., Ebner, P.-R., Kast, E., Wang, X. T., Schiebel, R., Sigman, D. M., Haug, G. H., and Martínez-García, A.: Enhanced ocean oxygenation during Cenozoic warm periods, *Nature*, 609, 77–82, <https://doi.org/10.1038/s41586-022-05017-0>, 2022.
- 2745 Azrieli-Tal, I., Matthews, A., Bar-Matthews, M., Almogi-Labin, A., Vance, D., Archer, C., and Teutsch, N.: Evidence from molybdenum and iron isotopes and molybdenum–uranium covariation for sulphidic bottom waters during Eastern Mediterranean sapropel S1 formation, *Earth Planet. Sc. Lett.*, 393, 0, 231–242, <https://doi.org/10.1016/j.epsl.2014.02.054>, 2014.
- 2750 Baas, J. H., Schönfeld, J., and Zahn, R.: Mid-depth oxygen drawdown during Heinrich events: evidence from benthic foraminiferal community structure, trace-fossil tiering, and benthic $\delta^{13}\text{C}$ at the Portuguese Margin, *Mar. Geol.*, 152, 25–55, [https://doi.org/10.1016/S0025-3227\(98\)00063-2](https://doi.org/10.1016/S0025-3227(98)00063-2), 1998.
- Bahl, A., Gnanadesikan, A., Pradal, M.A.: Variations in ocean deoxygenation across earth system models: isolating the role of parameterized lateral mixing, *Global Biogeochem. Cy.*, 33, 703–724, 2019.
- 2755 Bale, N.J., Hopmans, E.C., Zell, C., Sobrinho, R.L., Kim, J.-H., Sinninghe Damsté, J.S., Villareal, T.A., and Schouten, S.: Long chain glycolipids with pentose head groups as biomarkers for marine endosymbiotic heterocystous cyanobacteria, *Org. Geochem.*, 81, 1–7, <https://doi.org/10.1016/j.orggeochem.2015.01.004>, 2015.
- Bale, N.J., Hennekam, R., Hopmans, E.C., Dorhout, D., Reichart, G.-J., Meer, M. van der, Villareal, T.A., Damsté, J.S.S., and Schouten, S.: Biomarker evidence for nitrogen-fixing cyanobacterial blooms in a brackish surface layer in the Nile River plume during sapropel deposition, *Geology*, 47, 1088–1092, <https://doi.org/10.1130/G46682.1>, 2019.
- 2760 Bandy, O. L.: Ecology and paleoecology of some California foraminifera. Part I. The frequency distribution of recent foraminifera off California, *J. Paleontol.*, 161–182, <http://www.jstor.org/stable/1300051>, 1953.
- Barker, S., and Elderfield, H.: Foraminifera calcification response to glacial-interglacial changes in atmospheric CO_2 , *Science*, 297, 833–836, <https://doi.org/10.1126/science.1072815>, 2002.
- 2765 Barker, S., Greaves, M. and Elderfield, H.: A study of cleaning procedures used for foraminiferal Mg/Ca paleothermometry. *Geochem. Geophys. Geosy.*, 4, 1525–2027, <https://doi.org/10.1029/2003GC000559>, 2003.
- Barmawidjaja, D. M., Van der Zwaan, G. J., Jorissen, F. J., and Puskaric, S.: 150 years of eutrophication in the northern Adriatic Sea: evidence from a benthic foraminiferal record, *Mar. Geol.*, 122, 367–384, [https://doi.org/10.1016/0025-3227\(94\)00121-Z](https://doi.org/10.1016/0025-3227(94)00121-Z), 1995.
- 2770 Barnes, C.E. and Cochran, J.K.: Uranium removal in oceanic sediments and the oceanic U balance, *Earth Planet. Sc. Lett.*, 97(1–2), pp.94–101, [https://doi.org/10.1016/0012-821X\(90\)90101-3](https://doi.org/10.1016/0012-821X(90)90101-3), 1990.
- Barras, C., Mouret, A., Nardelli, M.P., Metzger, E., Petersen, J., La, C., Filipsson, H.L. and Jorissen, F.: Experimental calibration of manganese incorporation in foraminiferal calcite. *Geochim. Cosmochim. Ac.*, 237, 49–64, <https://doi.org/10.1016/j.gca.2018.06.009>, 2018.
- 2775 Barrenechea Angeles, I., Romero-Martinez, M.L., Cavaliere, M., Varella, S., Francescangeli, F., Schirone, A., Delbono, I., Margiotta, F., Corinaldesi, C., Chiavarini, S., Montereali, M.R., Rimauro, J., Parrella, L., Musco, L., Dell’Anno, A., Tangherlini, M., Pawloski, J., Frontalini, F.: Encapsulated in sediments: eDNA deciphers the ecosystem history of one of the

- most polluted European marine sites, *Environment International*, 172, 107738. <https://doi.org/10.1016/j.envint.2023.107738>, 2023.
- 2780 Batista, F.C., Ravelo, A.C., Crusius, J., Casso, M.A. and McCarthy, M.D.: Compound specific amino acid $\delta^{15}\text{N}$ in marine sediments: A new approach for studies of the marine nitrogen cycle. *Geochim. Cosmochim. Ac.*, 142, 553-569, <https://doi.org/10.1016/j.gca.2014.08.002>, 2014.
- Bauersachs, T., Compaoré, J., Hopmans, E.C., Stal, L.J., Schouten, S., Sinninghe Damsté, J.S.: Distribution of heterocyst glycolipids in cyanobacteria, *Phytochemistry*, 70, 2034–2039, <https://doi.org/10.1016/j.phytochem.2009.08.014>, 2009a.
- 2785 Bauersachs, T., Hopmans, E.C., Compaoré, J., Stal, L.J., Schouten, S., Sinninghe Damsté, J.S.: Rapid analysis of long-chain glycolipids in heterocystous cyanobacteria using high-performance liquid chromatography coupled to electrospray ionization tandem mass spectrometry, *Rapid Commun. Mass Sp.*, 23, 1387–1394, <https://doi.org/10.1002/rcm.4009>, 2009b.
- Bauersachs, T., Speelman, E.N., Hopmans, E.C., Reichart, G.-J., Schouten, S., Sinninghe Damsté, J.S.: Fossilized glycolipids reveal past oceanic N_2 fixation by heterocystous cyanobacteria, *P. Natl. Acad. Sci.*, 107, 19190–19194, <https://doi.org/10.1073/pnas.1007526107>, 2010.
- 2790 Bé, A. W. H.: Shell Porosity of Recent Planktonic Foraminifera as a Climatic Index, *Science*, 161, 881-884, <https://doi.org/10.1126/science.161.3844.881>, 1968.
- Bé, A.W.H., Jongebloed, W.L. and McIntyre, A.: X-ray microscopy of recent planktonic Foraminifera, *J. Paleontol.*, 43, 1384–1396, <http://www.jstor.org/stable/1302521>, 1969.
- 2795 Becker, K.W., Elling, F.J., Schröder, J.M., Lipp, J.S., Goldhammer, T., Zabel, M., Elvert, M., Overmann, J., and Hinrichs, K.-U.: Isoprenoid Quinones Resolve the Stratification of Redox Processes in a Biogeochemical Continuum from the Photic Zone to Deep Anoxic Sediments of the Black Sea, *Appl. Environ. Microb.*, 84, e02736-17, <https://doi.org/10.1128/AEM.02736-17>, 2018.
- 2800 Belanger, C. L.: Volumetric analysis of benthic foraminifera: Intraspecific test size and growth patterns related to embryonic size and food resources. *Mar. Micropaleontol.*, 176, 102170, <https://doi.org/10.1016/j.marmicro.2022.102170>, 2022.
- Bender, M. L., Klinkhammer, G. P., and Spencer, D. W.: Manganese in seawater and the marine manganese balance, *Deep-Sea Res.*, 24, 9, 799-812, [https://doi.org/10.1016/0146-6291\(77\)90473-8](https://doi.org/10.1016/0146-6291(77)90473-8), 1977.
- Bennett, W.W., and Canfield, D.E.: Redox-sensitive trace metals as paleoredox proxies: A review and analysis of data from modern sediments, *Earth-Sci. Rev.*, 204, 103175, <https://doi.org/10.1016/j.earscirev.2020.103175>, 2020.
- 2805 Berger, W. H.: Deep-sea carbonates: Pleistocene dissolution cycles, *J. Foramin. Res.*, 3, 187-195, <https://doi.org/10.2113/gsjfr.3.4.187>, 1973.
- Berndmeyer, C., Birgel, D., Brunner, B., Wehrmann, L.M., Jöns, N., Bach, W., Arning, E.T., Föllmi, K.B. and Peckmann, J., 2012.: The influence of bacterial activity on phosphorite formation in the Miocene Monterey Formation, California. *Palaeogeography, Palaeoclimatology, Palaeoecology*, 317, 171-181, <https://doi.org/10.1016/j.palaeo.2012.01.004>, 2012.
- Bernhard, J.M.: Characteristic assemblages and morphologies of benthic foraminifera from anoxic, organic-rich deposits; Jurassic through Holocene, *J. Foramin. Res.*, 16, 207–215, <https://doi.org/10.2113/gsjfr.16.3.207>, 1986.
- Bernhard, J. M.: Benthic foraminiferal distribution and biomass related to pore-water oxygen content central California continental slope and rise, *Deep-Sea Res. Pt I*, 39, 585-605, [https://doi.org/10.1016/0198-0149\(92\)90090-G](https://doi.org/10.1016/0198-0149(92)90090-G), 1992.

- 2815 Bernhard, J. M.: Experimental and field evidence of Antarctic foraminiferal tolerance to anoxia and hydrogen sulfide, *Mar. Micropaleontol.*, 20, 203-213, [https://doi.org/10.1016/0377-8398\(93\)90033-T](https://doi.org/10.1016/0377-8398(93)90033-T), 1993.
- Bernhard, J. M., and Alve, E.: Survival, ATP pool, and ultrastructural characterization of benthic foraminifera from Drammensfjord (Norway): response to anoxia, *Mar. Micropaleontol.*, 28, 5-17, [https://doi.org/10.1016/0377-8398\(95\)00036-4](https://doi.org/10.1016/0377-8398(95)00036-4), 1996.
- 2820 Bernhard, J. M., Sen Gupta, B. K., and Borne, P. F.: Benthic foraminiferal proxy to estimate dysoxic bottom-water oxygen concentrations; Santa Barbara Basin, US Pacific continental margin. *J. Foramin. Res.*, 27, 301-310, <https://doi.org/10.2113/gsjfr.27.4.301>, 1997. Bernhard, J.M., and Sen Gupta, B.K.: Foraminifera of oxygen-depleted environments, in: *Modern Foraminifera*, edited by: Sen Gupta, B.K., Springer, Dordrecht, Germany, 201-216, https://doi.org/10.1007/0-306-48104-9_12, 1999.
- 2825 Bernhard, J. M., Buck, K. R., Farmer, M. A., and Bowser, S.: The Santa Barbara Basin is a symbiosis oasis, *Nature*, 403, 77-80, <https://doi.org/10.1038/47476>, 2000.
- Bernhard, J. M., Barry, J. P., Buck, K. R., and Starczak, V. R.: Impact of intentionally injected carbon dioxide hydrate on deep-sea benthic foraminiferal survival. *Glob. Change Biol.*, 15, 2078-2088, <https://doi.org/10.1111/j.1365-2486.2008.01822.x>, 2009.
- 2830 Bernhard, J. M., Wit, J. C., Starczak, V. R., Beaudoin, D. J., Phalen, W. G., and McCorkle, D. C.: Impacts of Multiple Stressors on a Benthic Foraminiferal Community: A Long-Term Experiment Assessing Response to Ocean Acidification, Hypoxia and Warming, *Front. Mar. Sci.*, 8, 643339, <https://doi.org/10.3389/fmars.2021.643339>, 2021.
- Berner, R.A.: A new geochemical classification of sedimentary environments. *Journal of Sedimentary Petrology*, 51(2): 359-365, <https://doi.org/10.1306/212F7C7F-2B24-11D7-8648000102C1865D>, 1981.
- 2835 Berthold, W. -U.: Ultrastructure and function of wall perforations in *Patellina corrugata* Williamson, Foraminiferida, *J. Foramin. Res.*, 6, 22-29, <https://doi.org/10.2113/gsjfr.6.1.22>, 1976.
- Bianchi, T. S., Cui, X., Blair, N. E., Burdige, D. J., Eglinton, T. I., and Galy, V.: Centers of organic carbon burial and oxidation at the land-ocean interface, *Org. Geochem.*, 115, 138-155, <https://doi.org/10.1016/j.orggeochem.2017.09.008>, 2018.
- Bijma, J., Faber, W.W., Hemleben, C.: Temperature and salinity limits for growth and survival of some planktonic foraminifera in laboratory cultures, *Journal of Foraminifera Research* 20, 95-116, 1990.
- 2840 Bijma, J., Spero, H. J., and Lea, D. W.: Reassessing foraminiferal stable isotope geochemistry: impact of the oceanic carbonate system (experimental results), in: *Use of Proxies in Paleoceanography: Examples from the South Atlantic*, edited by: Fischer, G. and Wefer, G., Springer, Berlin, 489-512, https://doi.org/10.1007/978-3-642-58646-0_20, 1999.
- 2845 Bindoff, N. L., Cheung, W. W. L., Kairo, J. G., Arístegui, J., Guinder, V. A., Hallberg, R., Hilmi, N., Jiao, N., Karim, M. S., Levin, L., O'Donoghue, S., Purca Cuicapusa, S.R., Rinkevich, B., Suga, T., Tagliabue, A., and Williamson, P.: Changing Ocean, Marine Ecosystems, and Dependent Communities, in: *IPCC Special Report on the Ocean and Cryosphere in a Changing Climate*, edited by: Pörtner, H. -O., Roberts, D. C., Masson-Delmotte, V., Zhai, P., Tignor, M., Poloczanska, E., Mintenbeck, K., Alegría, A., Nicolai, M., Okem, A., Petzold, J., Rama, B., and Weyer, N. M., Cambridge University Press, Cambridge, UK and New York, NY, USA, 447-587. <https://doi.org/10.1017/9781009157964.007>, 2019.
- 2850 Blaga, C. I., Reichart, G. -J., Heiri, O., and Sinninghe Damsté, J. S.: Tetraether membrane lipid distributions in water-column particulate matter and sediments: a study of 47 European lakes along a north-south transect, *J. Paleolimnol.*, 41, 523-540, <https://doi.org/10.1007/s10933-008-9242-2>, 2009.
- Blair, N. E., and Aller, R. C.: The Fate of Terrestrial Organic Carbon in the Marine Environment, *Annu. Rev. Mar. Sci.*, 4, 401-423, <https://doi.org/10.1146/annurev-marine-120709-142717>, 2012.
- 2855 Blumenberg, M., Seifert, R., Reitner, J., Pape, T., and Michaelis, W.: Membrane lipid patterns typify distinct anaerobic methanotrophic consortia, *P. Nat. Acad. Sci. USA*, 101, 11111-11116, <https://doi.org/10.1073/pnas.0401188101>, 2004.

- Blumenberg, M., Krüger, M., Nauhaus, K., Talbot, H. M., Oppermann, B. I., Seifert, R., Pape, T., and Michaelis, W.: Biosynthesis of hopanoids by sulfate-reducing bacteria (genus *Desulfovibrio*), *Environ. Microbiol.*, 8, 1220–1227, <https://doi.org/10.1111/j.1462-2920.2006.01014.x>, 2006.
- 2860 Blumenberg, M., Hoppert, M., Krüger, M., Dreier, A., and Thiel, V.: Novel findings on hopanoid occurrences among sulfate reducing bacteria: Is there a direct link to nitrogen fixation? *Org. Geochem.*, 49, 1–5, <https://doi.org/10.1016/j.orggeochem.2012.05.003>, 2012.
- 2865 Bodelier, P. L. E., Gillisen, M. -J. B., Hordijk, K., Sinninghe Damsté, J. S., Rijpstra, W. I. C., Geenevasen, J. A. J., and Dunfield, P. F.: A reanalysis of phospholipid fatty acids as ecological biomarkers for methanotrophic bacteria, *ISME J.*, 3, 606–617, <https://doi.org/10.1038/ismej.2009.6>, 2009.
- Boer, W., Nordstad, S., Weber, M., Mertz-Kraus, R., Hönisch, B., Bijma, J., Raitzsch, M., Wilhelms-Dick, D., Foster, G.L., Goring-Harford, H. and Nürnberg, D.: New calcium carbonate nano-particulate pressed powder pellet (NFHS-2-NP) for LA-ICP-OES, LA-(MC)-ICP-MS and μ XRF, *Geostand. Geoanal. Res.*, 46, 411–432, <https://doi.org/10.1111/ggr.12425>, 2022.
- 2870 Boersma, A., Silva, I. P., and Shackleton, N. J.: Atlantic Eocene planktonic foraminiferal paleohydrographic indicators and stable isotope paleoceanography, *Paleoceanography*, 2, 287–331, <https://doi.org/10.1029/PA002i003p00287>, 1987.
- Boersma, A., and Silva, I. P.: Atlantic Paleogene biserial heterohelicid foraminifera and oxygen minima. *Paleoceanography*, 4, 271–286, <https://doi.org/10.1029/PA004i003p00271>, 1989.
- 2875 Boetius, A., Ravensschlag, K., Schubert, C. J., Rickert, D., Widdel, F., Gieseke, A., Amann, R., Jorgensen, B. B., Witte, U., and Pfannkuche, O.: A marine microbial consortium apparently mediating anaerobic oxidation of methane, *Nature*, 407, 623–626, <https://doi.org/10.1038/35036572>, 2000.
- Boiteau, R., Greaves, M. and Elderfield, H.: Authigenic uranium in foraminiferal coatings: A proxy for ocean redox chemistry. *Paleoceanography and Paleoclimatology*, 27, PA3227, <https://doi.org/10.1029/2012PA002335>, 2012.
- Bograd, S. J., Castro, C. G., Di Lorenzo, E., Palacios, D. M., Bailey, H., Gilly, W., and Chavez, F. P.: Oxygen declines and the shoaling of the hypoxic boundary in the California Current, *Geophys. Res. Lett.*, 35, L12607, <https://doi.org/10.1029/2008GL034185>, 2008.
- 2880 Böning, P., Brumsack, H.-J., Böttcher, M. E., Schnetger, B., Kriete, C., Kallmeyer, J., and Borchers, S. L.: Geochemistry of Peruvian near-surface sediments, *Geochim. Cosmochim. Ac.*, 68, 4429–4451, <https://doi.org/10.1016/j.gca.2004.04.027>, 2004.
- 2885 Böning, P., Bard, E., & Rose, J. : Toward direct, micron-scale XRF elemental maps and quantitative profiles of wet marine sediments. *Geochemistry, Geophysics, Geosystems*, 8(5), <https://doi.org/10.1029/2006GC001480>, 2007.
- Böning, P., Brumsack, H.-J., Schnetger, B., Grunwald, M.: Trace element signatures of Chilean upwelling sediments at ~36S, *Marine Geology* 259, 112–121, 2009.
- Böning, P., Shaw, T., Pahnke, K., and Brumsack, H. J.: Nickel as indicator of fresh organic matter in upwelling sediments, *Geochim. Cosmochim. Ac.*, 162, 99–108, <https://doi.org/10.1016/j.gca.2015.04.027>, 2015.
- 2890 Bouchet, V. M., Alve, E., Rygg, B., and Telford, R. J.: Benthic foraminifera provide a promising tool for ecological quality assessment of marine waters, *Ecol. Indic.*, 23, 66–75, <https://doi.org/10.1016/j.ecolind.2012.03.011>, 2012.
- BouDagher-Fadel, M.K: *Biostatigraphic and Geological Significance of Planktonic Foraminifera*. UCL Press, London, 2015.
- 2895 Boussafir, M., Gelin, F., Lallier-Vergès, E., Derenne, S., Bertrand, P., and Largeau, C.: Electron Microscopy and pyrolysis of kerogens from the Kimmeridge Clay Formation, UK: Source organisms, preservation processes, and origin of microcycles, *Geochim. Cosmochim. Ac.*, 59, 3731–47, [https://doi.org/10.1016/0016-7037\(95\)00273-3](https://doi.org/10.1016/0016-7037(95)00273-3), 1995.

- Boussafir, M., and Lallier-Vergès, E.: Accumulation of organic matter in the Kimmeridge Clay Formation (KCF): An update fossilisation model for marine petroleum source-rocks, *Mar. Petrol. Geol.*, 14, 75–83, [https://doi.org/10.1016/S0264-8172\(96\)00050-5](https://doi.org/10.1016/S0264-8172(96)00050-5), 1997.
- 2900 Boyle, E.A. and Keigwin, L.D.: Comparison of Atlantic and Pacific paleochemical records for the last 215,000 years: changes in deep ocean circulation and chemical inventories, *Earth Planet. Sc. Lett.*, 76, 135-150, [https://doi.org/10.1016/0012-821X\(85\)90154-2](https://doi.org/10.1016/0012-821X(85)90154-2), 1985.
- Boyle, R.A., Dahl, T.W., Dale, A.W., Shields-Zhou, G.A., Zhu, M.Y., Brasier, M.D., Canfield, D.E. and Lenton, T.M.: Stabilization of the coupled oxygen and phosphorus cycles by the evolution of bioturbation. *Nature Geosci*, 7(9), 671-676, 2905 <https://doi.org/10.1038/ngeo2213>, 2014.
- Bradbury, H. J., Turchyn, A. V., Bateson, A., Antler, G., Fotherby, A., Druhan, J. L., Greaves, M., Sevilgen, D. S., and Hodell, D. A.: The Carbon-Sulfur Link in the Remineralization of Organic Carbon in Surface Sediments, *Front. Earth Sci.*, 9, <https://doi.org/10.3389/feart.2021.652960>, 2021.
- Bradbury, H.J., Thomas, N.C., Mleneck-Vautravers, M., Hodell, D.A.: Revisiting the relationship between the pore water carbon isotope gradient and bottom water oxygen concentrations, *Geochimica et Cosmochimica Acta*, 366, 84-94, 2910 <https://doi.org/10.1016/j.gca.2023.12.011>, 2024.
- Bradley, A. S., Fredricks, H., Hinrichs, K. -U., and Summons, R. E.: Structural diversity of diether lipids in carbonate chimneys at the Lost City Hydrothermal Field, *Org. Geochem.*, 40, 1169–1178, <https://doi.org/10.1016/j.orggeochem.2009.09.004>, 2009.
- 2915 Branson, O., Bonnin, E. A., Perea, D. E., Spero, H. J., Zhu, Z., Winters, M., Honisch, B., Russell, A. D., Fehrenbacher, J. S., and Gagnon, A. C.: Nanometer-scale chemistry of a calcite biomineralization template: Implications for skeletal composition and nucleation. *P. Natl. Acad. Sci. USA*, 113, 12934-12939, <https://doi.org/10.1073/pnas.1522864113>, 2016.
- Brassell, S. C., Wardroper, A. M. K., Thomson, I. D., Maxwell, J. R., and Eglinton, G.: Specific acyclic isoprenoids as biological markers of methanogenic bacteria in marine sediments, *Nature*, 290, 693–696, <https://doi.org/10.1038/290693a0>, 2920 1981.
- Brassell, S. C.: Molecular changes in sediment lipids as indicators of systematic early diagenesis, *Philos. T. R. Soc. S-A*, 315, 57–75, <https://doi.org/10.1098/rsta.1985.0029>, 1985.
- Bratsch, Steven G.: Standard electrode potentials and temperature coefficients in water at 298.15 K, *J. Phys. Chem. Ref. Data*, 18, 1-21, <https://doi.org/10.1063/1.555839>, 1989.
- 2925 Breitbart, D., Levin, L. A., Oschlies, A., Grégoire, M., Chavez, F. P., Conley, D. J., Garçon, V., Gilbert, D., Gutiérrez, D., Isensee, K., Jacinto, G. S., Limburg, K. E., Montes, I., Naqvi, S. W. A., Pitcher, G. C., Rabalais, N. N., Roman, M. R., Rose, K. A., Seibel, B. A., Telszewski, M., Yasuhara, M., and Zhang, J.: Declining oxygen in the global ocean and coastal waters, *Science*, 359, eaam7240, <https://doi.org/10.1126/science.aam7240>, 2018.
- Briggs, D.E.G., and Summons, R.E.: Ancient biomolecules: Their origins, fossilization, and role in revealing the history of life, *BioEssays*, 36, 482–490, <https://doi.org/10.1002/bies.201400010>, 2930 2014.
- Briguglio, A.: Hydrodynamic behaviour of nummulitids, Ph.D. thesis, Universität Wien, Austria, 185 pp., 2010.
- Brinkmann, I., Ni, S., Schweizer, M., Oldham, V.E., Quintana Krupinski, N.B., Medjoubi, K., Somogyi, A., Whitehouse, M.J., Hansel, C.M., Barras, C., Bernhard, J.M., and Fillipson, H.L.: Foraminiferal Mn/Ca as Bottom-Water Hypoxia Proxy: An Assessment of *Nonionella stella* in the Santa Barbara Basin, USA, *Paleoceanography and Paleoclimatology*, 36, 2935 p.e2020PA004167, <https://doi.org/10.1029/2020PA004167>, 2021.
- Brinkmann, I., Barras, C., Jilbert, T., Paul, K. M., Somogyi, A., Ni, S., Schweizer, M., Bernhard, J.M. and Filipsson, H.L.: Benthic foraminiferal Mn/Ca as low-oxygen proxy in fjord sediments, *Global Biogeochem. Cy.*, e2023GB007690, <https://doi.org/10.1029/2023GB007690>, 2023.

- 2940 Brocks, J. J., and Schaeffer, P.: Okenane, a biomarker for purple sulfur bacteria (Chromatiaceae), and other new carotenoid derivatives from the 1640 Ma Barney Creek Formation. *Geochim. Cosmochim. Ac.*, 72, 1396-1414, <https://doi.org/10.1016/j.gca.2007.12.006>, 2008.
- Broecker, W., and Clark, E.: An evaluation of Lohmann's foraminifera weight dissolution index, *Paleoceanography and Paleoclimatology*, 16, 531– 534, <https://doi.org/10.1029/2000PA000600>, 2001
- 2945 Brown, S. T., Basu, A., Ding, X., Christensen, J. N., and DePaolo, D. J.: Uranium isotope fractionation by abiotic reductive precipitation, *P. Natl. Acad. Sci. USA* , 115, 8688-8693, <https://doi.org/10.1073/pnas.1805234115>, 2018.
- Bruland, K.W.: Trace elements in seawater. *Chemical Oceanography* 8. 157-200, 1983.
- Bruland, K.W., Lohan, M.C., Controls of Trace Metals in Seawater, *Treatise on Geochemistry, Volume 6*. Editor: Henry Elderfield. Executive Editors: Heinrich D. Holland and Karl K. Turekian. pp. 625. ISBN 0-08-043751-6. Elsevier, 2003, p.23-47 2003/
- 2950 Brunner, B., Contreras, S., Lehmann, M. F., Matantseva, O., Rollog, M., Kalvelage, T., Klockgether, G., Lavik, G., Jetten, M. S. M., Kartal, B., and Kuypers, M. M. M.: Nitrogen isotope effects induced by anammox bacteria, *Proc. Natl. Acad. Sci.*, 110, 18994–18999, <https://doi.org/10.1073/pnas.1310488110>, 2013.
- 2955 Brüske, A., Weyer, S., Zhao, M.-Y., Planavsky, N., Wegwerth, A., Neubert, N., Dellwig, O., Lau, K., and Lyons, T.: Correlated molybdenum and uranium isotope signatures in modern anoxic sediments: Implications for their use as paleo-redox proxy, *Geochim. Cosmochim. Ac.*, 270, 449-474, <https://doi.org/10.1016/j.gca.2019.11.031>, 2020.
- Burdige, D. J., and Gieskes, J. M.: A pore water/solid phase diagenetic model for manganese in marine sediments, *Am. J. Sci.*, 283, 29–47. <https://doi.org/10.2475/ajs.283.1.29>, 1983.
- 2960 Burdige, D.J.: The biogeochemistry of manganese and iron reduction in marine sediments, *Earth-Sci. Rev.*, 35, 249-284, [https://doi.org/10.1016/0012-8252\(93\)90040-E](https://doi.org/10.1016/0012-8252(93)90040-E), 1993.
- Burdige, D. J.: Preservation of organic matter in marine sediments: Controls, mechanisms, and an imbalance in sediment organic carbon budgets?, *Chemical Reviews*, 107, 467-485, <https://doi.org/10.1021/cr050347q>, 2007.
- 2965 Burke, J., Renema, W., Henehan, M. J., Elder, L. E., Davis, C. V., Maas, A. E., Foster, G. L., Schiebel, R., and Hull, P. M.: Factors influencing test porosity in planktonic foraminifera, *Biogeosciences*, 15, 6607-6619, <https://doi.org/10.5194/bg-15-6607-2018>, 2018.
- Burke, J. E., Renema, W., Schiebel, R., and Hull, P. M.: Three-dimensional analysis of inter- and intraspecific variation in ontogenetic growth trajectories of planktonic foraminifera, *Mar. Micropaleontol.*, 155, 1–12, <https://doi.org/10.1016/j.marmicro.2019.101794>, 2020.
- 2970 Busecke, J., Resplandy, L., Dunne, J.P.: The Equatorial Undercurrent and the Oxygen Minimum Zone in the Pacific, *Geophys. Res. Lett.*, 46, 6716-6725, <https://doi.org/10.1029/2019GL082692>, 2019.
- Buzas, M. A., Culver, S. J., and Jorissen, F. J.: A statistical evaluation of the microhabitats of living (stained) infaunal benthic foraminifera, *Mar. Micropaleontol.*, 20, 311–320, [https://doi.org/https://doi.org/10.1016/0377-8398\(93\)90040-5](https://doi.org/https://doi.org/10.1016/0377-8398(93)90040-5), 1993.
- 2975 Callbeck, C.M., Canfield, D.E., Kuypers, M.M.M., Yilmaz, P., Lavik, G., Thamdrup, B., Schubert, C.J., and Bristow, L.A.: Sulfur cycling in oceanic oxygen minimum zones, *Limnol. Oceanogr.*, 66, 2360–2392, <https://doi.org/10.1002/lno.11759>, 2021.
- Calvert, S. E., and Pedersen, T. F.: Sedimentary geochemistry of manganese; implications for the environment of formation of manganeseiferous black shales, *Econ. Geol.*, 91, 36–47, <https://doi.org/10.2113/gsecongeo.91.1.36>, 1996.

- Calvert, S. E. and Pedersen, T. F.: Elemental Proxies for Palaeoclimatic and Palaeoceanographic Variability in Marine Sediments: Interpretation and Application, in: *Paleoceanography of the Late Cenozoic, Part 1, Methods*, edited by: Hillaire-Marcel, C. and de Vernal, A., Elsevier, New York, 567-644, [http://dx.doi.org/10.1016/S1572-5480\(07\)01019-6](http://dx.doi.org/10.1016/S1572-5480(07)01019-6), 2007.
- 2980 Campos, M. L. A. M., Farrenkopf, A. M., Jickells, T. D. and Luther III, G. W.: A comparison of dissolved iodine cycling at the Bermuda Atlantic Time-series Station and Hawaii Ocean Time-series Station, *Deep-Sea Res. Pt. II*, 43, 455-466, [https://doi.org/10.1016/0967-0645\(95\)00100-X](https://doi.org/10.1016/0967-0645(95)00100-X), 1996.
- 2985 Canfield, D. E.: Biogeochemistry of sulfur isotopes, *Rev. Mineral. Geochem.*, 43, 607-636, <https://doi.org/10.2138/gsrmg.43.1.607>, 2001.
- Canfield, D.E., Farquhar, J.: Animal evolution, bioturbation, and the sulfate concentration of the oceans, *P. Natl. Acad. Sci. USA*, 106, 8123-8127, <https://doi.org/10.1073/pnas.0902037106>, 2009.
- Canfield, D. E., and Thamdrup, B.: Towards a consistent classification scheme for geochemical environments, or, why we wish the term 'suboxic' would go away, *Geobiology*, 7, 385-392, <https://doi.org/10.1111/j.1472-4669.2009.00214.x>, 2009.
- 2990 Canfield, D. E., Stewart, F.J., Thamdrup, B., Brabandere, L.D., Dalsgaard, T., DeLong, E. F., Revsbech, N. P., and Ulloa, O.: A Cryptic Sulfur Cycle in Oxygen-Minimum-Zone Waters off the Chilean Coast, *Science*, 330, 1375-1378, <https://doi.org/10.1126/science.1196889>, 2010.
- Cardich, J., Morales, M., Quipúzcoa, L., Sifeddine, A., and Gutiérrez, D.: Benthic foraminiferal communities and microhabitat selection on the continental shelf off central Peru, in: *Anoxia*, edited by: Altenbach, A., Bernhard, J., Seckbach, J., Springer, Dordrecht, Germany, 323-340, https://doi.org/10.1007/978-94-007-1896-8_17, 2012.
- 2995 Cardich, J., Gutiérrez, D., Romero, D., Pérez, A., Quipúzcoa, L., Marquina, R., Yupanqui, W., Solís, J., Carhuapoma, W., Sifeddine, A., and Rathburn, A.: Calcareous benthic foraminifera from the upper central Peruvian margin: control of the assemblage by pore water redox and sedimentary organic matter, *Mar. Ecol. Prog. Series*, 535, 63-87, <https://doi.org/10.3354/meps11409>, 2015.
- 3000 Cardich, J., Sifeddine, A., Salvattecchi, R., Romero, D., Briceño-Zuluaga, F., Graco, M., Anculle, T., Almeida, C., and Gutiérrez, D.: Multidecadal Changes in Marine Subsurface Oxygenation Off Central Peru During the Last ca. 170 Years, *Front. Mar. Sci.*, 6, 270, <https://doi.org/10.3389/fmars.2019.00270>, 2019.
- Caromel, A. G. M., Schmidt, D. N., Fletcher, I., and Rayfield, E. J.: Morphological Change During The Ontogeny Of The Planktic Foraminifera, *J. Micropalaeontol.*, 35, 2-19, <https://doi.org/10.1144/jmpaleo2014-017>, 2016.
- 3005 Caromel, A. G. M., Schmidt, D. N., and Rayfield, E. J.: Ontogenetic constraints on foraminiferal test construction, *Evol. Dev.*, 19, 157-168, <https://doi.org/10.1111/ede.12224>, 2017.
- Carpenter, S. R., Elser, M. M., and Elser, J. J.: Chlorophyll production, degradation, and sedimentation: Implications for paleolimnology, *Limnol. Oceanogr.*, 31, 112-124, <https://doi.org/10.4319/lo.1986.31.1.0112>, 1986.
- 3010 Carter, S.C., Paytan, A., Griffith, E.M.: Toward an improved understanding of the marine barium cycle and the application of marine barite as a paleoproductivity proxy, *Minerals* 10, 421, <https://doi.org/10.3390/min10050421>, 2020.
- Casanova-Arenillas, S., Rodríguez-Tovar, F.J. and Martínez-Ruiz, F.: Ichnological evidence for bottom water oxygenation during organic rich layer deposition in the westernmost Mediterranean over the Last Glacial Cycle. *Mar. Geo.*, 443, 106673, <https://doi.org/10.1016/j.margeo.2021.106673>, 2022.
- 3015 Casciotti, K. L.: Nitrogen and Oxygen Isotopic Studies of the Marine Nitrogen Cycle, *Annu. Rev. Mar. Sci.*, 8, 379-407, <https://doi.org/10.1146/annurev-marine-010213-135052>, 2016.
- Castillo, A., Hromic, T., Uribe, R. A., Valdés, J., Sifeddine, A., Quezada, L., Vega, S. -E., Arenciba, A., Días-Ochoa, J., and Guíñez, M.: Living (stained) calcareous benthic foraminiferal assemblages (> 125µm) in a coastal upwelling zone of the

- 3020 Humboldt Current System, Northern Chile (~ 27° S), *Reg. Stud. Mar. Sci.*, 44, 101725, <https://doi.org/10.1016/j.rsma.2021.101725>, 2021.
- Castillo, A., Valdés, J., Sifeddine, A., Reyss, J., Bouloubassi, I., and Ortlieb, L.: Changes in biological productivity and ocean-climatic fluctuations during the last ~1.5 kyr in the Humboldt ecosystem off northern Chile (27°S): a multiproxy approach, *Palaeogeogr. Palaeoclimatol.*, 485, 798-815, <https://doi.org/10.1016/j.palaeo.2017.07.038>, 2017.
- 3025 Castillo, A., Valdés, J., Sifeddine, A., Vega, S. E., Díaz-Ochoa, J., and Marambio, Y.: Evaluation of redox-sensitive metals in marine surface sediments influenced by the oxygen minimum zone of the Humboldt Current System, Northern Chile, *Int. J. Sediment Res.*, 34, 178-190, <https://doi.org/10.1016/j.ijsrc.2018.08.005>, 2019.
- Caulle, C., Koho, K. A., Mojtahid, M., Reichart, G. J., and Jorissen, F. J.: Live (Rose Bengal stained) foraminiferal faunas from the northern Arabian Sea: faunal succession within and below the OMZ, *Biogeosciences*, 11, 1155-1175, <https://doi.org/10.5194/bg-11-1155-2014>, 2014.
- 3030 Caulle, C., Mojtahid, M., Gooday, A. J., Jorissen, F. J., and Kitazato, H.: Living (Rose-Bengal-stained) benthic foraminiferal faunas along a strong bottom-water oxygen gradient on the Indian margin (Arabian Sea), *Biogeosciences*, 12, 5005-5019, <https://doi.org/10.5194/bg-12-5005-2015>, 2015.
- Cayre, O., Beaufort, L., and Vincent, E.: Paleoproductivity in the Equatorial Indian Ocean for the last 260,000 yr: a transfer function based on planktonic foraminifera, *Quaternary Sci. Rev.*, 18, 839-857, [https://doi.org/10.1016/S0277-3791\(98\)00036-5](https://doi.org/10.1016/S0277-3791(98)00036-5), 1999.
- 3035 Chan, F., Barth, J. A., Lubchenco, J., Kirincich, A., Weeks, H., Peterson, W. T., & Menge, B. A. (2008). Emergence of anoxia in the California current large marine ecosystem. *Science*, 319(5865), 920-920.
- Chance, R., Baker, A. R., Carpenter, L., and Jickells, T. D.: The distribution of iodide at the sea surface, *Environ. Sci.-Proc. Imp.*, 16, 1841-1859, <https://doi.org/10.1039/C4EM00139G>, 2014.
- 3040 Chang, L., Hoogakker, B.A.A., Heslop, D., Zhao, X., Roberts, A., De Deckker, O., Xue, P., Zeng, F., Wang, S., Berndt, T.A., Stuut, J-B.W., Harrison, R.J.: Recurrence of glacial ocean deoxygenation and accumulated respired carbon storage in the Indian Ocean of the last 850,000 years, *Nature Communications* 14:4841, <https://doi.org/10.1038/s41467-023-40452-1>, 2023.
- Charrieau, L.M., Nagai, Y., Kimoto, K., Dissard, D., Below, B., Fujita, K., and Toyofuku, T.: The coral reef-dwelling *Peneroplis* spp. shows calcification recovery to ocean acidification conditions, *Sci. Rep.*, 12, 6373, <https://doi.org/10.1038/s41598-022-10375-w>, 2022.
- 3045 Chen, J. H., Edwards, R. L., and Wasserburg, G. J.: ²³⁸U, ²³⁴U and ²³²Th in seawater, *Earth Planet. Sc. Lett.*, 80, 241-251, [https://doi.org/10.1016/0012-821X\(86\)90108-1](https://doi.org/10.1016/0012-821X(86)90108-1), 1986.
- 3050 Chen, X., Ling, J.-F., Vance, D., Shields-Zhou, G.A., Zhu, M., Poulton, S.W., Och, L.M., Jiang, S.-Y., Li, D., Cremonese, L., Archer, C.: Rise to modern levels of ocean oxygenation coincided with the Cambrian radiation of animals, *Nature Communications* 6, ncomms8142, 2015.
- Chen, P., Yu, J., and Jin, Z.: An evaluation of benthic foraminiferal U/Ca and U/Mn proxies for deep ocean carbonate chemistry and redox conditions, *Geochem. Geophys. Geosyst.*, 18, 617-630, <https://doi.org/10.1002/2016GC006730>, 2017.
- 3055 Chen, X., Robinson, S.A., Romaniello, S. J., and Anbar, A. D.: ²³⁸U/²³⁵U in calcite is more susceptible to carbonate diagenesis. *Geochim. Cosmochim. Ac.*, 326, 273-287, <https://doi.org/10.1016/j.gca.2022.03.027>, 2022.
- Chiu, C. F., Sweere, T. C., Clarkson, M. O., de Souza, G. F., Hennekam, R., and Vance, D.: Co-variation systematics of uranium and molybdenum isotopes reveal pathways for descent into euxinia in Mediterranean sapropels, *Earth Planet. Sc. Lett.*, 585, 117527, <https://doi.org/10.1016/j.epsl.2022.117527>, 2022.
- 3060 Choquel, C., Mütter, D., Ni, S., Pirzamanbein, B., Charrieau, L.M., Hirose, K., Seto, Y., Schmiedl, G., and Filipsson, H.L.: 3D morphological variability in foraminifera unravel environmental changes in the Baltic Sea entrance over the last 200 years, *Front. Earth Sci.*, 11, 1120170, <https://doi.org/10.3389/feart.2023.1120170>, 2023.

- Clarkson, M. O., Stirling, C. H., Jenkyns, H. C., Dickson, A. J., Porcelli, D., Moy, C. M., Pogge von Strandmann, P. A. E., Cooke, I. R., and Lenton, T. M.: Uranium isotope evidence for two episodes of deoxygenation during Oceanic Anoxic Event 2, *P. Natl. Acad. Sci. USA*, 115, 2918-2923, <https://doi.org/10.1073/pnas.1715278115>, 2018.
- 3065 Clarkson, M. O., Hennekam, R., Sweere, T. C., Andersen, M. B., Reichart, G.-J., and Vance, D.: Carbonate associated uranium isotopes as a novel local redox indicator in oxidatively disturbed reducing sediments, *Geochim. Cosmochim. Ac.*, 311, 12-28, <https://doi.org/10.1016/j.gca.2021.07.025>, 2021a.
- Clarkson, M. O., Lenton, T. M., Andersen, M. B., Bagard, M.-L., Dickson, A. J., and Vance, D.: Upper limits on the extent of seafloor anoxia during the PETM from uranium isotopes, *Nat. Commun.*, 12, 1-9, <https://doi.org/10.1038/s41467-020-20486-5>, 2021b.
- 3070 Clement, B. G., Luther III, G. W., and Tebo, B. M.: Rapid, oxygen-dependent microbial Mn (II) oxidation kinetics at sub-micromolar oxygen concentrations in the Black Sea suboxic zone, *Geochim. Cosmochim. Ac.*, 73, 1878-1889, <https://doi.org/10.1016/j.gca.2008.12.023>, 2009.
- Cline, J. D., and Kaplan, I. R.: Isotopic fractionation of dissolved nitrate during denitrification in the eastern tropical north Pacific Ocean, *Mar. Chem.*, 3, 271-299, [https://doi.org/10.1016/0304-4203\(75\)90009-2](https://doi.org/10.1016/0304-4203(75)90009-2), 1975.
- 3075 Cole, D., Zhang, Sh., and Planavsky, N.: A new estimate of detrital redox-sensitive metal concentrations and variability in fluxes to marine sediments, *Geochim. Cosmochim. Ac.*, 215, 337-353, <http://dx.doi.org/10.1016/j.gca.2017.08.004>, 2017.
- Colley, S., and Thomson, J.: Recurrent uranium relocations in distal turbidites emplaced in pelagic conditions, *Geochim. Cosmochim. Ac.*, 49, 2339-2348, [https://doi.org/10.1016/0016-7037\(85\)90234-0](https://doi.org/10.1016/0016-7037(85)90234-0), 1985.
- 3080 Colley, S., Thomson, J., and Toole, J.: Uranium relocations and derivation of quasi-isochrons for a turbidite/pelagic sequence in the Northeast Atlantic, *Geochim. Cosmochim. Ac.*, 53, 1223-1234, [https://doi.org/10.1016/0016-7037\(89\)90058-6](https://doi.org/10.1016/0016-7037(89)90058-6), 1989.
- Colley, S., Thomson, J., Wilson, T.R.S., and Higgs, N.C.: Post-depositional migration of elements during diagenesis in brown clay and turbidite sequences in the North East Atlantic, *Geochim. Cosmochim. Ac.*, 48, 1223-1235, [https://doi.org/10.1016/0016-7037\(84\)90057-7](https://doi.org/10.1016/0016-7037(84)90057-7), 1984.
- 3085 Colodner, D., Edmond, J., and Boyle, E.: Rhenium in the Black Sea: comparison with molybdenum and uranium, *Earth Planet. Sc. Lett.*, 131, 1-15, [https://doi.org/10.1016/0012-821X\(95\)00010-A](https://doi.org/10.1016/0012-821X(95)00010-A), 1995.
- Conley, D. J., Carstensen, J., Aigars, J., Axe, P., Bonsdorff, E., Eremina, T., Hahti, B.-M., Humborg, C., Jonsson, P., Kotta, J., Lännegren, C., Larsson, U., Maximov, A., Medina, M. R., Lysiak-Pastuszek, E., Remeikaitė-Nikienė, N., Walve, J., Wilhelms, S., and Zillén, L.: Hypoxia Is Increasing in the Coastal Zone of the Baltic Sea, *Environ. Sci. Technol.*, 45, 6777-6783, <https://doi.org/10.1021/es201212r>, 2011.
- 3090 Connock, G.T., Owens, J.D., and Liu, X.-L.: Biotic induction and microbial ecological dynamics of Oceanic Anoxic Event 2, *Commun. Earth Environ.*, 3, 136, <https://doi.org/10.1038/s43247-022-00466-x>, 2022.
- Cook, M.K., Dial, A.R., and Hendy, I.L.: Iodine stability as a function of pH and its implications for simultaneous multi-element ICP-MS analysis of marine carbonates for paleoenvironmental reconstructions, *Mar. Chem.*, 245, 104148, <https://doi.org/10.1016/j.marchem.2022.104148>, 2022.
- 3095 Corfield, R. M., and Shackleton, N. J.: Productivity change as a control on planktonic foraminiferal evolution after the Cretaceous/Tertiary boundary, *Hist. Biol.*, 1, 323-343, <https://doi.org/10.1080/08912968809386482>, 1988.
- Corliss, B. H.: Microhabitats of benthic foraminifera within deep-sea sediments. *Nature*, 314, 435-438, <https://doi.org/10.1038/314435a0>, 1985.
- 3100 Corliss, B. H.: Morphology and microhabitat preferences of benthic foraminifera from the northwest Atlantic Ocean, *Mar. Micropaleontol.*, 17, 195-236, [https://doi.org/10.1016/0377-8398\(91\)90014-W](https://doi.org/10.1016/0377-8398(91)90014-W), 1991.
- Corliss, B. H., and Emerson, S.: Distribution of Rose Bengal stained deep-sea benthic foraminifera from the Nova Scotian continental margin and Gulf of Maine, *Deep-Sea Res.*, 37, 381-400, [https://doi.org/10.1016/0198-0149\(90\)90015-N](https://doi.org/10.1016/0198-0149(90)90015-N), 1990.

- 3105 Corliss, B.H., Sun, X., Brown, C.W., and Showers, W.J.: Influence of seasonal primary productivity on $\delta^{13}\text{C}$ of North Atlantic deep-sea benthic foraminifera, *Deep-Sea Res. Pt. I*, 53, 740–746, <https://doi.org/10.1016/j.dsr.2006.01.006>, 2006.
- Costa, K.M., Anderson, R.F., McManus, J.F., Winckler, G., Middleton, J.L., Langmuir, C.H.: Trace element (Mn, Zn, Ni, V) and authigenic uranium (aU) geochemistry reveal sedimentary redox history on the Juan de Fuca Ridge, North Pacific Ocean, *Geochim. Cosmochim. Ac.*, 236, 79–98, <https://doi.org/10.1016/j.gca.2018.02.016>, 2018.
- 3110 Costa, K. M., Nielsen, S. G., Wang, Y., Lu, W., Hines, S. K., Jacobel, A. W., and Oppo, D. W.: Marine sedimentary uranium to barium ratios as a potential quantitative proxy for Pleistocene bottom water oxygen concentrations, *Geochim. Cosmochim. Ac.*, 343, 1-16, <https://doi.org/10.1016/j.gca.2022.12.022>, 2023.
- Cowie, G., Mowbray, S., Kurian, S., Sarkar, A., White, C., Anderson, A., Vergnaud, B., Johnstone, G., Brear, S., Woulds, C., Naqvi, S. W. A., and Kitazato, H.: Comparative organic geochemistry of Indian margin (Arabian Sea) sediments: estuary to continental slope, *Biogeosciences*, 11, 6683-6696, <https://doi.org/10.5194/bg-11-6683-2014>, 2014.
- 3115 Coxall, H. K., Pearson, P. N., Wilson, P. A., and Sexton, P. F.: Iterative evolution of digitate planktonic foraminifera, *Paleobiology*, 33, 495-516, <https://doi.org/10.1666/06034.1>, 2007.
- Crusius, J., Calvert, S., Pedersen, T., and Sage, D.: Rhenium and molybdenum enrichments in sediments as indicators of oxic, suboxic and sulfidic conditions of deposition. *Earth Planet. Sc. Lett.*, 145, 65-78, [https://doi.org/10.1016/S0012-821X\(96\)00204-X](https://doi.org/10.1016/S0012-821X(96)00204-X), 1996.
- 3120 Crusius, J., Thomson, J.: Comparative behaviour of authigenic Re, U and Mo during reoxidation and subsequent long-term burial in marine sediments, *Geochimica et Cosmochimica Acta* 64, 2233-2242, 2000.
- Croudace, I. W., Rindby, A., & Rothwell, R. G.: ITRAX: description and evaluation of a new multi-function X-ray core scanner. Geological Society, London, Special Publications, 267(1), 51-63, <https://doi.org/10.1144/GSL.SP.2006.267.01.04>, 2006.
- 3125 Croudace, I. W., & Rothwell, R. G. (Eds.). *Micro-XRF Studies of Sediment Cores: Applications of a non-destructive tool for the environmental sciences* (Vol. 17, p. 668). Dordrecht: Springer, <https://doi.org/10.1007/978-94-017-9849-5>, 2015.
- Croudace, I. W., Löwemark, L., Tjallingii, R., & Zolitschka, B.: Current perspectives on the capabilities of high resolution XRF core scanners. *Quaternary International*, 514, 5-15, <https://doi.org/10.1016/j.quaint.2019.04.002>, 2019.
- 3130 Cutter, G. A., Moffett, J. W., Nielsdóttir, M. C., Sanial, V., and Nielsdottir, M. C.: Multiple oxidation state trace elements in suboxic waters off Peru: In situ redox processes and advective/diffusive horizontal transport, *Mar. Chem.*, 201, 77–89, <https://doi.org/10.1016/j.marchem.2018.01.003>, 2018.
- Dahl, T. W., Anbar, A. D., Gordon, G. W., Rosing, M. T., Frei, R., and Canfield, D. E.: The behavior of molybdenum and its isotopes across the chemocline and in the sediments of sulfidic Lake Cadagno, Switzerland, *Geochim. Cosmochim. Ac.*, 74, 144-163, <https://doi.org/10.1016/j.gca.2009.09.018>, 2010a.
- 3135 Dahl, T. W., Hammarlund, E. U., Anbar, A. D., Bond, D. P., Gill, B. C., Gordon, G. W., Knoll, A. H., Nielsen, A. T., Schovsbo, N. H., and Canfield, D. E.: Devonian rise in atmospheric oxygen correlated to the radiations of terrestrial plants and large predatory fish, *P. Natl. Acad. Sci. USA*, 107, 17911-17915, <https://doi.org/10.1073/pnas.1011287107>, 2010b.
- Dahl, T.W., Chappaz, A., Hoek, J., McCenzie, C.J., Svane, S., Canfield, D.E.: Evidence of molybdenum association with particulate organic matter under sulfidic conditions, *Geobiology* 15, 311-323, 2017.
- 3140 Dahl, T. W., Hammarlund, E. U., Rasmussen, C. M. Ø., Bond, D. P., and Canfield, D. E.: Sulfidic anoxia in the oceans during the Late Ordovician mass extinctions—insights from molybdenum and uranium isotopic global redox proxies, *Earth-Sci. Rev.*, 220, 103748, <https://doi.org/10.1016/j.earscirev.2021.103748>, 2021.
- 3145 Davis, C.V., Myhre, S. E., and Hill, T. M.: Benthic foraminiferal shell weight: Deglacial species-specific responses from the Santa Barbara Basin, *Mar. Micropaleontol.*, 124, 45-53, <https://doi.org/10.1016/j.marmicro.2016.02.002>, 2016.

- Davis, C. V., Wishner, K., Renema, W., and Hull, P. M.: Vertical distribution of planktic foraminifera through an oxygen minimum zone: how assemblages and test morphology reflect oxygen concentrations, *Biogeosciences*, 18, 977-992, <https://doi.org/10.5194/bg-18-977-2021>, 2021.
- 3150 Davis, C. V., Doherty, S., Fehrenbacher, J., Wishner, K.: Trace element composition of modern planktic foraminifera from an oxygen minimum zone: potential proxies for an enigmatic environment, *Front. Mar. Sci.*, 29, <https://doi.org/10.3389/fmars.2023.1145756>, 2023.
- Davis, C. V., Sibert, E. C., Jacobs, P. H., Burls, N., & Hull, P. M.: Intermediate water circulation drives distribution of Pliocene Oxygen Minimum Zones, *Nat. Commun.*, 14, 40, <https://doi.org/10.1038/s41467-022-35083-x>, 2023.
- 3155 Debenay, J. -P. (Ed.): A Guide to 1,000 Foraminifera from Southwestern Pacific New Caledonia, IRD Éditions, Publications scientifiques du Muséum, Muséum national d'Histoire naturelle, Paris, France, 384 pp., ISBN 978-2-7099-1729-2, 2012.
- Deflandre, B., Mucci, A., Gagné, J.-P., Guignard, C., and Sundby, B.: Early diagenetic processes in coastal marine sediments disturbed by a catastrophic sedimentation event, *Geochim. Cosmochim. Ac.*, 66, 2547–2558, [https://doi.org/10.1016/S0016-7037\(02\)00861-X](https://doi.org/10.1016/S0016-7037(02)00861-X), 2002
- 3160 De Lange, G. J.: Early Diagenetic Reactions in Interbedded Pelagic and Turbiditic Sediments in the Nares-Abyssal-Plain (Western North- Atlantic) Consequences for the Composition of Sediment and Interstitial Water, *Geochim. Cosmochim. Ac.*, 50, 2543-2561, [https://doi.org/10.1016/0016-7037\(86\)90209-7](https://doi.org/10.1016/0016-7037(86)90209-7), 1986.
- De Lange, G. J., Thomson, J., Reitz, A., Slomp, C. P., Principato, M. S., Erba, E., and Corselli, C.: Synchronous basin-wide formation and redox-controlled preservation of a Mediterranean sapropel, *Nat. Geoscience*, 1, 606-610, <https://doi.org/10.1038/ngeo283>, 2008.
- 3165 Dellinger, M., Hilton, R.G., Geoff M. Nowell, G.M.: Fractionation of rhenium isotopes in the Mackenzie River basin during oxidative weathering, *Earth Planet. Sc. Lett.*, 573, 117131, <https://doi.org/10.1016/j.epsl.2021.117131>, 2021.
- de Moel, H., Ganssen, G. M., Peeters, F. J. C., Jung, S. J. A., Kroon, D., Brummer, G. J. A., and Zeebe, R. E.: Planktic foraminiferal shell thinning in the Arabian Sea due to anthropogenic ocean acidification? *Biogeosciences*, 6, 1917–1925, <https://doi.org/10.5194/bg-6-1917-2009>, 2009.
- 3170 Den Dulk, M., Reichart, G. J., Memon, G. M., Roelofs, E. M. P., Zachariasse, W. J., and Van der Zwaan, G. J.: Benthic foraminiferal response to variations in surface water productivity and oxygenation in the northern Arabian Sea, *Mar. Micropaleontol.*, 35, 43-66, [http://dx.doi.org/10.1016/S0377-8398\(98\)00015-2](http://dx.doi.org/10.1016/S0377-8398(98)00015-2), 1998.
- De Nooijer, L.J., Sampedro, L.P., Jorissen, F.J., Pawlowski, J., Rosenthal, Y., Dissard, D., Reichart, G.J.: 500 million years of foraminiferal calcification. *Earth-Science Reviews* 243, <https://doi.org/10.1016/j.earscirev.2023.104484>, 2023.
- 3175 Detlef, H., Sosdian, S.M., Kender, S., Lear, C.H., and Hall, I.R.: Multi-elemental composition of authigenic carbonates in benthic foraminifera from the eastern Bering Sea continental margin (International Ocean Discovery Program Site U1343), *Geochim. Cosmochim. Ac.*, 268, 1-21, <https://doi.org/10.1016/j.gca.2019.09.025>, 2020.
- Deutsch, C., Brix, H., Ito, T., Frenzel, H., & Thompson, L. (2011). Climate-forced variability of ocean hypoxia. *science*, 333(6040), 336-339, <https://doi.org/10.1126/science.1202422>, 2011.
- 3180 Deutsch, C., Berelson, W., Thunell, R., Weber, T., Tems, C., McManus, J., Crusius, J., Ito, T., Baumgartner, T., Ferreira, V., Mey, J., and van Geen, A.: Centennial changes in North Pacific anoxia linked to tropical trade winds, *Science*, 345, 665–668, <https://doi.org/10.1126/science.1252332>, 2014.
- 3185 Dias, B. B., Hart, M. B., Smart, C. W., and Hall-Spencer, J. M.: Modern seawater acidification: the response of foraminifera to high-CO₂ conditions in the Mediterranean Sea, *J. Geol. Soc. London*, 167, 843-846, <https://doi.org/10.1144/0016-76492010-050>, 2010.
- Diaz, R. J. and Rosenberg, R.: Spreading Dead Zones and Consequences for Marine Ecosystems, *Science* (80-.), 321, 926–929, <https://doi.org/10.1126/science.1156401>, 2008.

- 3190 Dickson, A. J., and Cohen, A. S.: A molybdenum isotope record of Eocene Thermal Maximum 2: Implications for global ocean redox during the early Eocene, *Paleoceanography and Paleoclimatology*, 27, <https://doi.org/10.1029/2012PA002346>, 2012.
- Dickson, A. J., Jenkyns, H. C., Porcelli, D., van den Boorn, S., and Idiz, E.: Basin-scale controls on the molybdenum-isotope composition of seawater during Oceanic Anoxic Event 2 (Late Cretaceous), *Geochim. Cosmochim. Ac.*, 178, 291-306, <https://doi.org/10.1016/j.gca.2015.12.036>, 2016.
- 3195 Dickson, A.J., Hsieh, Y.-T., Bryan, A.: The rhenium isotope composition of Atlantic Ocean seawater, *Geochimica et Cosmochimica Acta* 287, 221-228, <https://doi.org/10.1016/j.gca.2020.02.020>, 2020.
- Diz, P., and Francés, G.: Distribution of live benthic foraminifera in the Ría de Vigo (NW Spain), *Mar. Micropaleontol.*, 66, 165-191, <https://doi.org/10.1016/j.marmicro.2007.09.001>, 2008.
- 3200 Diz, P., Gonzalez-Guitian, V., Gonzalez-Villanueva, R., Ovejero, A., Hernandez-Almeida, I.: BENFEP, a quantitative database of BENthic Foraminifera from surface sediments of the Eastern Pacific, *Earth Syst. Sci. Data*, 15, 697-722, <https://doi.org/10.5194/essd-15-697-2023>, 2023.
- Dorador, J., Rodríguez-Tovar, F. J., & Titschack, J.: Exploring computed tomography in ichnological analysis of cores from modern marine sediments. *Scientific reports*, 10(1), 201, <https://doi.org/10.1038/s41598-019-57028-z>, 2020.
- 3205 Dubois, N., Kienast, M., Kienast, S., Normandeau, C., Calvert, S. E., Herbert, T. D., and Mix, A.: Millennial-scale variations in hydrography and biogeochemistry in the Eastern Equatorial Pacific over the last 100 kyr, *Quat. Sci. Rev.*, 30, 210–223, <https://doi.org/10.1016/j.quascirev.2010.10.012>, 2011.
- Duijnste, I. A. P., Ernst, S. R., and Van der Zwaan, G. J.: Effect of anoxia on the vertical migration of benthic foraminifera. *Marine Ecology Progress Series*, 246, 85-94, <https://doi.org/10.3354/meps246085>, 2003.
- 3210 Dummann, W., Steinig, S., Hofmann, P., Lenz, M., Kusch, S., Flögel, S., Herrle, J.O., Hallmann, C., Rethemeyer, J., Kasper, H.U., and Wagner, T.: Driving mechanisms of organic carbon burial in the Early Cretaceous South Atlantic Cape Basin (DSDP Site 361), *Clim. Past*, 17, 469–490, <https://doi.org/10.5194/cp-17-469-2021>, 2021.
- Dunk, R.M., Mills, R.A., and Jenkins, W.J.: A reevaluation of the oceanic uranium budget for the Holocene, *Chem. Geol.*, 190, 45–67, [https://doi.org/10.1016/S0009-2541\(02\)00110-9](https://doi.org/10.1016/S0009-2541(02)00110-9), 2002.
- 3215 Eggins, S.M.: Laser Ablation ICP-MS Analysis of Geological Materials Prepared as Lithium Borate Glasses, *Geostandard. Newslett.*, 27, 147-162. <https://doi.org/10.1111/j.1751-908X.2003.tb00642.x>, 2003.
- Eglinton, T.I., and Eglinton, G.: Molecular proxies for paleoclimatology, *Earth and Planetary Science Letters* 275, 1–16, <https://doi.org/10.1016/j.epsl.2008.07.012>, 2008.
- 3220 Eglinton, T.I., and Repeta, D.J.: Organic matter in the contemporary ocean, in: *Treatise on Geochemistry: The Oceans and Marine Geochemistry*, edited by: Mottl, M.J., and Elderfield, H., Elsevier, Oxford, United Kingdom, 151-189, <https://doi.org/10.1016/B978-0-08-095975-7.00606-9>, 2014.
- Eiler, J., Cesar, J., Chimiak, L., Dallas, B., Grice, K., Griep-Raming, J., Juchelka, D., Kitchen, N., Lloyd, M., Makarov, A., Robins, R., and Schwieters, J.: Analysis of molecular isotopic structures at high precision and accuracy by Orbitrap mass spectrometry, *Int. J. Mass Spectrom.*, 422, 126–142, <https://doi.org/10.1016/j.ijms.2017.10.002>, 2017.
- 3225 Elling, F.J., Könneke, M., Lipp, J.S., Becker, K.W., Gagen, E.J., Hinrichs, K.-U.: Effects of growth phase on the membrane lipid composition of the thaumarchaeon *Nitrosopumilus maritimus* and their implications for archaeal lipid distributions in the marine environment, *Geochim. Cosmochim. Ac.*, 141, 579–597, <https://doi.org/10.1016/j.gca.2014.07.005>, 2014.
- Elling, F.J., Becker, K.W., Könneke, M., Schröder, J.M., Kellermann, M.Y., Thomm, M., and Hinrichs, K.-U.: Respiratory quinones in Archaea: phylogenetic distribution and application as biomarkers in the marine environment. *Environmental Microbiology* 18, 692–707, <https://doi.org/10.1111/1462-2920.13086>, 2016.

- 3230 Elling, F.J., Könneke, M., Nicol, G.W., Stieglmeier, M., Bayer, B., Spieck, E., Torre, J.R. de la, Becker, K.W., Thomm, M., Prosser, J.I., Herndl, G.J., Schleper, C., and Hinrichs, K.-U.: Chemotaxonomic characterisation of the thaumarchaeal lipidome, *Environ. Microbiol.*, 19, 2681–2700, <https://doi.org/10.1111/1462-2920.13759>, 2017.
- Elling, F.J., Hemingway, J.D., Evans, T.W., Kharbush, J.J., Spieck, E., Summons, R.E., and Pearson, A.: Vitamin B₁₂-dependent biosynthesis ties amplified 2-methylhopanoid production during oceanic anoxic events to nitrification, *P. Natl. Acad. Sci. USA*, 117, 32996–33004, <https://doi.org/10.1073/pnas.2012357117>, 2020.
- 3235 Elling, F.J., Hemingway, J.D., Kharbush, J.J., Becker, K.W., Polik, C.A., and Pearson, A.: Linking diatom-diazotroph symbioses to nitrogen cycle perturbations and deep-water anoxia: Insights from Mediterranean sapropel events, *Earth Planet. Sc. Lett.*, 571, 117110, <https://doi.org/10.1016/j.epsl.2021.117110>, 2021.
- Elling, F.J., Evans, T.W., Nathan, V., Hemingway, J.D., Kharbush, J.J., Bayer, B., Spieck, E., Husain, F., Summons, R.E., and Pearson, A.: Marine and terrestrial nitrifying bacteria are sources of diverse bacteriohopanepolyols, *Geobiology*, 20, 399–420, <https://doi.org/10.1111/gbi.12484>, 2022.
- 3240 Elvert, M., Suess, E., and Whiticar, M.J.: Anaerobic methane oxidation associated with marine gas hydrates: superlight C-isotopes from saturated and unsaturated C-20 and C-25 irregular isoprenoids, *Naturwissenschaften*, 86, 295–300, <https://doi.org/10.1007/s001140050619>, 1999.
- 3245 Endrizzi, F., and Linfeng R.: Chemical speciation of uranium (VI) in marine environments: complexation of calcium and magnesium ions with $[(\text{UO}_2)(\text{CO}_3)_3]^{4-}$ and the effect on the extraction of uranium from seawater, *Chem–Eur. J.*, 20, 14499–14506, <https://doi.org/10.1002/chem.201403262>, 2014.
- Enge, A. J., Wukovits, J., Wanek, W., Watzka, M., Witte, U. F., Hunter, W. R., and Heinz, P.: Carbon and nitrogen uptake of calcareous benthic foraminifera along a depth-related oxygen gradient in the OMZ of the Arabian Sea, *Front. Microbiol.*, 7, 71, <https://doi.org/10.3389/fmicb.2016.00071>, 2016.
- 3250 Erdem, Z., Schönfeld, J. Glock, N., Dengler, M., Mosch, T., Sommer, S., Elger, J., Eisenhauer, A.: Peruvian sediments as recorders of an evolving hiatus for the last 22 thousand years. *Quaternary Science Reviews* 137, 1–14, <http://dx.doi.org/10.1016/j.quascirev.2016.01.029>, 2016.
- Erdem, Z., and Schönfeld, J.: Pleistocene to Holocene benthic foraminiferal assemblages from the Peruvian continental margin, *Palaeontol. Electron.*, 20.2.35A, 1–32, <https://doi.org/10.26879/764>, 2017.
- 3255 Erdem, Z., Schönfeld, J., Rathburn, A. E., Pérez, M. E., Cardich, J., and Glock, N.: Bottom-water deoxygenation at the Peruvian margin during the last deglaciation recorded by benthic foraminifera, *Biogeosciences*, 17, 3165–3182, <https://doi.org/10.5194/bg-17-3165-2020>, 2020.
- Erickson, B. E., and Helz, G. R.: Molybdenum (VI) speciation in sulfidic waters: stability and lability of thiomolybdates, *Geochim. Cosmochim. Ac.*, 64, 1149–1158, [https://doi.org/10.1016/S0016-7037\(99\)00423-8](https://doi.org/10.1016/S0016-7037(99)00423-8), 2000.
- 3260 Ettwig, K.F., Butler, M.K., Paslier, D.L., Pelletier, E., Mangenot, S., Kuypers, M.M.M., Schreiber, F., Dutilh, B.E., Zedelius, J., Beer, D. de, Gloorich, J., Wessels, H.J.C.T., Alen, T. van, Luesken, F., Wu, M.L., Pas-Schoonen, K.T. van de, Camp, H.J.M.O. den, Janssen-Megens, E.M., Francoijs, K.-J., Stunnenberg, H., Weissenbach, J., Jetten, M.S.M., and Strous, M.: Nitrite-driven anaerobic methane oxidation by oxygenic bacteria, *Nature*, 464, 543–548, <https://doi.org/10.1038/nature08883>, 2010.
- 3265 Farrell, J. W., Pedersen, T. F., Calvert, S. E., and Nielsen, B.: Glacial–interglacial changes in nutrient utilization in the equatorial Pacific Ocean, *Nature*, 377, 514–517, <https://doi.org/10.1038/377514a0>, 1995.
- 3270 Fennel, K., Mattern, J.P., Doney, S.C., Bopp, L., Moore, A.M., and Wang, B., Y, L.: Ocean biogeochemical modelling, *Nat. Rev. Methods Primers* 2, 76, <https://doi.org/10.1038/s43586-022-00154-2>, 2022.
- Ferry, J.G., and Lessner, D.J.: Methanogenesis in marine sediments, *Ann. NY Acad. Sci.*, 1125, 147–157, <https://doi.org/10.1196/annals.1419.007>, 2008.

- 3275 Finney, B. P., Lyle, M. W., and Heath, G. R.: Sedimentation at MANOP Site H (eastern equatorial Pacific) over the past 400,000 years: climatically induced redox variations and their effects on transition metal cycling, *Paleoceanography and Paleoclimatology*, 3, 169-189, <https://doi.org/10.1029/PA003i002p00169>, 1988.
- Fontanier, C., Jorissen, F.J., Licari, L., Alexandre, A., Anschutz, P., and Carbonel, P.: Live benthic foraminiferal faunas from the Bay of Biscay: faunal density, composition, and microhabitats, *Deep-Sea Res. Pt. I*, 49, 751-785, [https://doi.org/10.1016/S0967-0637\(01\)00078-4](https://doi.org/10.1016/S0967-0637(01)00078-4), 2002.
- 3280 Fontanier, C., Jorissen, F. J., Chaillou, G., David, C., Anschutz, P., and Lafon, V.: Seasonal and interannual variability of benthic foraminiferal faunas at 550 m depth in the Bay of Biscay. *Deep-Sea Res. Pt. I*, 50, 457-494, [https://doi.org/10.1016/S0967-0637\(02\)00167-X](https://doi.org/10.1016/S0967-0637(02)00167-X), 2003.
- Fontanier, C., Jorissen, F. J., Chaillou, G., Anschutz, P., Grémare, A., & Griveaud, C.: Live foraminiferal faunas from a 2800 m deep lower canyon station from the Bay of Biscay: faunal response to focusing of refractory organic matter. *Deep-Sea Res. Pt. I*, 52, 1189-1227, <https://doi.org/10.1016/j.dsr.2005.01.006>, 2005.
- 3285 Fontanier, C., Jorissen, F.J., Michel, E., Cortijo, E., Vidal, L., Anschutz, P., Stable oxygen and carbon isotopes of live (stained) benthic foraminifera from Cap-Ferret Canyon (Bay of Biscay), *Journal of Foraminiferal Research* 38, 39-51, 2008.
- Fontanier, C., Koho, K. A., Goñi-Urriza, M. S., Deflandre, B., Galaup, S., Ivanovsky, A., Gayer, N., Dennielou, B., Grémare, A., Bichon, S., Gassie, C., Anschutz, P., Duran, and Reichart, G. J.: Benthic foraminifera from the deep-water Niger delta (Gulf of Guinea): Assessing present-day and past activity of hydrate pockmarks, *Deep-Sea Res. Pt. I*, 94, 87-106, <https://doi.org/10.1016/j.dsr.2014.08.011>, 2014.
- 3290 Fox, L., Stukins, S., Hill, T., and Miller, C.G.: Quantifying the Effect of Anthropogenic Climate Change on Calcifying Plankton, *Sci. Rep.-UK*, 10, 1620, <https://doi.org/10.1038/s41598-020-58501-w>, 2020.
- Franco-Fraguas, P., Badaraco Costa, K., and de Lima Toledo, F.: Stable isotope/test size relationship in *Cibicides* *wuellerstorfi*, *Braz. J. Oceanogr.*, 59, 2870291, <https://doi.org/10.1590/S1679-87592011000300010>, 2011.
- 3295 Francois, R.: A Study of Sulphur Enrichment in the Humic Fraction of Marine Sediments during Early Diagenesis, *Geochim. Cosmochim. Ac.*, 51, 17-27, [https://doi.org/10.1016/0016-7037\(87\)90003-2](https://doi.org/10.1016/0016-7037(87)90003-2), 1987.
- Frei, R., Gaucher, C., Døssing, L., and Sial, A.: Chromium isotopes in carbonates—a tracer for climate change and for reconstructing the redox state of ancient seawater, *Earth Planet. Sc. Lett.*, 312, 114-125, <https://doi.org/10.1016/j.epsl.2011.10.009>, 2011.
- 3300 Freitas, T.R., Bacalhau, E., and Bonetti, C.: ForImage: Foraminiferal Image Analysis and Test Measurement. R Package Version 0.1.0., 2021.
- French, K.L., Rocher, D., Zumberge, J.E., and Summons, R.E.: Assessing the distribution of sedimentary C40 carotenoids through time, *Geobiology*, 13, 139-151, <https://doi.org/10.1111/gbi.12126>, 2015.
- 3305 Fritz-Endres, T. and Fehrenbacher, J.: Preferential Loss of High Trace Element Bearing Inner Calcite in Foraminifera During Physical and Chemical Cleaning, *Geochemistry, Geophys. Geosystems*, 22, e2020GC009419, <https://doi.org/https://doi.org/10.1029/2020GC009419>, 2021.
- Froelich P. N., Klinkhammer G. P., Bender M. L., Luedtke N. A., Heath G. R., Cullen D., Dauphin P., Hammond D., Hartman B. and Maynard V.: Early oxidation of organic matter in pelagic sediments of the eastern equatorial Atlantic: suboxic diagenesis, *Geochim. Cosmochim. Ac.*, 43, 1075-1090, [https://doi.org/10.1016/0016-7037\(79\)90095-4](https://doi.org/10.1016/0016-7037(79)90095-4), 1979.
- 3310 Freund, C., Wishard, A., Brenner, R., Sobel, M., Mizelle, J., Kim, A., Meyer, D. A., and Morford, J. L.: The effect of a thiol-containing organic molecule on molybdenum adsorption onto pyrite, *Geochim. Cosmochim. Ac.*, 174, 222-235, <https://doi.org/10.1016/j.gca.2015.11.015>, 2016.

- 3315 Fyke, J.G., D'Orgeville, M., Weaver, A.J.: Drake Passage and Central American Seaway controls on the distribution of the oceanic carbon reservoir, *Glob. and Planet. Change* 128, 72-83, 2015
- Galbraith, E. D., Kienast, M., Pedersen, T. F., and Calvert, S. E.: Glacial-interglacial modulation of the marine nitrogen cycle by high-latitude O₂ supply to the global thermocline: MODULATION OF THE N CYCLE BY O₂ SUPPLY, *Paleoceanography and Paleoclimatology*, 19, n/a-n/a, <https://doi.org/10.1029/2003PA001000>, 2004.
- 3320 Galbraith, E. D., Kienast, M., Jaccard, S. L., Pedersen, T. F., Brunelle, B. G., Sigman, D. M., and Kiefer, T.: Consistent relationship between global climate and surface nitrate utilization in the western subarctic Pacific throughout the last 500 ka: EPHEMERAL HNLC IN SUBARCTIC PACIFIC, *Paleoceanography and Paleoclimatology*, 23, n/a-n/a, <https://doi.org/10.1029/2007PA001518>, 2008.
- 3325 Gambacorta, A., Pagnotta, E., Romano, I., Sodano, G., and Trincone, A.: Heterocyst glycolipids from nitrogen-fixing cyanobacteria other than Nostocaceae, *Phytochemistry*, 48, 801–805, [https://doi.org/10.1016/S0031-9422\(97\)00954-0](https://doi.org/10.1016/S0031-9422(97)00954-0), 1998.
- Ganeshram, R. S., Pedersen, T. F., Calvert, S. E., and Murray, J. W.: Large changes in oceanic nutrient inventories from glacial to interglacial periods, *Nature*, 376, 755–758, <https://doi.org/10.1038/376755a0>, 1995.
- 3330 Geslin, E., Heinz, P., Jorissen, F., and Hemleben, C.: Migratory responses of deep-sea benthic foraminifera to variable oxygen conditions: laboratory investigations, *Mar. Micropaleontol.*, 53, 227-243, <https://doi.org/10.1016/j.marmicro.2004.05.010>, 2004.
- Geslin, E., Risgaard-Petersen, N., Lombard, F., Metzger, E., Langlet, D., and Jorissen, F.: Oxygen respiration rates of benthic foraminifera as measured with oxygen microsensors, *J. Exp. Mar. Biol. Ecol.*, 396, 108-114, <https://doi.org/10.1016/j.jembe.2010.10.011>, 2011.
- 3335 Geslin, E., Barras, C., Langlet, D., Nardelli, M. P., Kim, J. H., Bonnin, J., Metzger, E., and Jorissen, F. J.: Survival, reproduction and calcification of three benthic foraminiferal species in response to experimentally induced hypoxia, in: *Approaches to Study Living Foraminifera*, edited by: Kitazato, H., M., and Bernhard, J., Springer, Tokyo, 163-193, https://doi.org/10.1007/978-4-431-54388-6_10, 2014.
- 3340 Giordano, L., Ferraro, L., Salvatore, M., Oscurato, S. L., and Maddalena, P.: Morphometric analysis on benthic foraminifera through atomic force microscopy, *Mar. Micropaleontol*, 153, 101775, <https://doi.org/10.1016/j.marmicro.2019.101775>, 2019.
- Glock, N., Eisenhauer, A., Milker, Y., Liebetrau, V., Schönfeld, J., Mallon, J., Sommer, S., and Hensen, C.: Environmental influences on the pore density of *Bolivina spissa* (Cushman), *J. Foraminifer. Res.*, 41, 22–32, <https://doi.org/10.2113/gsjfr.41.1.22>, 2011.
- 3345 Glock, N., Eisenhauer, A., Liebetrau, V., Wiedenbeck, M., Hensen, C., and Nehrke, G.: EMP and SIMS studies on Mn/Ca and Fe/Ca systematics in benthic foraminifera from the Peruvian OMZ: a contribution to the identification of potential redox proxies and the impact of cleaning protocols, *Biogeosciences*, 9, 341-359, <https://doi.org/10.5194/bg-9-341-2012>, 2012.
- 3350 Glock, N., Schönfeld, J., and Mallon, J.: The Functionality of Pores in Benthic Foraminifera in View of Bottom Water Oxygenation: A Review, in: *ANOXIA: Evidence for Eukaryote Survival and Paleontological Strategies, Cellular Origin, Life in Extreme Habitats and Astrobiology*, Vol. 21, edited by: Altenbach, A. V., Bernhard, J. M., and Seckbach, J., Springer, Dordrecht, Germany, 540–556, https://doi.org/10.1007/978-94-007-1896-8_28, 2012.
- Glock, N., Liebetrau, V., and Eisenhauer, A.: I/Ca ratios in benthic foraminifera from the Peruvian oxygen minimum zone: analytical methodology and evaluation as a proxy for redox conditions, *Biogeosciences*, 11, 7077-7095, <https://doi.org/10.5194/bg-11-7077-2014>, 2014.

- 3355 Glock, N., Liebetrau, V., Eisenhauer, A., and Rocholl, A.: High resolution I/Ca ratios of benthic foraminifera from the Peruvian oxygen-minimum-zone: A SIMS derived assessment of a potential redox proxy, *Chem. Geol.*, 447, 40-53, <https://doi.org/10.1016/j.chemgeo.2016.10.025>, 2016.
- Glock, N., Erdem, Z., Wallmann, K., Somes, C. J., Liebetrau, V., Schönfeld, J., Gorb, S. and Eisenhauer, A.: Coupling of oceanic carbon and nitrogen facilitates spatially resolved quantitative reconstruction of nitrate inventories. *Nat. Commun.*, 9, 1217, <https://doi.org/10.1038/s41467-018-03647-5>, 2018.
- 3360 Glock, N., Liebetrau, V., Vogts, A. and Eisenhauer, A.: Organic heterogeneities in foraminiferal calcite traced through the distribution of N, S, and I measured with nanoSIMS: a new challenge for element-ratio-based paleoproxies?, *Front. Earth Sci.*, 7, 175, <https://doi.org/10.3389/feart.2019.00175>, 2019.
- Glock, N., Roy, A. S., Romero, D., Wein, T., Weissenbach, J., Revsbech, N. P., Høglund, S., Clemens, D., Sommer, S., and Dagan, T.: Metabolic preference of nitrate over oxygen as an electron acceptor in foraminifera from the Peruvian oxygen minimum zone, *P. Natl. Acad. Sci. USA*, 116, 2860-2865, <https://doi.org/10.1073/pnas.1813887116>, 2019.
- 3365 Glock, N., Erdem, Z., and Schönfeld, J.: The Peruvian oxygen minimum zone was similar in extent but weaker during the Last Glacial Maximum than Late Holocene, *Commun. Earth Environ.*, 3, 307, <https://doi.org/10.1038/s43247-022-00635-y>, 2022.
- Glock, N.: Benthic foraminifera and graptolites from oxygen-depleted environments – survival strategies, biogeochemistry and trophic interactions, *Biogeosciences*, 20, 3423–3447, <https://doi.org/10.5194/bg-20-3423-2023>, 2023.
- 3370 Goldschmidt, V. M. (ed.): *Geochemistry*, The Clarendon Press, Oxford, 730 pp., ISBN: 0198512104, 1954.
- Gomaa, F., Utter, D. R., Powers, C., Beaudoin, D. J., Edgcomb, V. P., Filipsson, H. L., Hansel, C. M., Wankel, S., Zhang, Y., and Bernhard, J. M.: Multiple integrated metabolic strategies allow foraminiferan protists to thrive in anoxic marine sediments, *Sci. Adv.*, 7, eabf1586, <https://doi.org/10.1126/sciadv.abf1586>, 2021.
- 3375 Gooday, A. J.: Benthic foraminifera (Protista) as tools in deep-water palaeoceanography: environmental influences on faunal characteristics, *Adv. Mar. Biol.*, 46, 1-90, [https://doi.org/10.1016/S0065-2881\(03\)46002-1](https://doi.org/10.1016/S0065-2881(03)46002-1), 2003.
- Gooday, A. J., and Rathburn, A. E.: Temporal variability in living deep-sea benthic foraminifera: a review, *Earth-Sci. Rev.*, 46, 187-212, [https://doi.org/10.1016/S0012-8252\(99\)00010-0](https://doi.org/10.1016/S0012-8252(99)00010-0), 1999.
- 3380 Gooday, A. J., Bernhard, J. M., Levin, L. A., and Suhr, S. B.: Foraminifera in the Arabian Sea oxygen minimum zone and other oxygen-deficient settings taxonomic composition, diversity, and relation to metazoan faunas, *Deep-Sea Res. Pt. II*, 47, 25-54, [https://doi.org/10.1016/S0967-0645\(99\)00099-5](https://doi.org/10.1016/S0967-0645(99)00099-5), 2000.
- Gooday, A. J., Jorissen, F., Levin, L. A., Middelburg, J. J., Naqvi, S. W. A., Rabalais, N. N., Scranton, M., and Zhang, J.: Historical records of coastal eutrophication-induced hypoxia, *Biogeosciences*, 6, 1707-1745, <https://doi.org/10.5194/bg-6-1707-2009>, 2009.
- 3385 Gooday, A.J., Bett, B.J., Escobar, E., Ingole, B., Levin, L.A., Neira, C., Raman, A.V. and Sellanes, J.: Habitat heterogeneity and its influence on benthic biodiversity in oxygen minimum zones, *Mar. Ecol.*, 31, 125-147, <https://doi.org/10.1111/j.1439-0485.2009.00348.x>, 2010.
- Goossens, H., De Leeuw, J.W., Schenck, P.A., Brassell, S.C.: Tocopherols as likely precursors of pristane in ancient sediments and crude oils, *Nature*, 312, 440–442, <https://doi.org/10.1038/312440a0>, 1984.
- 3390 Gordon, G., Lyons, T., Arnold, G., Roe, J., Sageman, B., and Anbar, A.: When do black shales tell molybdenum isotope tales?, *Geology*, 37, 535-538, <https://doi.org/10.1130/G25186A.1>, 2009.
- Gottschalk, J., Skinner, L.C., Lippold, J., Vogel, H., Frank, N., Jaccard, S.L. and Waelbroeck, C.: Biological and physical controls in the Southern Ocean on past millennial-scale atmospheric CO₂ changes, *Nat. Commun.*, 7, 11539, <https://doi.org/10.1038/ncomms11539>, 2016a.
- 3395

- Gottschalk, J., Riveiros, N.V., Waelbroeck, C., Skinner, L.C., Michel, E., Duplessy, J.-C., Hodell, D.A., and Mackensen, A.: Carbon isotope offsets between species of the genus *Cibicides* (Cibicidoides) in the glacial sub-Antarctic Atlantic Ocean, *Paleoceanography and Paleoclimatology* 31, 1583–1602, <https://doi.org/10.1002/2016PA003029>, 2016b.
- 3400 Gottschalk, J., Skinner, L.C., Jaccard, S.L., Meniel, L., Nehrbass-Ahles, C., and Waelbroeck, C.: Southern Ocean link between changes in atmospheric CO₂ levels and northern-hemisphere climate anomalies during the last two glacial periods, *Quaternary Sci. Rev.*, 230, 106067, <https://doi.org/10.1016/j.quascirev.2019.106067>, 2020a.
- Gottschalk, J., Michel, E., Thöle, L. M., Studer, A. S., Hasenfratz, A. P., Schmid, N., Butzin, M., Mazaud, A., Martínez-García, A., Szidat, S., and Jaccard, S. L.: Glacial heterogeneity in Southern Ocean carbon storage abated by fast South Indian deglacial carbon release, *Nat. Commun.*, 11, 6192, <https://doi.org/10.1038/s41467-020-20034-1>, 2020b.
- 3405 Govindankutty Menon, A., Davis, C. V., Nürnberg, D., Nomaki, H., Salonen, I., Schmiedl, G., and Glock, N.: A deep-learning automated image recognition method for measuring pore patterns in closely related bolivinids and calibration for quantitative nitrate paleo-reconstructions, *Sci. Rep.*, 13, 19628, <https://doi.org/10.1038/s41598-023-46605-y>, 2023.
- Greaves, M., Caillon, N., Rebaubier, H., Bartoli, G., Bohaty, S., Cacho, I., Clarke, L., Cooper, M., Daunt, C., Delaney, M., DeMenocal, P., Dutton, A., Eggins, S., Elderfield, H., Garbe-Schoenberg, D., Goddard, E., Green, D., Groeneveld, J., Hastings, D., Hathorne, E., Kimoto, K., Klinkhammer, G., Labeyrie, L., Lea, D. W., Marchitto, T., Martínez-Botí, M. A., Mortyn, P. G., Ni, Y., Nuernberg, D., Paradis, G., Pena, L., Quinn, T., Rosenthal, Y., Russell, A., Sagawa, T., Sosdian, S., Stott, L., Tachikawa, K., Tappa, E., Thunell, R., and Wilson P. A.: Interlaboratory comparison study of calibration standards for foraminiferal Mg/Ca thermometry, *Geochem. Geophys. Geosy.*, 9, <https://doi.org/10.1029/2008GC001974>, 2008.
- 3415 Granger, J., Sigman, D. M., Needoba, J. A., and Harrison, P. J.: Coupled nitrogen and oxygen isotope fractionation of nitrate during assimilation by cultures of marine phytoplankton, *Limnol. Oceanogr.*, 49, 1763–1773, <https://doi.org/10.4319/lo.2004.49.5.1763>, 2004.
- 3420 Grice, K., Gibbison, R., Atkinson, J.E., Schwark, L., Eckardt, C.B., and Maxwell, J.R.: Maleimides (1H-pyrrole-2,5-diones) as molecular indicators of anoxygenic photosynthesis in ancient water columns, *Geochim. Cosmochim. Ac.*, 60, 3913–3924, [https://doi.org/10.1016/0016-7037\(96\)00199-8](https://doi.org/10.1016/0016-7037(96)00199-8), 1996.
- Groeneveld, J., and Filipsson, H.L.: Mg/Ca and Mn/Ca ratios in benthic foraminifera: The potential to reconstruct past variations in temperature and hypoxia in shelf regions, *Biogeosciences*, 10, 5125–5138, <http://dx.doi.org/10.5194/bg-10-5125-2013>, 2013.
- 3425 Groeneveld, J., Filipsson, H.L., Austin, W.E., Darling, K., McCarthy, D., Quintana Krupinski, N.B., Bird, C., and Schweizer, M.: Assessing proxy signatures of temperature, salinity, and hypoxia in the Baltic Sea through foraminifera-based geochemistry and faunal assemblages, *J. Micropalaeontol.*, 37, 403–429, <https://doi.org/10.5194/jm-37-403-2018>, 2018.
- 3430 Gueguen, B., Reinhard, C. T., Algeo, T. J., Peterson, L. C., Nielsen, S. G., Wang, X., Rowe, H., and Planavsky, N. J.: The chromium isotope composition of reducing and oxic marine sediments, *Geochim. Cosmochim. Ac.*, 184, 1–19, <https://doi.org/10.1016/j.gca.2016.04.004>, 2016.
- Gueneli, N., McKenna, A.M., Ohkouchi, N., Boreham, C.J., Beghin, J., Javaux, E.J., and Brocks, J.J.: 1.1-billion-year-old porphyrins establish a marine ecosystem dominated by bacterial primary producers, *P. Natl. Acad. Sci. USA*, 115, E6978–E6986, <https://doi.org/10.1073/pnas.1803866115>, 2018.
- 3435 Guerrero-Cruz, S., Vaksmaa, A., Horn, M.A., Niemann, H., Pijuan, M., and Ho, A.: Methanotrophs: Discoveries, environmental relevance, and a perspective on current and future applications, *Front. Microbiol.*, 12, 678057, <https://doi.org/10.3389/fmicb.2021.678057>, 2021.
- 3440 Gulev, S. K., Thorne, P. W., Ahn, J., Dentener, F. J., Domingues, C. M., Gerland, S., Gong, D., Kaufman, D. S., Nnamchi, H. C., Quaas, J., Rivera, J. A., Sathyendranath, S., Smith, S. L., Trewin, B., von Shuckmann, K., and Vose, R. S.: Changing State of the Climate System, in: *Climate Change 2021: The Physical Science Basis. Contribution of Working Group I to the Sixth Assessment Report of the Intergovernmental Panel on Climate Change*, edited by: Masson-Delmotte, V., Zhai, P., Pirani, A.,

- Connors, S. L., Péan, C., Berger, S., Caud, N., Chen, Y., Goldfarb, L., Gomis, M. I., Huang, M., Leitzell, K., Lonnoy, E., Matthews, J. B. R., Maycock, T. K., Waterfield, T., Yelekçi, O., Yu, R., and Zhou, B., Cambridge University Press, https://www.ipcc.ch/report/ar6/wg1/downloads/report/IPCC_AR6_WGI_Chapter_02.pdf (last access: 21 March 2022), 2021.
- 3445 Guo, X., Xu, B., Burnett, W.C., Yu, Z., Yang, S., Huang, X., Wang, F., Nan, H., Yao, P., and Sun, F.: A potential proxy for seasonal hypoxia: LA-ICP-MS Mn/Ca ratios in benthic foraminifera from the Yangtze River Estuary, *Geochim. Cosmochim. Ac.*, 245, 290-303, <https://doi.org/10.1016/j.gca.2018.11.007>, 2019.
- Gupta, B. K. S., and Machain-Castillo, M. L.: Benthic foraminifera in oxygen-poor habitats, *Mar. Micropaleontol.*, 20, 183-201, [https://doi.org/10.1016/0377-8398\(93\)90032-S](https://doi.org/10.1016/0377-8398(93)90032-S), 1993.
- 3450 Gutiérrez, D., Sifeddine, A., Field, D. B., Ortlieb, L., Vargas, G., Chávez, F. P., Velazco, F., Ferreira, V., Tapia, P., Salvatelli, R., Boucher, H., Morales, M. C., Valdés, J., Reyss, J.-L., Campusano, A., Boussafir, M., Mandeng-Yogo, M., García, M., and Baumgartner, T.: Rapid reorganization in ocean biogeochemistry off Peru towards the end of the Little Ice Age, *Biogeosciences*, 6, 835–848, <https://doi.org/10.5194/bg-6-835-2009>, 2009.
- 3455 Hain, M. P., Sigman, D. M., and Haug, G. H.: Carbon dioxide effects of Antarctic stratification, North Atlantic Intermediate Water formation, and subantarctic nutrient drawdown during the last ice age: Diagnosis and synthesis in a geochemical box model: ATMOSPHERIC CO₂ DURING THE LAST ICE AGE, *Glob. Biogeochem. Cycles*, 24, n/a-n/a, <https://doi.org/10.1029/2010GB003790>, 2010.
- Harayama, T., and Riezman, H.: Understanding the diversity of membrane lipid composition, *Nat. Rev. Mol. Cell. Biol.*, 19, 281–296, <https://doi.org/10.1038/nrm.2017.138>, 2018.
- 3460 Hardisty, D.S., Lu, Z., Planavsky, N.J., Bekker, A., Philippot, P., Zhou, X., Lyons, T.W.: An iodine record of Paleoproterozoic surface ocean oxygenation *Geology* 42, 619-622, 2014.
- Hardisty, D. S., Lu, Z., Bekker, A., Diamond, C. W., Gill, B. C., Jiang, G., Kah, L. C., Knoll, A. H., Loyd, S. J., Osburn, M. R., and Planavsky, N. J.: Perspectives on Proterozoic surface ocean redox from iodine contents in ancient and recent carbonate, *Earth Planet. Sc. Lett.*, 463, 159-170, <https://doi.org/10.1016/j.epsl.2017.01.032>, 2017.
- 3465 Hardisty, D. S., Horner, T. J., Evans, N., Moriyasu, R., Babbin, A. R., Wankel, S. D., Moffett, J. W. and Nielsen, S. G.: Limited iodate reduction in shipboard seawater incubations from the Eastern Tropical North Pacific oxygen deficient zone, *Earth Planet. Sc. Lett.*, 554, 116676, <https://doi.org/10.1016/j.epsl.2020.116676>, 2021.
- Hardisty, D. S., Riedinger, N., Planavsky, N. J., Asael, D., Bates, S. M., and Lyons, T. W.: Holocene spatiotemporal redox variations in the southern Baltic Sea, *Front. Earth Sci.*, 9, 344, <https://doi.org/10.3389/feart.2021.671401>, 2021.
- 3470 Harmann, R.A.: Distribution of foraminifera in the Santa Barbara Basin, California, *Micropaleontology*, 10, 81-96, <https://doi.org/10.2307/1484628>, 1964.
- Harris, P.G., Zhao, M., Rosell-Melé, A., Tiedemann, R., Sarnthein, M., and Maxwell, J.R.: Chlorin accumulation rate as a proxy for Quaternary marine primary productivity, *Nature*, 383, 63-65, <https://doi.org/10.1038/383063a0>, 1996.
- 3475 Hartnett, H. E., Keil, R. G., Hedges, J. I., and Devol, A. H.: Influence of oxygen exposure time on organic carbon preservation in continental margin sediments. *Nature*, 391, 572-574, <https://doi.org/10.1038/35351>, 1998.
- Hashim, M.S., Burke, J.E., Hardisty, D.S., and Kaczmarek, S.E.: Iodine incorporation into dolomite: Experimental constraints and implications for the iodine redox proxy and Proterozoic Ocean. *Geochim. Cosmochim. Ac.*, 338, 365-381, <https://doi.org/10.1016/j.gca.2022.10.027>, 2022.
- 3480 Hastings, D.W., Emerson, S.R., and Mix, A.C.: Vanadium in foraminiferal calcite as a tracer for changes in the areal extent of reducing sediments, *Paleoceanography and Paleoclimatology*, 11, 665–678, <https://doi.org/10.1029/96PA01985>, 1996.
- Hayes, C. T., Anderson, R. F., Cheng, H., Conway, T. M., Edwards, R. L., Fleisher, M. Q., Ho, P., Huang, K. F., John, S. G., Landing, W. M., Little, S. H., Lu, Y., Morton, P. L., Moran, S. B., Robinson, L. F., Shelley, R. U., Shiller, A. M., and Zheng,

- X. Y.: Replacement times of a spectrum of elements in the North Atlantic based on Thorium supply, *Global Biogeochem. Cy.*, 32, 1294–1311, <https://doi.org/10.1029/2017GB005839>, 2018.
- 3485 Hayes, C. T., Costa, K. M., Anderson, R. F., Calvo, E., Chase, Z., Demina, L. L., Dutay, J., German, C. R., Heimbürger-Boavida, L., Jaccard, S. L., Jacobel, A., Kohfeld, K. E., Kravchishina, M. D., Lippold, J., Mekik, F., Missiaen, L., Pavia, F. J., Paytan, A., Pedrosa-Pamies, R., Petrova, M. V., Rahman, S., Robinson, L. F., Roy-Barman, M., Sanchez-Vidal, A., Shiller, A., Tagliabue, A., Tessin, A. C., van Hulst, M., and Zhang, J.: Global Ocean Sediment Composition and Burial Flux in the Deep Sea, *Glob. Biogeochem. Cycles*, 35, <https://doi.org/10.1029/2020GB006769>, 2021.
- 3490 Hazel, J.R., and Williams, E.E.: The role of alterations in membrane lipid composition in enabling physiological adaptation of organisms to their physical environment, *Prog. Lipid Res.*, 29, 167–227, [https://doi.org/10.1016/0163-7827\(90\)90002-3](https://doi.org/10.1016/0163-7827(90)90002-3), 1990.
- He, Y., Gao, C., Wei, W., and Liu, Y.: Density Functional Theory Calculations of Equilibrium Mo Isotope Fractionation Factors among MoO₄²⁻ Species in the Aqueous Phase by the ONIOM Method, *ACS Earth and Space Chemistry*, <https://doi.org/10.1021/acsearthspacechem.2c00268.s002>, 2022.
- 3495 Hebbing, Y., Schaeffer, P., Behrens, A., Adam, P., Schmitt, G., Schneckenburger, P., Bernasconi, S.M., and Albrecht, P.: Biomarker Evidence for a Major Preservation Pathway of Sedimentary Organic Carbon, *Science*, 312, 1627–1631, <https://doi.org/10.1126/science.1126372>, 2006.
- Hecht, A. D., Eslinger, E. V., and Garmon, L. B.: Experimental studies on the dissolution of planktonic foraminifera, in: *Dissolution of Deep-sea Carbonates*, edited by: Sliter, W. V., Bé, A. W. H., and Berger W. H., Cushman Found. Foraminiferal Res., 13, New York, U. S. A., 56-69, 1975.
- 3500 Hedges, J. I., and Keil, R. G.: Sedimentary organic matter preservation: an assessment and speculative synthesis, *Mar., Chem.*, 49, 81-115, [https://doi.org/10.1016/0304-4203\(95\)00008-F](https://doi.org/10.1016/0304-4203(95)00008-F), 1995.
- Heggie, D., Kahn, D., and Fischer, K.: Trace metals in metalliferous sediments, MANOP Site M: interfacial pore water profiles, *Earth Planet. Sc. Lett.*, 80, 106–116, [https://doi.org/10.1016/0012-821X\(86\)90023-3](https://doi.org/10.1016/0012-821X(86)90023-3), 1986.
- 3505 Helz, G.R., Miller, C.V., Charnock, J.M., Mosselmans, J.F.W., Patrick, R.A.D., Garner, C.D., Vaughan, D.J.: Mechanism of molybdenum removal from the sea and its concentration in black shales: EXAFS evidence, *Geochimica et Cosmochimica Acta* 60, 3631-3642.
- Helz, G. R., Vorlicek, T. P., and Kahn, M. D.: Molybdenum scavenging by iron monosulfide, *Environ. Sci. Technol.*, 38, 4263-4268, <https://doi.org/10.1021/es034969t>, 2004.
- 3510 Helz, G. R., and Dolor, M. K.: What regulates rhenium deposition in euxinic basins? *Chem. Geol.*, 304, 131-141, <https://doi.org/10.1016/j.chemgeo.2012.02.011>, 2012.
- Helz, G.R., Vorlicek, T.P.: Precipitation of molybdenum from euxinic waters and the role of organic matter, *Chemical Geology* 509, 178-193.
- 3515 Helz, G.R.: The Re/Mo redox proxy reconsidered, *Geochim. Cosmochim. Ac.*, 317, 507-522, <https://doi.org/10.1016/j.gca.2021.10.029>, 2022.
- Hemingway, J.D., Kusch, S., Walter, S.R.S., Polik, C.A., Elling, F.J., and Pearson, A.: A novel method to measure the ¹³C composition of intact bacteriohopanepolyols, *Org. Geochem.*, 123, 144–147, <https://doi.org/10.1016/j.orggeochem.2018.07.002>, 2018.
- 3520 Hemingway, J. D., Rothman, D. H., Grant, K. E., Rosengard, S. Z., Eglinton, T. I., Derry, L. A., and Galy, V. V.: Mineral protection regulates long-term global preservation of natural organic carbon, *Nature*, 570, 228-231, <https://doi.org/10.1038/s41586-019-1280-6>, 2019.
- Hemleben, C., Spindler, M., and Anderson, O. R.: *Modern Planktonic Foraminifera*, Springer New York, New York, NY, <https://doi.org/10.1007/978-1-4612-3544-6>, 1989.

- 3525 Herbert, T. D., Lawrence, K. T., Tzanova, A., Peterson, L. C., Caballero-Gill, R., and Kelly, C. S.: Late Miocene global cooling and the rise of modern ecosystems, *Nat. Geosci.*, 9, 843–847, <https://doi.org/10.1038/ngeo2813>, 2016.
- Henderson, G. M., and Anderson, R. F.: The U-series Toolbox for Paleoceanography, *Rev. Mineral. Geochem.*, 52, 493–531, <https://doi.org/10.2113/0520493>, 2003.
- Hendy, I.L., Pedersen, T.F., Kennett, J.P., Tada, R.L.: Intermittent existence of a southern Californian upwelling cell during submillennial climate change of the past 60 kyr, *Paleoceanography* 19, 3, <https://doi.org/10.1029/2003PA000965>, 2004.
- 3530 Hepach, H., Hughes, C., Hogg, K., Collings, S., Chance, R.: Senescence as the main driver of iodide release from a diverse range of marine phytoplankton, *Biogeosciences*, 17, 2453–2471, <https://doi.org/10.5194/bg-17-2453-2020>, 2020.
- Hermelin, J. O. R. and Shimmield, G. B.: The importance of the oxygen minimum zone and sediment geochemistry in the distribution of Recent benthic foraminifera in the northwest Indian Ocean, *Mar. Geol.*, 91, 1–29, [https://doi.org/10.1016/0025-3227\(90\)90130-C](https://doi.org/10.1016/0025-3227(90)90130-C), 1990.
- 3535 Hernandez-Sanchez, M.T., Homoky, W.B., and Pancost, R.D.: Occurrence of 1-*O*-monoalkyl glycerol ether lipids in ocean waters and sediments, *Org. Geochem.*, 66, 1–13, <https://doi.org/10.1016/j.orggeochem.2013.10.003>, 2014.
- Hess, A. V, Auderset, A., Rosenthal, Y., Miller, K. G., Zhou, X., Sigman, D. M., and Martínez-García, A.: A well-oxygenated eastern tropical Pacific during the warm Miocene, *Nature*, 619, 521–525, <https://doi.org/10.1038/s41586-023-06104-6>, 2023.
- 3540 Higgins, M.B., Robinson, R.S., Carter, S.J., and Pearson, A.: Evidence from chlorin nitrogen isotopes for alternating nutrient regimes in the Eastern Mediterranean Sea, *Earth Planet. Sc. Lett.*, 290, 102–107, <https://doi.org/10.1016/j.epsl.2009.12.009>, 2010.
- 3545 Higgins, M.B., Robinson, R.S., Husson, J.M., Carter, S.J., and Pearson, A.: Dominant eukaryotic export production during ocean anoxic events reflects the importance of recycled NH₄⁺, *P. Natl. Acad. Sci. USA*, 109, 2269–2274, <https://doi.org/10.1073/pnas.1104313109>, 2012.
- Hinrichs, K.-U., Pancost, R.D., Summons, R.E., Sprott, G.D., Sylva, S.P., Sinninghe Damsté, J.S., and Hayes, J.M.: Mass spectra of sn-2-hydroxyarchaeol, a polar lipid biomarker for anaerobic methanotrophy, *Geochem. Geophys. Geosy.*, 1, 2000GC000042, <https://doi.org/10.1029/2000gc000042>, 2000.
- 3550 Hinrichs, K.-U., Hmelo, L.R., and Sylva, S.P.: Molecular fossil record of elevated methane levels in Late Pleistocene coastal waters, *Science*, 299, 1214–1217, <https://doi.org/10.1126/science.1079601>, 2003.
- 3555 Hlohowskyj, S., Chappaz, A., and Dickson, A. (Eds.): Molybdenum as a Paleoredox Proxy: Past, Present, and Future (Elements in Geochemical Tracers in Earth System Science), Cambridge: Cambridge University Press, United kingdom, ISBN 9781108993777, 2021.
- Høgslund, S., Revsbech, N. P., Cedhagen, T., Nielsen, L. P., and Gallardo, V. A.: Denitrification, nitrate turnover, and aerobic respiration by benthic foraminiferans in the oxygen minimum zone off Chile, *J. Exp. Mar. Biol. Ecol.*, 359, 85–91, <https://doi.org/10.1016/j.jembe.2008.02.015>, 2008.
- 3560 Hoogakker, B. A. A., Elderfield, H., Schmiedl, G., McCave, I. N., and Rickaby, R. E. M.: Glacial–interglacial changes in bottom-water oxygen content on the Portuguese margin, *Nat. Geosci.*, 8, 40–43, <https://doi.org/10.1038/ngeo2317>, 2015.

- Hoogakker, B. A. A., Thornalley, D. J. R., and Barker, S.: Millennial changes in North Atlantic oxygen concentrations, *Biogeosciences*, 13, 211–221, <https://doi.org/10.5194/bg-13-211-2016>, 2016.
- 3565 Hoogakker, B. A. A., Lu, Z., Umling, N., Jones, L., Zhou, X., Rickaby, R. E. M., Thunell, R., Cartapanis, O., and Galbraith, E.: Glacial expansion of oxygen-depleted seawater in the eastern tropical Pacific, *Nature*, 562, 410–413, <https://doi.org/10.1038/s41586-018-0589-x>, 2018.
- Hopmans, E.C., Smit, N.T., Schwartz-Narbonne, R., Sinninghe Damsté, J.S., and Rush, D.: Analysis of non-derivatized bacteriohopanepolyols using UHPLC-HRMS reveals great structural diversity in environmental lipid assemblages. *Organic Geochemistry* 160, 104285, <https://doi.org/10.1016/j.orggeochem.2021.104285>, 2021.
- 3570 Horn, M. G., Robinson, R. S., Rynearson, T. A., and Sigman, D. M.: Nitrogen isotopic relationship between diatom-bound and bulk organic matter of cultured polar diatoms: N isotopes in cultured polar diatoms, *Paleoceanography*, 26, PA3208, <https://doi.org/10.1029/2010PA002080>, 2011.
- Hsiang, A. Y., Brombacher, A., Rillo, M. C., Mleneck-Vautravers, M. J., Conn, S., Lordsmith, S., Jentzen, A., Henehan, M. J., Metcalfe, B., Fenton, I. S., Wade, B. S., Fox, L., Meilland, J., Davis, C. V., Baranowski, U., Groeneveld, J., Edgar, K. M., Movellan, A., Aze, T., Dowsett, H. J., Miller, C. G., Rios, N., and Hull, P. M.: Endless Forams:> 34,000 modern planktonic foraminiferal images for taxonomic training and automated species recognition using convolutional neural networks, *Paleoceanography and Paleoclimatology*, 34, 1157-1177, <https://doi.org/10.1029/2019PA003612>, 2019.
- 3575 Hu, R., Bostock, H.C., Gottschalk, J., Piotrowski, A.M.: Reconstructing ocean oxygenation changes from U/Ca and U/Mn in foraminiferal coatings: proxy validation and constraints on glacial oxygenation changes, *Quat. Sci. Rev.* 306, 108028, 2023.
- Hughes, C., Barton, E., Hepach, H., Chance, R., Pickering, M.D., Hogg, K., Pommerening-Röser, A., Wadley, M.R., Stevens, D.P. and Jickells, T.D.: Oxidation of iodide to iodate by cultures of marine ammonia-oxidising bacteria, *Mar. Chem.*, 234, 104000, <https://doi.org/10.1016/j.marchem.2021.104000>, 2021.
- 3585 Hull, P. M., Osborn, K. J., Norris, R. D., and Robison, B. H.: Seasonality and depth distribution of a mesopelagic foraminifer, *Hastigerinella digitata*, in Monterey Bay, California, *Limnol. Oceanogr.*, 56, 562-576, <https://doi.org/10.4319/lo.2011.56.2.0562>, 2011.
- Hupp, B. N., Kelly, D. C., and Williams, J. W.: Isotopic filtering reveals high sensitivity of planktic calcifiers to Paleocene–Eocene thermal maximum warming and acidification, *Proceedings of the National Academy of Sciences*, 119(9), e2115561119, 2022.
- 3590 Hupp, B. N., Kelly, D. C., Zachos, J. C., & Bralower, T. J.: Effects of size-dependent sediment mixing on deep-sea records of the Paleocene-Eocene Thermal Maximum. *Geology*, 47(8), 749-752, 2019.
- Hupp, B. N., Kelly, D. C., Kozdon, R., Orland, I. J., & Valley, J. W.: Secondary controls on the stratigraphic signature of the carbon isotope excursion marking the Paleocene-Eocene thermal maximum at Ocean Drilling Program Site 1135, *Chemical Geology*, 632, 121534, 2023.
- 3595 Hutchins, D. A., Mulholland, M. R., and Fu, F.: Nutrient cycles and marine microbes in a CO₂-enriched ocean, *Oceanography*, 22, 128-145, <https://doi.org/10.5670/oceanog.2009.103>, 2008.
- 3600 IPCC, 2021: Annex II: Models [Gutiérrez, J M., A.-M. Tréguier (eds.)]. In *Climate Change 2021: The Physical Science Basis. Contribution of Working Group I to the Sixth Assessment Report of the Intergovernmental Panel on Climate Change* [Masson-Delmotte, V., P. Zhai, A. Pirani, S.L. Connors, C. Péan, S. Berger, N. Caud, Y. Chen, L. Goldfarb, M.I. Gomis, M. Huang, K.

- Leitzell, E. Lonnoy, J.B.R. Matthews, T.K. Maycock, T. Waterfield, O. Yelekçi, R. Yu, and B. Zhou (eds.]. Cambridge University Press, Cambridge, United Kingdom and New York, NY, USA, pp. 2087–2138, doi:10.1017/9781009157896.016.
- 3605 Ishikawa, N. F., Ogawa, N. O., Sun, Y., Chikaraishi, Y., Takano, Y., and Ohkouchi, N.: Integrative assessment of amino acid nitrogen isotopic composition in biological tissue samples determined by GC /C/ IRMS , LC × EA / IRMS , and LC × GC /C/ IRMS, *Limnol. Oceanogr.-Meth.*, 20, 531–542, <https://doi.org/10.1002/lom3.10502>, 2022.
- Ito, T., Minobe, S., Long, M. C., and Deutsch, C.: Upper ocean O₂ trends: 1958–2015, *Geophys. Res. Lett.*, 44, 4214–4223, <https://doi.org/10.1002/2017GL073613>, 2017.
- 3610 Iwasaki, S., Kimoto, K., Sasaki, O., Kano, H., Honda, M.C., Okazaki, Y., Observations of the dissolution process of *Globigerina bulloides* tests (planktic foraminifera) by X-ray microcomputed tomography, *Paleoceanography and Paleoclimatology* 30, 317-331, 2015.
- Iwasaki, S., Kimoto, K., Okazaki, Y., and Ikehara, M.: X-ray micro-CT scanning of tests of three planktic foraminiferal species to clarify dissolution process and progress, *Geochem. Geophys. Geosyst.*, 20, 6051– 6065. <https://doi.org/10.1029/2019GC008456>, 2019a.
- 3615 Iwasaki, S., Kimoto, K., Sasaki, O., Kano, H., and Uchida, H.: Sensitivity of planktic foraminiferal test bulk density to ocean acidification, *Sci. Rep. UK*, 9, 1–9, <https://doi.org/10.1038/s41598-019-46041-x>, 2019b.
- Jacobel, A.W., Anderson, R.F., Jaccard, S.L., McManus, J.F., Pavia, F.J., and Winckler, G.: Deep Pacific storage of respired carbon during the last ice age: Perspectives from bottom water oxygen reconstructions, *Quat. Sci. Rev.*, 230, 106065, <https://doi.org/10.1016/j.quascirev.2019.106065>, 2020.
- 3620 Jahn, B.: Elektronenmikroskopische Untersuchungen an Foraminiferenschalen, *Zeitschrift für Wissenschaftliche Mikroskopie und Mikrotechnik*, 61, 294-297, 1953.
- Jaeschke, A., Ziegler, M., Hopmans, E.C., Reichart, G., Lourens, L.J., Schouten, S., and Sinninghe Damsté, J.S.: Molecular fossil evidence for anaerobic ammonium oxidation in the Arabian Sea over the last glacial cycle, *Paleoceanography and Paleoclimatology*, 24, PA2202, <https://doi.org/10.1029/2008PA001712>, 2009.
- 3625 Jahnke, L. L., Summons, R. E., Hope, J. M., and Marais, D. J. D.: Carbon isotopic fractionation in lipids from methanotrophic bacteria II: the effects of physiology and environmental parameters on the biosynthesis and isotopic signatures of biomarkers, *Geochim. Cosmochim. Ac.*, 63, 79–93, [https://doi.org/10.1016/S0016-7037\(98\)00270-1](https://doi.org/10.1016/S0016-7037(98)00270-1), 1999.
- Jannink, N. T., Zachariasse, W. J., and Van der Zwaan, G. J.: Living (Rose Bengal stained) benthic foraminifera from the Pakistan continental margin (northern Arabian Sea), *Deep-Sea Res. Pt. I*, 45, 1483-1513, [https://doi.org/10.1016/S0967-0637\(98\)00027-2](https://doi.org/10.1016/S0967-0637(98)00027-2), 1998.
- 3630 Jannink, N. T.: Seasonality, biodiversity and microhabitats in benthic foraminiferal communities, Ph. D. thesis, Utrecht University, Netherlands, 192 pp., 2001.
- Jarvis, I., and Higgs, N.: Trace-element mobility during early diagenesis in distal turbidites: late Quaternary of the Madeira Abyssal Plain, N Atlantic, *Geol. Soc. Sp.*, 31, 179–214, <https://doi.org/10.1144/GSL.SP.1987.031.01.14>, 1987.
- 3635 Jayakumar, A., Chang, B.X., Widner, B., Bernhardt, P., Mulholland, M.R., and Ward, B.B.: Biological nitrogen fixation in the oxygen-minimum region of the eastern tropical North Pacific ocean, *ISME J.*, 11, 2356-2367, <https://doi.org/10.1038/ismej.2017.97>, 2017.
- Jenkyns, H. C.: Geochemistry of oceanic anoxic events, *Geochem. Geophys. Geosyst.*, 11, Q03004, <https://doi.org/10.1029/2009GC002788>, 2010.
- 3640 Jochum, K. P., Weis, U., Stoll, B., Kuzmin, D., Yang, Q., Raczek, I., Jacob, D. E., Stracke, A., Birbaum, K., Frick, D. A., and Günther, D.: Determination of reference values for NIST SRM 610–617 glasses following ISO guidelines, *Geostand. Geoanal. Res.*, 35, 397-429, <https://doi.org/10.1111/j.1751-908X.2011.00120.x>, 2011.

- Jochum, K.P., Scholz, D., Stoll, B., Weis, U., Wilson, S.A., Yang, Q., Schwab, A., Börner, N., Jacob, D. E., and Andreae, M. O., 2012. Accurate trace element analysis of speleothems and biogenic calcium carbonates by LA-ICP-MS, *Chem. Geol.*, 318, 31-44, <https://doi.org/10.1016/j.chemgeo.2012.05.009>, 2012.
- Johnson, K. S., Riser, S. C., and Ravichandran, M.: Oxygen variability controls denitrification in the Bay of Bengal oxygen minimum zone, *Geophys. Res. Lett.*, 46, 804–811, <https://doi.org/10.1029/2018GL079881>, 2019.
- Johnstone, H. J. H., Schulz, M., Barker, S., and Elderfield, H.: Inside story: An X-ray computed tomography method for assessing dissolution in the tests of planktonic foraminifera, *Mar. Micropaleontol.*, 77, 58–70, <https://doi.org/10.1016/j.marmicro.2010.07.004>, 2010.
- Johnstone, H. J. H., Yu, J., Elderfield, H., and Schulz, M.: Improving temperature estimates derived from Mg/Ca of planktonic foraminifera using X-ray computed tomography–based dissolution index, XDX, *Paleoceanography and Paleoclimatology*, 26, 1–17, <https://doi.org/10.1029/2009pa001902>, 2011.
- Jones, B., Manning, D.A.C.: Comparison of Geochemical Indices Used for the Interpretation of Palaeoredox Conditions in Ancient Mudstones, *Chemical Geology*, 111, 111-129, 1994.
- Jones, C. A., Closset, I., Riesselman, C. R., Kelly, R. P., Brzezinski, M. A., and Robinson, R. S.: New Constraints on Assemblage-Driven Variation in the Relationship Amongst Diatom-Bound, Biomass, and Nitrate Nitrogen Isotope Values, *Paleoceanogr. Paleoclimatology*, 37, <https://doi.org/10.1029/2022PA004428>, 2022.
- Jonkers, L., Bothe, O., and Kucera, M.: Preface: Advances in paleoclimate data synthesis and analysis of associated uncertainty: towards data–model integration to understand the climate, *Climate of the Past*, 17, 2577–2581, <https://doi.org/10.5194/cp-17-2577-2021>, 2021a.
- Jorissen, F. J., de Stigter, H. C., and Widmark, J. G.: A conceptual model explaining benthic foraminiferal microhabitats, *Mar. Micropaleontol.*, 26, 3-15, [https://doi.org/10.1016/0377-8398\(95\)00047-X](https://doi.org/10.1016/0377-8398(95)00047-X), 1995.
- Jorissen, F. J., Wittling, I., Peypouquet, J. P., Rabouille, C., and Relexans, J. C.: Live benthic foraminiferal faunas off Cape Blanc, NW-Africa: Community structure and microhabitats, *Deep-Sea Res. Pt. I*, 45, 2157-2188, [https://doi.org/10.1016/S0967-0637\(98\)00056-9](https://doi.org/10.1016/S0967-0637(98)00056-9), 1998.
- Jorissen, F. J., Fontanier, C., and Thomas, E.: Chapter seven paleoceanographical proxies based on deep-sea benthic foraminiferal assemblage characteristics. *Developments in marine geology*, 1, 263-325, [https://doi.org/10.1016/S1572-5480\(07\)01012-3](https://doi.org/10.1016/S1572-5480(07)01012-3), 2007.
- Jorissen, F.J., Meyers, S.R., Kelly-Gerreyn, B.A., Huchet, L., Mouret, A., Anschutz, P.: The 4GFOR model–Coupling 4G early diagenesis and benthic foraminiferal ecology, *Marine Micropaleontology*, 170, 102078, 2022.
- Junium, C. K., Freeman, K. H., and Arthur, M. A.: Controls on the stratigraphic distribution and nitrogen isotopic composition of zinc, vanadyl and free base porphyrins through Oceanic Anoxic Event 2 at Demerara Rise, *Org. Geochem.*, 80, 60-71, <https://doi.org/10.1016/j.orggeochem.2014.10.009>, 2015.
- Junium, C.K. and Arthur, M.A.: Nitrogen cycling during the Cretaceous, Cenomanian-Turonian oceanic anoxic event II, *Geochem. Geophys. Geosy.*, 8, n/a-n/a, <https://doi.org/10.1029/2006GC001328>, 2007.
- Kaiho, K.: Benthic foraminiferal dissolved-oxygen index and dissolved-oxygen levels in the modern ocean, *Geology*, 22, 719-722, [https://doi.org/10.1130/0091-7613\(1994\)022<0719:BFDIOA>2.3.CO;2](https://doi.org/10.1130/0091-7613(1994)022<0719:BFDIOA>2.3.CO;2), 1994.
- Kaiho, K.: Effect of organic carbon flux and dissolved oxygen on the benthic foraminiferal oxygen index (BFOI), *Mar. Micropaleontol.*, 37, 67-76, [https://doi.org/10.1016/S0377-8398\(99\)00008-0](https://doi.org/10.1016/S0377-8398(99)00008-0), 1999.
- Kaiho, K., Takeda, K., Petrizzo, M. R., and Zachos, J. C.: Anomalous shifts in tropical Pacific planktonic and benthic foraminiferal test size during the Paleocene-Eocene thermal maximum, *Palaeogeogr. Palaeoclimatol.*, 237, 456–464, <https://doi.org/10.1016/j.palaeo.2005.12.017>, 2006.

- 3685 Kalvelage, T., Jensen, M. M., Contreras, S., Revsbech, N. P., Lam, P., Günter, M., LaRoche, J., Lavik, G., and Kuypers, M. M.: Oxygen sensitivity of anammox and coupled N-cycle processes in oxygen minimum zones, *PLoS ONE* 6, e29299-12, <https://doi.org/10.1371/journal.pone.0029299>, 2011.
- Kaneko, M., Takano, Y., Kamo, M., Morimoto, K., Nunoura, T., and Ohkouchi, N.: Insights into the methanogenic population and potential in subsurface marine sediments based on coenzyme F430 as a function-specific biomarker, *JACS Au*, 1, 1743–1751, <https://doi.org/10.1021/jacsau.1c00307>, 2021.
- 3690 Kaplan, I.R., Rittenberg, S.C.: Microbiological fractionation of sulphur isotopes, *J. Gen. Microbiol.*, 34, 195–212, <https://doi.org/10.1099/00221287-34-2-195>, 1964.
- Kappler, A., and Bryce, C.: Cryptic biogeochemical cycles: unravelling hidden redox reactions, *Environ. Microbiol.*, 19, 842–846, <https://doi.org/10.1111/1462-2920.13687>, 2017.
- 3695 Kast, E. R., Stolper, D. A., Auderset, A., Higgins, J. A., Ren, H., Wang, X. T., Martínez-García, A., Haug, G. H., and Sigman, D. M.: Nitrogen isotope evidence for expanded ocean suboxia in the early Cenozoic, *Science*, 364, 386–389, <https://doi.org/10.1126/science.aau5784>, 2019.
- Keating-Bitonti CR, and Payne J. L.: Ecophenotypic responses of benthic foraminifera to oxygen availability along an oxygen gradient in the California Borderland, *Mar. Ecol.*, 38, e12430, <https://doi.org/10.1111/maec.12430>, 2017.
- 3700 Keeling, R. F., and García, H. E.: The change in oceanic O₂ inventory associated with recent global warming, *Proc. Natl. Acad. Sci. USA*, 99, 7848–7853, <https://doi.org/10.1073/pnas.122154899>, 2002.
- Keeling, R. F., Körtzinger, A., and Gruber, N.: Ocean Deoxygenation in a Warming World, *Annu. Rev. Mar. Sci.*, 2, 199–229, <https://doi.org/10.1146/annurev.marine.010908.163855>, 2010.
- 3705 Keil, R. G., and Cowie, G. L.: Organic matter preservation through the oxygen-deficient zone of the NE Arabian Sea as discerned by organic carbon: mineral surface area ratios, *Mar. Geol.*, 161, 13-22, [https://doi.org/10.1016/S0025-3227\(99\)00052-3](https://doi.org/10.1016/S0025-3227(99)00052-3), 1999.
- Kendall, B., Dahl, T. W., and Anbar, A. D.: The stable isotope geochemistry of molybdenum, *Rev. Mineral. Geochem.*, 82, 683-732, <https://doi.org/10.2138/rmg.2017.82.16>, 2017.
- 3710 Kendall, B., Komiya, T., Lyons, T. W., Bates, S. M., Gordon, G. W., Romaniello, S. J., Jiang, G., Creaser, R. A., Xiao, S., McFadden, K., Sawaki, Y., Tahata, M., Shu, D., Han, J., Li, Y., Chu, X., and Anbar, A. D.: Uranium and molybdenum isotope evidence for an episode of widespread ocean oxygenation during the late Ediacaran Period, *Geochim. Cosmochim. Ac.*, 156, 173-193, <https://doi.org/10.1016/j.gca.2015.02.025>, 2015.
- Kennedy, H.A. and Elderfield, H.: Iodine diagenesis in pelagic deep-sea sediments. *Geochim. Cosmochim. Ac.*, 51, 2489-2504, [https://doi.org/10.1016/0016-7037\(87\)90300-0](https://doi.org/10.1016/0016-7037(87)90300-0), 1987a.
- 3715 Kennedy, H.A. and Elderfield, H.: Iodine diagenesis in non-pelagic deep-sea sediments. *Geochim. Cosmochim. Ac.*, 51, pp.2505-2514, [https://doi.org/10.1016/0016-7037\(87\)90301-2](https://doi.org/10.1016/0016-7037(87)90301-2), 1987b.
- Kerisit, S.N., Smith, F.N., Saslow, S.A., Hoover, M.E., Lawter, A.R., and Qafoku, N.P.: Incorporation modes of iodate in calcite, *Environ. Sci. Technol.*, 52, 5902-5910, <https://doi.org/10.1021/acs.est.8b00339>, 2018.
- 3720 Kerl, C. F., Lohmayer, R., Bura-Nakic, E., Vance, D., and Planer-Friedrich, B.: Experimental confirmation of isotope fractionation in thiomolybdates using ion chromatographic separation and detection by multicollector ICPMS, *Anal. Chem.*, 89, 3123-3129, <https://doi.org/10.1021/acs.analchem.6b04898>, 2017.
- 3725 Khider, D., Geay, J.E., McKay, N.P., Gil, Y., Garijo, D., Ratnakar, V., Garcia, M.A., Bertrand, S., Bothe, O., Brewer, P., Bunn, A., Chevalier, M., Bru, L.C., Csank, A., Dassié, E., DeLong, K., Felis, T., Francus, P., Frappier, A., Gray, W., Goring, S., Jonkers, L., Kahle, M., Kaufman, D., Kehrwald, N.M., Martrat, B., McGregor, H., Richey, J., Schmittner, A., Scroxton, N., Sutherland, E., Thirumalai, K., Allen, K., Arnaud, F., Axford, Y., Barrows, T., Bazin, L., Birch, S.E.P., Bradley, E., Bregy,

- J., Capron, E., Cartapanis, O., Chiang, H.W., Cobb, K.M., Debret, M., Dommmain, R., Du, J., Dyez, K., Emerick, S., Erb, M.P., Falster, G., Finsinger, W., Fortier, D., Gauthier, N., George, S., Grimm, E., Hertzberg, J., Hibbert, F., Hillman, A., Hobbs, W., Huber, M., Hughes, A.L.C., Jaccard, S., Ruan, J., Kienast, M., Konecky, B., Roux, G.L., Lyubchich, V., Novello, V.F., Olaka, L., Partin, J.W., Pearce, C., Phipps, S.J., Pignol, C., Piotrowska, N., Poli, M.S., Prokopenko, A., Schwanck, F., Stepanek, C., Swann, G.E.A., Telford, R., Thomas, E., Thomas, Z., Truebe, S., Gunten, L., Waite, A., Weitzel, N., Wilhelm, B., Williams, J., Williams, J.J., Winstrup, M., Zhao, N., and Zhou, Y.: PaCTS 1.0: A Crowdsourced Reporting Standard for Paleoclimate Data, *Paleoceanography and Paleoclimatology*, 34, 1570–1596, <https://doi.org/10.1029/2019pa003632>, 2019.
- 3730 Khon, V.C., Hoogakker, B.A.A., Schneider, B., Segschneider, J., Park, W.: Effect of an Open Central American Seaway on Ocean Circulation and the Oxygen Minimum Zone in the Tropical Pacific From Model Simulations, *Geophysical Research Letters* 50, e2023GL103728. <https://doi.org/10.1029/2023GL103728>, 2023
- Killops, S.D., and Killops, V.J. (Eds.) *Introduction to Organic Geochemistry*. Wiley-Blackwell, New Jersey, USA, 408 p., ISBN 0632065044, 2005.
- Kim, B., and Zhang, Y.G.: Methane Index: Towards a quantitative archaeal lipid biomarker proxy for reconstructing marine sedimentary methane fluxes, *Geochim. Cosmochim. Ac.*, 354, 74–87, <https://doi.org/10.1016/j.gca.2023.06.008>, 2023.
- 3740 King, K. and Hare, P. E.: Amino Acid Composition of Planktonic Foraminifera: A Paleobiochemical Approach to Evolution, *Science*, 175, 1461–1463, <https://doi.org/10.1126/science.175.4029.1461>, 1972.
- Kinoshita, S., Kuroyanagi, A., Kawahata, H., Fujita, K., Ishimura, T., Suzuki, A., Sasaki, O., and Nishi, H.: Temperature effects on the shell growth of a larger benthic foraminifer (*Sorites orbiculus*): Results from culture experiments and micro X-ray computed tomography, *Mar. Micropaleontol.*, 163, <https://doi.org/10.1016/j.marmicro.2021.101960>, 2021.
- 3745 Kipp, N. G.: New transfer function for estimating past sea-surface conditions from sea-bed distribution of planktonic foraminiferal assemblages in the North Atlantic, in: *Investigation of Late Quaternary Paleoceanography and Paleoclimatology*, edited by: Cune, R. M. and Hays, J. D., Geol. Soc. Am., USA, <https://doi.org/10.1130/MEM145-p3>, 1976.
- Klinkhammer, G. P., and Bender, M. L.: The distribution of manganese in the Pacific Ocean, *Earth Planet. Sc. Lett.*, 46, 361–384, [https://doi.org/10.1016/0012-821X\(80\)90051-5](https://doi.org/10.1016/0012-821X(80)90051-5), 1980.
- 3750 Klinkhammer, G.P., and Palmer, M.R.: Uranium in the oceans: Where it goes and why, *Geochim. Cosmochim. Ac.*, 55, 1799–1806, [https://doi.org/10.1016/0016-7037\(91\)90024-Y](https://doi.org/10.1016/0016-7037(91)90024-Y), 1991.
- Klinkhammer, G.P., Mix, A.C., and Haley, B.A.: Increased dissolved terrestrial input to the coastal ocean during the last deglaciation, *Geochem. Geophys. Geosy.*, 10, n/a-n/a, <https://doi.org/10.1029/2008GC002219>, 2009.
- 3755 Knapp, A. N., Casciotti, K. L., Berelson, W. M., Prokopenko, M. G., and Capone, D. G.: Low rates of nitrogen fixation in eastern tropical South Pacific surface waters, *Proc. Natl. Acad. Sci.*, 113, 4398–4403, <https://doi.org/10.1073/pnas.1515641113>, 2016.
- Kobayashi, K., Makabe, A., Yano, M., Oshiki, M., Kindaichi, T., Casciotti, K. L., and Okabe, S.: Dual nitrogen and oxygen isotope fractionation during anaerobic ammonium oxidation by anammox bacteria, *ISME J.*, 13, 2426–2436, <https://doi.org/10.1038/s41396-019-0440-x>, 2019.
- 3760 Koga, Y., Nishihara, M., Morii, H., and Akagawa-Matsushita, M.: Ether polar lipids of methanogenic bacteria - structures, comparative aspects, and biosyntheses, *Microbiol. Rev.*, 57, 164–182, <https://doi.org/10.1128/mr.57.1.164-182.1993>, 1993.
- Koga, Y., Morii, H., Akagawa-Matsushita, M., and Ohga, M.: Correlation of polar lipid composition with 16S rRNA phylogeny in methanogens. Further analysis of lipid component parts, *Biosci. Biotech. Bioch.*, 62, 230–236, <https://doi.org/10.1271/bbb.62.230>, 1998.
- 3765

- Kohnen, M.E.L., Sinninghe Damsté, J.S., ten Haven, H.L., and de Leeuw, J.W.: Early incorporation of polysulphides in sedimentary organic matter, *Nature*, 341, 640–41, <https://doi.org/10.1038/341640a0>, 1989.
- Kohnen, M.E.L., Damste, J.S.S., and Leeuw, J.W.D.: Biases from natural sulphurization in palaeoenvironmental reconstruction based on hydrocarbon biomarker distributions, *Nature*, 349, 775–778, <https://doi.org/10.1038/349775a0>, 1991.
- 3770 Koho, K. A., Kouwenhoven, T. J., De Stigter, H. C., and Van Der Zwaan, G. J.: Benthic foraminifera in the Nazaré Canyon, Portuguese continental margin: Sedimentary environments and disturbance, *Mar. Micropaleontol.*, 66, 27-51, <https://doi.org/10.1016/j.marmicro.2007.07.005>, 2007.
- 3775 Koho, K. A., García, R. D., De Stigter, H. C., Epping, E., Koning, E., Kouwenhoven, T. J., and Van der Zwaan, G. J.: Sedimentary labile organic carbon and pore water redox control on species distribution of benthic foraminifera: A case study from Lisbon–Setúbal Canyon (southern Portugal), *Progr. Oceanogr.*, 79, 55-82, <https://doi.org/10.1016/j.pocean.2008.07.004>, 2008.
- 3780 Koho, K. A., Langezaal, A. M., Van Lith, Y. A., Duijnste, I. A. P., and Van der Zwaan, G. J.: The influence of a simulated diatom bloom on deep-sea benthic foraminifera and the activity of bacteria: a mesocosm study, *Deep-Sea Res. Pt. I*, 55, 696-719, <https://doi.org/10.1016/j.dsr.2008.02.003>, 2008.
- Koho, K. A., Nierop, K. G. J., Moodley, L., Middelburg, J. J., Pozzato, L., Soetaert, K., van der Plicht, J., and Reichart, G. J.: Microbial bioavailability regulates organic matter preservation in marine sediments, *Biogeosciences*, 10, 1131-1141, <https://doi.org/10.5194/bg-10-1131-2013>, 2013.
- 3785 Koho, K.A., De Nooijer, L.J., and Reichart, G.J.: Combining benthic foraminiferal ecology and shell Mn/Ca to deconvolve past bottom water oxygenation and paleoproductivity, *Geochim. Cosmochim. Ac.*, 165, 294-306, <https://doi.org/10.1016/j.gca.2015.06.003>, 2015.
- Kok, M.D., Rijpstra, W.I.C, Robertson, L., Volkman, J.K., and Sinninghe Damsté, J.S.: Early Steroid sulfurisation in surface sediments of a permanently stratified lake (Ace Lake, Antarctica), *Geochim. Cosmochim. Ac.* 64, 1425–36, [https://doi.org/10.1016/S0016-7037\(99\)00430-5](https://doi.org/10.1016/S0016-7037(99)00430-5), 2000.
- 3790 Kolouchová, I., Timkina, E., Mařátková, O., Kyselová, L., and Řezanka, T.: Analysis of bacteriohopanoids from thermophilic bacteria by liquid chromatography–mass spectrometry, *Microorganisms*, 9, 2062, <https://doi.org/10.3390/microorganisms9102062>, 2021.
- Kool, D.M., Talbot, H.M., Rush, D., Ettwig, K., Damsté, J.S.S.: Rare bacteriohopanepolyols as markers for an autotrophic, intra-aerobic methanotroph, *Geochim. Cosmochim. Ac.*, 136, 114–125, <https://doi.org/10.1016/j.gca.2014.04.002>, 2014.
- 3795 Kraft, B., Jehmlich, N., Larsen, M., Bristow, L.A., Könneke, M., Thamdrup, B., and Canfield, D.E.: Oxygen and nitrogen production by an ammonia-oxidizing archaeon, *Science*, 375, 97–100, <https://doi.org/10.1126/science.abe6733>, 2022.
- Kranner, M., Harzhauser, M., Beer, C., Auer, G., and Piller, W. E.: Calculating dissolved marine oxygen values based on an enhanced Benthic Foraminifera Oxygen Index, *Sci. Rep.*, 12, 1-13, <https://doi.org/10.1038/s41598-022-05295-8>, 2022.
- 3800 Kristiansen, K. D., Kristensen, E. and Jensen, E. M. H.: The influence of water column hypoxia on the behaviour of manganese and iron in sandy coastal marine sediment, *Estuar. Coast. Shelf S.*, 55, 645-654, <https://doi.org/10.1006/ecss.2001.0934>, 2002.
- Ku, T.L., Mathieu, G.G. and Knauss, K.G.: Uranium in open ocean: concentration and isotopic composition, *Deep-Sea Res.*, 24, 1005-1017, [https://doi.org/10.1016/0146-6291\(77\)90571-9](https://doi.org/10.1016/0146-6291(77)90571-9), 1977.
- 3805 Kucera, M., Weinelt, M., Kiefer, T., Pflaumann, U., Hayes, A., Weinelt, M., Chen, M. W., Mix, A. C., Barrows, T. T., Cortijo, E., Duprat, J., Juggins, S., and Waelbroeck, C.: Reconstruction of sea-surface temperatures from assemblages of planktonic foraminifera: multi-technique approach based on geographically constrained calibration data sets and its application to glacial Atlantic and Pacific Oceans, *Quaternary Sci. Rev.*, 24, 951-998, <https://doi.org/10.1016/j.quascirev.2004.07.014>, 2005.
- Kucera, M., Chapter six planktonic foraminifera as tracers of past ocean envri

- 3810 Kühn, H., Lembke-Jene, L., Gersonde, R., Esper, O., Lamy, F., Arz, H., Kuhn, G. and Tiedemann, R.: Laminated sediments in the Bering Sea reveal atmospheric teleconnections to Greenland climate on millennial to decadal timescales during the last deglaciation. *Climate of the Past*, 10(6), 2215-2236, <https://doi.org/10.5194/cp-10-2215-2014>, 2014.
- Kuhnt, T., Friedrich, O., Schmiedl, G., Milker, Y., Mackensen, A., and Lückge, A.: Relationship between pore density in benthic foraminifera and bottom-water oxygen content. *Deep-Sea Res. Pt. I*, 76, 85–95, <https://doi.org/10.1016/j.dsr.2012.11.013>, 2013.
- 3815 Kuhnt, T., Schiebel, R., Schmiedl, G., Milker, Y., Mackensen, A., and Friedrich, O.: Automated and manual analyses of the pore density-to-oxygen relationship in *Globobulimina Turgida* (Bailey), *J. Foraminifer. Res.*, 44, 5–16, <https://doi.org/10.2113/gsjfr.44.1.5>, 2014.
- Kuroda, J., Ohkouchi, N., Ishii, T., Tokuyama, H., & Taira, A.: Lamina-scale analysis of sedimentary components in Cretaceous black shales by chemical compositional mapping: Implications for paleoenvironmental changes during the Oceanic Anoxic Events. *Geochimica et Cosmochimica Acta*, 69(6), 1479-1494, <https://doi.org/10.1016/j.gca.2004.06.039>, 2005.
- 3820 Kuroyanagi, A., da Rocha, R. E., Bijma, J., Spero, H. J., Russell, A. D., Eggins, S. M., and Kawahata, H.: Effect of dissolved oxygen concentration on planktonic foraminifera through laboratory culture experiments and implications for oceanic anoxic events, *Mar. Micropaleontol.*, 101, 28–32, <https://doi.org/10.1016/j.marmicro.2013.04.005>, 2013.
- Kuroyanagi, A., Iriem T., Kinoshita, S., Kawahata, H., Suzuki, A., Nishi, H., Sasaki, O., Takashima, R., and Fujita, K.: Decrease in volume and density of foraminiferal shells with progressing ocean acidification, *Sci. Rep.*, 11, 19988, <https://doi.org/10.1038/s41598-021-99427-1>, 2021.
- 3825 Kusch, S., Kashiyama, Y., Ogawa, N.O., Altabet, M., Butzin, M., Friedrich, J., Ohkouchi, N., Mollenhauer, G.: Implications for chloro-and pheopigment synthesis and preservation from combined compound-specific $\delta^{13}\text{C}$, $\delta^{15}\text{N}$, and $\Delta^{14}\text{C}$ analysis. *Biogeosciences* 7, 4105–4118, <https://doi.org/10.5194/bg-7-4105-2010>, 2010.
- 3830 Kusch, S., and Rush, D.: Revisiting the precursors of the most abundant natural products on Earth: a look back at 30+ years of bacteriohopanepolyol (BHP) research and ahead to new frontiers, *Org. Geochem.*, 172, 104469, <https://doi.org/10.1016/j.orggeochem.2022.104469>, 2022.
- Kusch, S., Wakeham, S.G., Dildar, N., Zhu, C., and Sepúlveda, J.: Bacterial and archaeal lipids trace chemo(auto)trophy along the redoxcline in Vancouver Island fjords, *Geobiology*, 19, 521–541, <https://doi.org/10.1111/gbi.12446>, 2021.
- 3835 Kusch, S., Wakeham, S.G., and Sepúlveda, J.: Bacteriohopanepolyols across the Black Sea redoxcline trace diverse bacterial metabolisms, *Org. Geochem.*, 172, 104462, <https://doi.org/10.1016/j.orggeochem.2022.104462>, 2022.
- Kutuzov, I., Rosenberg, Y.O., Bishop, A., and Amrani, A.: The origin of organic sulphur compounds and their impact on the paleoenvironmental record, in: *Hydrocarbons, Oils and Lipids: Diversity, Origin, Chemistry and Fate*, edited by: Wilkes, H., Springer, Cham, 1–54, <https://doi.org/10.1007/978-3-319-54529-5>, 2019.
- 3840 Kuypers, M. M. M., Breugel, Y. van, Schouten, S., Erba, E., Sinninghe Damsté, J. S.: N_2 -fixing cyanobacteria supplied nutrient N for Cretaceous oceanic anoxic events, *Geology*, 32, 853–856, <https://doi.org/10.1130/G20458.1>, 2004.
- 3845 Kwiatkoski, L., Torres, O., Bopp, L., Aumont, O., Chamberlain, M., Christian, J.R., Dunne, J.P., Gehlen, M., Ilyina, T., John, J.G., Lenton, A., Li, H., Lovenduski, N.S., Orr, J.C., Palmieri, J., Santana-Falcón, Y., Schwinger, J., Séférian, R., Stock, C.A., Tagliabue, A., Takano, Y., Tjiputra, J., Toyama, L., Tsujino, H., Watanabe, M., Yamamoto, A., Yool, A., Ziehn, T.: Twenty-first century ocean warming, acidification, deoxygenation, and upper-ocean nutrient and primary production decline from CMIP6 model projections, *Biogeosciences* 17, 3439-3470, 2020.
- Lam, P., and Kuypers, M. M. M.: Microbial nitrogen cycling processes in oxygen minimum zones, *Annu. Rev. Mar. Sci.*, 3, 317–345, <https://doi.org/10.1146/annurev-marine-120709-142814>, 2011.
- Langmuir, D.: Uranium solution-mineral equilibria at low temperatures with applications to sedimentary ore deposits, *Geochim. Cosmochim. Ac.*, 42, 547–569, [https://doi.org/10.1016/0016-7037\(78\)90001-7](https://doi.org/10.1016/0016-7037(78)90001-7), 1978.

- 3850 Large, R.R., Halpin, J.A., Danyushevsky, L.V., Maslennikov, V.V., Bull, S.W., Long, J.A., Gregory, D.D., Lounejeva, E., Lyons, T.W., Sack, P.J. and McGoldrick, P.J.: Trace element content of sedimentary pyrite as a new proxy for deep-time ocean–atmosphere evolution. *Earth and Planetary Science Letters*, 389, 209-220, <https://doi.org/10.1016/j.epsl.2013.12.020>, 2014.
- 3855 Large, R.R., Halpin, J.A., Danyushevsky, L.V., Maslennikov, V.V., Bull, S.W., Long, J.A., Gregory, D.D., Lounejeva, E., Lyons, T.W., Sack, P.J. and McGoldrick, P.J.: Trace element content of sedimentary pyrite as a new proxy for deep-time ocean–atmosphere evolution, *Earth Planet. Sc. Lett.*, 389, 209-220, <https://doi.org/10.1016/j.epsl.2013.12.020>, 2014.
- Lau, K. V., Romaniello, S. J., and Zhang, F. (Eds.): *The uranium isotope paleoredox proxy*, Cambridge University Press, Cambridge, United Kingdom, ISBN 9781108584142, 2019.
- 3860 Lau, K. V., Lyons, T. W., and Maher, K.: Uranium reduction and isotopic fractionation in reducing sediments: Insights from reactive transport modeling, *Geochim. Cosmochim. Ac.*, 287, 65-92, <https://doi.org/10.1016/j.gca.2020.01.021>, 2020.
- Lau, K. V., and Hardisty, D. S.: Modeling the impacts of diagenesis on carbonate paleoredox proxies, *Geochim. Cosmochim. Ac.*, 337, 123-139, <https://doi.org/10.1016/j.gca.2022.09.021>, 2022.
- Le Calvez, J.: Les perforations du test de *Discorbis erecta* (Foraminifère), *Bulletin de Laboratoire Maritime de Dinard*, 29, 1-4, 1947.
- 3865 Legeleux, F., Reyss, J., Bonte, P., and Organo, C.: Concomitant enrichments of uranium, molybdenum and arsenic in suboxic continental-margin sediments, *Oceanol. Acta*, 17, 417–429, 1994.
- Leiter, C., and Altenbach, A. V.: Benthic foraminifera from the diatomaceous mud belt off Namibia: characteristic species for severe anoxia, *Palaeontol. Electron.*, 13.2.11A, 1-19, http://palaeo-electronica.org/2010_2/188/index.html, 2010.
- 3870 LeKieffre, C., Spangenberg, J. E., Mabilieu, G., Escrig, S., Meibom, A., and Geslin, E.: Surviving anoxia in marine sediments: The metabolic response of ubiquitous benthic foraminifera (*Ammonia tepida*), *PLOS ONE*, 12, e0177604, <https://doi.org/10.1371/journal.pone.0177604>, 2017.
- 3875 Lengger, S. K., Rush, D., Mayser, J. P., Blewett, J., Narbonne, R. S., Talbot, H. M., Middelburg, J. J., Jetten, M. S. M., Schouten, S., Sinninghe Damsté, J. S., and Pancost, R.D.: Dark carbon fixation in the Arabian Sea oxygen minimum zone contributes to sedimentary organic carbon (SOM), *Global Biogeochem. Cy.*, 33, 1715–1732, <https://doi.org/10.1029/2019GB006282>, 2019.
- 3880 Levin, L. A., Etter, R. J., Rex, M. A., Gooday, A. J., Smith, C. R., Pineda, J., Stuart, C. T., Hessler, R. R., and Pawson, D.: Environmental influences on regional deep-sea species diversity, *Annu. Rev. Ecol. Syst.*, 51-93, <https://doi.org/10.1146/annurev.ecolsys.32.081501.114002>, 2001.
- Levin, L., Gutiérrez, D., Rathburn, A., Neira, C., Sellanes, J., Muñoz, P., Gallardo, V., and Salamanca, M.: Benthic processes on the Peru margin: a transect across the oxygen minimum zone during the 1997–98 El Niño, *Prog. Oceanogr.*, 53, 1-27, [https://doi.org/10.1016/S0079-6611\(02\)00022-8](https://doi.org/10.1016/S0079-6611(02)00022-8), 2002.
- 3885 Levin, L. A.: Oxygen minimum zone Benthos: Adaptation and community response to hypoxia, *Oceanogr. Mar. Biol.*, 41, 1-45, 2003.
- Levin, L. A.: Manifestation, drivers, and emergence of open ocean deoxygenation. *Annual review of marine science*, 10, 229-260, 2018.

- 3890 Li, C., Jian, Z., Jia, G., Dang, H., and Wang, J.: Nitrogen fixation changes regulated by upper water structure in the South China Sea during the last two glacial cycles, *Global Biogeochem. Cy.*, 33, 1010-1025, <https://doi.org/10.1029/2019GB006262>, 2019.
- Li, J., Wang, Y., Guo, W., Xie, X., Zhang, L., Liu, Y., and Kong, S.: Iodine mobilization in groundwater system at Datong basin, China: evidence from hydrochemistry and fluorescence characteristics, *Sci. Total Environ.*, 468, 738-745, <https://doi.org/10.1016/j.scitotenv.2013.08.092>, 2014.
- 3895 Linke, P. and Lutze, G. F.: Microhabitat preferences of benthic foraminifera—a static concept or a dynamic adaptation to optimize food acquisition?, *Mar. Micropaleontol.*, 20, 215-234, [https://doi.org/10.1016/0377-8398\(93\)90034-U](https://doi.org/10.1016/0377-8398(93)90034-U), 1993.
- Liu, J., Algeo, T.J.: Beyond redox: Control of trace-metal enrichment in anoxic marine facies by water mass chemistry and sedimentation rates, *Geochimica et Cosmochimica Acta* 287, 269-317, 2020.
- 3900 Liu, K.-K. and Kaplan, I. R.: The eastern tropical Pacific as a source of ^{15}N -enriched nitrate in seawater off southern California: Origin of ^{15}N -rich nitrate, *Limnol. Oceanogr.*, 34, 820–830, <https://doi.org/10.4319/lo.1989.34.5.0820>, 1989.
- Liu, X.-L., Summons, R.E., and Hinrichs, K.-U.: Extending the known range of glycerol ether lipids in the environment: structural assignments based on tandem mass spectral fragmentation patterns, *Rapid Commun. Mass Sp.*, 26, 2295–2302, <https://doi.org/10.1002/rcm.6355>, 2012.
- 3905 Liu, X.-L., Zhu, C., Wakeham, S.G., and Hinrichs, K.-U.: In situ production of branched glycerol dialkyl glycerol tetraethers in anoxic marine water columns, *Mar. Chem.*, 166, 1–8, <https://doi.org/10.1016/j.marchem.2014.08.008>, 2014.
- Liu, Z., Altabet, M. A., and Herbert, T. D.: Plio-Pleistocene denitrification in the eastern tropical North Pacific: Intensification at 2.1 Ma: ETNP denitrification intensification at 2.1 Ma, *Geochem. Geophys. Geosystems*, 9, n/a-n/a, <https://doi.org/10.1029/2008GC002044>, 2008.
- 3910 Loeblich, A. R., Jr. and Tappan, H. (Eds.): *Foraminiferal Genera and Their Classification*, Van Nostrand Reinhold, New York, 868 pp., ISBN 9781489957627, 1988.
- Loescher, C. R., Großkopf, T., Desai, F. D., Gill, D., Schunck, H., Croot, P. L., Schlosser, C., Neulinger, S.C., Pinnow, N., Lavik, G., Kuypers, M.M.M., LaRoche, J., and Schmitz, R.A.: Facets of diazotrophy in the oxygen minimum zone waters off Peru, *ISME J.*, 8, 2180–2192, <https://doi.org/10.1038/ismej.2014.71>, 2014.
- 3915 Lohmann, G. P.: A model for variation in the chemistry of planktonic foraminifera due to secondary calcification and selective dissolution, *Paleoceanography and Paleoclimatology*, 10, 445–457, <https://doi.org/10.1029/95PA00059>, 1995.
- Loubere, P., Gary, A., and Lagoe, M.: Generation of the benthic foraminiferal assemblage: Theory and preliminary data, *Mar. Micropaleontol.*, 20, 165-181, [https://doi.org/10.1016/0377-8398\(93\)90031-R](https://doi.org/10.1016/0377-8398(93)90031-R), 1993.
- 3920 Loubere, P.: Quantitative estimation of surface ocean productivity and bottom water oxygen concentration using benthic foraminifera, *Paleoceanography and Paleoclimatology*, 9, 723-737, <https://doi.org/10.1029/94PA01624>, 1994.
- Lovley, D. R., Phillips, E. J., Gorby, Y. A., and Landa, E. R.: Microbial reduction of uranium, *Nature*, 350, 413-416, <https://doi.org/10.1038/350413a0>, 1991.
- 3925 Löwemark, L., Chen, H.F., Yang, T.N., et al., Normalizing XRF-scanner data: a cautionary note on the interpretation of high resolution records from organic rich lakes, *Journal of Asian Earth Sci.* 40, 1250-1256., 2010.
- Löwemark, L., Bloemsma, M., Croudace, I., Daly, J.S., Edwards, R.J., Francus, P., Galloway, J.M., Gregory, B.R., Huang, J.J.S., Jones, A.F. and Kylander, M.: Practical guidelines and recent advances in the Itrax XRF core-scanning procedure. *Quaternary International*, 514, 16-29, <https://doi.org/10.1016/j.quaint.2018.10.044>, 2019.

- 3930 Lu, W., Ridgwell, A., Thomas, E., Hardisty, D. S., Luo, G., Algeo, T. J., Saltzman, M. R., Gill, B. C., Shen, Y., Ling, H. F., and Edwards, C. T.: Late inception of a resiliently oxygenated upper ocean, *Science*, 361, 174-177, <https://doi.org/10.1126/science.aar5372>, 2018.
- Lu, W., Dickson, A.J., Thomas, E., Rickaby, R.E., Chapman, P., and Lu, Z.: Refining the planktic foraminiferal I/Ca proxy: Results from the Southeast Atlantic Ocean, *Geochim. Cosmochim. Ac.*, 287, 318-327, <https://doi.org/10.1016/j.gca.2019.10.025>, 2020.
- 3935 Lu, W., Wang, Y., Oppo, D. W., Nielsen, S. G., and Costa, K. M.: Comparing paleo-oxygenation proxies (benthic foraminiferal surface porosity, I/Ca, authigenic uranium) on modern sediments and the glacial Arabian Sea, *Geochim. Cosmochim. Ac.*, 331, pp.69-85, <https://doi.org/10.1016/j.gca.2022.06.001>, 2022.
- Lu, W., Costa, K.M., Oppo, D. W. Reconstructing the oxygen depth profile in the Arabian Sea during the last glacial period. *Paleoceanography and Paleoclimatology*, 38, e2023PA004632. <https://doi.org/10.1029/2023PA004632>, 2023.
- 3940 Lu, Z., Jenkyns, H. C., and Rickaby, R. E.: Iodine to calcium ratios in marine carbonate as a paleo-redox proxy during oceanic anoxic events, *Geology*, 38, 1107-1110, <https://doi.org/10.1130/G31145.1>, 2010.
- Lu, Z., Hoogakker, B. A., Hillenbrand, C. D., Zhou, X., Thomas, E., Gutchess, K. M., Lu, W., Jones, L., and Rickaby, R. E.: Oxygen depletion recorded in upper waters of the glacial Southern Ocean, *Nat. Commun.*, 7, 11146, <https://doi.org/10.1038/ncomms11146>, 2016.
- 3945 Luciani, V., D'Onofrio, R., Filippi, G., and Moretti, S.: Which was the habitat of early Eocene planktic foraminifer *Chiloguembelina*? Stable isotope paleobiology from the Atlantic Ocean and implication for paleoceanographic reconstructions, *Global Planet. Change*, 191, 103216, <https://doi.org/10.1016/j.gloplacha.2020.103216>, 2020.
- Luo, G., Yang, H., Algeo, T.J., Hallmann, C., and Xie, S.: Lipid biomarkers for the reconstruction of deep-time environmental conditions, *Earth-Sci. Rev.*, 189, 99–124, <https://doi.org/10.1016/j.earscirev.2018.03.005>, 2019.
- 3950 Luther, G.W.: Review on the physical chemistry of iodine transformations in the oceans, *Front. Mar. Sci.*, 10, 20, <https://doi.org/10.3389/fmars.2023.1085618>, 2023.
- Lutze, G. F.: Variationsstatistik und Ökologie bei rezenten Foraminiferen, *Paläontologische Zeitschrift*, 36, 252-264, <https://doi.org/10.1007/BF02986977>, 1962.
- 3955 Lutze, G. F.: Statistical investigations on the variability of *Bolivina argentea* Cushman, *Contributions from the Cushman Foundation for Foraminiferal Research*, 15, 105-116, 1964.
- Lutze, G. F., and Coulbourn, W. T.: Recent benthic foraminifera from the continental margin of northwest Africa: community structure and distribution, *Mar. Micropaleontol.*, 8, 361-401, [https://doi.org/10.1016/0377-8398\(84\)90002-1](https://doi.org/10.1016/0377-8398(84)90002-1), 1984.
- Lynn D. C. and Bonatti E.: Mobility of manganese in diagenesis of deep-sea sediments, *Mar. Geol.*, 3, 457–474, [https://doi.org/10.1016/0025-3227\(65\)90046-0](https://doi.org/10.1016/0025-3227(65)90046-0), 1965.
- 3960 Ma, J., French, K. L., Cui, X., Bryant, D. A., and Summons, R. E.: Carotenoid biomarkers in Namibian shelf sediments: Anoxygenic photosynthesis during sulfide eruptions in the Benguela Upwelling System, *P. Natl. Acad. Sci. USA*, 118, e2106040118, <https://doi.org/10.1073/pnas.2106040118>, 2021.
- Mackensen, A. and Douglas, R. G.: Down-core distribution of live and dead deep-water benthic foraminifera in box cores from the Weddell Sea and the California continental borderland, *Deep-Sea Res.*, 36, 879-900, [https://doi.org/10.1016/0198-0149\(89\)90034-4](https://doi.org/10.1016/0198-0149(89)90034-4), 1989.
- 3965 Mackensen, A., Hubberten, H. W., Bickert, T., Fischer, G., and Fütterer, D. K.: The $\delta^{13}\text{C}$ in benthic foraminiferal tests of *Fontbotia wuellerstorfi* (Schwager) Relative to the $\delta^{13}\text{C}$ of dissolved inorganic carbon in Southern Ocean Deep Water: Implications for glacial ocean circulation models, *Paleoceanography and Paleoclimatology*, 8, 587–610, <https://doi.org/10.1029/93pa01291>, 1993.
- 3970

- Mackensen, A., Licari, L.: Carbon Isotopes of Live Benthic Foraminifera from the South Atlantic: Sensitivity to Bottom Water Carbonate Saturation State and Organic Matter Rain Rates, *The South Atlantic in the Late Quaternary: Reconstruction of material budgets and current systems*, 623-644, Springer Berlin Heidelberg, 2004.
- 3975 Madison A. S., Tebo B. M., Mucci A., Sundby B., and Luther G. W.: Abundant porewater Mn(III) is a major component of the sedimentary redox system, *Science*, 341, 875–878, <https://doi.org/10.1126/science.1241396>, 2013.
- Mallon, J., Glock, N., and Schönfeld, J.: The response of benthic foraminifera to low-oxygen conditions of the Peruvian oxygen minimum zone, in: *Anoxia*, edited by: Altenbach, A., Bernhard, J., Seckbach, J., Springer, Dordrecht, Germany, 305-321, https://doi.org/10.1007/978-94-007-1896-8_16, 2012.
- 3980 Mangini, A., Jung, M., and Laukenmann, S.: What do we learn from peaks of uranium and of manganese in deep sea sediments?, *Mar. Geol.*, 177, 63–78, [https://doi.org/10.1016/S0025-3227\(01\)00124-4](https://doi.org/10.1016/S0025-3227(01)00124-4), 2001.
- Manno, C., Morata, N., and Bellerby, R.: Effect of ocean acidification and temperature increase on the planktonic foraminifer *Neoglobobulimina pachyderma* (sinistral), *Polar Biol.*, 5, 1–9, <https://doi.org/10.1029/2003GC000670>, 2012.
- 3985 Marchant, R., Tetard, M., Pratiwi, A., Adebayo, M., and de Garidel-Thoron, T.: Automated analysis of foraminifera fossil records by image classification using a convolutional neural network, *J. Micropalaeontol.*, 39, 183-202, <https://doi.org/10.5194/jm-39-183-2020>, 2020.
- Marconi, D., Kopf, S., Rafter, P. A., and Sigman, D. M.: Aerobic respiration along isopycnals leads to overestimation of the isotope effect of denitrification in the ocean water column, *Geochim. Cosmochim. Ac.*, 197, 417–432, <https://doi.org/10.1016/j.gca.2016.10.012>, 2017.
- 3990 Marshall, B. J., Thunell, R. C., Henehan, M. J., Astor, Y., and Wejnert, K. E.: Planktonic foraminiferal area density as a proxy for carbonate ion concentration: A calibration study using the Cariaco Basin ocean time series, *Paleoceanography and Paleoclimatology*, 28, 363-376, <https://doi.org/10.1002/palo.20034>, 2013.
- Martínez-García, A., Jung, J., Ai, X. E., Sigman, D. M., Auderset, A., Duprey, N. N., Foreman, A., Fripiat, F., Leichliter, J., Lüdecke, T., Moretti, S., and Wald, T.: Laboratory Assessment of the Impact of Chemical Oxidation, Mineral Dissolution, and Heating on the Nitrogen Isotopic Composition of Fossil-Bound Organic Matter, *Geochem. Geophys. Geosy.*, 23, e2022GC010396, <https://doi.org/10.1029/2022GC010396>, 2022.
- 3995 Margreth, S., Rueggeberg, A., and Spezzaferri, S.: Benthic foraminifera as bioindicator for cold-water coral reef ecosystems along the Irish margin, *Deep-Sea Res. Pt. I*, 56, 2216-2234, <https://doi.org/10.1016/j.dsr.2009.07.009>, 2009.
- 4000 Matthews, A., Azrieli-Tal, I., Benkovitz, A., Bar-Matthews, M., Vance, D., Poulton, S. W., Teutsch, N., Almogi-Labin, A., and Archer, C.: Anoxic development of sapropel S1 in the Nile Fan inferred from redox sensitive proxies, Fe speciation, Fe and Mo isotopes, *Chem. Geol.*, 475, 24-39, <https://doi.org/10.1016/j.chemgeo.2017.10.028>, 2017.
- Matys, E. D., Sepúlveda, J., Pantoja, S., Lange, C. B., Caniupán, M., Lamy, F., and Summons, R. E.: Bacterioplanepolyols along redox gradients in the Humboldt Current System off northern Chile, *Geobiology*, 15, 844–857, <https://doi.org/10.1111/gbi.12250>, 2017.
- 4005 Mayer, M. H., Parenteau, M. N., Kempfer, M. L., Madigan, M. T., Jahnke, L. L., and Welander, P. V.: Anaerobic 3-methylhopanoid production by an acidophilic photosynthetic purple bacterium, *Arch. Microbiol.*, 203, 6041–6052, <https://doi.org/10.1007/s00203-021-02561-7>, 2021.
- McCarthy, M.D., Lehman, J., and Kudela, R.: Compound-specific amino acid $\delta^{15}\text{N}$ patterns in marine algae: Tracer potential for cyanobacterial vs. eukaryotic organic nitrogen sources in the ocean, *Geochim. Cosmochim. Ac.*, 103, 104-120, <https://doi.org/10.1016/j.gca.2012.10.037>, 2013.
- 4010 McConnaughey, T. A., Burdett, J., Whelan, J. F., and Paull, C. K.: Carbon isotopes in biological carbonates: respiration and photosynthesis, *Geochim. Cosmochim. Ac.*, 61, 611–622, [https://doi.org/10.1016/S0016-7037\(96\)00361-4](https://doi.org/10.1016/S0016-7037(96)00361-4), 1997.
- McCorkle, D.C., and Emerson, S.R.: The relationship between pore water carbon isotopic composition and bottom water oxygen concentration, *Geochim. Cosmochim. Ac.*, 52, 1169–1178, [https://doi.org/10.1016/0016-7037\(88\)90270-0](https://doi.org/10.1016/0016-7037(88)90270-0), 1988.

- 4015 McCormick, L. R., Levin, L. A., and Oesch, N. W.: Vision is highly sensitive to oxygen availability in marine invertebrate larvae, *J. Exp. Biol.*, 222, jeb200899, <https://doi.org/10.1242/jeb.200899>, 2019.
- McIlvin, M. R. and Altabet, M. A.: Chemical Conversion of Nitrate and Nitrite to Nitrous Oxide for Nitrogen and Oxygen Isotopic Analysis in Freshwater and Seawater, *Anal. Chem.*, 77, 5589–5595, <https://doi.org/10.1021/ac050528s>, 2005.
- 4020 McKay, C.L., Groeneveld, J., Filipsson, H.L., Gallego-Torres, D., Whitehouse, M.J., Toyofuku, T., and Romero, O.E.: A comparison of benthic foraminiferal Mn/Ca and sedimentary Mn/Al as proxies of relative bottom-water oxygenation in the low-latitude NE Atlantic upwelling system, *Biogeosciences*, 12, 5415–5428, <https://doi.org/10.5194/bg-12-5415-2015>, 2015.
- McKay, J. L., and Pedersen, T. F.: Geochemical response to pulsed sedimentation: implications for the use of Mo as a paleoproxy, *Chem. Geol.*, 382, 83–94, <https://doi.org/10.1016/j.chemgeo.2014.05.009>, 2014.
- 4025 McMahan, K. W., McCarthy, M. D., Sherwood, O. A., Larsen, T., and Guilderson, T. P.: Millennial-scale plankton regime shifts in the subtropical North Pacific Ocean, *Science*, 350, 1530–1533, <https://doi.org/10.1126/science.aaa9942>, 2015.
- McManus, J., Berelson, W.M., Klinkhammer, G.P., Hammond, D.E., and Holm, C.: Authigenic uranium: Relationship to oxygen penetration depth and organic carbon rain, *Geochim. Cosmochim. Ac.*, 69, 95–108, <https://doi.org/10.1016/j.gca.2004.06.023>, 2005.
- 4030 McManus, J., Berelson, W. M., Severmann, S., Poulson, R. L., Hammond, D. E., Klinkhammer, G. P., and Holm, C.: Molybdenum and uranium geochemistry in continental margin sediments: paleoproxy potential, *Geochim. Cosmochim. Ac.*, 70, 4643–4662, <https://doi.org/10.1016/j.gca.2006.06.1564>, 2006.
- Meckler, A. N., Ren, H., Sigman, D. M., Gruber, N., Plessen, B., Schubert, C. J., and Haug, G. H.: Deglacial nitrogen isotope changes in the Gulf of Mexico: Evidence from bulk sedimentary and foraminifera-bound nitrogen in Orca Basin sediments, *Paleoceanography*, 26, 2011PA002156, <https://doi.org/10.1029/2011PA002156>, 2011.
- 4035 Mees, F., Swennen, R., Geet, M. V., and Jacobs, P.: Applications of X-ray computed tomography in the geosciences, *Geol. Soc. Spec. Publ.*, 215, 1–6, <https://doi.org/10.1144/GSL.SP.2003.215.01.01>, 2003.
- Mena, A., Frances, G., Pérez-Arlucea, M., Aguiar, P., Barreiro-Vázquez, J. D., Iglesias, A., & Barreiro-Lois, A.: A novel sedimentological method based on CT-scanning: Use for tomographic characterization of the Galicia Interior Basin. *Sedimentary Geology*, 321, 123–138, <https://doi.org/10.1016/j.sedgeo.2015.03.007>, 2015.
- 4040 Menzel, D., Hopmans, E. C., Schouten, S., and Sinninghe Damsté, J. S.: Membrane tetraether lipids of planktonic Crenarchaeota in Pliocene sapropels of the eastern Mediterranean Sea, *Palaeogeogr. Palaeoclimatol.*, 239, 1–15, <https://doi.org/10.1016/j.palaeo.2006.01.002>, 2006.
- 4045 Metcalf, W. W., Griffin, B. M., Cicchillo, R. M., Gao, J., Janga, S. C., Cooke, H. A., Circello, B. T., Evans, B. S., Martens-Habbena, W., Stahl, D. A., Donk, W. A. van der: Synthesis of methylphosphonic acid by marine microbes: A source for methane in the aerobic ocean, *Science*, 337, 1104–1107, <https://doi.org/10.1126/science.1219875>, 2012.
- Miller, C.A., Peucker-Ehrenbring, B., Walker, B.D., Marcantonio, F.: Re-assessing the surface cycling of molybdenum and rhenium, *Geochimica et Cosmochimica Acta* 15, 7146–7179, 2011.
- 4050 Miller, N., Dougherty, M., Du, R., Sauers, T., Yan, C., Pines, J. E., Meyers, K. L., Dang Y M., Nagle, E., Ni, Z., Pungsrissai, T., Wetherington, M. T., Vorlicek, T. P., Plass, K. E., and Morford, J. L.: Adsorption of Tetrathiomolybdate to Iron Sulfides and its Impact on Iron Sulfide Transformations, *ACS Earth Space Chem.*, 4, 2246–2260, <https://doi.org/10.1021/acsearthspacechem.0c00176>, 2020.
- 4055 Mitra, R., Marchitto, T. M., Ge, Q., Zhong, B., Kanakiya, B., Cook, M. S., Fehrenbacher, J. S., Ortiz, J. D., Tripathi, A., and Lobaton, E.: Automated species-level identification of planktic foraminifera using convolutional neural networks, with comparison to human performance, *Mar. Micropaleontol.*, 147, 16–24, <https://doi.org/10.1016/j.marmicro.2019.01.005>, 2019.

- Moffitt, S. E., Hill, T. M., Ohkushi, K., Kennett, J. P., and Behl, R. J.: Vertical oxygen minimum zone oscillations since 20 ka in Santa Barbara Basin: A benthic foraminiferal community perspective, *Paleoceanography*, 29, 44-57, <https://doi.org/10.1002/2013PA002483>, 2014.
- 4060 Mojtahid, M., Toucanne, S., Fentimen, R., Barras, C., Le Houedec, S., Soulet, G., Bourillet, J. -G. and Michel, E.: Changes in northeast Atlantic hydrology during Termination 1: Insights from Celtic margin's benthic foraminifera, *Quaternary Sci. Rev.*, 175, 45-59, <https://doi.org/10.1016/j.quascirev.2017.09.003>, 2017.
- Moodley, L., and Hess, C.: Tolerance of Infaunal Benthic Foraminifera for low and high Oxygen concentrations, *Biol. Bull*, 183, 94-98, <https://doi.org/10.2307/1542410>, 1992.
- 4065 Moodley, L., Van der Zwaan, G. J., Herman, P. M. J., Kempers, L., and Van Breugel, P.: Differential response of benthic meiofauna to anoxia with special reference to Foraminifera (Protista: Sarcodina), *Mar. Ecol. Prog. Ser.*, 158, 151-163, <https://doi.org/10.3354/meps158151>, 1997.
- Moretti, S., Auderset, A., Deutsch, C., Schmitz, R., Gerber, L., Thomas, E., Luciani, V., Petrizzo, M.R., Schiebel, R., Tripathi, A., Sexton, P., Norris, R., D'Onofrio, R., Zachos, J., Sigman, D.M., Haug, G.H., Martínez-García, A.: Oxygen rise in the tropical upper ocean during the Paleocene-Eocene Thermal Maximum, *Science*, 383, 727–731, <https://doi.org/10.1126/science.adh4893>, 2024
- 4070 Morford, J. L., and Emerson, S.: The geochemistry of redox sensitive trace metals in sediments, *Geochim. Cosmochim. Ac.*, 63, 1735–1750, [https://doi.org/10.1016/S0016-7037\(99\)00126-X](https://doi.org/10.1016/S0016-7037(99)00126-X), 1999.
- 4075 Morford, J. L., Martin, W. R., and Carney, C. M.: Uranium diagenesis in sediments underlying bottom waters with high oxygen content, *Geochim. Cosmochim. Ac.*, 73, 2920-2937, <https://doi.org/10.1016/j.gca.2009.02.014>, 2009.
- Morgan, J. J.: Kinetics of reaction between O₂ and Mn (II) species in aqueous solutions, *Geochim. Cosmochim. Ac.*, 69, 35-48, <https://doi.org/10.1016/j.gca.2004.06.013>, 2005.
- 4080 Moriyasu, R., Evans, N., Bolster, K. M., Hardisty, D. S., and Moffett, J. W.: The distribution and redox speciation of iodine in the eastern tropical North Pacific Ocean, *Global Biogeochem. Cy.*, 34, e2019GB006302, <https://doi.org/10.1029/2019GB006302>, 2020.
- Moriyasu, R., Bolster, K.M., Hardisty, D.S., Kadko, D.C., Stephens, M.P., Moffett, J.W., Meridional Survey of the Central Pacific Reveals Iodide Accumulation in Equatorial Surface Waters and Benthic Sources in the Abyssal Plain, *Global Biogeochemical Cycling*, 37, <https://doi.org/10.1029/2021GB007300>, 2023.
- 4085 Morrill, C., Thrasher, B., Lockshin, S. N., Gille, E.P., McNeill, S., Shepherd, E., Gross, W. S., Bauer, B. A.: The Paleoenvironmental Standard Terms (PaST) Thesaurus: Standardizing Heterogeneous Variables in Paleoscience, *Paleoceanography and Paleoclimatology*, 36, e2020PA004193, <https://doi.org/10.1029/2020PA004193>, 2021.
- Moss, F. R., Shuken, S. R., Mercer, J. A. M., Cohen, C. M., Weiss, T. M., Boxer, S. G., and Burns, N. Z.: Ladderane phospholipids form a densely packed membrane with normal hydrazine and anomalously low proton/hydroxide permeability, *P. Natl. Acad. Sci. USA*, 115, 9098–9103, <https://doi.org/10.1073/pnas.1810706115>, 2018.
- 4090 Mouret, A., Anschutz, P., Lecroart, P., Chaillou, G., Hyacinthe, C., Deborde, J., Jorissen, F.J., Deflandre, B., Schmidt, S., and Jouanneau, J.M.: Benthic geochemistry of manganese in the Bay of Biscay, and sediment mass accumulation rate, *Geo-Mar. Lett.*, 29, 133-149, <https://doi.org/10.1007/s00367-008-0130-6>, 2009.
- Moy, A. D., Howard, W. R., Bray, S. G., and Trull, T. W.: Reduced calcification in modern southern ocean planktonic foraminifera, *Nat. Geosci.*, 2, 276–280, <https://doi.org/10.1038/ngeo460>, 2009.
- 4095 Mucci, A.: The behavior of mixed Ca–Mn carbonates in water and seawater: controls of manganese concentrations in marine porewaters, *Aquat. Geochem.*, 10, 139-169, <https://doi.org/10.1023/B:AQUA.0000038958.56221.b4>, 2004.

- 4100 Muglia, J., Mulitza, S., Repschläger, J., Schmittner, A., Lembke-Jene, L., Lisiecki, L., Mix, A., Saraswat, R., Sikes, E., Waelbroeck, C., Gottschalk, J., Lippold, J., Lund, D., Martinez-Mendez, G., Michel, E., Muschitiello, F., Naik, S., Okazaki, Y., Stott, L., Voelker, A., and Zhao, N.: A global synthesis of high-resolution stable isotope data from benthic foraminifera of the last deglaciation, *Scientific Data*, 10, <https://doi.org/10.1038/s41597-023-02024-2>, 2023.
- 4105 Mulitza, S., Bickert, T., Bostock, H. C., Chiessi, C. M., Donner, B., Govin, A., Harada, N., Huang, E., Johnstone, H., Kuhnert, H., Langner, M., Lamy, F., Lembke-Jene, L., Lisiecki, L., Lynch-Stieglitz, J., Max, L., Mohtadi, M., Mollenhauer, G., Muglia, J., Nürnberg, D., Paul, A., Rühlemann, C., Repschläger, J., Saraswat, R., Schmittner, A., Sikes, E. L., Spielhagen, R. F., and Tiedemann, R.: World Atlas of late Quaternary Foraminiferal Oxygen and Carbon Isotope Ratios, *Earth System Science Data*, 14, 2553–2611, <https://doi.org/10.5194/essd-14-2553-2022>, 2022.
- Muñoz, P., Dezilaeau, L., Lange, C., Cardenas, L., Sellanes, J., Salamanca, M.A., Maldonado, A.: Evaluation of sediment trace metal records as paleoproductivity and paleoxygenation proxies in the upwelling center off Concepción, Chile, *Prog. Oceanogr.*, <https://doi.org/10.1016/j.pocean.2011.07.010>, 2012.
- 4110 Muñoz, P., Hevía-Hormazabal, V., Araya, K., Maldonado, A., and Salamanca, M.: Metal enrichment evolution in marine sediments influenced by oxygen-deficient waters in a mineral loading zone, Atacama, Chile (27°S), *Mar. Environ. Res.*, 177, 105619, <https://doi.org/10.1016/j.marenvres.2022.105619>, 2023.
- Muñoz, P., Castillo, A., Valdés, J., and Dewitte, B.: Oxidative conditions along the continental shelf of the Southeast Pacific during the last two millennia: a multiproxy interpretation of the oxygen minimum zone variability from sedimentary records, *Front. Mar. Sci.*, 10, 1134164, <https://doi.org/10.3389/fmars.2023.1134164>, 2023.
- 4115 Murray, J. W.: The niche of benthic foraminifera, critical thresholds and proxies, *Mar. Micropaleontol.*, 41, 1-7, [https://doi.org/10.1016/S0377-8398\(00\)00057-8](https://doi.org/10.1016/S0377-8398(00)00057-8), 2001.
- Myhre, S. E., Kroeker, K. J., Hill, T. M., Roopnarine, P., and Kennett, J. P.: Community benthic paleoecology from high-resolution climate records: Mollusca and foraminifera in post-glacial environments of the California margin, *Quaternary Sci. Rev.*, 155, 179-197, <https://doi.org/10.1016/j.quascirev.2016.11.009>, 2017.
- 4120 Nakashima, Y., & Komatsubara, J.: Seismically induced soft-sediment deformation structures revealed by X-ray computed tomography of boring cores. *Tectonophysics*, 683, 138-147, <https://doi.org/10.1016/j.tecto.2016.05.044>, 2016.
- Nardelli, M. P., Barras, C., Metzger, E., Mouret, A., Filipsson, H. L., Jorissen, F., and Geslin, E.: Experimental evidence for foraminiferal calcification under anoxia, *Biogeosciences*, 11, 4029-4038, <https://doi.org/10.5194/bg-11-4029-2014>, 2014.
- 4125 Naeher, S., Schaeffer, P., Adam, P., and Schubert, C. J.: Maleimides in recent sediments – Using chlorophyll degradation products for palaeoenvironmental reconstructions, *Geochim. Cosmochim. Acta.*, 119, 248–263, <https://doi.org/10.1016/j.gca.2013.06.004>, 2013.
- Nägler, T. F., Anbar, A. D., Archer, C., Goldberg, T., Gordon, G. W., Greber, N. D., Siebert, C., Sohrin, Y., and Vance, D.: Proposal for an international molybdenum isotope measurement standard and data representation, *Geostand. Geoanal. Res.*, 38, 149-151, <https://doi.org/10.1111/j.1751-908X.2013.00275.x>, 2013.
- 4130 Nakagawa, Y., Takano, S., Firdaus, M. L., Norisuye, K., Hirata, T., Vance, D., and Sohrin, Y.: The molybdenum isotopic composition of the modern ocean, *Geochem. J.*, 46, 131-141, <https://doi.org/10.2343/geochemj.1.0158>, 2012.
- Nameroff, T. J., Balistrieri, L.S., Murray, J.W.: Suboxic trace metal geochemistry in the eastern tropical north Pacific, *Geochim. Cosmochim. Acta*, 66, 1139–1158, 2003.
- 4135 Nameroff, T. J., Calvert, S. E., and Murray, J. W.: Glacial-interglacial variability in the eastern tropical North Pacific oxygen minimum zone recorded by redox-sensitive trace metals, *Paleoceanography*, 19, n/a-n/a, <https://doi.org/10.1029/2003PA000912>, 2004.
- Neubert, N., Nägler, T. F., and Böttcher, M. E.: Sulfidity controls molybdenum isotope fractionation into euxinic sediments: Evidence from the modern Black Sea, *Geology*, 36, 775-778, <https://doi.org/10.1130/G24959A.1>, 2008.

- Nguyen, T. M. P., Petrizzo, M. R., and Speijer, R. P.: Experimental dissolution of a fossil foraminiferal assemblage (Paleocene–Eocene Thermal Maximum, Dababiya, Egypt): Implications for paleoenvironmental reconstructions, *Mar. Micropaleontol.*, 73, 241–258, <https://doi.org/10.1016/j.marmicro.2009.10.005>, 2009.
- Nguyen, T. M. P., Petrizzo, M. R., Stassen, P., and Speijer, R. P.: Dissolution susceptibility of Paleocene–Eocene planktic foraminifera: Implications for palaeoceanographic reconstructions, *Mar. Micropaleontol.*, 81, 1–21, <https://doi.org/10.1016/j.marmicro.2011.07.001>, 2011.
- Nguyen, T. M. P., and Speijer, R. P.: A new procedure to assess dissolution based on experiments on Pliocene–Quaternary foraminifera (ODP Leg 160, Eratosthenes Seamount, Eastern Mediterranean), *Mar. Micropaleontol.*, 106, 22–39, <https://doi.org/10.1016/j.marmicro.2013.11.004>, 2014.
- Ni, S., Krupinski, N. Q., Groeneveld, J., Persson, P., Somogyi, A., Brinkmann, I., Knudsen, K. L., Seidenkrantz, M. S. and Filipsson, H. L.: Early diagenesis of foraminiferal calcite under anoxic conditions: A case study from the Landsort Deep, Baltic Sea (IODP Site M0063), *Chem. Geol.*, 558, 119871, <https://doi.org/10.1016/j.chemgeo.2020.119871>, 2020.
- Nicolo, M.J., Dickens, G.R. and Hollis, C.J.: South Pacific intermediate water oxygen depletion at the onset of the Paleocene–Eocene thermal maximum as depicted in New Zealand margin sections. *Paleoceanography*, 25(4), <https://doi.org/10.1029/2009PA001904>, 2010.
- Nielsen, S. G., Rehkämper, M., Baker, J., and Halliday, A. N.: The precise and accurate determination of thallium isotope compositions and concentrations for water samples by MC-ICPMS, *Chem. Geol.*, 204, 109–124, <https://doi.org/10.1016/j.chemgeo.2003.11.006>, 2004.
- Nielsen, S. G., Goff, M., Hesselbo, S. P., Jenkyns, H. C., LaRowe, D. E., and Lee, C.-T. A.: Thallium isotopes in early diagenetic pyrite – A paleoredox proxy?, *Geochim. Cosmochim. Ac.*, 75, 6690–6704. <https://doi.org/10.1016/j.gca.2011.07.047>, 2011.
- Nielsen, S. G., Owens, J. D., & Horner, T. J.: Analysis of high-precision vanadium isotope ratios by medium resolution MC-ICP-MS, *J. Anal. Atom. Spectrom.*, 31, 531–536, <https://doi.org/10.1039/C5JA00397K>, 2016.
- Nielsen, S. G., Rehkämper, M., and Prytulak, J.: Investigation and Application of Thallium Isotope Fractionation, *Rev. Mineral. Geochem.*, 82, 759–798. <https://doi.org/10.2138/rmg.2017.82.18>, 2017.
- Nielsen, S. G. (Ed.): *Vanadium Isotopes: A Proxy for Ocean Oxygen Variations*, Cambridge University Press, Cambridge, United Kingdom, 32 pp., ISBN 9781108863438, 2020.
- Nielsen, S. G., Wasylenki, L. E., Rehkämper, M., Peacock, C. L., Xue, Z., and Moon, E. M.: Towards an understanding of thallium isotope fractionation during adsorption to manganese oxides, *Geochim. Cosmochim. Ac.*, 117, 252–265. <https://doi.org/10.1016/j.gca.2013.05.004>, 2013.
- Niemann, H., and Elvert, M.: Diagnostic lipid biomarker and stable carbon isotope signatures of microbial communities mediating the anaerobic oxidation of methane with sulphate, *Org. Geochem.*, 39, 1668–1677, <https://doi.org/10.1016/j.orggeochem.2007.11.003>, 2008.
- Nomaki, H., Chikaraishi, Y., Tsuchiya, M., Toyofuku, T., Suga, H., Sasaki, Y., Uematsu, K., Tame, A., and Ohkouchi, N., 2015. Variation in the nitrogen isotopic composition of amino acids in benthic foraminifera: Implications for their adaptation to oxygen-depleted environments, *Limnol. Oceanogr.*, 60, 1906–1916, <https://doi.org/10.1002/lno.10140>, 2015.
- Nomaki, H., Chen, C., Oda, K., Tsuchiya, M., Tame, A., Uematsu, K. and Isobe, N.: Abundant Chitinous Structures in *Chilostomella* (Foraminifera, Rhizaria) and Their Potential Functions, *J. Eukaryot. Microbiol.*, 68, e12828, <https://doi.org/10.1111/jeu.12828>, 2021.

- 4180 Nordberg, K., Gustafsson, M., and Krantz, A. L.: Decreasing oxygen concentrations in the Gullmar Fjord, Sweden, as confirmed by benthic foraminifera, and the possible association with NAO, *J. Marine Syst.*, 23, 303-316, [https://doi.org/10.1016/S0924-7963\(99\)00067-6](https://doi.org/10.1016/S0924-7963(99)00067-6), 2000.
- Not, C., Brown, K., Ghaleb, B., and Hillaire-Marcel, C.: Conservative behavior of uranium vs. salinity in Arctic sea ice and brine, *Mar. Chem.*, 130, 33-39, <https://doi.org/10.1016/j.marchem.2011.12.005>, 2012.
- 4185 Nowicka, B., and Kruk, J.: Occurrence, biosynthesis and function of isoprenoid quinones, *BBA – Bioenergetics*, 1797, 1587–1605, <https://doi.org/10.1016/j.bbabi.2010.06.007>, 2010.
- Ofstad, S., Zamelczyk, K., Kimoto, K., Chierici, M., Fransson, A., and Rasmussen, T. L.: Shell density of planktonic foraminifera and pteropod species *Limacina helicina* in the Barents Sea: Relation to ontogeny and water chemistry, *PLoS ONE*, 16, e0249178, <https://doi.org/10.1371/journal.pone.0249178>, 2021.
- 4190 Ohkouchi, N., Kashiyama, Y., Kuroda, J., Ogawa, N. O., and Kitazato, H.: The importance of diazotrophic cyanobacteria as primary producers during Cretaceous Oceanic Anoxic Event 2, *Biogeosciences*, 3,467-478, <https://doi.org/10.5194/bg-3-467-2006>, 2006.
- Ohkouchi, N., Chikaraishi, Y., Close, H. G., Fry, B., Larsen, T., Madigan, D. J., McCarthy, M. D., McMahon, K. W., Nagata, T., Naito, Y. I., Ogawa, N. O., Popp, B. N., Steffan, S., Takano, Y., Tayasu, I., Wyatt, A. S. J., Yamaguchi, Y. T., and Yokoyama, Y.: Advances in the application of amino acid nitrogen isotopic analysis in ecological and biogeochemical studies, *Org. Geochem.*, 113, 150–174, <https://doi.org/10.1016/j.orggeochem.2017.07.009>, 2017.
- 4195 Ohkushi, K., Kennett, J. P., Zeleski, C. M., Moffitt, S. E., Hill, T. M., Robert, C., Beaufort, L., and Behl, R. J.: Quantified intermediate water oxygenation history of the NE Pacific: A new benthic foraminiferal record from Santa Barbara basin, *Paleoceanography*, 28, 453-467, <https://doi.org/10.1002/palo.20043>, 2013.
- 4200 Ogawa, N. O., Nagata, T., Kitazato, H., and Ohkouchi, N.: Ultra-sensitive elemental analyzer/isotope ratio mass spectrometer for stable nitrogen and carbon isotope analyses, in: *Earth Life Isotopes*, edited by: Ohkouchi, N., Tayasu, I., and Koba, K., Kyoto University Press, Kyoto, Japan, 339–353, 2010.
- Oldham V. E., Owings S. M., Jones M. R., Tebo B. M., and Luther G. W.: Evidence for the presence of strong Mn(III)- binding ligands in the water column. *Mar. Chem.* 171, 58–66, <https://doi.org/10.1016/j.marchem.2015.02.008>, 2015.
- 4205 Oldham, V. E., Mucci, A., Tebo, B. M., and Luther III, G. W.: Soluble Mn (III)–L complexes are abundant in oxygenated waters and stabilized by humic ligands, *Geochim. Cosmochim. Ac.*, 199, 238-246, <https://doi.org/10.1016/j.gca.2016.11.043>, 2017.
- Oldham, V. E., Jones, M. R., Tebo, B. M., and Luther III, G. W.: Oxidative and reductive processes contributing to manganese cycling at oxic-anoxic interfaces, *Marine Chemistry*, 195, 122-128, <https://doi.org/10.1016/j.marchem.2017.06.002>, 2017.
- 4210 Orsi, T. H., Edwards, C. M., & Anderson, A. L.: X-ray computed tomography: a nondestructive method for quantitative analysis of sediment cores. *Journal of Sedimentary Research*, 64(3a), 690-693, <https://doi.org/10.1306/D4267E74-2B26-11D7-8648000102C1865D>, 1994.
- 4215 Orsi, W. D., Morard, R., Vuillemin, A., Eitel, M., Wörheide, G., Milucka, J., and Kucera, M.: Anaerobic metabolism of Foraminifera thriving below the seafloor, *ISME J.*, 14, 2580-2594, <https://doi.org/10.1038/s41396-020-0708-1>, 2020.
- Oschlies, A., Brandt, P., Stramma, L., and Schmidtko, S.: Drivers and mechanisms of ocean deoxygenation, *Nat. Geosci.*, 11, 467-473, <https://doi.org/10.1038/s41561-018-0152-2>, 2018.
- Oschlies, A.: A committed fourfold increase in ocean oxygen loss, *Nat. Commun.*, 12, 2307, <https://doi.org/10.1038/s41467-021-22584-4>, 2021.
- 4220

- Owens, J. D., Nielsen, S. G., Horner, T. J., Ostrander, C. M., and Peterson, L. C.: Thallium-isotopic compositions of euxinic sediments as a proxy for global manganese-oxide burial, *Geochim. Cosmochim. Ac.*, 213, 291–307, <https://doi.org/10.1016/j.gca.2017.06.041>, 2017.
- 4225 Owens, J.D.: Application of thallium isotopes: Tracking marine oxygenation through manganese oxide burial. Cambridge University Press, Cambridge, United Kingdom, 21 pp., ISBN 9781108688697, <https://doi.org/10.1017/9781108688697>, 2019.
- Paoloni, T., Hoogakker, B., Navarro Rodriguez, A., Pereira, R., McClymont, E.L., Jovane, L., Magill, C.: Composition of planktonic foraminifera test-bound organic material and implications for carbon cycle reconstructions, *Frontiers of Marine Science* 10:1237440, doi: 10.3389/fmars.2023.1237440, 2023.
- 4230 Paradis, S., Nakajima, K., Van der Voort, T. S., Gies, H., Wildberger, A., Blattmann, T. M., Bröder, L., and Eglinton, T. I.: The Modern Ocean Sediment Archive and Inventory of Carbon (MOSAIC): version 2.0, *Earth Syst. Sci. Data*, 15, 4105–4125, <https://doi.org/10.5194/essd-15-4105-2023>, 2023.
- Pardo, A., Keller, G., Molina, E., & Canudo, J.: Planktic foraminiferal turnover across the Paleocene-Eocene transition at DSDP site 401, Bay of Biscay, North Atlantic, *Mar. Micropaleontol.*, 29, 129-158, [https://doi.org/10.1016/S0377-8398\(96\)00035-7](https://doi.org/10.1016/S0377-8398(96)00035-7), 1997.
- 4235 Paropkari, A. L., Babu, C. P., and Mascarenhas, A.: A Critical-Evaluation of Depositional Parameters Controlling the Variability of Organic-Carbon in Arabian Sea Sediments, *Mar. Geol.*, 107, 213-226, [https://doi.org/10.1016/0025-3227\(92\)90168-H](https://doi.org/10.1016/0025-3227(92)90168-H), 1992.
- Paropkari, A. L., Mascarenhas, A., and Babu, C. P.: Lack of Enhanced Preservation of Organic-Matter in Sediments under the Oxygen Minimum on the Oman Margin – Comment, *Geochim. Cosmochim. Ac.*, 57, 2399-2401, [https://doi.org/10.1016/0016-7037\(93\)90578-K](https://doi.org/10.1016/0016-7037(93)90578-K), 1993.
- 4240 Pavia, F. J., Wang, S., Middleton, J., Murray, R. W., and Anderson, R. F.: Trace metal evidence for deglacial ventilation of the abyssal Pacific and Southern Oceans, *Paleoceanography and Paleoclimatology*, 36, e2021PA004226, <https://doi.org/10.1029/2021PA004226>, 2021.
- 4245 Pawłowska, J., Pawłowski, J., and Zajączkowski, M.: Ancient foraminiferal DNA: A new paleoceanographic proxy., EGU General Assembly 2022, Vienna, Austria, 23–27 May 2022, EGU22-9392, <https://doi.org/10.5194/egusphere-egu22-9392>, 2022.
- Pearson, A., Hurley, S.J., Walter, S.R.S., Kusch, S., Lichtin, S., and Zhang, Y.G.: Stable carbon isotope ratios of intact GDGTs indicate heterogeneous sources to marine sediments, *Geochim. Cosmochim. Ac.*, 181, 18–35, <https://doi.org/10.1016/j.gca.2016.02.034>, 2016.
- 4250 Pedersen, T. F., Shimmiel, G. B., and Price, N. B.: Lack of enhanced preservation of organic matter in sediments under the oxygen minimum on the Oman Margin, *Geochim. Cosmochim. Ac.*, 56, 545-551, [https://doi.org/10.1016/0016-7037\(92\)90152-9](https://doi.org/10.1016/0016-7037(92)90152-9), 1992.
- 4255 Penn, J.L., and Deutch, C.: Avoiding ocean mass extinction from climate warming, *Science*, 376, 6592, <https://doi.org/10.1126/science.abe9039>, 2022.
- Perez-Cruz, L. L., and Machain-Castillo, M.L.: Benthic foraminifera of the oxygen minimum zone, continental shelf of the Gulf of Tehuantepec, Mexico, *J. Foramin. Res.*, 20, 312-325, <https://doi.org/10.2113/gsjfr.20.4.312>, 1990.
- 4260 Peters, K. E., Walters, C.C., and Moldowan, J.M. (Eds.): The biomarker guide. Vol. 1. Biomarkers in the environment and human history, Cambridge University Press, Cambridge, UK, 471 pp., ISBN 9780511524868, 2005.

Petersen, J., Riedel, B., Barras, C., Pays, O., Guihéneuf, A., Mabilieu, G., Schweizer, M., Meysman, F. J. R., and Jorissen, F.: Improved methodology for measuring pore patterns in the benthic foraminiferal genus *Ammonia*, *Mar. Micropaleontol.*, 128, 1–13, <https://doi.org/10.1016/j.marmicro.2016.08.001>, 2016.

4265

Phleger, F. B., and Soutar, A.: Production of benthic foraminifera in three east Pacific oxygen minima, *Micropaleontology*, 19, 110-115, <https://doi.org/10.2307/1484973>, 1973.

Pike, J., Bernard, J.M., Moreton, S.G., Butkler, I.B.: Microirrigation of marine sediments in dysoxic environments: implications for early sediment fabric formation and diagenetic processes, *Geology* 29, 923-926, 2001.

4270 Piña-Ochoa, E., Høgslund, S., Geslin, E., Cedhagen, T., Revsbech, N. P., Nielsen, L. P., Schweizer, M., Jorissen, F., Rysgaard, S., and Risgaard-Petersen, N.: Widespread occurrence of nitrate storage and denitrification among Foraminifera and Gromiida, *P. Natl. Acad. Sci. USA*, 107, 1148-1153, <https://doi.org/10.1073/pnas.0908440107>, 2010a.

Piña-Ochoa, E., Koho, K. A., Geslin, E., and Risgaard-Petersen, N.: Survival and life strategy of the foraminiferan *Globobulimina turgida* through nitrate storage and denitrification, *Mar. Ecol. Prog. Ser.*, 417, 39-49, <https://doi.org/10.3354/meps08805>, 2010b.

4275

Podder, J., Lin, J., Sun, W., Botis, S.M., Tse, J., Chen, N., Hu, Y., Li, D., Seaman, J. and Pan, Y.: Iodate in calcite and vaterite: Insights from synchrotron X-ray absorption spectroscopy and first-principles calculations, *Geochim. Cosmochim. Ac.*, 198, 218-228, <https://doi.org/10.1016/j.gca.2016.11.032>, 2017.

4280 Polik, C.A., Elling, F.J., and Pearson, A.: Impacts of Paleocology on the TEX86 Sea Surface Temperature Proxy in the Pliocene-Pleistocene Mediterranean Sea, *Paleoceanography and Paleoclimatology*, 33, 1472–1489, <https://doi.org/10.1029/2018PA003494>, 2018.

Polissar, P. J., Fulton, J. M., Junium, C. K., Turich, C. C., and Freeman, K. H.: Measurement of ^{13}C and ^{15}N Isotopic Composition on Nanomolar Quantities of C and N, *Anal. Chem.*, 81, 755–763, <https://doi.org/10.1021/ac801370c>, 2009.

4285 Prah, F. G., De Lange, G. J., Lyle, M., and Sparrow, M. A.: Post-Depositional Stability of Long-Chain Alkenones under Contrasting Redox Conditions, *Nature*, 341, 434-437, <https://doi.org/10.1038/341434a0>, 1989.

Prah, F.G., Pinto, L.A., and Sparrow, M.A.: Phytane from chemolytic analysis of modern marine sediments: a product of desulfurization or not?, *Geochim. Cosmochim. Ac.*, 60, 1065–73, [https://doi.org/10.1016/0016-7037\(95\)00450-5](https://doi.org/10.1016/0016-7037(95)00450-5), 1996.

4290 Prah, F.G., Pilska, C.H., Sparrow, M.A.: Seasonal record for alkenones in sedimentary particles from the Gulf of Maine, *Deep Sea Research Part I: Oceanographic Research Papers* 48, 515-518, 2001.

Prazeres, M., Uthicke, S., and Pandolfi, J. M.: Ocean acidification induces biochemical and morphological changes in the calcification process of large benthic foraminifera, *Proc. R. Soc. B Biol. Sci.*, 282, 20142782, <https://doi.org/10.1098/rspb.2014.2782>, 2015.

4295 Qin, L. and Wang, X.: Chromium Isotope Geochemistry, *Reviews in Mineralogy and Geochemistry*, 82 (1), 379–414, <https://doi.org/10.2138/rmg.2017.82.10>, 2017.

Rabalais, N.N., Turner, R.E., and Wiseman, W.J.: Gulf of Mexico hypoxia, aka “The dead zone”, *Annu. Rev. Ecol. Syst.*, 33, 253-263, <https://doi.org/10.1146/annurev.ecolsys.33.010802.150513>, 2002.

Rabalais, N. N. (2010). Eutrophication of estuarine and coastal ecosystems. *Environmental microbiology*, 115-134.

4300 Rabalais, N.N., Diaz, R.J., Levin, L.A., Turner, R.E., Gilbert, D., Zhang, J.: Dynamics and distribution of natural and human-caused hypoxia. *Biogeosciences* 7, 585–619, <https://doi.org/10.5194/bg-7-585-2010>, 2010.

Raiswell, R., Hardisty, D.S., Lyons, T.W., Canfield, D.E., Owens, J.D., Planavsky, N.J., Poulton, S.W. and Reinhard, C.T.,: The iron paleoredox proxies: A guide to the pitfalls, problems and proper practice. *American Journal of Science*, 318(5), 491-526, <https://doi.org/10.2475/05.2018.03>, 2018.

4305

Raitzsch, M., Kuhnert, H., Hathorne, E.C., Groeneveld, J., and Bickert, T.: U/Ca in benthic foraminifers: A proxy for the deep-sea carbonate saturation, *Geochem. Geophys. Geosy.*, 12, <https://doi.org/10.1029/2010GC003344>, 2011.

4310 Rapp, I., Schlosser, C., Browning, T.J., Wolf, F., Le Moigne, F.A., Gledhill, M., and Achterberg, E.P.: El Niño-driven oxygenation impacts Peruvian shelf iron supply to the South Pacific Ocean, *Geophys. Res. Lett.*, 47, e2019GL086631, <https://doi.org/10.1029/2019GL086631>, 2020.

Rathburn, A. E., Willingham, J., Ziebis, W., Burkett, A. M., and Corliss, B. H.: A New biological proxy for deep-sea paleo-oxygen: Pores of epifaunal benthic foraminifera, *Sci. Rep.*, 8, 9456, <https://doi.org/10.1038/s41598-018-27793-4>, 2018.

4315 Raven, M. R., Fike, D. A., Gomes, M. L., Webb, S. M., Bradley, A. S., and McClelland, H.-L. O.: Organic carbon burial during OAE2 driven by changes in the locus of organic matter sulfurization, *Nat. Commun.*, 9, 3409. <https://doi.org/10.1038/s41467-018-05943-6>, 2018.

Raven, M., Adkins, J.F., Werne, J.P., Lyons, T.W., and Sessions, A.L.: Sulfur isotopic composition of individual organic compounds from Cariaco Basin sediments, *Org. Geochem.*, 80, 53–59, <https://doi.org/10.1016/j.orggeochem.2015.01.002>, 2015.

4320 Raven, M. R., Keil, R.G., Webb, S.M.: Microbial sulfate reduction and organic sulfur formation in sinking marine particles, *Science*, 371, 178–181, <https://doi.org/10.1126/science.abc6035>, 2021a.

Raven, M. R., Keil, R.G., Webb, S.M.: Rapid, Concurrent formation of organic sulfur and iron sulfides during experimental sulfurization of sinking marine particles, *Global Biogeochem. Cy.*, 35, <https://doi.org/10.1029/2021GB007062>, 2021b.

Reddin, C. J., Nätscher, P. S., Kocsis, Á. T., Pörtner, H. O., & Kiessling, W.: Marine clade sensitivities to climate change conform across timescales. *Nature Climate Change*, 10(3), 249-253, <https://doi.org/10.1038/s41558-020-0690-7>, 2020.

4325

Reinhard, C. T., Planavsky, N. J., Wang, X., Fischer, W. W., Johnson, T. M., and Lyons, T. W.: The isotopic composition of authigenic chromium in anoxic marine sediments: A case study from the Cariaco Basin, *Earth Planet. Sc. Lett.*, 407, 9-18, <https://doi.org/10.1016/j.epsl.2014.09.024>, 2014.

4330 Ren, H., Sigman, D. M., Meckler, A. N., Plessen, B., Robinson, R. S., Rosenthal, Y., and Haug, G. H.: Foraminiferal Isotope Evidence of Reduced Nitrogen Fixation in the Ice Age Atlantic Ocean, *Science*, 323, 244–248, <https://doi.org/10.1126/science.1165787>, 2009.

Ren, H., Sigman, D. M., Chen, M.-T., and Kao, S.-J.: Elevated foraminifera-bound nitrogen isotopic composition during the last ice age in the South China Sea and its global and regional implications: FB- $\delta^{15}\text{N}$ RECORD IN SOUTH CHINA SEA, *Glob. Biogeochem. Cycles*, 26, n/a-n/a, <https://doi.org/10.1029/2010GB004020>, 2012a.

4335 Ren, H., Sigman, D. M., Thunell, R. C., and Prokopenko, M. G.: Nitrogen isotopic composition of planktonic foraminifera from the modern ocean and recent sediments, *Limnol. Oceanogr.*, 57, 1011–1024, <https://doi.org/10.4319/lo.2012.57.4.1011>, 2012b.

4340

Řezanka, T., Siristova, L., Melzoch, K., and Sigler, K.: N-acylated bacteriohopanehexol-mannosamides from the thermophilic bacterium *Alicyclobacillus acidoterrestris*, *Lipids* 46, 249–261, <https://doi.org/10.1007/s11745-010-3482-4>, 2011.

- Rhoads, D. C., & Morse, J. W. (1971). Evolutionary and ecologic significance of oxygen-deficient marine basins. *Lethaia*, 4(4), 413-428, <https://doi.org/10.1111/j.1502-3931.1971.tb01864.x>, 1971.
- 4345 Richirt, J., Champmartin, S., and Schweizer, M., Mouret, A., Petersen, J., Ambari, A., and Jorissen, F.: Scaling laws explain foraminiferal pore patterns, *Sci. Rep.*, 9, 9149, <https://doi.org/10.1038/s41598-019-45617-x>, 2019.
- Richmond, T., Cole, J., Dangler, G., Daniele, M., Marchitto, T., and Lobaton, E.: Forabot: Automated planktic foraminifera isolation and imaging, *Geochem. Geophys. Geosy.*, 23, e2022GC010689, <https://doi.org/10.1029/2022GC010689>, 2022.
- 4350 Risgaard-Petersen, N., Langezaal, A. M., Ingvardsen, S., Schmid, M. C., Jetten, M. S., Op den Camp, H. J., Derksen, J. W., Piña-Ochoa, E., Eriksson, S. P., Nielsen, L. P., Revsbech, N. P., Cedhagen, T., and van der Zwaan, G. J.: Evidence for complete denitrification in a benthic foraminifer, *Nature*, 443, 93-96, <https://doi.org/10.1038/nature05070>, 2006.
- Robinson, R. S., and Sigman, D. M.: Nitrogen isotopic evidence for a poleward decrease in surface nitrate within the ice age Antarctic, *Quat. Sci. Rev.*, 27, 1076–1090, <https://doi.org/10.1016/j.quascirev.2008.02.005>, 2008.
- 4355 Robinson, R. S., Kienast, M., Luiza Albuquerque, A., Altabet, M., Contreras, S., De Pol Holz, R., Dubois, N., Francois, R., Galbraith, E., Hsu, T.-C., Ivanochko, T., Jaccard, S., Kao, S.-J., Kiefer, T., Kienast, S., Lehmann, M., Martinez, P., McCarthy, M., Möbius, J., Pedersen, T., Quan, T. M., Ryabenko, E., Schmittner, A., Schneider, R., Schneider-Mor, A., Shigemitsu, M., Sinclair, D., Somes, C., Studer, A., Thunell, R., and Yang, J.-Y.: A review of nitrogen isotopic alteration in marine sediments: N isotopic alteration in marine sediment, *Paleoceanography*, 27, <https://doi.org/10.1029/2012PA002321>, 2012.
- 4360 Robinson, R. S., Etourneau, J., Martinez, P. M., and Schneider, R.: Expansion of pelagic denitrification during early Pleistocene cooling, *Earth Planet. Sci. Lett.*, 389, 52–61, <https://doi.org/10.1016/j.epsl.2013.12.022>, 2014.
- Robinson, R. S., Moore, T. C., Erhardt, A. M., and Scher, H. D.: Evidence for changes in subsurface circulation in the late Eocene equatorial Pacific from radiolarian-bound nitrogen isotope values: Radiolarian N Isotope Values From EOT, *Paleoceanography*, 30, 912–922, <https://doi.org/10.1002/2015PA002777>, 2015.
- 4365 Rodrigo-Gámiz, M., Rampen, S. W., Schouten, S., and Damsté, J. S. S.: The impact of oxic degradation on long chain alkyl diol distributions in Arabian Sea surface sediments, *Org. Geochem.*, 100, 1-9, <https://doi.org/10.1016/j.orggeochem.2016.07.003>, 2016.
- Rodríguez-Tovar, F.J. and Uchman, A.: Ichnological data as a useful tool for deep-sea environmental characterization: a brief overview and an application to recognition of small-scale oxygenation changes during the Cenomanian–Turonian anoxic event. *Geo-Mar Lett*, 31, 525-536, <https://doi.org/10.1007/s00367-011-0237-z>, 2011.
- 4370 Rodríguez-Tovar, F.J.: Ichnology of the Toarcian Oceanic Anoxic Event: An underestimated tool to assess palaeoenvironmental interpretations. *Earth-Science Reviews*, 216, 103579, <https://doi.org/10.1016/j.earscirev.2021.103579>, 2021.
- Rodríguez-Tovar, F.J.: Ichnological analysis: A tool to characterize deep-marine processes and sediments, *Earth-Science Reviews* 228, <https://doi.org/10.1016/j.earscirev.2022.104014>, 2022
- 4375 Rohmer, M., Bouvier-Nave, P., Ourisson, G.: Distribution of hopanoid triterpenes in prokaryotes, *Microbiology*, 130, 1137–1150, <https://doi.org/10.1099/00221287-130-5-1137>, 1984.
- Rolison, J. M., Stirling, C. H., Middag, R., & Rijkenberg, M. J.: Uranium stable isotope fractionation in the Black Sea: Modern calibration of the $^{238}\text{U}/^{235}\text{U}$ paleo-redox proxy, *Geochim. Cosmochim. Ac.*, 203, 69-88, <https://doi.org/10.1016/j.gca.2016.12.014>, 2017.
- 4380 Rontani, J. F., and Volkman, J. K.: Phytol degradation products as biogeochemical tracers in aquatic environments, *Org. Geochem.*, 34, 1–35, [https://doi.org/10.1016/S0146-6380\(02\)00185-7](https://doi.org/10.1016/S0146-6380(02)00185-7), 2003.
- Rosenberg, Y.O., Kutuzov, I., and Amrani, A.: Sulfurization as a preservation mechanism for the $\delta^{13}\text{C}$ of biomarkers, *Org. Geochem.*, 125, 66–69, <https://doi.org/10.1016/j.orggeochem.2018.08.010>, 2018.

- 4385 Rosenberg, Y.O., Meshoulam, A., Said-Ahmad, W., Shawar, L., Dror, G., Reznik, I.J., Feinstein, S., and Amrani, A.: Study of thermal maturation processes of sulfur-rich source rock using compound specific sulfur isotope analysis, *Org. Geochem.*, 112, 59–74, <https://doi.org/10.1016/j.orggeochem.2017.06.005>, 2017.
- Ross, B. J., and Hallock, P.: Dormancy in the foraminifera: A review, *J. Foramin. Res.*, 46, 358–368, <https://doi.org/10.2113/gsjfr.46.4.358>, 2016.
- 4390 Rossel, P.E., Elvert, M., Ramette, A., Boetius, A., and Hinrichs, K.-U.: Factors controlling the distribution of anaerobic methanotrophic communities in marine environments: Evidence from intact polar membrane lipids, *Geochim. Cosmochim. Ac.*, 75, 164–184, <https://doi.org/10.1016/j.gca.2010.09.031>, 2011.
- Rudnick, R. L., Gao, S.: Composition of the continental crust, in: *Treatise on Geochemistry* vol. 3, edited by: Holland, H. D., and Turekian, K. K., Elsevier Science, USA, 1–64, <https://doi.org/10.1016/B0-08-043751-6/03016-4>, 2003.
- 4395 Rue, E. L., Smith, G. J., Cutter, G. A., and Bruland, K. W.: The response of trace element redox couples to suboxic conditions in the water column, *Deep-Sea Res. Pt. I*, 44, 113–134, [https://doi.org/10.1016/S0967-0637\(96\)00088-X](https://doi.org/10.1016/S0967-0637(96)00088-X), 1997.
- Rush, D., Jaeschke, A., Hopmans, E. C., Geenevasen, J. A. J., Schouten, S., Damsté, J. S. S.: Short chain ladderanes: Oxidic biodegradation products of anammox lipids, *Geochim. Cosmochim. Ac.*, 75, 1662–1671, <https://doi.org/10.1016/j.gca.2011.01.013>, 2011.
- 4400 Rush, D., Wakeham, S. G., Hopmans, E. C., Schouten, S., Sinninghe Damsté, J. S.: Biomarker evidence for anammox in the oxygen minimum zone of the Eastern Tropical North Pacific, *Org. Geochem.*, 53, 80–87, <https://doi.org/10.1016/j.orggeochem.2012.02.005>, 2012.
- Rush, D., Sinninghe Damsté, J. S., Poulton, S. W., Thamdrup, B., Garside, A. L., González, J. A., Schouten, S., Jetten, M. S. M., Talbot, H. M.: Anaerobic ammonium-oxidising bacteria: A biological source of the bacteriohopanetetrol stereoisomer in marine sediments, *Geochim. Cosmochim. Ac.*, 140, 50–64, <https://doi.org/10.1016/j.gca.2014.05.014>, 2014.
- 4405 Rush, D., Osborne, K. A., Birgel, D., Kappler, A., Hirayama, H., Peckmann, J., Poulton, S. W., Nickel, J. C., Mangelsdorf, K., Kalyuzhnaya, M., Sidgwick, F. R., Talbot, H. M.: The bacteriohopanepolyol inventory of novel aerobic methane oxidising bacteria reveals new biomarker signatures of aerobic methanotrophy in marine systems, *PLoS ONE*, 11, e0165635–27, <https://doi.org/10.1371/journal.pone.0165635>, 2016.
- Rush, D., and Sinninghe Damsté, J. S.: Lipids as paleomarkers to constrain the marine nitrogen cycle: Lipids as paleomarkers, *Environ. Microbiol.*, 19, 2119–2132, <https://doi.org/10.1111/1462-2920.13682>, 2017.
- Rush, D., Talbot, H. M., Meer, M. van der, Hopmans, E. C., Douglas, B., and Sinninghe Damsté, J. S.: Biomarker evidence for the occurrence of anaerobic ammonium oxidation in the eastern Mediterranean Sea during Quaternary and Pliocene sapropel formation, *Biogeosciences*, 16, 2467–2479, <https://doi.org/10.5194/bg-16-2467-2019>, 2019.
- 4415
- Russell, A. D., Emerson, S., Nelson, B. K., Erez, J., and Lea, D. W.: Uranium in foraminiferal calcite as a recorder of seawater uranium concentrations, *Geochim. Cosmochim. Ac.*, 58, 671–681, [https://doi.org/10.1016/0016-7037\(94\)90497-9](https://doi.org/10.1016/0016-7037(94)90497-9), 1994.
- Ryabenko, E.: Stable Isotope Methods for the Study of the Nitrogen Cycle, in: *Topics in Oceanography*, edited by: Zambianchi, E., InTech, <https://doi.org/10.5772/56105>, 2013.
- 4420 Sachs, J. P., and Repeta, D. J.: Oligotrophy and Nitrogen Fixation During Eastern Mediterranean Sapropel Events, *Science*, 286, 2485–2488, <https://doi.org/10.1126/science.286.5449.2485>, 1999.
- Sáenz, J. P., Waterbury, J. B., Eglinton, T. I., and Summons, R. E.: Hopanoids in marine cyanobacteria: probing their phylogenetic distribution and biological role, *Geobiology*, 10, 311–319, <https://doi.org/10.1111/j.1472-4669.2012.00318.x>, 2012.

- 4425 Sakata, S., Hayes, J. M., Rohmer, M., Hooper, A. B., and Seemann, M.: Stable carbon-isotopic compositions of lipids isolated from the ammonia-oxidizing chemoautotroph *Nitrosomonas europaea*, *Org. Geochem.*, 39, 1725–1734, <https://doi.org/10.1016/j.orggeochem.2008.08.005>, 2008.
- Sampaio, E., Santos, C., Rosa, I.C., Ferreira, V., Pörtner, H.O., Duarte, C.M., Levin, L.A. and Rosa, R.,: Impacts of hypoxic events surpass those of future ocean warming and acidification. *Nature Ecology & Evolution*, 5(3), 311–321, <https://doi.org/10.1038/s41559-020-01370-3>, 2021.
- 4430 Sarmiento, J. L., and Gruber, N. (Eds.): *Ocean Biogeochemical Dynamics*, Princeton University Press, New Jersey, USA, 528 pp., ISBN 9780691017075, 2006.
- Schaeffer, P., Adam, P., Wehrung, P., and Albrecht, P.: Novel aromatic carotenoid derivatives from sulfur photosynthetic bacteria in sediments, *Tetrahedron Lett.*, 38, 8413–8416, [https://doi.org/10.1016/S0040-4039\(97\)10235-0](https://doi.org/10.1016/S0040-4039(97)10235-0), 1997.
- 4435 Schiebel, R., and Hemleben, C.: *Planktic Foraminifers in the Modern Ocean*, 2nd ed., Springer Berlin, Heidelberg, Berlin, Germany, 358 pp., <https://doi.org/10.1007/978-3-662-50297-6>, 2017.
- Schlitzer, R., Anderson, R. F., Masferrer Dodas, E., Lohan, M., Geibert, W., Tagliabue, A., Bowie, A., Jeandel, C., Maldonado, M. T., Landing, W. M., Cockwell, D., Abadie, C., Abouchami, W., Achterberg, E. P., Agather, A., Aguliar-Islas, A., et al.: The GEOTRACES Intermediate Data Product 2017, *Chem. Geol.*, <https://doi.org/10.1016/j.chemgeo.2018.05.040>, 2018.
- 4440 Schmidt, R. A. M.: Microradiography of microfossils with X-ray diffraction equipment, *Science*, 115, 94–95, <https://doi.org/10.1126/science.115.2978.94>, 1952.
- Schmidt, D. N., Rayfield, E. J., Cocking, A., and Marone, F.: Linking evolution and development: Synchrotron radiation X-ray tomographic microscopy of planktic foraminifers, *Palaeontology*, 56, 741–749, <https://doi.org/10.1111/pala.12013>, 2013.
- 4445 Schmidt, D. N., Thomas, E., Authier, E., Saunders, D., and Ridgwell, A.: Strategies in times of crisis—insights into the benthic foraminiferal record of the Palaeocene–Eocene Thermal Maximum, *Phil. Trans. R. Soc. A.*, 376; <http://doi.org/10.1098/rsta.2017.0328>, 2018.
- Schmidtko, S., Stramma, L., and Visbeck, M.: Decline in global oceanic oxygen content during the past five decades, *Nature*, 542, 335–339, <https://doi.org/10.1038/nature21399>, 2017.
- 4450 Schmiedl, G., Mitschele, A., Beck, S., Emeis, K. C., Hemleben, C., Schulz, H., ... & Weldeab, S.: Benthic foraminiferal record of ecosystem variability in the eastern Mediterranean Sea during times of sapropel S5 and S6 deposition, *Palaeogeogr. Palaeoclimatol.*, 190, 139–164, [https://doi.org/10.1016/S0031-0182\(02\)00603-X](https://doi.org/10.1016/S0031-0182(02)00603-X), 2003.
- Schmiedl, G., Mackensen, A.: Multispecies stable isotopes of benthic foraminifers reveal past changes of organic matter decomposition and deepwater oxygenation in the Arabian Sea, *Paleoceanography and Paleoclimatology* 21, PA4213, doi:10.1029/2006PA001284, 2006.
- 4455 Schmittner, A., Gruber, N., Mix, A.C., Key, R.M., Tagliabue, A., Westberry, T.K., Biology and air-sea gas exchange controls on the distribution of carbon isotopes ratios in the ocean, *Biogeosciences* 10, 5793–5816, doi:10.5194/bg-10-5793-2013, 2013.
- Schmittner, A., Bostock, H. C., Cartapanis, O., Curry, W. B., Filipsson, H. L., Galbraith, E. D., Gottschalk, J., Herguera, J. C., Hoogakker, B., Jaccard, S. L., Lisiecki, L. E., Lund, D. C., Méndez, G. M., Stieglitz, J. L., Mackensen, A., Michel, E., Mix, A. C., Oppo, D. W., Peterson, C. D., Repschläger, J., Sikes, E. L., Spero, H. J., Waelbroeck, C.: Calibration of the carbon isotope composition ($\delta^{13}\text{C}$) of benthic foraminifera, *Paleoceanography* 32, 512–530, <https://doi.org/10.1002/2016PA003072>, 2017.
- 4460 Schouten, S., Hopmans, E. C., Sinninghe Damsté, J. S.: The organic geochemistry of glycerol dialkyl glycerol tetraether lipids: A review, *Org. Geochem.*, 54, 19–61, <https://doi.org/10.1016/j.orggeochem.2012.09.006>, 2013a.

- Schouten, S., Villareal, T. A., Hopmans, E. C., Mets, A., Swanson, K. M., Sinninghe Damsté, J. S.: Endosymbiotic heterocystous cyanobacteria synthesize different heterocyst glycolipids than free-living heterocystous cyanobacteria, *Phytochemistry*, 85, 115–121, <https://doi.org/10.1016/j.phytochem.2012.09.002>, 2013b.
- 4470 Schwark, L., and Frimmel, A.: Chemostratigraphy of the Posidonia Black Shale, SW-Germany II. Assessment of extent and persistence of photic-zone anoxia using aryl isoprenoid distributions, *Chem. Geol.*, 206, 231-248, <https://doi.org/10.1016/j.chemgeo.2003.12.008>, 2004.
- Schubert, C. J., and Calvert, S. E.: Nitrogen and carbon isotopic composition of marine and terrestrial organic matter in Arctic Ocean sediments: implications for nutrient utilization and organic matter composition, *Deep-Sea Res. Pt. I.*, 48, 789-810, [https://doi.org/10.1016/S0967-0637\(00\)00069-8](https://doi.org/10.1016/S0967-0637(00)00069-8), 2001.
- 4475 Schumacher, S., Jorissen, F. J., Dissard, D., Larkin, K. E., & Gooday, A. J.: Live (Rose Bengal stained) and dead benthic foraminifera from the oxygen minimum zone of the Pakistan continental margin (Arabian Sea), *Mar. Micropaleontol.*, 62, 45-73, <https://doi.org/10.1016/j.marmicro.2006.07.004>, 2007.
- Schwartz-Narbonne, R., Schaeffer, P., Hopmans, E. C., Schenese, M., Charlton, E. A., Jones, D. M., Sinninghe Damsté, J. S., Haque, M. F. U., Jetten, M. S. M., Lengger, S. K., Murrell, J. C., Normand, P., Nuijten, G. H. L., Talbot, H. M., Rush, D.: A unique bacteriohopanetetrol stereoisomer of marine anammox, *Org. Geochem.*, 143, 103994, <https://doi.org/10.1016/j.orggeochem.2020.103994>, 2020.
- 4480 Sen Gupta, B. K., and Machain-Castillo, M. L.: Benthic foraminifera in oxygen-poor habitats, *Mar. Micropaleontol.*, 20, 183-201, [https://doi.org/10.1016/0377-8398\(93\)90032-S](https://doi.org/10.1016/0377-8398(93)90032-S), 1993.
- 4485 Sen Gupta, B. K., Platon, E., Bernhard, J. M. and Aharon, P.: Foraminiferal colonization of hydrocarbon-seep bacterial mats and underlying sediment, Gulf of Mexico slope, *J. Foramin. Res.*, 27, 292–300, <https://doi.org/10.2113/gsjfr.27.4.292>, 1997.
- Sen Gupta, B. K.: Systematics of modern Foraminifera BT - Modern Foraminifera, edited by: Sen Gupta, B. K., Springer Netherlands, Dordrecht, 7–36, https://doi.org/10.1007/0-306-48104-9_2, 2003.
- 4490 Seralathan, P., and Hartmann, M.: Molybdenum and vanadium in sediment cores from the NW-African continental margin and their relations to climatic and environmental conditions, *Meteor Forschungsergebnisse: Reihe C, Geologie und Geophysik*, 40, 1–17, 1986.
- Service, R. F.: New dead zone off Oregon coast hints at sea change in currents, *Science*, 305, 1099, <https://doi.org/10.1126/science.305.5687.1099>, 2004.
- 4495 Severmann, S., Lyons, T. W., Anbar, A., McManus, J., and Gordon, G.: Modern iron isotope perspective on the benthic iron shuttle and the redox evolution of ancient oceans, *Geology*, 36, 487-490, <https://doi.org/10.1130/G24670A.1>, 2008.
- Sharon, Belanger, C., Du, J., and Mix, A.: Reconstructing paleo-oxygenation for the last 54,000 years in the Gulf of Alaska using cross-validated benthic foraminiferal and geochemical records, *Paleoceanography and Paleoclimatology*, 36, e2020PA003986. <https://doi.org/10.1029/2020PA003986>, 2021.
- 4500 Shatz, M., Yosief, T., and Kashman, Y.: Bacteriohopanehexol, a new triterpene from the marine sponge *Petrosia* species, *J. Nat. Prod.*, 63, 1554–1556, <https://doi.org/10.1021/np000190r>, 2000.
- Shaw, T. J., Gieskes, J. M., and Jahnke, R. A.: Early diagenesis in differing depositional environments: The response of transition metals in pore water, *Geochim. Cosmochim. Ac.* 54, 1233–1246, [https://doi.org/10.1016/0016-7037\(90\)90149-F](https://doi.org/10.1016/0016-7037(90)90149-F), 1990.
- 4505 Shaw, T.J., Sholkovitz, E.R., and Klinkhammer, G.: Redox dynamics in the Chesapeake Bay: The effect on sediment/water uranium exchange, *Geochim. Cosmochim. Ac.* 58, 2985–2995, [https://doi.org/10.1016/0016-7037\(94\)90173-2](https://doi.org/10.1016/0016-7037(94)90173-2), 1994.

- 4510 Shawar, L., Said-Ahmad, W., Ellis, G.S., and Amrani, A.: Sulfur Isotope composition of individual compounds in immature organic-rich rocks and possible geochemical implications, *Geochim. Cosmochim. Ac.*, 274, 20–44, <https://doi.org/10.1016/j.gca.2020.01.034>, 2020.
- Shawar, L., Grice, K., Holman, A.I., and Amrani, A.: Carbon and Sulfur Isotopic Composition of Alkyl- and Benzo-Thiophenes Provides Insights into Their Origins and Formation Pathways, *Org. Geochem.*, 151, 104163, <https://doi.org/10.1016/j.orggeochem.2020.104163>, 2021.
- 4515 Sherwood, O. A., Guilderson, T. P., Batista, F. C., Schiff, J. T., and McCarthy, M. D.: Increasing subtropical North Pacific Ocean nitrogen fixation since the Little Ice Age, *Nature*, 505, 78–81, <https://doi.org/10.1038/nature12784>, 2014.
- Shiller, A.M., and Boyle, E.A.: Dissolved vanadium in rivers and estuaries, *Earth Planet. Sc. Lett.*, 86, 214–224, [https://doi.org/10.1016/0012-821X\(87\)90222-6](https://doi.org/10.1016/0012-821X(87)90222-6), 1987.
- 4520 Siccha, M., Trommer, G., Schulz, H., Hemleben, C., and Kucera, M.: Factors controlling the distribution of planktonic foraminifera in the Red Sea and implications for the development of transfer functions, *Mar. Micropaleontol.*, 72, 146-156, <https://doi.org/10.1016/j.marmicro.2009.04.002>, 2009.
- Sigman, D. M., Altabet, M. A., Francois, R., McCorkle, D. C., and Gaillard, J.-F.: The isotopic composition of diatom-bound nitrogen in Southern Ocean sediments, *Paleoceanography*, 14, 118–134, <https://doi.org/10.1029/1998PA900018>, 1999.
- 4525 Sigman, D. M., Casciotti, K. L., Andreani, M., Barford, C., Galanter, M., and Böhlke, J. K.: A Bacterial Method for the Nitrogen Isotopic Analysis of Nitrate in Seawater and Freshwater, *Anal. Chem.*, 73, 4145–4153, <https://doi.org/10.1021/ac010088e>, 2001.
- Sigman, D. M. and Fripiat, F.: Nitrogen Isotopes in the Ocean, in: *Encyclopedia of Ocean Sciences*, Elsevier, 263–278, <https://doi.org/10.1016/B978-0-12-409548-9.11605-7>, 2019.
- 4530 Sigman, D. M., DiFiore, P. J., Hain, M. P., Deutsch, C., Wang, Y., Karl, D. M., Knapp, A. N., Lehmann, M. F., and Pantoja, S.: The dual isotopes of deep nitrate as a constraint on the cycle and budget of oceanic fixed nitrogen, *Deep-Sea Res. Pt. I*, 56, 1419-1439, <https://doi.org/10.1016/j.dsr.2009.04.007>, 2009a.
- Sigman, D. M., Karsh, K. L., and Casciotti, K. L.: Ocean process tracers: Nitrogen isotopes in the ocean, in: *Encyclopedia of Ocean Sciences*, edited by: Steele, J. H., Academic Press, Cambridge, Massachusetts, USA, 4138-4153, <https://doi.org/10.1006/rwos.2001.0172>, 2009b.
- 4535
- Sinninghe Damsté, J. S., Rijpstra, W. I. C., de Leeuw, J., Schenck, P. A.: Origin of organic sulphur compounds and sulphur-containing high molecular weight substances in sediments and immature crude oils, *Org. Geochem.*, 13, 593–606, [https://doi.org/10.1016/0146-6380\(88\)90079-4](https://doi.org/10.1016/0146-6380(88)90079-4), 1988.
- 4540
- Sinninghe Damsté, J. S., Strous, M., Rijpstra, W. I. C., Hopmans, E. C., Geenevasen, J. A. J., Duin, A. C. T. van, Niftrik, L. A. van, Jetten, M. S. M.: Linearly concatenated cyclobutane lipids form a dense bacterial membrane, *Nature*, 419, 708–712, <https://doi.org/10.1038/nature01128>, 2002a.
- 4545
- Sinninghe Damsté, J. S., Schouten, S., Hopmans, E. C., van Duin, A. C. T., Geenevasen, J. A. J.: Crenarchaeol: the characteristic core glycerol dibiphytanyl glycerol tetraether membrane lipid of cosmopolitan pelagic crenarchaeota, *J. Lipid Res.*, 43, 1641–1651, <https://doi.org/10.1194/jlr.m200148-jlr200>, 2002b.
- Sinninghe Damsté, J. S., Rijpstra, W. I. C., and Reichart, G. J.: The influence of oxic degradation on the sedimentary biomarker record II. Evidence from Arabian Sea sediments, *Geochim. Cosmochim. Ac.*, 66, 2737-2754, [https://doi.org/10.1016/S0016-7037\(02\)00865-7](https://doi.org/10.1016/S0016-7037(02)00865-7), 2002c.

- 4550 Sinninghe Damsté, J. S., Kuypers, M. M. M., Schouten, S., Schulte, S., and Rullkötter, J.: The lycopane/C31 n-alkane ratio as a proxy to assess palaeoacidity during sediment deposition, *Earth Planet. Sc. Lett.* 209, 215–226, [https://doi.org/10.1016/S0012-821X\(03\)00066-9](https://doi.org/10.1016/S0012-821X(03)00066-9), 2003.
- Skinner, L. C., Sadekov, A., Brandon, M., Greaves, M., Plancherel, Y., de La Fuente, M., Gottschalk, J., Souanef-Ureta, S., Sevilgen, D. S., and Scrivner, A. E.: Rare Earth Elements in early-diagenetic foraminifer ‘coatings’: Pore-water controls and potential palaeoceanographic applications, *Geochim. Cosmochim. Ac.*, 245, 118-132, <https://doi.org/10.1016/j.gca.2018.10.027>, 2019.
- 4555 Sliter, W. V.: Test ultrastructure of some living benthic foraminifers: *Lethaia*, 7, 5-16, <https://doi.org/10.1111/j.1502-3931.1974.tb00880.x>, 1974.
- Smart, C. W., King, S. C., Gooday, A. J., Murray, J. W., and Thomas, E.: A benthic foraminiferal proxy of pulsed organic matter paleofluxes, *Mar. Micropaleontol.*, 23, 89-99, [https://doi.org/10.1016/0377-8398\(94\)90002-7](https://doi.org/10.1016/0377-8398(94)90002-7), 1994.
- 4560 Smith, P. B.: Ecology of benthonic species, *Geol. Surv. Prof. Paper*, 429-B, n/a-n/a, <https://doi.org/10.3133/pp429B>, 1964.
- Smit, N. T., Rush, D., Sahonero-Canavesi, D. X., Verweij, M., Rasigraf, O., Cruz, S. G., Jetten, M. S. M., Sinninghe Damsté, J. S., and Schouten, S.: Demethylated hopanoids in “*Ca. Methyloirabilis oxyfera*” as biomarkers for environmental nitrite-dependent methane oxidation, *Org. Geochem.*, 137, 103899, <https://doi.org/10.1016/j.orggeochem.2019.07.008>, 2019.
- 4565 Sollai, M., Hopmans, E. C., Schouten, S., Keil, R. G., and Sinninghe Damsté, J. S.: Intact polar lipids of Thaumarchaeota and anammox bacteria as indicators of N cycling in the eastern tropical North Pacific oxygen-deficient zone, *Biogeosciences*, 12, 4725–4737, <https://doi.org/10.5194/bg-12-4725-2015>, 2015.
- Speijer, R. P., Van Loo, D., Masschaele, B., Vlassenbroeck, J., Cnudde, V., and Jacobs P.: Quantifying foraminiferal growth with high-resolution x-ray computed tomography: New opportunities in foraminiferal ontogeny, phylogeny, and paleoceanographic applications, *Geosphere*, 4, 760-763, <https://doi.org/10.1130/GES00176.1>, 2008.
- 4570 Sperling, E. A., Frieder, C. A., Raman, A. V., Girguis, P. R., Levin, L. A., & Knoll, A. H.: Oxygen, ecology, and the Cambrian radiation of animals. *Proceedings of the National Academy of Sciences*, 110(33), 13446-13451, <https://doi.org/10.1073/pnas.1312778110>, 2013.
- 4575 Sperling, E. A., Knoll, A. H., & Girguis, P. R.: The ecological physiology of Earth's second oxygen revolution. *Annual Review of Ecology, Evolution, and Systematics*, 46, 215-235, [10.1146/annurev-ecolsys-110512-135808](https://doi.org/10.1146/annurev-ecolsys-110512-135808), 2015.
- Sperling, E.A., Boag, T.H., Duncan, M.I., Endriga, C.R., Marquez, J.A., Mills, D.B., Monarrez, P.M., Sclafani, J.A., Stockey, R.G. and Payne, J.L.: Breathless through time: oxygen and animals across Earth’s history. *The Biological Bulletin*, 243(2), 184-206, <https://doi.org/10.1086/721754>, 2022.
- 4580 Stal, L. J.: Is the distribution of nitrogen-fixing cyanobacteria in the oceans related to temperature?, *Environ. Microbiol.*, 11, 1632–1645, <https://doi.org/10.1111/j.1758-2229.2009.00016.x>, 2009.
- Stassen, P., Thomas, E., & Speijer, R. P.: Paleocene–Eocene Thermal Maximum environmental change in the New Jersey Coastal Plain: benthic foraminiferal biotic events, *Marine Micropaleontology*, 115, 1-23, 2015.
- 4585 Steen, A. D., Kusch, S., Abdulla, H. A., Cakić, N., Coffinet, S., Dittmar, T., Fulton, J. M., Galy, V., Hinrichs, K. -U., Ingalls, A. E., Koch, B. P., Kujawinski, E., Liu, Z., Osterholz, H., Rush, D., Seidel, M., Sepúlveda, J., and Wakeham, S.G.: Analytical and computational advances, opportunities, and challenges in marine organic biogeochemistry in an era of “omics.”, *Front. Mar. Sci.*, 7, 3815, <https://dx.doi.org/10.3389/fmars.2020.00718>, 2020.
- Steinhardt, J., Cléroux, C., Ullgren, J., de Nooijer, L., Durgadoo, J.V., Brummer, G.J. and Reichart, G.J.: Anti-cyclonic eddy imprint on calcite geochemistry of several planktonic foraminiferal species in the Mozambique Channel, *Mar. Micropaleontol.*, 113, 20-33, <https://doi.org/10.1016/j.marmicro.2014.09.001>, 2014.
- 4590

- Stirling, C. H., Andersen, M. B., Warthmann, R., and Halliday, A. N.: Isotope fractionation of ²³⁸U and ²³⁵U during biologically-mediated uranium reduction, *Geochim. Cosmochim. Ac.*, 163, 200-218, <https://doi.org/10.1016/j.gca.2015.03.017>, 2015.
- 4595 St-Onge, G., Mulder, T., Francus, P., and Long, B.: Chapter two continuous physical properties of cored marine sediments, *Developments in marine geology*, 1, 63-98, [https://doi.org/10.1016/S1572-5480\(07\)01007-X](https://doi.org/10.1016/S1572-5480(07)01007-X), 2007.
- Stramma, L., Johnson, G. C., Sprintall, J., and Mohrholz, V.: Expanding Oxygen-Minimum Zones in the Tropical Oceans, *Science* (80-.), 320, 655 LP – 658, 2008.
- Stramma, L., Schmidtko, S., Levin, L. A., and Johnson, G. C.: Ocean oxygen minima expansions and their biological impacts, *Deep Sea Res. Part I Oceanogr. Res. Pap.*, 57, 587–595, <https://doi.org/10.1016/J.DSR.2010.01.005>, 2010.
- 4600 Studer, A.S., Martinez-Garcia, A., Jaccard, S.L., Girault, F.E., Sigman, D.M., Haug, G.H.: Enhanced stratification and seasonality in the Subarctic Pacific upon Northern Hemisphere Glaciation—New evidence from diatom-bound nitrogen isotopes, alkenones and archaeal tetraethers, *Earth and Planetary Science Letters* 351-352, 84-94, 2012.
- Studer, A. S., Ellis, K. K., Oleynik, S., Sigman, D. M., Haug, G. H.: Size-specific opal-bound nitrogen isotope measurements in North Pacific sediments, *Geochimica et Cosmochimica Acta* 120, 179-194, <https://doi.org/10.1016/j.gca.2013.06.041>, 2013.
- 4605 Studer, A. S., Sigman, D. M., Martínez-García, A., Benz, V., Winckler, G., Kuhn, G., Esper, O., Lamy, F., Jaccard, S. L., Wacker, L., Oleynik, S., Gersonde, R., and Haug, G. H.: Antarctic Zone nutrient conditions during the last two glacial cycles: Antarctic zone nutrient conditions, *Paleoceanography*, 30, 845–862, <https://doi.org/10.1002/2014PA002745>, 2015.
- Studer, A. S., Mekik, F., Ren, H., Hain, M. P., Oleynik, S., Martínez-García, A., Haug, G. H., and Sigman, D. M.: Ice Age-Holocene Similarity of Foraminifera-Bound Nitrogen Isotope Ratios in the Eastern Equatorial Pacific, *Paleoceanogr. Paleoclimatology*, 36, <https://doi.org/10.1029/2020PA004063>, 2021.
- 4610 Summons, R.E., and Powell, T.G.: Identification of aryl isoprenoids in source rocks and crude oils: biological markers for the green sulphur bacteria, *Geochim. Cosmochim. Ac.*, 51, 557–566, [https://doi.org/10.1016/0016-7037\(87\)90069-X](https://doi.org/10.1016/0016-7037(87)90069-X), 1987.
- Sun, X., Kop, L. F. M., Lau, M. C. Y., Frank, J., Jayakumar, A., Lückner, S., Ward, B.B.: Uncultured Nitrospina-like species are major nitrite oxidizing bacteria in oxygen minimum zones, *ISME J.*, 13, 2391–2402, <https://doi.org/10.1038/s41396-019-0443-7>, 2019.
- 4615 Sundby, B., and Silverberg, N.: Manganese fluxes in the benthic boundary layer 1, *Limnol. Oceanogr.*, 30, 372-381, <https://doi.org/10.4319/lo.1985.30.2.0372>, 1985.
- Sundby, B., Martinez, P., and Gobeil, C.: Comparative geochemistry of cadmium, rhenium, uranium, and molybdenum in continental margin sediments, *Geochim. Cosmochim. Ac.*, 68, 2485–2493, <https://doi.org/10.1016/j.gca.2003.08.011>, 2004.
- 4620 Suokhrie, T., Saraswat, R., and Nigam, R.: Lack of denitrification causes a difference in benthic foraminifera living in the oxygen deficient zones of the Bay of Bengal and the Arabian Sea, *Mar. Pollut. Bull.*, 153, 110992, <https://doi.org/10.1016/j.marpolbul.2020.110992>, 2020.
- 4625 Sweere, T., van den Boorn, S., Dickson, A.J., Reichart, G.-J.: Definition of new trace-metal proxies for the controls on organic matter enrichment in marine sediments based on Mn, Co, Mo and Cd concentrations, *Chemical Geology* 441, 235-245, 2016.
- Sweere, T., Hennekam, R., Vance, D., and Reichart, G.-J.: Molybdenum isotope constraints on the temporal development of sulfidic conditions during Mediterranean sapropel intervals, *Geochem. Perspect.*, 17, 16-20, <https://doi.org/10.7185/geochemlet.2108>, 2021.
- 4630 Szymczak-Żyła, M., Kowalewska, G., and Louda, J.W.: The influence of microorganisms on chlorophyll a degradation in the marine environment, *Limnol. Oceanogr.*, 53, 851–862, <https://doi.org/10.4319/lo.2008.53.2.0851>, 2008.

- Szymczak-Żyła, M., Krajewska, M., Winogradow, A., Zaborska, A., Breedveld, G.D. and Kowalewska, G.: Tracking trends in eutrophication based on pigments in recent coastal sediments, *Oceanologia*, 59, 1-17, <https://doi.org/10.1016/j.oceano.2016.08.003>, 2017.
- 4635 Takana, Y., Illyina, T., Tiputra, T., Eddebbar, Y.A., Berthet, S., Bopp, L., Buitenhuis, E., Butenschön, M., Christian, J.R., Dunne, J.P., Gröger, M., Hayashida, H., Hieronymus, J., Koenigk, T., Krasting, J., Long, M.C., Lovato, T., Nakano, H., Palmieri, J., Schwinger, J., Séférian, R., Suntharalingam, P., Tatebe, H., Tsujino, H., Urawaka, S., Watanabe, M., Yool, A.: Simulations of ocean deoxygenation in the historical era: insights from forced and coupled models, *Frontiers of Marine Science* 10, <https://doi.org/10.3389/fmars.2023.1139917>, 2023.
- 4640 Talbot, H. M., Watson, D. F., Murrell, J. C., Carter, J. F., and Farrimond, P.: Analysis of intact bacteriohopanepolyols from methanotrophic bacteria by reversed-phase high-performance liquid chromatography-atmospheric pressure chemical ionisation mass spectrometry, *J. Chromatogr. A*, 921, 175–185, [https://doi.org/10.1016/S0021-9673\(01\)00871-8](https://doi.org/10.1016/S0021-9673(01)00871-8), 2001.
- Talbot, H.M., Summons, R.E., Jahnke, L.L., Cockell, C.S., Rohmer, M., and Farrimond, P.: Cyanobacterial bacteriohopanepolyol signatures from cultures and natural environmental settings, *Org. Geochem.*, 39, 232–263, <https://doi.org/10.1016/j.orggeochem.2007.08.006>, 2008.
- 4645 Talbot, H. M., Bischoff, J., Inglis, G. N., Collinson, M. E., and Pancost, R. D.: Polyfunctionalised bio- and geohopanoids in the Eocene Cobham Lignite, *Org. Geochem.*, 96, 77–92, <https://doi.org/10.1016/j.orggeochem.2016.03.006>, 2016.
- Tanaka, A., Nakano, T., & Ikehara, K.: X-ray computerized tomography analysis and density estimation using a sediment core from the Challenger Mound area in the Porcupine Seabight, off Western Ireland. *Earth, planets and space*, 63, 103-110, <https://doi.org/10.5047/eps.2010.12.006>, 2011.
- 4650 Tarhan, L. G., Droser, M. L., Planavsky, N. J., & Johnston, D. T.: Protracted development of bioturbation through the early Palaeozoic Era. *Nature Geoscience*, 8(11), 865-869, <https://doi.org/10.1038/ngeo2537>, 2015.
- Tavera Martínez, L., Marchant, M., Muñoz, P., & Abdala Díaz, R. T.: Spatial and Vertical Benthic Foraminifera Diversity in the Oxygen Minimum Zone of Mejillones Bay, Northern Chile, *Front. Mar. Sci.*, 9, 357, <https://doi.org/10.3389/fmars.2022.821564>, 2022.
- 4655 Tebo, B. M., Bargar, J. R., Clement, B., Dick, G., Murray, K. J., Parker, D., Verity, R., and Webb, S. M.: Biogenic manganese oxides: properties and mechanisms of formation, *Annu. Rev. Earth Pl. Sc.*, 32, 287–328, <https://doi.org/10.1146/annurev.earth.32.101802.120213>, 2004.
- 4660 ten Haven, H. L., de Leeuw, J. W., Rullkötter, J., Sinninghe Damsté J. S.: Restricted utility of the pristane/phytane ratio as a palaeoenvironmental indicator, *Nature*, 330, 641–643, <https://doi.org/10.1038/330641a0>, 1987.
- Tesdal, J.-E., Galbraith, E. D., and Kienast, M.: Nitrogen isotopes in bulk marine sediment: linking seafloor observations with subseafloor records, *Biogeosciences*, 10, 101–118, <https://doi.org/10.5194/bg-10-101-2013>, 2013.
- 4665 Teske, A., Wawer, C., Muyzer, G., and Ramsing, N.B.: Distribution of sulfate-reducing bacteria in a stratified fjord (Mariager Fjord, Denmark) as evaluated by most-probable-number counts and denaturing gradient gel electrophoresis of PCR-amplified ribosomal DNA fragments, *Appl. Environ. Microb.*, 62, 1405–1415, <https://doi.org/10.1128/aem.62.4.1405-1415.1996>, 1996.
- Tetard, M., Licari, L., and Beaufort, L.: Oxygen history off Baja California over the last 80 kyr: A new foraminiferal-based record, *Paleoceanography*, 32, 246-264, <https://doi.org/10.1002/2016PA003034>, 2017.
- 4670 Tetard, M., Licari, L., Ovsepyan, E., Tachikawa, K., & Beaufort, L.: Toward a global calibration for quantifying past oxygenation in oxygen minimum zones using benthic Foraminifera, *Biogeosciences*, 18, 2827-2841, <https://doi.org/10.5194/bg-18-2827-2021>, 2021a.

- Tetard, M., Ovsepyan, E., and Licari, L.: Eubuliminella Tenuata as a New Proxy for Quantifying Past Bottom Water Oxygenation, *Mar. Micropaleontol.*, 166, 102016, <https://doi.org/10.1016/j.marmicro.2021.102016>, 2021b.
- 4675 Tetard, M., Prebble, J., Cortese, G.: Dissolved oxygen affinities of hundreds of benthic foraminiferal species. *Mar. Micropaleontol.*, 190, 102380, <https://doi.org/10.1016/j.marmicro.2024.102380>, 2024.
- Thamdrup, B.: New pathways and processes in the global nitrogen cycle, *Annu. Rev. Ecol. Evol. S.*, 43, 407–428, <https://doi.org/10.1146/annurev-ecolsys-102710-145048>, 2012.
- 4680 Thamdrup, B., Fossing, H., and Jørgensen, B.B.: Manganese, iron and sulfur cycling in a coastal marine sediment, Aarhus Bay, Denmark, *Geochim. Cosmochim. Ac.*, 58, 5115-5129, [https://doi.org/10.1016/0016-7037\(94\)90298-4](https://doi.org/10.1016/0016-7037(94)90298-4), 1994a.
- Thamdrup, B., Glud, R. N., and Hansen, J. W.: Manganese oxidation and in situ manganese fluxes from a coastal sediment, *Geochim. Cosmochim. Ac.*, 58, 2563-2570, [https://doi.org/10.1016/0016-7037\(94\)90032-9](https://doi.org/10.1016/0016-7037(94)90032-9), 1994b.
- Thamdrup, B., Dalsgaard, T., and Revsbech N. P.: Widespread functional anoxia in the oxygen minimum zone of the Eastern South Pacific, *Deep-Sea Res. Pt. I*, 65, 36–45, <https://doi.org/10.1016/j.dsr.2012.03.001>, 2012.
- 4685 Thiel, V., Peckmann, J., Seifert, R., Wehrung, P., Reitner, J., and Michaelis, W.: Highly isotopically depleted isoprenoids: Molecular markers for ancient methane venting, *Geochim. Cosmochim. Ac.*, 63, 3959–3966, [https://doi.org/10.1016/S0016-7037\(99\)00177-5](https://doi.org/10.1016/S0016-7037(99)00177-5), 1999.
- Thomas, N.C., Bradbury, H.J., Hodell, D.A.: Changes in North Atlantic deep-water oxygenation across the Middle Pleistocene Transition, *Science* 377, 654-659, 2022.
- 4690
- Thomson, J., Wallace, H.E., Colley, S., and Toole, J.: Authigenic uranium in Atlantic sediments of the last glacial stage - a diagenetic phenomenon, *Earth Planet. Sc. Lett.*, 98, 222–232, [https://doi.org/10.1016/0012-821X\(90\)90061-2](https://doi.org/10.1016/0012-821X(90)90061-2), 1990.
- Tissot, F.L.H., Chen, S., Go, B.M., Naziemiec, M., Healy, G., Bekker, A., Swart, P.K., Dauphas, N. Controls of eustacy and diagenesis on the 238U/235U of carbonates and evolution of the seawater (234U.238U) during the last 1.4 Myr. *Geochimica et Cosmochimica Acta* 242, 233-265, <https://doi.org/10.1016/j.gca.2018.08.022>, 2018.
- 4695 Titelboim D., Lord O. T., and Schmidt D. N.: Thermal Stress Reduces Carbonate Production of Benthic Foraminifera and Changes the Material Properties of Their Shells, *ICES J. Mar. Sci.*, 78, 3202–3211, <https://doi.org/10.1093/icesjms/fsab186>, 2021.
- 4700 Todd C. L., Schmidt D. N., Robinson M. M., and De Schepper S.: Planktic Foraminiferal Test Size and Weight Response to the Late Pliocene Environment, *Paleoceanography and Paleoclimatology*, 35, e2019PA003738, <https://doi.org/10.1029/2019PA003738>, 2020.
- Tossell, J.: Calculating the partitioning of the isotopes of Mo between oxidic and sulfidic species in aqueous solution, *Geochim. Cosmochim. Ac.*, 69, 2981-2993, <https://doi.org/10.1016/j.gca.2005.01.016>, 2005.
- 4705
- Tribouillard, N., Algeo, T. J., Lyons, T., and Riboulleau, A.: Trace metals as paleoredox and paleoproductivity proxies: An update, *Chem. Geol.*, 232, 12–32, <https://doi.org/10.1016/j.chemgeo.2006.02.012>, 2006.
- Truesdale, V. W., and Bailey, G. W.: Dissolved iodate and total iodine during an extreme hypoxic event in the Southern Benguela system, *Estuar. Coast. Shelf S.*, 50, 751-760, <https://doi.org/10.1006/ecss.2000.0609>, 2000.
- 4710 Trust, B. A., and Fry, B.: Stable sulphur isotopes in plants: A review, *Plant Cell Environ.*, 15, 1105–10, <https://doi.org/10.1111/j.1365-3040.1992.tb01661.x>, 1992.

- Umling, N. E., and Thunell, R. C.: Mid-depth respired carbon storage and oxygenation of the eastern equatorial Pacific over the last 25,000 years, *Quaternary Sci. Rev.*, 189, 43-56, <https://doi.org/10.1016/j.quascirev.2018.04.002>, 2018.
- 4715 Vairavamurthy, A., Mopper, K., and Taylor, B.F.: Occurrence of particle-bound polysulfides and significance of their reaction with organic matters in marine sediments, *Geophys. Res. Lett.*, 19, 2043–46, <https://doi.org/10.1029/92GL01995>, 1992.
- Vairavamurthy, A.: Using X-Ray Absorption to Probe Sulfur Oxidation States in Complex Molecules, *Spectrochim. Acta A*, 54, 2009–2017, [https://doi.org/10.1016/S1386-1425\(98\)00153-X](https://doi.org/10.1016/S1386-1425(98)00153-X), 1998.
- 4720 Valdés, J., and Tapia, J.: Spatial monitoring of metals and As in coastal sediments of northern Chile: An evaluation of background values for the analysis of local environmental conditions, *Mar. Pollut. Bull.*, 145, 624-640, <https://doi.org/10.1016/j.marpolbul.2019.06.036>, 2019.
- Valdés, J., Sifeddine, A., Boussafir, M., and Ortlieb, L.: Redox conditions in a coastal zone of the Humboldt system (Mejillones, 23°S). Influence on the preservation of redox-sensitive metals, *J. Geochem. Explor.*, 140, 1-10, <https://doi.org/10.1016/j.gexplo.2014.01.002>, 2014.
- 4725 Valdés, J., Sifeddine, A., Guíñez, M., and Castillo, A.: Oxygen minimum zone variability during the last 700 years in a coastal upwelling area of the Humboldt system (Mejillones, 23°S, Chile). A new approach from geochemical signature, *Prog. Oceanogr.*, 193, 102520. <https://doi.org/10.1016/j.poccean.2021.102520>, 2021.
- Valdés, J., Ortlieb, L., Sifeddine, A., and Castillo, A.: Human-induced metals accumulation in sediments of an industrialized bay of northern Chile. An enrichment and ecological risk assessment based on preindustrial values, *Mar. Pollut. Bull.*, 189, 114723, <https://doi.org/10.1016/j.marpolbul.2023.114723>, 2023.
- 4730 Van De Velde, S., Mills, B. J., Meysman, F. J., Lenton, T. M., & Poulton, S. W.: Early Palaeozoic ocean anoxia and global warming driven by the evolution of shallow burrowing. *Nature communications*, 9(1), 2554, <https://doi.org/10.1038/s41467-018-04973-4>, 2018.
- 4735 Van der Weijden, C. H.: Pitfalls of normalization of marine geochemical data using a common divisor, *Mar. Geol.*, 184, 167-187, [https://doi.org/10.1016/S0025-3227\(01\)00297-3](https://doi.org/10.1016/S0025-3227(01)00297-3), 2002.
- Van der Zwaan, G. J., Duijnste, A. I., Den Dulk, M., Ernst, S. R., Jannink, N. T., and Kouwenhoven, T. J.: Benthic foraminifers: proxies or problems?: a review of paleoecological concepts, *Earth Sci. Rev.*, 46, 213-236, [https://doi.org/10.1016/S0012-8252\(99\)00011-2](https://doi.org/10.1016/S0012-8252(99)00011-2), 1999.
- 4740 Van Dijk, I., Mouret, A., Cotte, M., Le Houedec, S., Oron, S., Reichart, G.J., Reyes-Herrera, J., Filipsson, H.L. and Barras, C.: Chemical heterogeneity of Mg, Mn, Na, S, and Sr in benthic foraminiferal calcite, *Front. Earth Sci.*, 7, 281, <https://doi.org/10.3389/feart.2019.00281>, 2019.
- Van Dijk, I., De Nooijer, L. J., Barras, C., and Reichart, G. J.: Mn Incorporation in Large Benthic Foraminifera: Differences Between Species and the Impact of p CO₂, *Front. Earth Sci.*, 8, 567701, <https://doi.org/10.3389/feart.2020.567701>, 2020.
- 4745 van Dongen, B. E., Talbot, H. M., Schouten, S., Pearson, P. N., and Pancost, R. D.: Well preserved Palaeogene and Cretaceous biomarkers from the Kilwa area, Tanzania, *Org. Geochem.*, 37, 539–557, <https://doi.org/10.1016/j.orggeochem.2006.01.003>, 2006.
- 4750 van Dongen, B. E., Schouten, S., and Sinninghe Damsté, J. S.: Preservation of carbohydrates through sulfurization in a Jurassic euxinic shelf sea: Examination of the Blackstone Band TOC cycle in the Kimmeridge Clay Formation, UK, *Org. Geochem.*, 37, 1052–73, <https://doi.org/10.1016/j.orggeochem.2006.05.007>, 2006.
- Van Kaam-Peters, H. M. E., Schouten, S., Köster, J., and Sinninghe Damsté, J. S.: Controls on the molecular and carbon isotopic composition of organic matter deposited in a Kimmeridgian euxinic shelf sea: evidence for preservation of

- carbohydrates through sulfurisation, *Geochim. Cosmochim. Ac.*, 62, 3259–83, [https://doi.org/10.1016/S0016-7037\(98\)00231-2](https://doi.org/10.1016/S0016-7037(98)00231-2), 1998.
- 4755 van Kemenade, Z. R., Villanueva, L., Hopmans, E. C., Kraal, P., Witte, H. J., Sinninghe Damsté, J. S., and Rush, D.: Bacteriohopanetetrol-x: constraining its application as a lipid biomarker for marine anammox using the water column oxygen gradient of the Benguela upwelling system, *Biogeosciences*, 19, 201–221, <https://doi.org/10.5194/bg-19-201-2022>, 2022.
- 4760 van Meer, G., Voelker, D. R., and Feigenson, G. W.: Membrane lipids: where they are and how they behave, *Nat. Rev. Mol. Cell Biol.*, 9, 112–124, <https://doi.org/10.1038/nrm2330>, 2008.
- Van Vliet, D. M., Meijerfeldt, F. A. B., Dutilh, B. E., Villanueva, L., Sinninghe Damsté, J. S., Stams, A. J. M., and Sánchez-Andrea, I.: The bacterial sulfur cycle in expanding dysoxic and euxinic marine waters, *Environ. Microbiol.*, 23, 2834–2857, <https://doi.org/10.1111/1462-2920.15265>, 2021.
- 4765 Vaquer-Sunyer, R., and Duarte, C.M.: Thresholds of hypoxia for marine biodiversity, *P. Natl. Acad. Sci. USA*, 105, 15452–15457, <https://doi.org/10.1073/pnas.0803833105>, 2008.
- Vedamati, J., Chan, C., and Moffett, J. W.: Distribution of dissolved manganese in the Peruvian Upwelling and Oxygen Minimum Zone, *Geochim. Cosmochim. Ac.*, 156, 222–240, <https://doi.org/10.1016/j.gca.2014.10.026>, 2015.
- 4770 Vickerman, K.: The diversity and ecological significance of Protozoa. *Biodivers Conserv* 1, 334–341, <https://doi.org/10.1007/BF00693769>, 1992.
- Vorlicek, T. P., Chappaz, A., Groskreutz, L. M., Young, N., and Lyons, T. W.: A new analytical approach to determining Mo and Re speciation in sulfidic waters, *Chem. Geol.*, 403, 52–57, <https://doi.org/10.1016/j.chemgeo.2015.03.003>, 2015.
- 4775 Wagner, C. L., Stassen, P., Thomas, E., Lippert, P. C., & Lasca, I.: Magnetofossils and benthic foraminifera record changes in food supply and deoxygenation of the coastal marine seafloor during the paleocene-eocene thermal maximum, *Paleoceanography and Paleoclimatology*, 37(10), e2022PA004502, 2022.
- 4780 Wakeham, S. G., Freeman, K. H., Pease, T. K., and Hayes, J. M.: A photoautotrophic source for lycopane in marine water columns, *Geochim. Cosmochim. Ac.*, 57, 159–165, [https://doi.org/10.1016/0016-7037\(93\)90476-d](https://doi.org/10.1016/0016-7037(93)90476-d), 1993.
- Wakeham, S. G., Sinninghe Damsté, J. S., Kohnen, M. E. L., and De Leeuw, J. W.: Organic sulfur compounds formed during early diagenesis in Black Sea sediments, *Geochim. Cosmochim. Ac.*, 59, 521–33, [https://doi.org/10.1016/0016-7037\(94\)00361-O](https://doi.org/10.1016/0016-7037(94)00361-O), 1995.
- 4785 Wakeham, S. G., Lee, C., Hedges, J. I., Hernes, P. J., and Peterson, M. J.: Molecular indicators of diagenetic status in marine organic matter, *Geochim. Cosmochim. Ac.*, 61, 5363–5369, [https://doi.org/10.1016/S0016-7037\(97\)00312-8](https://doi.org/10.1016/S0016-7037(97)00312-8), 1997.
- 4790 Wakeham, S. G., Amann, R., Freeman, K. H., Hopmans, E. C., Jørgensen, B. B., Putnam, I. F., Schouten, S., Sinninghe Damsté, J. S., Talbot, H. M., and Woebken, D.: Microbial ecology of the stratified water column of the Black Sea as revealed by a comprehensive biomarker study, *Org. Geochem.*, 38, 2070–2097, <https://doi.org/10.1016/j.orggeochem.2007.08.003>, 2007.
- Wakeham, S. G.: Organic biogeochemistry in the oxygen-deficient ocean: A review, *Org. Geochem.*, 149, 104096, <https://doi.org/10.1016/j.orggeochem.2020.104096>, 2020.

- Wang, W. -L., Moore, J. K., Martiny, A. C., and Primeau, F. W.: Convergent estimates of marine nitrogen fixation, *Nature*, 566, 205–211, <https://doi.org/10.1038/s41586-019-0911-2>, 2019.
- 4795 Wang, X., Planavsky, N. J., Reinhard, C. T., Hein, J. R., and Johnson, T. M.: A Cenozoic seawater redox record derived from $^{238}\text{U}/^{235}\text{U}$ in ferromanganese crusts, *Am. J. Sci.*, 316, 64–83, <https://doi.org/10.2475/01.2016.02>, 2016.
- Wang, X., Algeo, T. J., Li, C., & Zhu, M. Spatial pattern of marine oxygenation set by tectonic and ecological drivers over the Phanerozoic. *Nat. Geo.*, 16(11), 1020–1026, <https://doi.org/10.1038/s41561-023-01296-y>, 2023.
- 4800 Wang, X. T., Prokopenko, M. G., Sigman, D. M., Adkins, J. F., Robinson, L. F., Ren, H., Oleynik, S., Williams, B., and Haug, G. H.: Isotopic composition of carbonate-bound organic nitrogen in deep-sea scleractinian corals: A new window into past biogeochemical change, *Earth Planet. Sci. Lett.*, 400, 243–250, <https://doi.org/10.1016/j.epsl.2014.05.048>, 2014.
- Wang, X. T., Sigman, D. M., Cohen, A. L., Sinclair, D. J., Sherrell, R. M., Weigand, M. A., Erler, D. V., and Ren, H.: Isotopic composition of skeleton-bound organic nitrogen in reef-building symbiotic corals: A new method and proxy evaluation at Bermuda, *Geochim. Cosmochim. Ac.*, 148, 179–190, <https://doi.org/10.1016/j.gca.2014.09.017>, 2015.
- 4805 Wang, X. T., Sigman, D. M., Cohen, A. L., Sinclair, D. J., Sherrell, R. M., Cobb, K. M., Erler, D. V., Stolarski, J., Kitahara, M. V., and Ren, H.: Influence of open ocean nitrogen supply on the skeletal $\delta^{15}\text{N}$ of modern shallow-water scleractinian corals, *Earth Planet. Sci. Lett.*, 441, 125–132, <https://doi.org/10.1016/j.epsl.2016.02.032>, 2016.
- Wang, X. T., Wang, Y., Auderset, A., Sigman, D. M., Ren, H., Martínez-García, A., Haug, G. H., Su, Z., Zhang, Y. G., Rasmussen, B., Sessions, A. L., and Fischer, W. W.: Oceanic nutrient rise and the late Miocene inception of Pacific oxygen-deficient zones, *Proc. Natl. Acad. Sci.*, 119, e2204986119, <https://doi.org/10.1073/pnas.2204986119>, 2022.
- 4810 Wang, Y., Hendy, I. L., Latimer, J. C., and Bilardello, D.: Diagenesis and iron paleo-redox proxies: New perspectives from magnetic and iron speciation analyses in the Santa Barbara Basin, *Chem. Geol.*, 519, 95–109, <https://doi.org/10.1016/j.chemgeo.2019.04.018>, 2019.
- 4815 Wang, Y., Costa, K. M., Lu, W., Hines, S. K., & Nielsen, S. G. Global oceanic oxygenation controlled by the Southern Ocean through the last deglaciation. *Sci. Adv.*, 10(3), <https://doi.org/10.1126/sciadv.adk2506>, 2024.
- Wang, Y., Lu, W., Costa, K. M., and Nielsen, S. G.: Beyond anoxia: Exploring sedimentary thallium isotopes in paleo-redox reconstructions from a new core top collection, *Geochim. Cosmochim. Ac.*, 333, 347–361, <https://doi.org/10.1016/j.gca.2022.07.022>, 2022.
- 4820 Waser, N., Yin, K., Yu, Z., Tada, K., Harrison, P., Turpin, D., and Calvert, S.: Nitrogen isotope fractionation during nitrate, ammonium and urea uptake by marine diatoms and coccolithophores under various conditions of N availability, *Mar. Ecol. Prog. Ser.*, 169, 29–41, <https://doi.org/10.3354/meps169029>, 1998.
- Wehrli, B., and Stumm, W.: Vanadyl in natural waters: Adsorption and hydrolysis promote oxygenation, *Geochim. Cosmochim. Ac.*, 53, 69–77, [https://doi.org/10.1016/0016-7037\(89\)90273-1](https://doi.org/10.1016/0016-7037(89)90273-1), 1989.
- 4825 Weigand, M. A., Foriel, J., Barnett, B., Oleynik, S., and Sigman, D. M.: Updates to instrumentation and protocols for isotopic analysis of nitrate by the denitrifier method: Denitrifier method protocols and instrumentation updates, *Rapid Commun. Mass Spectrom.*, 30, 1365–1383, <https://doi.org/10.1002/rcm.7570>, 2016.
- Weijers, J. W. H., Lim, K. L. H., Aquilina, A., Sinninghe Damsté, J. S., Pancost, R. D.: Biogeochemical controls on glycerol dialkyl glycerol tetraether lipid distributions in sediments characterized by diffusive methane flux, *Geochem. Geophys. Geosy.*, 12, n/a-n/a, <https://doi.org/10.1029/2011GC003724>, 2011.
- 4830 Welander, P. V., and Summons, R. E.: Discovery, taxonomic distribution, and phenotypic characterization of a gene required for 3-methylhopanoid production, *P. Natl. Acad. Sci. USA*, 109, 12905–12910, <https://doi.org/10.1073/pnas.1208255109>, 2012.
- 4835 Weltje & Tjallingii 2008 Weltje, G.J., Tjallingii, R.: Calibration of XRF core scanners for quantitative geochemical logging of sediment cores: Theory and application, *Earth and Planetary Science Letters* 274 (3–4), 423–438, <https://doi.org/10.1016/j.epsl.2008.07.054>, 2008.

- Werne, J. P., Hollander, D. J., Behrens, A., Schaeffer, P., Albrecht, P., and Sinninghe Damsté, J. S.: Timing of Early Diagenetic Sulfurization of Organic Matter: A Precursor-Product Relationship in Holocene Sediments of the Anoxic Cariaco Basin, Venezuela, *Geochim. Cosmochim. Ac.*, 64, 1741–51, [https://doi.org/10.1016/S0016-7037\(99\)00366-X](https://doi.org/10.1016/S0016-7037(99)00366-X), 2000.
- 4840 Westerhold, T., Marwan, N., Drury, A. J., Liebrand, D., Agnini, C., Anagnostou, E., Barnet, J. S. K., Bohaty, S. M., De Vleeschouwer, D., Florindo, F., Frederichs, T., Hodell, D. A., Holbourn, A. E., Kroon, D., Laurentano, V., Littler, K., Lourens, L. J., Lyle, M., Pälike, H., Röhl, U., Tian, J., Wilkens, R. H., Wilson, P. A., and Zachos, J. C.: An astronomically dated record of Earth's climate and its predictability over the last 66 million years, *Science*, 369, 1383–1387, <https://doi.org/10.1126/science.aba6853>, 2020.
- 4845 White, A. E., Foster, R. A., Benitez-Nelson, C. R., Masqué, P., Verdeny, E., Popp, B. N., Arthur, K. E., and Prahl, F.G.: Nitrogen fixation in the Gulf of California and the eastern tropical North Pacific, *Prog. Oceanogr.*, 109, 1-17, <https://doi.org/10.1016/j.pocean.2012.09.002>, 2013.
- Wignall, P. B., & Newton, R.: Pyrite framboid diameter as a measure of oxygen deficiency in ancient mudrocks. *American Journal of Science*, 298(7), 537-552, <https://doi.org/10.2475/ajs.298.7.537>, 1998.
- 4850 Wignall, P. B., Newton, R., & Brookfield, M. E.: Pyrite framboid evidence for oxygen-poor deposition during the Permian–Triassic crisis in Kashmir. *Palaeogeography, Palaeoclimatology, Palaeoecology*, 216(3-4), 183-188, <https://doi.org/10.1016/j.palaeo.2004.10.009>, 2005.
- Wilfert, P., Krause, S., Liebetau, V., Schönfeld, J., Haeckel, M., Linke, P., and Treude, T.: Response of anaerobic methanotrophs and benthic foraminifera to 20 years of methane emission from a gas blowout in the North Sea, *Mar. Petrol. Geol.*, 68, 731-742, <https://doi.org/10.1016/j.marpetgeo.2015.07.012>, 2015.
- 4855 Wilkin, R. T., Barnes, H. L., & Brantley, S. L.: The size distribution of framboidal pyrite in modern sediments: an indicator of redox conditions. *Geochimica et cosmochimica acta*, 60(20), 3897-3912, [https://doi.org/10.1016/0016-7037\(96\)00209-8](https://doi.org/10.1016/0016-7037(96)00209-8), 1996.
- 4860 Wilkin, R. T., Arthur, M. A., & Dean, W. E.: History of water-column anoxia in the Black Sea indicated by pyrite framboid size distributions. *Earth and Planetary Science Letters*, 148(3-4), 517-525, [https://doi.org/10.1016/S0016-7037\(01\)00552-X](https://doi.org/10.1016/S0016-7037(01)00552-X), 1997a.
- Wilkin, R. T., & Barnes, H. L.: Pyrite formation in an anoxic estuarine basin. *American Journal of Science*, 297(6), 620-650, <https://doi.org/10.2475/ajs.297.6.620>, 1997b.
- 4865 Wilkinson, M. D., Dumontier, M., Aalbersberg, Ij. J., Appleton, G., Axton, M., Baak, A., Blomberg, N., Boiten, J.-W., Santos, L. B. da S., Bourne, P. E., Bouwman, J., Brookes, A. J., Clark, T., Crosas, M., Dillo, I., Dumon, O., Edmunds, S., Evelo, C. T., Finkers, R., Gonzalez-Beltran, A., Gray, A. J. G., Groth, P., Goble, C., Grethe, J. S., Heringa, J., Hoen, P. A. C. 't, Hooft, R., Kuhn, T., Kok, R., Kok, J., Lusher, S. J., Martone, M. E., Mons, A., Packer, A. L., Persson, B., Rocca-Serra, P., Roos, M., van Schaik, R., Sansone, S.-A., Schultes, E., Sengstag, T., Slater, T., Strawn, G., Swertz, M. A., Thompson, M., Lei, J. van der, van Mulligen, E., Velterop, J., Waagmeester, A., Wittenburg, P., Wolstencroft, K., Zhao, J., and Mons, B.: The FAIR Guiding Principles for scientific data management and stewardship, *Scientific Data*, 3, 1–9, <https://doi.org/10.1038/sdata.2016.18>, 2016.
- 4870 Winkelbauer, H. A., Cordova-Rodriguez, K., Reyes-Macaya, D., Scott, J., Glock, N., Lu, Z., Hamilton, E., Chenery, S., Holdship, P., Dormon, C., and Hoogakker, B.: Foraminifera iodine to calcium ratios: approach and cleaning, *Geochem. Geophys. Geosy.*, 22, e2021GC009811, <https://doi.org/10.1029/2021GC009811>, 2021.
- 4875 Winkelbauer, H. A., Hoogakker, B. A., Chance, R. J., Davis, C. V., Anthony, C. J., Bischoff, J., Carpenter, L. J., Chenery, S., Hamilton, E. M., Holdship, P., and Peck, V. L.: Planktic foraminifera iodine/calcium ratios from plankton tows, *Front. Mar. Sci.*, 10, 179, <https://doi.org/10.3389/fmars.2023.1095570>, 2023.
- Woehle, C., Roy, A. S., Glock, N., Wein, T., Weissenbach, J., Rosenstiel, P., Hiebenthal, C., Michels, J., Schönfeld, J., and Dagan, T.: A novel eukaryotic denitrification pathway in foraminifera, *Current Biology*, 28, 2536-2543, <https://doi.org/10.1016/j.cub.2018.06.027>, 2018.

- 4880 Woehle, C., Roy, A.-S., Glock, N., Wein, T., Weissenbach, J., Rosenstiel, P., Hiebenthal, C., Michels, J., Schonfeld, J., and Dagan, T.: A Novel Eukaryotic Denitrification Pathway in Foraminifera, *Curr. Biol.*, 28, 2536–2543, <https://doi.org/10.1016/j.cub.2018.06.027>, 2018.
- Woehle, C., Roy, A.-S., Glock, N., Michels, J., Wein, T., Weissenbach, J., Romero, D., Hiebenthal, C., Gorb, S.N., Schönfeld, J., and Dagan, T.: Denitrification in foraminifera has an ancient origin and is complemented by associated bacteria, *P. Natl. Acad. Sci. USA*, 119, e2200198119, <https://doi.org/10.1073/pnas.2200198119>, 2022.
- 4885 Wörmer, L., Lipp, J. S., Schröder, J. M., and Hinrichs, K. -U.: Application of two new LC–ESI–MS methods for improved detection of intact polar lipids (IPLs) in environmental samples, *Org. Geochem.*, 59, 10–21, <https://doi.org/10.1016/j.orggeochem.2013.03.004>, 2013.
- Woulds, C., Andersson, J. H., Cowie, G. L., Middelburg, J. J., and Levin, L. A.: The short-term fate of organic carbon in marine sediments: Comparing the Pakistan margin to other regions, *Deep-Sea Res. Pt. II*, 56, 393–402, <https://doi.org/10.1016/j.dsr2.2008.10.008>, 2009.
- 4890 Wu, F., Qi, Y., Yu, H., Tian, S., Hou, Z., and Huang, F.: Vanadium isotope measurement by MC-ICP-MS, *Chem. Geol.*, 421, 17–25, <https://doi.org/10.1016/j.chemgeo.2015.11.027>, 2016.
- 4895 Yu, J., Elderfield, H., Jin, Z., and Booth, L.: A strong temperature effect on U/Ca in planktonic foraminiferal carbonates, *Geochim. Cosmochim. Ac.*, 72, 4988–5000, <https://doi.org/10.1016/j.gca.2008.07.011>, 2008.
- Xie, S., Liu, X. -L., Schubotz, F., Wakeham, S. G., and Hinrichs, K. -U.: Distribution of glycerol ether lipids in the oxygen minimum zone of the Eastern Tropical North Pacific Ocean, *Org. Geochem.*, 71, 60–71, <https://doi.org/10.1016/j.orggeochem.2014.04.006>, 2014.
- 4900 Zarkogiannis, S. D., Iwasaki, S., Rae, J. W. B., Schmidt, M. W., Mortyn, P. G., Kontakiotis, G., Hertzberg, J. E., and Rickaby, R. E. M.: Calcification, Dissolution and Test Properties of Modern Planktonic Foraminifera From the Central Atlantic Ocean, *Front. Mar. Sci.*, 9, <https://doi.org/10.3389/fmars.2022.864801>, 2022.
- Zarriess, M., and Mackensen, A.: Testing the impact of seasonal phytodetritus deposition on $\delta^{13}\text{C}$ of epibenthic foraminifer *Cibicoides wuellerstorfi*: A 31,000 year high-resolution record from the northwest African continental slope, *Paleoceanography* 26, <https://doi.org/10.1029/2010PA001944>, 2011.
- 4905 Zhang, F., Romaniello, S. J., Algeo, T. J., Lau, K. V., Clapham, M. E., Richoz, S., Herrmann, A. D., Smith, H., Horacek, M., and Anbar, A. D.: Multiple episodes of extensive marine anoxia linked to global warming and continental weathering following the latest Permian mass extinction, *Sci. Adv.*, 4, e1602921, <https://doi.org/10.1126/sciadv.1602921>, 2018.
- Zhang, F., Lenton, T. M., del Rey, Á., Romaniello, S. J., Chen, X., Planavsky, N. J., Clarkson, M. O., Dahl, T. W., Lau, K. V., and Wang, W.: Uranium isotopes in marine carbonates as a global ocean paleoredox proxy: a critical review, *Geochim. Cosmochim. Ac.*, 287, 27–49, <https://doi.org/10.1016/j.gca.2020.05.011>, 2020.
- 4910 Zhang, F., Stockey, R.G., Xiao, S., Shen, S.-Z., Dahl, T.W., Wei, G.-Y., Cao, M., Li, Z., Kang, J., Anbar, A.D., Planavsky, N.J.: Uranium isotope evidence for extensive shallow water anoxia in the early Tonian oceans, *Earth and Planetary Science Letters* 583, 117437.
- 4915 Zheng, Y., Anderson, R. F., van Geen, A., and Fleisher, M. Q.: Preservation of particulate non-lithogenic uranium in marine sediments. *Geochim. Cosmochim. Ac.*, 66, 3085–3092, [https://doi.org/10.1016/S0016-7037\(01\)00632-9](https://doi.org/10.1016/S0016-7037(01)00632-9), 2002a.
- Zheng, Y., Anderson, R. F., van Geen, A., Fleisher, M. Q.: Remobilization of authigenic uranium in marine sediments by bioturbation, *Geochim. Cosmochim. Ac.*, 66, 1759–1772. [https://doi.org/10.1016/S0016-7037\(01\)00886-9](https://doi.org/10.1016/S0016-7037(01)00886-9), 2002b.
- 4920 Zehr, J. P.: Nitrogen fixation by marine cyanobacteria, *Trends Microbiol.*, 19, 162–173, <https://doi.org/10.1016/j.tim.2010.12.004>, 2011.

- Zhou, X., Thomas, E., Rickaby, R. E. M., Winguth, A. M. E., and Lu, Z.: I/Ca evidence for upper ocean deoxygenation during the PETM, *Paleoceanography*, 29, 964-975, <https://doi.org/10.1002/2014PA002702>, 2014.
- 4925 Zhou, X., Thomas, E., Winguth, A. M. E., Ridgwell, A., Scher, H., Hoogakker, B. A. A., Rickaby, R. E. M., and Z. Lu: Expanded oxygen minimum zones during the late Paleocene-early Eocene: Hints from multiproxy comparison and ocean modeling, *Paleoceanography* 31, 1532-1546, <https://doi.org/10.1002/2016PA003020>, 2016.
- Zhou, X., Hess, A. V., Bu, K., Sagawa, T., and Rosenthal, Y.: Simultaneous determination of I/Ca and other elemental ratios in foraminifera: comparing results from acidic and basic solutions, *Geochem. Geophys. Geosy.*, 23, e2022GC010660, <https://doi.org/10.1029/2022GC010660>, 2022.
- 4930 Zhou, Y., and McManus, J.F.: Authigenic uranium deposition in the glacial North Atlantic: Implications for changes in oxygenation, carbon storage, and deep water-mass geometry, *Quaternary Science Reviews* 300, 107914, <https://doi.org/10.1016/j.quascirev.2022.107914>, 2023.
- 4935 Zindorf, M., Rush, D., Jaeger, J., Mix, A., Penkrot, M. L., Schnetger, B., Sidgwick, F. R., Talbot, H. M., Land, C. van der, Wagner, T., Walczak, M., and März, C.: Reconstructing oxygen deficiency in the glacial Gulf of Alaska: Combining biomarkers and trace metals as paleo-redox proxies, *Chem. Geol.*, 558, 119864, <https://doi.org/10.1016/j.chemgeo.2020.119864>, 2020.
- 4940 Zonneveld, K. A. F., Versteegh, G. J. M., Kasten, S., Eglinton, T.I., Emeis, K. C., Huguet, C., Koch, B. P., de Lange, G. J., de Leeuw, J. W., Middelburg, J. J., Mollenhauer, G., Prahl, F. G., Rethemeyer, J., and Wakeham, S. G.: Selective preservation of organic matter in marine environments; processes and impact on the sedimentary record, *Biogeosciences*, 7, 483-511, <https://doi.org/10.5194/bg-7-483-2010>, 2010.